New phenomenological tests for supersymmetric theories with SU(5)-like unification

Yannick Stoll

UNIVERSITÉ GRENOBLE ALPES

THÈSE

Pour obtenir le grade de

DOCTEUR DE L'UNIVERSITÉ DE GRENOBLE ALPES

Spécialité : **Physique théorique**

Arrêté ministériel : 7 août 2006

Présentée par

Yannick STOLL

Thèse dirigée par **Fawzi BOUDJEMA**
et codirigée par **Björn HERRMANN**

préparée au sein du **Laboratoire d'Annecy-Le-Vieux de Physique Théorique**
et de **l'Ecole Doctorale de Physique de Grenoble**

Nouveaux tests phénoménologiques pour les théories supersymétriques avec unification de type $SU(5)$

Thèse soutenue publiquement le **25 Septembre 2015**,
devant le jury composé de :

Jean-Loïc KNEUR
Directeur de recherche, L2C - Montpellier , Président
Farvah Nazila MAHMOUDI
Maître de conférences, Université de Lyon, Rapporteur
Sabine KRAML
Directrice de recherche, LPSC - Grenoble, Examinatrice
Stéphane LAVIGNAC
Chargé de recherche , CEA - Saclay, Examinateur
Fawzi BOUDJEMA
Directeur de recherche, LAPTh, Directeur de thèse
Björn HERRMANN
Maître de conférences, Université Savoie Mont Blanc - LAPTh , Co-Directeur de thèse

Résumé

Dans cette thèse, nous explorons les conséquences aux basses énergies des modèles supersymétriques de grande unification (SUSY-GUT) basés sur le groupe de Lie $SU(5)$. Ces modèles constituent les prototypes des modèles SUSY-GUT et, en tant que tels, ont reçu beaucoup d'attention au cours des dernières décennies. En particulier, l'unification quark-lepton dans le secteur de Yukawa a été l'objet de nombreuses études.

L'originalité de notre approche est de rester confiné au secteur des squarks hauts, où nous avons montré qu'une relation de symétrie induite par $SU(5)$ apparait, à notre connaissance jusqu'à présent non étudiée, et bien moins dépendante de la réalisation particulière du modèle que l'unification quark-lepton. En effet, nous avons démontré qu'un modèle supersymétrique équipé d'une symétrie de jauge $SU(5)$ implique de manière générale un couplage trilinéaire dans le secteur des squarks hauts A_U symétrique i.e. $A_U = A_U^T$ à l'échelle GUT. Cette relation reste bien préservée par les équations du groupe de renormalisation durant son évolution jusqu'à l'échelle du TeV, laissant ainsi une empreinte de la symétrie de grande unification dans le spectre supersymétrique aux basses énergies. Cela étant établie, nous pouvons construire une série de tests phénoménologiques sur les spectres SUSY de basses énergies, potentiellement accessibles au LHC. La plupart de ces tests consistent à déterminer une certaine relation parmi les observables de basses énergies.

Nous avons réussi à exhiber de telles relations dans trois sortes de spectre SUSY, à savoir les spectres "SUSY lourds" dans lesquels l'échelle de brisure de la SUSY est bien plus élevée que l'échelle du TeV, les spectres de "SUSY naturels" où la troisième génération de scalaire est légère et enfin les spectres de "SUSY Top-Charm" dans lesquels seule la première génération de scalaire est gardée lourde. Nous avons développé une méthode générique, basée sur des tests statistiques fréquentistes reposant sur le calcul d'une valeur p, pour quantifier avec quelle significativité des écarts à ces relations de contrainte peuvent être détectés, dans chacun des trois cas mentionnés plus haut. Typiquement, pour chacun des tests, environ $\mathcal{O}(10 - 100)$ événements sont nécessaires dans chacun des processus considérés, pour établir un écart de 50% des relations tests à un niveau de significativité de 3σ. Notons que des techniques expérimentales telles que l'identification des jets charmés ou la polarimétrie du top, jouent un rôle essentiel dans la mise en œuvre de ces tests aux collisionneurs actuels, tel que le LHC.

La seconde partie de cette thèse est consacrée à une analyse numérique plus globale, basée sur les techniques bayésiennes de comparaison de modèles et applicable à toutes sortes de spectres quelque soit leurs hiérarchies. Dans ce contexte, nous avons développé une méthode numérique basée sur un algorithme de simulation de Monte Carlo par Chaine de Markov. Cette algorithme permet de tester, étant donné un certain spectre, avec quelle significativité celui-ci pointe ou non vers une symétrie $SU(5)$ à haute énergie. À nouveau, nous avons considéré plusieurs cas, selon la quantité d'information qui pourrait être collecté au LHC sur le spectre des squarks hauts. Nous trouvons que typiquement, ces informations ne contraignent pas suffisamment le spectre pour pouvoir tirer une conclusion quant à la présence d'une symétrie $SU(5)$ à haute énergie, exception faite de certains cas, où les incertitudes des observables sont réduites à des valeurs de l'ordre de $\mathcal{O}(1\%)$ et/ou des spectres loin d'être symétriques sous $SU(5)$ sont considérés. Dans cette dernière situation, cette analyse semble défavoriser la présence d'une symétrie $SU(5)$ à l'échelle GUT avec une évidence faible.

Abstract

In this thesis, we explore the consequences at low energies of supersymmetric grand unified theories (SUSY-GUT) based on the Lie group $SU(5)$. These models constitute the prototype of minimal SUSY-GUT and as such, have been intensively studied in the last decades. In particular, the quark-lepton unification in the Yukawa sector has received a lot of attention.

The originality of our approach is to stay within the up-squark sector, where we have shown that a so far unnoticed $SU(5)$ induced symmetry relation emerges, way less model dependent than the one aforementioned. Indeed, we demonstrate that a supersymmetric model, equipped with a $SU(5)$ gauge symmetry generically implies that the up-squark trilinear term A_U is symmetric at the GUT scale, namely that $A_U = A_U^T$. This relation is only mildly spoiled by the renormalization group running, and remains well preserved at the TeV scale, leaving thus a $SU(5)$ footprint in the low scale SUSY spectrum. This allows to build a series of phenomenological $SU(5)$ tests on low scale SUSY spectra, potentially accessible at the LHC. Most of these tests generically consist in determining a certain relation among low scale observables.

We exhibit such relations for three different sort of SUSY spectra, namely "Heavy SUSY" spectra which feature a SUSY breaking scale well above the TeV scale, "Natural SUSY" spectra which feature a light third scalar generation and "Top Charm SUSY" spectra in which only the first scalar generation is kept heavy. We have developed a generic method, based on a p-value frequentist statistical test to quantify to which significance one can assess a departure from these low scale constraints relations, in the three above-mentioned types of SUSY spectra. Typically, for each of the tests, $\mathcal{O}(10-100)$ events are necessary in the processes considered, to assess a departure of 50% at 3σ level of significance. It should be mentioned that experimental techniques such as charm tagging or top-polarimetry play a crucial role to apply these tests at current colliders, such as the LHC.

The second part of this thesis is devoted to a more global numerical analysis, based on Bayesian model comparison methods, and applicable to any kind of spectrum whatever its hierarchy. In this context, we have developed a numerical method based on a Markov Chain Monte Carlo algorithm allowing to test, given an observed low energy spectrum, with which significance it points or not toward a high scale $SU(5)$ dynamic. Again, we have considered several cases depending on the amount of information that will be collected on the squark spectrum at the LHC. We find that typically, the constraining power of these would-be collected information is too low to draw any conclusion on a possible $SU(5)-$like high scale dynamic, except in certain cases, when the uncertainties attached to the observables considered are reduced to $\mathcal{O}(1\%)$ and/or when spectra far from being $SU(5)$-symmetric are considered. In this last case, this analysis seems to disfavor the presence of a GUT scale $SU(5)$ symmetry with weak evidence.

À ma mère, à mes amis...

Contents

Remerciements

En tout premier lieu, je tiens à chaleureusement remercier mon directeur de thèse, Björn Herrmann pour m'avoir soutenu lors de la préparation de cette thèse. Ces conseils quotidiens ont été inestimables à mes yeux et m'ont permis de beaucoup progresser lors de ces trois ans de recherche.
Je tiens aussi à remercier Fawzi Boudjema, pour m'avoir accueilli au sein de son laboratoire et avoir servi de directeur de thèse officiel.
Je voudrais remercier Farvah Nazila Mahmoudi et Werner Porod, tous les deux chercheurs de stature internationale à l'emploi du temps extrêmement chargé et qui malgré tout, ont accepté de prendre le rôle de rapporteur de ma thèse. Leurs remarques ont grandement contribué à améliorer la qualité de ce manuscrit. Merci à eux.
Je souhaiterais aussi remercier Diego Guadagnoli qui a accepté de parrainer ma thèse et m'a soutenu tout au long de mon séjour au LAPTh.
Bien sûr, je profite de cette tribune pour affirmer avec force que notre laboratoire fermerait sans doute ses portes en une semaine sans notre équipe administrative de choc. Celle-ci est emportée par Dominique Turc en tant que responsable administrative, Véronique Jonnery à la comptabilité et Virginie Malaval au secrétariat. Je n'ai pas la place ici pour commencer à décrire à quel point leurs dévouements, leurs professionnalismes, sont essentiels au bon fonctionnement du laboratoire. Je me contenterai donc de leur dire un grand merci.
Je voudrais aussi remercier Mathieu Gauthier-Lafaye, le magicien du laboratoire comme je l'ai nommé, qui constitue la clé de voute du service informatique du LAPTh. Sa disponibilité, son sérieux, ses conseils et sa maitrise du monde du logiciel libre m'ont été grandement utile un nombre incalculable de fois.
Je voudrais aussi remercier Andreas Goudelis, aujourd'hui post-doc à Vienne, qui a été un véritable ami pour moi, quasiment un grand frère, lors de mes deux premières années de thèse. C'est une personne que j'apprécie énormément et avec laquelle j'espère sincèrement maintenir un contact au-delà du monde de la recherche. En particulier, merci à lui de m'avoir hébergé lorsque je me suis retrouvé quasi-SDF une semaine avant de partir en séjour à Hambourg. J'ai aussi une pensée particulière pour sa chère et tendre, Aoife Bharucha, CR à Marseille. Je ne peux que leur souhaiter tout le bonheur du monde pour la suite.
Je tiens aussi à remercier tous les doctorants avec lesquels j'ai pu passer de bons moments tel que Mathieu Vanicat, Mathieu Boudaud, Vincent Bizouard, Vivian Poulin, Yoann Genolini... En particulier, je souhaite bon courage à ceux qui restent, la route va être longue les gars, mais je sais que vous y arriverai.
Je souhaiterais aussi remercier ma mère, Nadia Stoll, qui m'a soutenu de manière indéfectible depuis toujours et m'a permit de mener ma thèse à bien. Son amour, son soutien quotidien ont été crucial dans la bonne réussite de mes études, cette thèse lui est dédiée.
Enfin, je souhaiterais remercier tous les amis chère à mon cœur. En particulier, Sinan et Nicolas qui mènent tous les deux de brillantes carrières en mathématiques. Nous nous sommes construits ensemble et ils m'ont apporté énormément, à tel point que nos personnalités respectives sont irrémédiablement liées. Eux aussi ont joué un rôle déterminant dans la réussite de ma thèse, merci. Parmi les autres copains, je souhaiterais citer pêle-mêle : Jean-Loup, Sylvie, Sébastien, Ariane, Éric, Sabine, Élie, Caroline, Odile, Rozenn, Vincent, Samuel. Cette thèse leur est aussi dédiée.

Introduction

It is fair to say that modern particle physics has started with the Rutherford experiments conducted in 1909 by Hans Geiger, Ernest Marsden and Ernest Rutherford. These scattering experiments have shown the existence of the atomic nucleus, the positively charged part of the atom. Most importantly, this experiment has lead in 1912 to the planetary model: atoms are composed of a very dense, very heavy, positively charged nucleus whose size is completely negligible in front of the electronic cloud. Hence, this has lead to the conclusion that matters is mostly composed of void.

The second founding experiment might be the discovering by Carl David Anderson in 1932 of the positron, the antimatter electron counterpart, theorized four years earlier by Paul Dirac. Finally, the third experiment I would like to mentioned is the discovery of the Higgs boson in 2012 by the LHC's ATLAS and CMS experiments. This discovery has put a final dot to the Standard Model, the theory in which are interpreted most of the results in particle physics today. However, one knows that this is not the end of the story and that the Standard Model (SM) is not an ultimate theory of nature, failing for example to include massive neutrinos or suitable dark matter candidates.

At the time these lines are written (July 2015), the LHC has just restarted to record data at its nominal energy. One can say that, currently, the situation is quite inquiring, even though not yet worrying. Indeed, new physics have been waited for a while now, and the simplest extensions of the Standard Model have been put more and more under pressure.

Among the best motivated frameworks to extend the Standard Model, there is Supersymmetry (SUSY), which postulates the existence of a new type of space-time symmetry between bosons, which are integer spin particles, and fermions, which are half-integer spin particles. However, the non-observation of light superpartners clearly indicates that SUSY, if realized in nature, must be a broken symmetry. In any case, the simplest SUSY extension of the SM, the Minimal Supersymmetric Standard Model (MSSM) is of special interest for phenomenologists, resolving most of the questions unanswered by the SM.

On the other hand, the lack of experimental signals makes that theoretically, SUSY remains poorly understood. Crucially, one misses a clear understanding of the mechanism responsible for the spontaneous breaking of SUSY. To parameterize this ignorance, a way around have been found by introducing a lot (about a hundred) of "soft" -in a sens that will be precised later- parameters. However, the price to pay to apply such procedure is a clear drop of predictability of the theory, unless a breaking mechanism is imposed, the soft terms are seen as free parameters.

One cure to the point raised above might be to embed the SM's Lie gauge group into a larger one, for example $SU(5)$, $SO(10)$ or $E(6)$. Such Grand Unified Theory (GUT) allows to unify the three fundamental forces of the SM into a single one, through the unification of their respective gauge couplings. Beside, when a GUT is combined with SUSY, fitting the low energy gauge couplings to their measured values is easier and suppression of proton decay can be obtained to a reasonable level, phenomenon otherwise generically predicted by GUT theories. Furthermore, in a SUSY context, the soft terms get unified as well, thus reducing the hundred free soft parameters needed in the MSSM to only a few independent high scale terms.

The present thesis is interested in the simplest of such SUSY/GUT theory, the one based on the Lie group $SU(5)$. This SUSY/GUT have been the subject of multiple studies during the last decades, in particular the quark-lepton unification have received a lot of attention. Indeed, this SUSY/GUT predicts that Yukawa couplings in the quarks and leptons sectors unify at a scale $M \sim \mathcal{O}(10^{16})$ GeV, called the GUT scale. Evolving these down to a scale accessible to experiments with the renormalization group's techniques, one can then scrutinize their low scale values to see if these are compatible with a

possible high scale unification. In the simplest model, the conclusion is quite pessimistic. Indeed, this unification seems to work only for the third generation and even there, extra-care have to be taken, introducing for example threshold corrections originating from the dynamic above the GUT scale.

On the other hand, the originality of this thesis is to investigate the low scale consequences of this type of unification not on Yukawa couplings but on soft parameters, restricting our study to the up-squarks sector. Indeed, we have shown that a so-far unstudied feature of $SU(5)$ SUSY/GUTs is that the up-squarks trilinear coupling is symmetric at the GUT scale. This symmetry relation is well preserved by the renormalization group equations, the asymmetry introduced by the running remaining small at the TeV scale. Hence, if the GUT scale is symmetric under $SU(5)$, we expect that a footprint should remain in the low scale up-squarks spectrum, allowing to build a series of phenomenological tests.

This thesis is organized as follows:

1. The chapter 1 is dedicated to a presentation of the Standard Model. Its gauge structure as well as its matter content are presented. Also, the Higgs mechanism, responsible for the electroweak symmetry breaking as well as the fermions mixing mechanisms are outlined. We conclude this chapter by giving some hints on why we believe that the SM needs to be extended by a more complete theory.

2. The chapter 2 gives an introduction to supersymmetry, focusing on the MSSM. The SUSY algebra and the elegant formalism of superfields are presented. We then give some arguments to understand why SUSY spontaneous breaking cannot be achieved in a SUSY theory whose breaking scale lies near the TeV scale, thus motivating the introduction of a soft sector. Finally, the MSSM is described, its virtues and limitations exposed, and the three main paradigms used to maintain the superpartners contributions to low scale observables outlined.

3. The chapter 3 presents the $SU(5)$ GUT, both in a non-SUSY and in a SUSY-context. A special attention is paid to the flavor sector of this GUT, in particular one shows that the symmetry relations which hold in the Yukawa sector propagate to the soft breaking terms. We conclude this chapter by presenting a few of the physical consequences that derive from this kind of unification.

4. The chapter 4 contains the main contribution of this thesis. In this chapter, we have build a series of phenonomenological tests on up-type squarks spectra, using frequentist statistical methods. In particular, three types of typical SUSY spectra are considered, for which we provide constraint relations on low scale observables deriving from a $SU(5)$-like GUT symmetry. These relations are only midly spoiled, should a $SU(5)$-like GUT be realized in nature.

5. Finally, in the chapter 5, we build more global $SU(5)$ tests, using Bayesian model comparison methods. Indeed, in this chapter, we compute Bayes factors numerically, using Markov Chains Monte Carlo techniques, to discriminate the possible presence of remnants of a high scale $SU(5)$ symmetry into low scale squarks spectra. We hence start this chapter by providing an introduction to Bayesian statistics. The numerical strategy is then exhibited and the results commented.

Introduction en français

La physique des particules moderne a commencé avec les expériences de Rutherfords, conduites en 1909 par Hans Geiger, Ernest Marsden et Ernest Rutherford. Ces expériences de diffusion ont démontré l'existence du noyau atomique, la partie chargée positivement de l'atome. Plus important peut-être, cette expérience a conduit en 1912, à l'émergence du modèle planétaire : les atomes sont constitués d'un noyau chargé positivement, très dense et très lourd, dont la taille est complètement négligeable devant celle du nuage électronique, en conséquence de quoi la matière est surtout composée de vide.

La deuxième expérience fondatrice pourrait être la découverte par Carl David Anderson en 1932 du positron, la particule d'antimatière associée à l'électron, théorisée quatre années plus tôt par Paul Dirac. Finalement, la troisième expérience que je voudrais citer est la découverte du boson de Higgs en 2012 par les expériences ATLAS et CMS du LHC. Cette découverte a mis un point final au Modèle Standard (MS), théorie dans laquelle sont interprétés la plupart des résultats expérimentaux aujourd'hui. Cependant, nous savons que l'histoire ne s'arrête pas là, le modèle standard n'étant pas une théorie ultime de la nature, échouant par example à inclure des termes de masse pour les neutrinos ou à inclure des particules qui pourraient être de bon candidats de matière noire.

Au moment où ces lignes sont écrites (Juillet 2015), le LHC vient juste de reprendre sa prise de donnée à son énergie nominale. On peut dire que pour l'instant la situation est assez troublante, bien que pas encore inquiétante. En effet, la nouvelle physique se fait attendre depuis un moment maintenant, et les extensions les plus simples du MS sont de plus en plus sous pression.

Parmi les cadres bien motivés pour étendre le MS se trouve la supersymétrie (SUSY), qui postule l'existence d'un nouveau type de symétrie d'espace-temps entre les bosons, particules au spin entier, et les fermions, particules au spin demi-entier. Cependant, la non-observation de superpartenaires légers indique clairement que la SUSY, si elle est réalisée dans la nature, se doit d'être une symétrie brisée. Dans tous les cas, l'extension la plus simple du MS compatible avec la SUSY, le modèle standard supersymétrique minimal (MSSM) continu d'être d'une grande aide pour les phénoménologistes, résolvant la plupart des questions laissées sans réponse par le MS.

D'un autre côté, le manque de signaux expérimentaux font que la SUSY reste théoriquement encore assez mal comprise. Essentiellement, une compréhension claire du mécanisme responsable de la brisure de la SUSY nous manque. Afin de paramétrer cette ignorance, une solution a été trouvée qui consiste à introduire beaucoup (environ une centaine) de paramètres « doux »[1]. Cependant, le prix à payer pour appliquer cette procédure est une nette baisse de la prédictibilité de la théorie, à moins qu'un mécanisme de brisure ne soit imposé, ces paramètres doux étant vus comme libres.

Une solution au point soulevé plus haut peut consister à plonger le groupe de jauge du MS dans un groupe plus grand, par example $SU(5)$, $SO(10)$ ou $E(6)$. Une telle théorie de grande unification (GUT) permet d'unifier les trois forces fondamentales du MS en une seule, au travers de l'unification de leurs couplages de jauge respectifs. De plus, lorsqu'une GUT est supersymétrisée, il est plus facile d'ajuster les couplages de jauge de basse énergie à leurs valeurs mesurées expérimentalement. Il est alors aussi plus facile d'abaisser le taux de désintégration du proton à un niveau acceptable, phénomène autrement généralement prédit par les théories de grande unification. En outre, dans un contexte supersymétrique, les termes doux deviennent aussi unifiés, réduisant ainsi à très haute énergie, la centaine de paramètre du MSSM à seulement quelques termes indépendants.

Cette thèse s'intéresse à la plus simple des théories SUSY/GUT, celle basée sur le groupe de jauge $SU(5)$. Cette théorie a été l'objet de nombreuses études durant les dernières décennies, en particulier

[1] La signification de l'adjectif « doux »pour caractériser ces paramètres sera précisée plus tard dans cette thèse.

l'unification quark-lepton a reçue beaucoup d'attention. En effet, ces théories SUSY/GUT prédisent que les couplages de Yukawa des leptons et des quarks s'unifient, à une échelle de l'ordre de $M \sim \mathcal{O}(10^{16})$ GeV, appelée l'échelle GUT. En faisant évoluer ces couplages à des échelles accessibles aux expériences, via les techniques du groupe de renormalisation, il est alors possible de tester leurs compatibilités avec une possible unification à haute énergie en scrutant leurs valeurs à basse énergie. Dans le cas le plus simple, la conclusion est clairement négative. En effet, cette unification ne semble fonctionner que pour la troisième génération et, même dans ce cas, des précautions supplémentaires doivent être prises, par example en introduisant des corrections de seuils qui pourraient naitre de la dynamique au dessus de l'échelle GUT.

D'un autre côté, l'originalité de cette thèse est d'investir les conséquences à basse énergie de ce type d'unification non plus dans le secteur de Yukawa, mais dans le secteur doux, en restant confiné au secteur des squarks hauts. En effet, nous avons montré qu'une caractéristique jusque là non étudiée de ces modèles est que le couplage trilinéaire des squarks hauts est symétrique à l'échelle GUT. Cette relation de symétrie est bien préservée par les équations du groupe de renormalisation, l'asymétrie introduite par l'évolution des couplages restant petite à l'échelle du TeV. Si l'échelle GUT est gouvernée par une symétrie $SU(5)$, on s'attend donc à ce qu'une empreinte de cette symétrie puisse subsister dans le spectre des squarks hauts à l'échelle du TeV, autorisant ainsi la construction d'une série de tests phénoménologiques.

Cette thèse est organisée de la manière suivante :

1. Le chapitre 1 est dédié à la présentation du Modèle Standard. Sa structure de jauge ainsi que son spectre de matière sont présentés. De plus, le mécanisme de Higgs, responsable de la brisure de symétrie électrofaible, et les mécanismes de mélange des fermions sont exposés. Ce chapitre se conclut sur une discussion des principaux indices qui nous pousse à penser que le MS a besoin d'être étendu par une théorie plus complète.

2. Le chapitre 2 constitue une introduction à la supersymétrie, en se concentrant sur le MSSM. L'algèbre supersymétrique ainsi que l'élégant formalisme des super-champs sont présentés. Des arguments sont ensuite donnés permettant de comprendre pourquoi la brisure spontanée de la SUSY ne peut être achevée dans le secteur visible, motivant ainsi l'introduction d'un secteur doux. Finalement, le MSSM est décrit, ses vertus et limitations exposées, et les trois grands paradigmes utilisés pour maintenir sous contrôle les contributions des super-partenaires aux observables de basse énergie ébauchés.

3. Le chapitre 3 présente la théorie GUT $SU(5)$, à la fois dans un contexte SUSY et non-SUSY. Une attention particulière est dévouée au secteur de la saveur, en particulier il est montré que les relations de symétrie qui existent dans le secteur de Yukawa se propagent aux termes doux. Ce chapitre se conclut par une présentation de quelques unes des conséquences physiques de ce type d'unification.

4. Le chapitre 4 contient la contribution principale de cette thèse. Dans ce chapitre, nous avons construit une série de tests phénoménologiques sur les spectres de squarks hauts, en utilisant des méthodes statistiques fréquentistes. En particulier, trois types de spectre SUSY sont considérés, pour lesquels nous fournissons des relations de contrainte sur les observables de basse énergie, relations qui ne devraient être que peu détruites si une théorie GUT de type $SU(5)$ est réalisée dans la nature.

5. Finalement, dans le chapitre 5, nous construisons des tests $SU(5)$ plus globaux, en utilisant des méthodes bayésiennes de comparaison de modèles. En effet, dans ce chapitre, nous calculons des facteurs de Bayes numériquement, en utilisant des algorithmes de Monte Carlo par Chaine de Markov, afin de discriminer la présence éventuelle de rémanents d'une symétrie $SU(5)$ dans les spectres de squarks hauts à basse énergie. Nous commençons donc ce chapitre en donnant une introduction aux statistiques bayésiennes. La stratégie numérique utilisée est ensuite présentée et les résultats commentés.

Part I

The Big Picture

Chapter 1

The Standard Model of particle physics

1.1 Introduction

The Standard Model of particle physics is, by its abilities to accurately fit most of the experimental results, one of the greatest theoretical achievements in particle physics in the second half of the twentieth century. It was able to predict new particles before their observation in experiments, with for some of them, their masses, to set order in the jungle of new bound states which were discovered in the 1960's by introducing the quark model and to predict the value of the intrinsic magnetic moment of the electron. This last value has turned out to be in agreement with the measured one to an extraordinary accuracy of the order of $\mathcal{O}(10^{-13})$.

From a theoretical point of view, the SM has assessed the importance of *gauge symmetries* (see [1]) in modern physics which now find applications well beyond the scope of particle physics. However, despite its successes, the SM leaves several questions unanswered. This has lead the high energy physics community to believe that a more fundamental theory in particle physics should exist of which the SM should be a low energy *effective theory*.

In this chapter we give a general overview of the SM. In section 1.2 we start by presenting the theoretical structure of the SM with an emphasis on the fermions mixing mechanisms. This will allow us to fix a certain number of notations which will be useful for the rest of this work. Section 1.5 is devoted to the presentation of the Cabbibo Kobayashi Maskawa (CKM) matrix, which drives flavor violation in the SM, and the unitary triangle fit which tests the consistency of the CKM mechanism with data. In section 1.6, we comment on the questions which are left unanswered by the SM. This will serve as a transition to the next chapter. Although it is a very insightful topic, the historical construction of the SM is not presented in this work, the interested reader is invited to refer to [2] and [3] as well as to the first chapter of [4].

1.2 Theoretical framework

The SM is a quantum field theory which describes three out of the four fundamental interactions of nature, namely the electromagnetic interaction, the weak interaction, and the strong interaction. The gravitational interaction is left aside as it requires special care. Quantum field theory (QFT) allows to properly reconcile quantum mechanics with special relativity and is based on analytical mechanics using the Lagrangian formalism. For a complete tour of QFT, see the classical book of Peskin and Schroeder [5] although other references such as [6] or [7] should be more appropriate for graduate students. Precisely, the SM is a Yang-Mills theory (see [8]) invariant under the semi-simple non-abelian gauge group $G_{SM} = SU(3)_C \times SU(2)_L \times U(1)_Y$. The subscripts (C, L, Y) have no mathematical meaning and refer to the physical content of the charges of the factors. The factor $SU(3)_C$ is the gauge group of Quantum Chromodynamic (QCD) which describes the strong interaction responsible for maintaining the quarks inside the nucleons bound. To the quarks is associated an intrinsic quantum number called "color". It was first introduced to preserve the spin statistic theorem where in certain bounds states, without color, several quarks (which are fermions) would be in the same quantum state. The factor $SU(2)_L \times U(1)_Y$ is associated to the electroweak interaction which unifies the weak and the Quantum

Electrodynamic (QED) interactions, the quantum version of electromagnetism. The subscript L refers to the "weak isospin" introduced to explain why certain pairs of fermions in the SM have similar quantum properties under the weak interaction. Finally, Y refers to the "weak hypercharge" introduced to maintain the consistency of the SM and defined through the Gell-Mann–Nishijima formula:

$$\frac{Y}{2} = Q - T_L^3 \tag{1.1}$$

with T_L^3 the eigenvalue of the third generator of $SU(2)_L$ (see eqs (1.5) and (1.6)) and Q the usual electric charge. To each factor in G_{SM} are associated spin-1 bosons which transmit the force from one fermion to another. Their number is equal to the dimension of the group which is, for $SU(N)$ factors:

$$\dim(SU(N)) = \frac{N}{N(N-1)} \tag{1.2}$$

and 1 for the abelian $U(1)$ factor. In the case of QCD, we have $\frac{3(3-1)}{2} = 8$ bosons, called gluons, and noted $\{G^i\}_{\{i=1..8\}}$. For the electroweak interaction, three bosons $\{W^i\}_{\{i=1..3\}}$ are associated to the $SU(2)$ factor and one boson B to the $U(1)$ factor. It has to be noted that as long as the symmetry group remains exact, the gauge bosons as well as the fermions remain massless, a mass term in the Lagrangian breaking explicitly the gauge invariance. This has lead Francois Englert, Robert Brout, Peter Higgs, Gerald Guralnik, Carl Richard Hagen and Thomas Kibble in the mid-1960s to apply to the SM a mechanism inherited from solid state physics, the so-called Higgs mechanism [9, 10] [1].

Digression on the paramagnetic $\rightarrow$ ferromagnetic transition One can have a feeling about the physics of the Higgs mechanism by making a parallel with the ferromagnetic/paramagnetic transition in solid state physics. Let us consider an electric conductor which can be thought of as a spin assembly. If the temperature of the system is high enough the directions of the different spins are randomly distributed. The macroscopic magnetization vector, which is proportional to the vectorial sum of the spins, is null. The system is said to be in the paramagnetic phase, the solid being isotrop the symmetry group is $SO(3)$, the group of 3D space rotations. If one decreases the temperature below a certain threshold, the Curie point T_C, a macroscopic direction in the system appears among the spins, the magnetization vector is not null anymore and the system is said to be in the ferromagnetic phase. The symmetry group of the ferromagnetic phase is $SO(2)$ (subgroup of $SO(3)$), the symmetry group of the plane rotations whose axis is set by the magnetization direction. Hence, during the paramagnetic $\rightarrow$ ferromagnetic transition, the symmetry group of the system has been reduced from $SO(3)$ to $SO(2)$. As this phase transition didn't occur due to an external element, for instance a magnet, but because the temperature i.e. the energy of the system has decreased, it is called a *spontaneous symmetry breaking*.

Back to particle physics, the Higgs mechanism describes the spontaneous symmetry breaking (SSB) of the $SU(2)_L \times U(1)_Y$ factor down to $U(1)_Q$, the gauge group of QED. To perform this SSB, we need to introduce an extra scalar, the Higgs boson, which plays an analogous role to the magnetization vector, and reduces the symmetry group of the system when picking specific directions in the scalar potential of the theory. This occurs when the system falls in its ground state which in a QFT framework is called the vacuum. In this process, the gauge bosons $\{W^{1,2}\}$ acquire a non-vanishing mass and mix to give the electrically charged $W^{+,-}$ physical states. The others gauge bosons $\{W^3, B\}$ mix to give the massive boson Z^0, the third electrically neutral gauge boson of the weak interaction, and the photon, the gauge boson of QED, which remains massless as the Higgs mechanism preserves an abelian group, $U(1)_Q$, to guarantee the conservation of the electric charge. The gluons remain also massless as the $SU(3)_C$ factor of G_{SM} is left invariant by the Higgs mechanism. The states (W^+, W^-, Z^0) have been observed at the UA1 and UA2 experiments at the CERN in 1983 with properties which match the quantum numbers predicted by the SM [11–14]. Lastly and, although further investigations are needed, a scalar boson has been discovered in 2012 independently by the ATLAS [15] and CMS [16] experiments with properties which seem to match to the Higgs boson as predicted by the SM Higgs mechanism.

[1] History has forgotten most of the authors in the used name which one can consider as not very fair. Alternatively, if one believes that a discovery belong to anybody, a more radical solution could be to use a name for the mechanism in which no authors appears.

After this qualitative description of the Standard Model, we want to adopt now a more quantitative approach by presenting the details of the theory. Specifically, the SM Lagrangian can be split into four parts:

$$\mathcal{L}_{SM} = \mathcal{L}_{Gauge} + \mathcal{L}_{Matter} + \mathcal{L}_{Yukawa} + \mathcal{L}_{Higgs} \tag{1.3}$$

In the following, we shall have a tour at each of these sectors.

1.3 The Gauge sector

We start with the gauge sector which describes both the kinetic terms and self-interactions of the gauge bosons. The gauge sector of the standard model can be written as:

$$\mathcal{L}_{Gauge} = -\frac{1}{2}\mathrm{Tr}(G_{\mu\nu}G^{\mu\nu}) - \frac{1}{2}\mathrm{Tr}(W_{\mu\nu}W^{\mu\nu}) - \frac{1}{2}\mathrm{Tr}(B_{\mu\nu}B^{\mu\nu}), \tag{1.4}$$

where the rank 2 tensors $G_{\mu\nu}, W_{\mu\nu}$ and $B_{\mu\nu}$ are called the *field strength tensors* of respectively the $SU(3)$, $SU(2)$, and $U(1)$ factors. These can be decomposed, for instance in the case of $SU(2)$, as:

$$W_{\mu\nu} = W^i_{\mu\nu} T_i \tag{1.5}$$

with $\{T_i\}$, the *generators* of the group. The greek indices $(\mu, \nu...)$ are lorentz indices and indicate how the fields transform under the group of special relativity spacetime symmetry, the Poincaré group $R^{1,3} \rtimes SO(1,3)$ (see [17]) which can be reduced, by a proper choice of frame, to the Lorentz group $SO(1,3)$ [2]. Here, we take the usual metric convention in QFT, $\eta_{\mu\nu} = diag(+1,-1,-1,-1)$.. The generators can be thought of as "basis vectors" of the group encoding infinitesimal transformations defined by the following commutation relations :

$$[T_i, T_j] = g c_{ijk} T_k \tag{1.6}$$

These commutation relations form a Lie algebra [3]. $\{c_{ijk}\}$ are called the structure constants of the group with, in the case of $SU(2)$ $c_{ijk} = \epsilon_{ijk}$ the totally antisymmetric Levi-Civita tensor defined such that $\epsilon_{123} = +1$. g is called the coupling constant of the group and sets the interaction strength. For the three factors of G_{SM}, the field strength tensors can be expressed in term of the gauge bosons as:

$$\begin{aligned} G^i_{\mu\nu} &= \partial_\mu G^i_\nu - \partial_\nu G^i_\mu - g_3 f_{ijk} G^j_\mu G^k_\mu \quad i,j,k = 1...8, \\ W^i_{\mu\nu} &= \partial_\mu W^i_\nu - \partial_\nu W^i_\mu - g_1 \epsilon_{ijk} W^j_\mu W^k_\mu \quad i,j,k = 1..3, \\ B_{\mu\nu} &= \partial_\mu B_\nu - \partial_\nu B_\mu, \end{aligned} \tag{1.7}$$

with $\{f_{ijk}\}$, the structure constants of $SU(3)$ define by Gell Mann [18]. The indices $i, j, k...$ live in the adjoint representation of the group [4]. We want to emphasize that the structure constants vanish in the case of an abelian group or, in equivalent terms, when their gauge bosons are neutral under the group. The consequence is that, in such a case, no gauge bosons self-interaction vertices are present. This is typically the case for $U(1)_Y$ or in QED for $Q(1)_Q$ for which structure constants are zero and no photon self-interactions exist. On the other hand, $SU(3)$ and $SU(2)$ being non-abelian, three and four point self interactions vertices are present among the gluons and W bosons as illustrated in figure 1.1.

[2] The Lorentz group $SO(1,3)$ is defined as the group of matrices which leave the metric invariant i.e. $\Lambda \in SO(1,3)$: $\eta = \Lambda\eta\Lambda^T$.

[3] A nice view of this machinery can be developed if we remember that, in the context of differential geometry, a Lie group is isomorphic to a manifold. The generators of the group then really form a basis of vectors on the tangential space of this manifold.

[4] That means that a gauge transformation acts on the field strength tensor, for instance in the case of $SU(3)$, as: $U \in SU(3), G^i \to UG^iU^\dagger$.

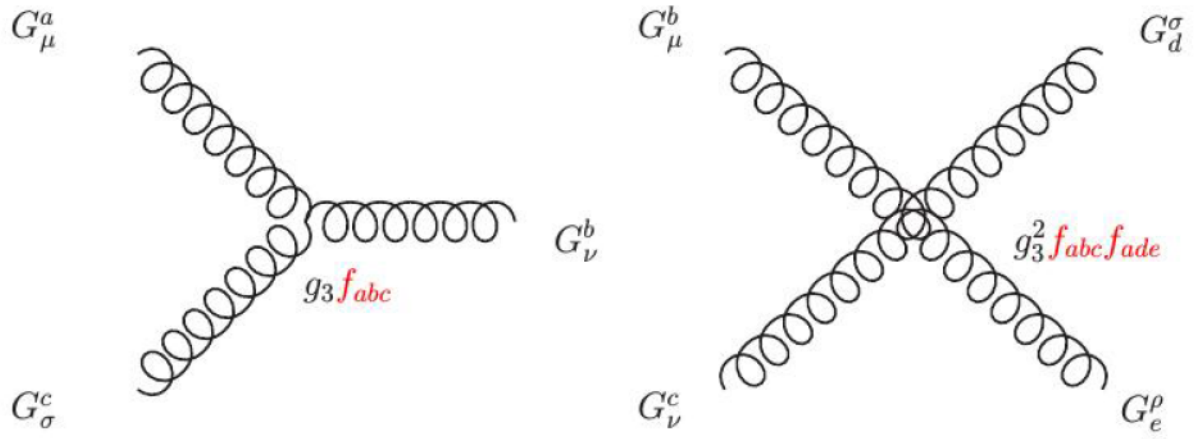

Figure 1.1 – Three and four point gluon self interactions. The vertices arises due to the non abelian nature of $SU(3)$ i.e. these are proportional to the structure constants f_{abc}.

1.4 The matter sector

The matter sector of the SM describes the 24 spin 1/2 fermions forming the matter and their associate anti-particles. These can be gathered in two families depending on their sensitivity to the strong interaction. The fermions sensitive to the strong interaction are called quarks and their electric charges are quantified to be either $+\frac{2}{3}e$ (the "up-type" quarks) or $-\frac{1}{3}e$ (the "down-type" quarks) with e the elementary electric charge. On the other hand, leptons are not sensitive to the strong interaction and can be split in two sub-families depending on their electric charges, the electrically neutral leptons being called "neutrinos" and the electrically charged being called "charged leptons".

In the context of group representation theory, we can restrict the Lorentz group mentioned above to the subgroup of Lorentz transformations preserving both the orientation of space and the direction of time, noted $SO(1,3)^\uparrow$, the *orthochronous* proper Lorentz group [5]. One can show that there is an isomorphism between the fundamental representation of $SO(1,3)^\uparrow$ and a direct product of two fundamental representations of $SU(2)$, i.e. $SO(1,3)^\uparrow \sim SU(2) \otimes SU(2)$. This suggests that the fermions of the SM can be decomposed as a combination of two Weyl spinors which are merged in an object called a Dirac spinor Ψ. More precisely, a Dirac spinor can be decomposed as:

$$\Psi = P_L \Psi_L + P_R \Psi_R, \tag{1.8}$$

where P_L and P_R are *chirality* projector operators defined as:

$$P_L = \frac{1-\gamma_5}{2}, \; P_R = \frac{1+\gamma_5}{2} \tag{1.9}$$

with γ_5, the fifth gamma matrix (see appendix A.1).

Let us consider a fermion described by a Dirac spinor Ψ and also consider its associate anti-spinor $\Psi^C = C\Psi C^{-1}$ with C the charge conjugate operator. We can define the chirality operator h as the operator which projects the spin $\vec{S}$ over the momentum $\vec{p}$ direction $h = \vec{S} \cdot \frac{\vec{p}}{|\vec{p}|}$. In the massless limit, one can show that Ψ always has a negative helicity and is in a pure Ψ_L state ($h\Psi = -1, \Psi = \Psi_L$) and Ψ^C always has a positive helicity and is in a pure Ψ_R state ($h\Psi^C = +1, \Psi^C = \Psi^C_R$). For this reason, Ψ_R is called a "right"-handed spinor and Ψ_L a "left"-handed spinor.

If now Dirac mass terms are present in the electroweak broken phase as it results from the Higgs mechanism, a chirality mixing is introduced through a Yukawa coupling to the Higgs boson (see subsection 1.4.1). Hence, particles and anti-particles are in a superposition of both left-handed and right-handed states. It turns out that the weak interaction couples exclusively to the left-handed component

[5] Hence $SO(1,3)^\uparrow$ is defined as : $\Lambda \in SO(1,3)^\uparrow$ if $\det(\Lambda) = +1$ and $\Lambda^0_0 > 0$.

of Ψ, that is why a subscript L is added to the gauge group name $SU(2)_L$ and the weak interaction is said to break maximally the parity symmetry. This enforces the fact that left-handed components are fold in two-dimensional representations of $SU(2)_L$ i.e. particle physicist say they form $SU(2)$ doublets. whereas the right-handed components will be fold in 1-dimensional representations of $SU(2)_L$ i.e. they form $SU(2)$ singlets. More generally, the fields of the SM can be classified in multiplets according to which representation spaces they are living in for the $SU(3)$, $SU(2)$, and $U(1)$ factors. The notation is the following: we use a 3-plets $\{\mathbf{n_C}, \mathbf{n_L}, Y\}_\Psi$ where $\mathbf{n_C}$ and $\mathbf{n_L}$ are bold integers denoting the dimension of $SU(3)_C$ and $SU(2)_L$ representations, Y being the common multiplet hypercharge value. For instance, left-handed quarks form $SU(2)$ doublets composed of an up and a down-quark and are noted:

$$Q^0_{mL} = \begin{pmatrix} u^0_m \\ d^0_m \end{pmatrix}_L . \tag{1.10}$$

These doublets are uniquely defined by the 3-plet $\{\mathbf{3}, \mathbf{2}, \frac{1}{3}\}_{Q_L}$ indicating that they live in a 3-dimensional representation of $SU(3)_C$ (quarks exist in three color states), in a 2-dimensional representation of $SU(2)$ and the up and down quarks share a common hypercharge value of $Y_{Q_L} = \frac{1}{3}$. The electric charge of u^0_m and d^0_m can then be easily deduced from eq (1.1). Here, the superscript 0 defines these states as weak eigenstates i.e. they possess definite transformation properties under $SU(2)_L$ and the subscript m refers to the family index. Indeed, it is an empirical fact of nature that each fermion type in the SM (charged leptons: e^{-0} , neutrinos: ν^0 , up quarks: u^0 and down quarks: d^0) exist in three copies (m=1,2,3) named "generation" or "family". The full content of the m-th family of fermions can then be summarized as follows:

$$\begin{aligned} Q^0_{mL} = \begin{pmatrix} u^0_m \\ d^0_m \end{pmatrix}_L : \{\mathbf{3}, \mathbf{2}, \frac{1}{3}\}_{Q_L} \qquad & L^0_{mL} = \begin{pmatrix} \nu^0_m \\ e^{-0}_m \end{pmatrix}_L : \{\mathbf{1}, \mathbf{2}, -1\}_{L^0_{mL}} \\ u^0_{mR} : \{\mathbf{3}, \mathbf{1}, \frac{4}{3}\}_{u^0_{mR}} \qquad & d^0_{mR} : \{\mathbf{3}, \mathbf{1}, -\frac{2}{3}\}_{d^0_{mR}} \\ e^{-0}_{mR} : \{\mathbf{1}, \mathbf{1}, -2\}_{e^{-0}_{mR}} \qquad & \nu^0_{mR} : \{\mathbf{1}, \mathbf{1}, 0\}_{\nu^0_{mR}} \end{aligned} \tag{1.11}$$

We emphasize the fact that despite we have introduced right-handed neutrinos ν^0_{mR} above, strictly speaking, they do not belong to the SM spectrum since they are completely neutral under G_{SM}. As ν^0_{mR} does not interact through any of the gauge interaction of the SM with the rest of the spectrum, it is called a *sterile* particle. Beside, currently, right-handed neutrinos should still be seen as hypothetical particles as no experiment has allowed to disentangle the exact spinorial nature (Majorana or Dirac, see subsubsection 1.4.2.2 and appendix A) of neutrinos until now. However their existence might be needed, depending on the exact neutrino nature, as suggested by the experiments which have proven that neutrinos can oscillate from one family to another and hence, own a non-vanishing mass.

The matter part of the SM Lagrangian can then be written:

$$\mathcal{L}_{Matter} = \sum_{m=1}^{3} \left(\overline{Q}^0_{mL} i \not{D} Q^0_{mL} + \overline{L}^0_{mL} i \not{D} L^0_{mL} + \overline{u}^0_{mR} i \not{D} u^0_{mR} + \overline{d}^0_{mR} i \not{D} d^0_{mR} + \overline{e}^0_{mR} i \not{D} e^0_{mR} + \overline{\nu}^0_{mR} i \not{D} \nu^0_{mR} \right) \tag{1.12}$$

Note that mass terms of the form $\mathcal{L}_{mass} = -m\overline{\Psi}\Psi$ are absolutely forbidden at this stage as these are equal to $\mathcal{L}_{mass} = -m\left(\overline{\Psi}_L \Psi_R + \overline{\Psi}_R \Psi_L\right)$ using the decomposition (1.8) and thus violate explicitly the $SU(2)_L$ invariance.

An important remark is that $\mathcal{L}_{matter}$ owns a $U(3)^6$ global flavor symmetry. For example, a global transformation of the form $U_{Q_L} \in U(3), Q_L \to U_{Q_L} Q_L$ leaves $\mathcal{L}_{Matter}$ invariant. As this symmetry is not imposed explicitly when constructing the theory, we call it an *accidental symmetry*. $\mathcal{L}_{Matter}$ contains all kinetic terms for the fermions but also fermion-gauge boson interactions as can be seen if we develop the gauge covariant derivative $\not{D} = D^\mu \gamma_\mu$ in the first term of (1.12):

$$\overline{Q}^0_{mL} i \not{D} Q^0_{mL} = i \left(\overline{u}^{0\alpha}_{mL} \overline{d}^{0\alpha}_{mL} \right) \gamma^\mu \times \left[\left(\partial_\mu I + i g_1 T^1_i W^i_\mu + \frac{i g_2}{3} T^2 B_\mu \right) \delta_{\alpha\beta} + i g_3 T^3_{\alpha\beta i} G^i_\mu I \right] \begin{pmatrix} u^0_{mL\beta} \\ d^0_{mL\beta} \end{pmatrix} . \tag{1.13}$$

Here I is the $SU(2)$ identity matrix and α, β are the color indices of the quarks. $T^1_{i=1..3}$ and $T^3_{i=1..8}$ are respectively the $SU(2)$ and $SU(3)$ generators which can be represented by Pauli and Gell-Mann

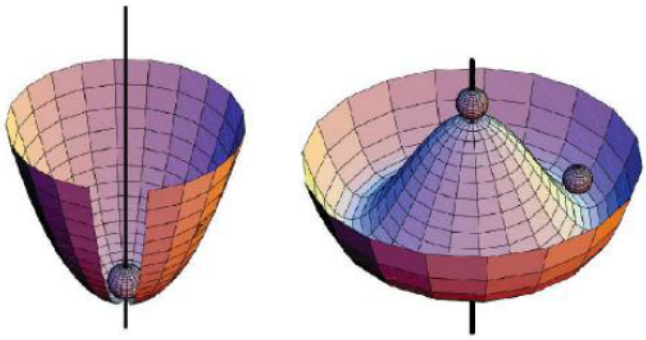

Figure 1.2 – Single complex scalar field case: The scalar potential V with, on the left $\mu^2 > 0$ and, on the right $\mu^2 < 0$. Taken from [19].

matrices. For a definition of the Pauli matrices, see appendix A. The unique $U(1)_Y$ generator is simply equal to $T^2 = I\frac{Y}{2}$. We use the usual Einstein convention which implies implicit sums over all repeated indices.

1.4.1 The Higgs mechanism

In this subsection, we give details on the above mentioned Higgs mechanism which generates dynamically mass terms for the gauge bosons and for the fermions through, respectively, the Higgs kinetic terms and the Yukawa interactions with the Higgs boson. The Higgs part of the SM Lagrangian $\mathcal{L}_{Higgs}$ is:

$$\mathcal{L}_{Higgs} = (D^\mu \Phi)^\dagger D_\mu \Phi - V(\Phi) \tag{1.14}$$

where Φ is composed of one electrically charged complex scalar ϕ^+ and one electrically neutral ϕ^0 forming an $SU(2)$ doublet $\Phi = \begin{pmatrix} \phi^+ \\ \phi^0 \end{pmatrix}$ transforming as $\{\mathbf{1}, \mathbf{2}, \frac{1}{2}\}_\phi$. The gauge derivative takes the form:

$$D^\mu \Phi = \left(\partial_\mu + igT_i^1 W_\mu^i + ig'T^2 B_\mu\right) \Phi \tag{1.15}$$

as the Higgs doublet is not charged under $SU(3)_C$. The simultaneous need for renormalizability and $SU(2) \times U(1)$ gauge invariance restricts the scalar potential V to the form:

$$V(\Phi) = +\mu^2 \Phi^\dagger \Phi + \lambda (\Phi^\dagger \Phi)^2 \tag{1.16}$$

with $\lambda > 0$ in order to enforce vacuum stability. The minimum of this potential will depend on the sign of μ^2 as depicted in figure 1.2 in the case of a single complex scalar field.

We see that in the case $\mu^2 > 0$, V presents a stable minimum at $\Phi = 0$ whereas for $\mu^2 < 0$ an all set of degenerate minima appears at a non-vanishing distance from the origin, all those minima being related by a $SO(2) \sim U(1)$ symmetry. The Higgs doublet can be rewritten in terms of 4 real fields $\{\phi\}_{i=1..4}$ as:

$$\Phi = \begin{pmatrix} \phi^+ \\ \phi^0 \end{pmatrix} = \begin{pmatrix} \frac{1}{\sqrt{2}}(\phi_1 + i\phi_2) \\ \frac{1}{\sqrt{2}}(\phi_3 + i\phi_4) \end{pmatrix} \tag{1.17}$$

and the scalar potential becomes:

$$V(\Phi) = \frac{1}{2}\mu^2 \left(\sum_{i=1}^{4} \phi_i^2\right) + \frac{1}{4}\lambda \left(\sum_{i=1}^{4} \phi_i^2\right)^2 \tag{1.18}$$

The spontaneous symmetry breaking of the electroweak phase is triggered when the neutral components $\{\phi_i\}_{\{i=3,4\}}$ fall in one of those degenerate minima which are related, in the case of a doublet, by a

$SO(4)$ symmetry. In a QFT context ϕ_i is said to take a non-vanishing vacuum expectation value (VEV) as it does not annihilate the vacuum $|0\rangle$ anymore, meaning $\langle 0|\phi_i|0\rangle \neq 0$. We can then use this $SO(4)$ symmetry to set all but one VEVs to zero $\langle 0|\phi_i|0\rangle = 0, i = 1,2,4$ and $\langle 0|\phi_3|0\rangle = \nu > 0$. With this in mind, the value at these minima of the scalar doublet Φ and of the potential V are:

$$\begin{aligned} \Phi \to \langle 0|\Phi|0\rangle \equiv v = \frac{1}{\sqrt{2}}\begin{pmatrix} 0 \\ \nu \end{pmatrix} \\ V(\Phi) \to V(v) = \frac{1}{2}\mu^2\nu^2 + \frac{1}{4}\lambda\nu^4 \end{aligned} \tag{1.19}$$

and the value of ν is obtained by minimizing the potential $V(\nu)$:

$$\nu = \sqrt{\frac{-\mu^2}{\lambda}} \tag{1.20}$$

Let us have a look at the action of the generators of $SU(2)_L \times U(1)_Y$ once the Higgs doublet has taken a VEV:

$$\begin{aligned} T_i^1 v = \frac{\tau_i}{2}\frac{1}{\sqrt{2}}\begin{pmatrix} 0 \\ \nu \end{pmatrix} \neq 0, \\ Yv = \frac{I}{2}\frac{1}{\sqrt{2}}\begin{pmatrix} 0 \\ \nu \end{pmatrix} \neq 0. \end{aligned} \tag{1.21}$$

We see that the action of the generators of $SU(2)_L \times U(1)_Y$ do not leave the vacuum invariant anymore. This means that the vacuum has got charged under these groups and the electroweak symmetry has indeed been spontaneously broken. However, a combination of these generators corresponding to the electric charge, $Q = (T_3^1 + \frac{Y}{2})$ (see (1.1)) remains intact since $Qv = 0$. This enforces the fact that the electric charge is conserved as it should be, and the following electroweak spontaneous symmetry breaking (EWSSB) pattern $SU(2)_L \times U(1)_Y \to U(1)_Q$ has been established. However, if a charged component of ϕ would have taken a VEV, this would not be true anymore and the $SU(2)_L \times U(1)_Y$ would have been broken to nothing. When spontaneously breaking a gauge symmetry, it is thus mandatory that only fields neutral under the symmetries we want to preserve in the low energy theory are allowed to take a non-vanishing VEV.

On the other hand, the complex scalar ϕ_3 is expected to oscillate around its minimum due to its quantum nature. We can thus shift it around v and write $\phi_3 = v + h^0$ with h^0 the physical neutral Higgs boson which has a vanishing VEV $\langle 0|h^0|0\rangle = 0$. Going back to the situation where Φ is not aligned on the real axis, a useful polar parametrization has been introduced by Kibble and can be written as:

$$\Phi = \frac{1}{\sqrt{2}} e^{\left(i\sum_{i=1}^{3}\zeta_i(x)L'^i\right)}\begin{pmatrix} 0 \\ v + h^0 \end{pmatrix} \tag{1.22}$$

with L'^i being the three electroweak broken generators $T_1^1, T_2^1, T_3^1 - Y$ and we have made the space-time dependence of $\zeta(x)_i$ explicit. Supposed that we were dealing with a global symmetry, the gauge parameters $\zeta(x)_i$ would then correspond to the so-called massless Goldstone bosons and there would be as many as broken generators, here 3. However, precisely due to the local nature of the gauge symmetry, we can eliminate these using the following gauge transformation:

$$\Phi \to \Phi = e^{\left(-i\sum_i \zeta_i L'^i\right)}\Phi = \frac{1}{\sqrt{2}}\begin{pmatrix} 0 \\ v + h^0 \end{pmatrix} \tag{1.23}$$

called the *unitary* gauge. From now on, unless otherwise stated, we will always work in the unitary gauge. With the disappearance of the Goldstone bosons, we seem to have lost physical degrees of freedom in our theory, however these will reemerge somewhere else as we will now see. Indeed, if we have a look at the Higgs kinetic term in eq (1.14) after EWSSB, it takes the form:

$$(D_\mu\Phi)^\dagger (D^\mu\Phi) = \frac{1}{2}\begin{pmatrix} 0 & \nu \end{pmatrix}\left[g_1 T_i^1 W_\mu^i + g_2 T^2 B_\mu\right]^2 \begin{pmatrix} 0 \\ \nu \end{pmatrix} + h^0 \text{ terms.} \tag{1.24}$$

d.o.f	Before EWSSB	After EWSSB
gauge bosons	8	11
Goldstone bosons	3	0
Higgs field	1	1

Figure 1.3 – The distribution of d.o.f among the fields before and after EWSSB. The Goldstone bosons have disappeared into the gauges bosons, these have been "eaten".

We can perform the following change of basis:

$$W^{\pm} = \frac{W^1 \mp iW^2}{\sqrt{2}}, \quad T^{1\pm} = T_1^1 \pm T_2^1 \tag{1.25}$$

to see that eq. (1.24) contains the terms:

$$\frac{g_1^2\nu^2}{4}W^{+\mu}W_{\mu}^{-} + \frac{1}{2}\left(g_1^2+g_2^2\right)\frac{\nu^2}{4}\left[\frac{g_1W_{\mu}^3 - g_2B_{\mu}}{\sqrt{g_1^2+g_2^2}}\right]^2 \equiv M_W^2W^{+\mu}W_{\mu}^{-} + \frac{M_Z^2}{2}Z^{\mu}Z_{\mu}, \tag{1.26}$$

and see that the charged gauge bosons $W^{\pm}$ have acquired a non-vanishing mass term $M_W = \frac{g_1\nu}{2}$. $W^{\pm}$ are the only physical states in the SM which allow at tree level to mediate the decay of a particle changing its flavor. As we will see in subsection 1.4.2, and as $W^{\pm}$ own an electric charge, such flavor transition is inevitably followed by a change of the electric charge of the decaying particle. For this reason, we say that the $W^{\pm}$ are the only mediators of flavor changing charged currents (FCCC) in the SM. A third neutral physical Z boson has also appeared with a mass term $M_Z = \frac{M_W}{\cos\theta_W}$. Z is defined as a linear combination of the B_{μ} and W_{μ}^3 bosons:

$$Z_{\mu} = \frac{g_1W_{\mu}^3 - g_2B_{\mu}}{\sqrt{g_1^2+g_2^2}} \equiv -\sin\theta_W B_{\mu} + \cos\theta_W W_{\mu}^3 \tag{1.27}$$

where we have defined the weak mixing angle θ_W as:

$$\tan\theta_W \equiv \frac{g_2}{g_1} \rightarrow \sin\theta_W = \frac{g_2}{g_Z}, \ \cos\theta_W = \frac{g_1}{g_Z}, \tag{1.28}$$

and $g_Z = \sqrt{g_1^2+g_2^2}$ the Z boson coupling constant. The combination orthogonal to Z can then be easily defined as $A = \cos\theta_W B + \sin\theta_W W^3$ and is identified as the photon. The photon remains massless at all order in perturbation theory as its associated gauge group $U(1)_Q$ is left unbroken by the EWSSB. As stated above, it seems that physical degrees of freedom have disappeared during the EWSSB when absorbing the Goldstone bosons using the unitary gauge. Let us have a closer look and count the number of degrees of freedom (d.o.f.) before and after EWSSB. Before EWSSB, we had 4 massless vectors bosons associated with the $SU(2)_L \times U(1)_Y$ gauge group. As it is very well known, massless vectors bosons only have two d.o.f. corresponding to two transverse polarizations. The electroweak bosons hence bring a total of $4 \times 2 = 8$ d.o.f. to the theory.

On the other hand, there are three massless Goldstone real bosons corresponding to the three broken generators and one massless Higgs boson. All these four fields own only one d.o.f. each. The total number of d.o.f. before EWSSB is hence $8 + 3 + 1 = 12$. After EWSSB, the now massive three eletroweak gauge bosons W^+, W^-, Z have 3 degrees of freedom each corresponding to two transverse and one longitudinal polarization states. We also have a massless vector photon A with two d.o.f. and one massive real scalar h with one d.o.f. The total number of d.o.f. after EWSSB is also 12, however we see that the d.o.f. which have disappeared when absorbing the three Goldstone bosons have reappeared in the now massive gauge bosons as transverse polarizations. The accepted expression to designate this re-balancing is that the Goldstone bosons have been "eaten" by the massive gauge bosons. Table 1.3 summarizes the distribution of d.o.f. among the fields before and after EWSSB.

1.4.2 The Yukawa sector

As stated above, the fermions of the SM can be split into two groups, the quarks and the leptons, depending on their sensitivity to the strong interaction. To match experimental observations, each group has to be duplicated three times into three copies named family or generation. In this subsection, we have a closer look at the Yukawa sector $\mathcal{L}_{Yukawa}$ of $\mathcal{L}_{SM}$. The Yukawa sector allows to generate masses for the three families of leptons and quarks through coupling to the Higgs boson. Although the Yukawa sector is discussed in its full generality, we postpone comments on the experimental values of the mass spectrum to subsection 1.6.4.

1.4.2.1 Quarks

We start with the quarks. They are six types (or flavors) of quarks in the SM which exist in three different colors each. As seen in section 1.4, each family is composed of one quark of electric charge $\frac{2}{3}e$ and of one quark of electric charge $-\frac{1}{3}e$. Their left-handed (resp: right-handed) components forming $SU(2)$ doublets (resp: singlets). The lightest family of quarks constitutes the components of the proton and the neutron which form the atomic nucleus. For this reason, the quarks of the first family are simply named up "u" and down "d" quarks. The four heavier flavors are named for historical reasons strange "s", charm "c", bottom "b" and top "t" quarks. These can only be produced in higher energy processes for example when a proton of cosmic rays hits the high atmosphere or when two protons collide in a hadron collider. Indeed, a very specific feature of "QCD" named "confinement" makes that quarks can never be seen as free states and can only be detected as bound states called hadrons themselves colorless. The down-type strange and the up-type charm quarks form the second family of the SM. Finally, the down-type bottom and the up-type top quarks form the third and heavier family of the SM. The quarks Yukawa sector can be written as:

$$-\mathcal{L}_{Yukawa}^{quarks} = y^u_{m,n}\overline{Q}^0_{mL}\widetilde{\Phi}u^0_{nR} + y^d_{m,n}\overline{Q}^0_{mL}\Phi d^0_{nR} + \text{h.c.} \tag{1.29}$$

with $\widetilde{\Phi} = i\sigma_2\Phi^\dagger$, the conjugate Higgs field transforming as $\{\mathbf{1},\mathbf{2},-\frac{1}{2}\}_{\widetilde{\Phi}}$ needed to write invariant terms of the form $\overline{Q}^0_{mL}\Phi u^0_{nR} + h.c$ in the up-sector [6]. y^u, y^d are 3×3 arbitrary Yukawa matrices determining the strength of the coupling to the Higgs boson. The Yukawa matrices are completely arbitrary and do not have to be Hermitian, real nor diagonal. They introduce most of the SM free parameters and break most of the $U(3)^6$ family symmetries of the rest of $\mathcal{L}_{matter}$, only two global $U(1)$ symmetries, the total baryon and lepton numbers are accidentally conserved. After EWSSB, $\mathcal{L}_{Yukawa}^{quarks}$ becomes:

$$-\mathcal{L}_{Yukawa}^{quarks} = \overline{u}^0_{mL}y^u_{mn}\left(\frac{\nu+h^0}{\sqrt{2}}\right)u^0_{nR} + \overline{d}^0_{mL}y^d_{mn}\left(\frac{\nu+h^0}{\sqrt{2}}\right)d^0_{nR} + h.c \tag{1.30}$$

where Dirac mass terms have been generated for the up and down quarks:

$$M^u_{mn} = y^u_{mn}\frac{\nu}{\sqrt{2}},\ M^d_{mn} = y^d_{mn}\frac{\nu}{\sqrt{2}} \tag{1.31}$$

In order to identify the physical states, those which will actually propagate, it is still needed to perform a change of basis to bring the mass matrices to diagonal forms. As the left and right handed components of the fields transform independently, we have to perform separate transformations on them. Since the electroweak symmetry is now broken, we also need to perform independent transformations on the up and down components, e.g.:

$$u^0_L = V_{u_L}u_L,\quad u^0_R = V_{u_R}u_R,\quad d^0_L = V_{d_L}d_L,\quad d^0_R = V_{d_R}d_R, \tag{1.32}$$

where we have switched to indice free notations and simply note $u = (u,c,t)^T$, $d = (d,s,b)^T$. We emphasize that all the matrices in eq. (1.32) must be unitary in order to preserve the canonical form

[6] Let us be explicit, if we consider the hypercharge we have $Y\left(\overline{Q}_L\right) = -\frac{1}{3}$ and $Y\left(u_R\right) = \frac{4}{3}$ or we have to impose $Y\left(\overline{Q}_L\Phi u_R\right) = 0 \to Y\left(\widetilde{\Phi}\right) = -\frac{1}{2}$.

of the kinetic terms into $\mathcal{L}_{matter}$. This change of basis rotates the mass matrices to diagonal form, e.g.:

$$\begin{aligned} V_{u_L}^{\dagger} M^u V_{u_R} &\equiv M_D^u = diag(m_u, m_c, m_t) \\ V_{d_L}^{\dagger} M^d V_{d_R} &\equiv M_D^d = diag(m_d, m_s, m_b). \end{aligned} \tag{1.33}$$

with m_f the real and positive physical mass of the fermion f. For this reason the states Ψ, without the superscript 0, are called the mass eigenstates of the theory. Now that we have switched to the mass basis, we still have to scrutinize the consequences of the change of basis (1.32) on the rest of the Lagrangian. The Higgs and gauge part remain invariant as they do not depend on the fermions fields. However, if we rewrite $\mathcal{L}_{Matter}$ in terms of the physical weak bosons $W^{\pm}$, one can show with a little bit of algebra that the following term is included in the SM Lagrangian:

$$\begin{aligned} \mathcal{L}_{SM} \ni & -\frac{g_1}{2\sqrt{2}} \left[\overline{u}^0 \gamma^\mu (1-\gamma_5) d^0\right] W_\mu^+ + h.c \\ = & -\frac{g_1}{2\sqrt{2}} \left[\overline{u}_m (V_{u_L}^{\dagger} V_{d_L} \gamma^\mu (1-\gamma_5))_{mn} d_n\right] W_\mu^+ + h.c \end{aligned} \tag{1.34}$$

where we have switched to the mass basis in the last line of eq. (1.34). We see that this term induces charged flavor transitions between the up and down sectors through coupling to the W bosons. Furthermore, if the up and down quarks are not aligned in flavor space, that is if $V_{u_L} \neq V_{d_L}$, the coupling of these transitions is set by the unitary matrix $V_{CKM} = V_{u_L}^{\dagger} V_{d_L}$ called the Cabibbo-Kobayashi-Maskawa (CKM) matrix (see [20]) and section 1.5.

1.4.2.2 Leptons

We now discuss briefly the leptonic Yukawa sector. As stated in section 1.4, the three families of leptons in the SM can be split in two groups according to their electric charges. Charged leptons e_m^- own an electric charge equal to $-e$ whereas neutrinos are electrically neutral. Left-handed components of charged leptons are fold in the down-part of $SU(2)$ doublets ($T_3^1(e_{Lm}^-) = -\frac{1}{2}$) whereas left handed components of neutrinos are fold in the up-part of $SU(2)$ doublets ($T_3^1(\nu_{Lm}) = +\frac{1}{2}$), their right-handed components being again $SU(2)$ singlets. The lightest charged lepton belonging to the first leptonic family is simply the usual electron noted e^-, the mediator of chemical reactions. The second lepton is named the muon and noted μ^-. The muon has as particularity that it is able to travel on long distances due to its long proper lifetime of $\tau(\mu^-) = 2.2\mu s$. Opposite to that, the third lepton, the tauon noted τ^- has a much smaller lifetime of $\tau(\tau^-) = 2.9 \times 10^{-1}$ps and thus decays much more quickly. On the other hand, the neutrinos are named after their charged leptons $SU(2)$ counterparts. Hence the three neutrinos are the electronic, muonic and tauic neutrinos, noted respectively ν_e, ν_μ and ν_τ. The leptonic Yukawa Lagrangian is then:

$$\mathcal{L}_{Yukawa}^{leptons} = y^e \overline{L}_L^0 \Phi e_R^0 + y^\nu \overline{L}_L^0 \widetilde{\Phi} \nu_{nR}^0 + h.c. \tag{1.35}$$

where we have define the following vectors in flavor space $e^0 = (e^0, \mu^0, \tau^0)^T$, $\nu^0 = (\nu_e^0, \nu_\mu^0, \nu_\tau^0)^T$. As in the quark sector, $\mathcal{L}_{Yukawa}^{leptons}$ generates Dirac mass terms for the leptons and the neutrinos once the neutral component of Φ has taken a VEV ν:

$$M^e = y^e \frac{\nu}{\sqrt{2}}, \; M^\nu = y^\nu \frac{\nu}{\sqrt{2}} \tag{1.36}$$

One can then perform unitary rotations on the fields to bring the mass matrices to diagonal form:

$$V_L^{e\dagger} M^e V_R^e \equiv M_D^e = diag(m_e, m_\mu, m_\tau) \quad V_L^{\nu\dagger} M^\nu V_R^\nu \equiv M_D^\nu = diag(m_{\nu_1}, m_{\nu_2}, m_{\nu_3}) \tag{1.37}$$

which define the mass eigenstate basis for the charged leptons $e_{L,R}^0 = V_{L,R}^e e_{L,R}$ and for the neutrinos $\nu_{L,R}^0 = V_{L,R}^\nu (\nu_1, \nu_2, \nu_3)_{L,R}^T$. We have labeled the three neutrino mass eigenstates ν_1, ν_2 and ν_3 because, opposite to the quark case, the mixing in the leptonic sector is significantly higher, each mass eigenstate ν_1, ν_2 and ν_3 being truly a superposition of all three weak eigenstates ν_e, ν_μ and ν_τ. This change of basis will in turn induce charged flavor violating transitions as in (1.34) whose coupling is set by the

mismatch in the rotations of the left-handed leptons and neutrinos. This mismatch is parameterized by the unitary Pontecorvo-Maki-Nakagawa-Sakata (PMNS) matrix $V_{PMNS} = V_L^{\nu\dagger} V_L^e$ (see [21]). Note that the PMNS matrix is different from unity only in the case where mass terms for the neutrinos are present. Indeed, if no neutrinos mass terms are present in the Lagrangian one can adjust V_L^ν freely and set $V_L^\nu = V_L^e \rightarrow V_{PMNS} = \mathbb{1}$.

A caveat on neutrino masses: In this paragraph, we want to point out that the approach we have considered until here -with neutrino Dirac mass terms generated via the Higgs mechanism-, although having the virtue of symmetrizing the quarks and leptonic sectors ask serious naturalness problems. Indeed, the masses of the neutrinos being extremely small ($\sum_{i=1,2,3} m_i < 0.49$ eV @ 95 CL from cosmology [22]), Dirac mass terms would imply extremely high fine tuning of the Yukawa couplings. However, it is possible to construct models beyond the SM in which these tiny neutrinos masses arise naturally thanks to the presence of one or several heavy right-handed sterile neutrinos N_R. To this end, neutrinos need to be viewed as Majoranas particles. A 4-components Majorana spinor Ψ^M is a field in which the left-handed component is the charge conjugate of the right handed one i.e. $\Psi^M_{L,R} = C(\overline{\Psi}^M_{R,L})^T$. This imply that a Majorana particle should be its own anti-particle i.e. $\nu = \nu^c = C\overline{\nu}^T$ and should not carry any conserved quantum numbers. Or, this is indeed the case of the neutrinos in the SM. Several experiments are trying to disentangle the Dirac/Majorana nature of the neutrino by seeking, for example, for neutrinoless double beta decays $0\nu\beta\beta$ in which a neutrino annihilates with its antineutrino to nothing (see [23] for a review). In these so-called "seesaw" mechanisms small neutrinos masses are then generated when integrating out right-handed neutrinos N_R. This results in non-renormalizable, dimension five operators of the form:

$$\delta\mathcal{L}^M_{mass} = \frac{1}{2}\frac{gv^2}{\Lambda}\nu_L^T C^\dagger \nu_L + h.c \tag{1.38}$$

where Λ is the cut-off of the effective operator $\Lambda \sim M_{N_R}$ which suppress the light neutrinos masses.

However, as this thesis is focusing on the hadronic sector, these questions will not be further investigated and we refer to references [4], [24] for a tour of seesaw models.

1.5 A focus on the CKM matrix

As stated in subsubsection 1.4.2.1, the CKM matrix arises from a mismatch between the fermion gauge and Yukawa interactions i.e. between the weak and mass eigenstates basis. Furthermore, after EWSSB, a mismatch appears between the up and down sector and the CKM can be seen as the composition of the rotations in these two sectors i.e. $V_{CKM} = V_{u_L}^\dagger V_{d_L}$, only left-handed components being involved due to the chiral nature of the electroweak theory. It is thus a unitary 3 by 3 complex matrix which sets the strength of FCCC processes in the SM. In this section, we want to give more details on the CKM matrix as it plays a prominent role for flavor physics in the SM and beyond. Let us start by counting the number of d.o.f. in V_{CKM}. A general $F \times F$ complex matrix has $2F^2$ independents parameters. Out of those $2F^2$ parameters, one can subtract F^2 parameters due to unitary conditions $(V_{CKM}^\dagger V_{CKM})_{mn} = \delta_{mn}$. We can further remove $2F-1$ parameters thanks to a redefinition of phases on the up and down quarks. These are of the type $u_L \rightarrow K_{u_L} u_L$ with $K_{u_L} = diag\left(e^{i\phi_1}, e^{i\phi_2}, e^{i\phi_3}\right)$. We are thus left with $F^2 - (2F-1) = (F-1)^2 \overset{F=3}{\longrightarrow} 4$ independent real parameters in the CKM matrix. These 4 real parameters can be further split in 3 mixing angles θ_{ij} and 1 CP violating phase δ_{CKM}. There are many ways to parameterize the CKM matrix but here we follow the one given by the Particle Data Group [25]:

$$\begin{aligned} V_{CKM} \equiv \begin{pmatrix} V_{ud} & V_{us} & V_{ub} \\ V_{cd} & V_{cs} & V_{cb} \\ V_{td} & V_{ts} & V_{tb} \end{pmatrix} &= \begin{pmatrix} 1 & 0 & 0 \\ 0 & c_{23} & s_{23} \\ 0 & -s_{12} & c_{23} \end{pmatrix} \begin{pmatrix} c_{13} & 0 & s_{13}e^{-i\delta} \\ 0 & 1 & 0 \\ -s_{13}e^{i\delta} & 0 & c_{13} \end{pmatrix} \begin{pmatrix} c_{12} & s_{12} & 0 \\ -s_{12} & c_{12} & 0 \\ 0 & 0 & 1 \end{pmatrix} \\ &= \begin{pmatrix} c_{12}c_{13} & s_{12}c_{13} & s_{13}e^{-i\delta} \\ -s_{12}c_{23} - c_{12}s_{23}s_{13}e^{i\delta} & c_{12}c_{23} - s_{12}s_{23}s_{13}e^{i\delta} & s_{23}c_{13} \\ s_{12}s_{23} - c_{12}c_{23}s_{13}e^{i\delta} & -c_{12}s_{23} - s_{12}c_{23} - s_{12}c_{23}s_{13}e^{i\delta} & c_{23}s_{13} \end{pmatrix} \end{aligned} \tag{1.39}$$

with $c_{ij} = \cos(\theta_{ij})$ and $s_{ij} = \sin(\theta_{ij})$. The magnitude of the elements of the CKM matrix have been measured through processes involving different flavor transitions and are equal to:

$$|V_{ij}| = \begin{pmatrix} 0.9742 & 0.226 & 0.0036 \\ 0.226 & 0.973 & 0.042 \\ 0.0087 & 0.041 & 0.9991 \end{pmatrix} \tag{1.40}$$

which implies $s_{12} \sim 0.23$, while $s_{13} << s_{23} << s_{12}$. The important point to notice is that the elements modulus decrease of one order of magnitude each time we take one step away from the diagonal. This suggests to use 4 parameters $\lambda, A, \overline{\rho}, \overline{\eta}$ defined as:

$$\begin{aligned} s_{12} = \lambda = \frac{|V_{us}|}{\sqrt{|V_{ud}|^2 + |V_{us}|^2}},\ s_{23} = A\lambda^2 = \lambda \left|\frac{V_{cb}}{V_{us}}\right|, \\ s_{13}e^{i\delta} = V_{ub}^* = A\lambda^3 (\overline{\rho} + i\overline{\eta}) = \frac{A\lambda^3(\overline{\rho} + i\overline{\eta})\sqrt{1 - A^2\lambda^4}}{\sqrt{1-\lambda^2}\left[1 - A^2\lambda^4(\overline{\rho} + i\overline{\eta})\right]} \end{aligned} \tag{1.41}$$

to write an expansion of V_{CKM}, using λ as expansion parameter. Following this procedure, a parameterization has been proposed by Wolfenstein [26], and we end up with, at $O(\lambda^3)$:

$$V_{CKM} = \begin{pmatrix} 1 - \frac{\lambda^2}{2} & \lambda & A\lambda^3(\rho - i\eta) \\ -\lambda & 1 - \frac{\lambda^2}{2} & A\lambda^2 \\ A\lambda^3(1 - \rho - i\eta) & -A\lambda^2 & 1 \end{pmatrix} + O(\lambda^4) \tag{1.42}$$

Moreover, we can safely check that V_{CKM} stays unitary at all orders in the Wolfenstein expansion, the CP violation phase δ_{CKM} being associated with η through $\tan\delta = \frac{\eta}{\rho}$. There are various possible conventions for defining the CP phase in V_{CKM} however, $\overline{\rho} + i\overline{\eta} \equiv -\frac{V_{ub}^* V_{ud}}{V_{cb}^* V_{cd}}$ is phase-convention-independent.

It is especially important for phenomenology to get accurate measures of the elements of V_{CKM} and to test its features, especially its unitarity. In particular, we want to check if sums of the type $\sum_j V_{ij}V_{kj}^*$ really vanish for $i \neq k$. Using the Wolfenstein parameterization, these relations take for example the form:

$$\begin{aligned} \left(V^\dagger V\right)_{31} &= V_{ub}^* V_{ud} + V_{cb}^* V_{cd} + V_{tb}^* V_{td} \\ &\sim \left(1 - \frac{\lambda^2}{2}\right) A\lambda^3 (\rho + i + \eta) - A\lambda^3 + A\lambda^3(1 - \rho - i\eta) \\ &\sim A\lambda^3(\overline{\rho} + i\overline{\eta}) - A\lambda^3 + A\lambda^3(1 - \overline{\rho} - i\overline{\eta}) = 0 \end{aligned} \tag{1.43}$$

but, $|V_{cb}^* V_{cd}| \sim A\lambda^3$ is known with great accuracy, so that it can be used to normalized eq. (1.43):

$$\frac{\left(V^\dagger V\right)_{31}}{A\lambda^3} \sim \overline{\rho} + i\overline{\eta} - 1 + 1 - \overline{\rho} - i\overline{\eta} \tag{1.44}$$

and eq. (1.44) can be represented by a normalized triangle in the complex plane $(\overline{\rho}, \overline{\eta})$ with the vertices at $(0,0)$; $(1,0)$ and $(\overline{\rho}, \overline{\eta})$. One can then apply different constraints from flavor observables to fit the Wolfenstein parameters and to check if the sum of the angles are really equal to 180° i.e to check that unitarity is indeed satisfied. For example, the length of the triangles can be obtained from CP conserving observables, as in the $b \to u$ decay rate whereas the angles are obtained from CP violating effects such as neutral mesons mixing. Figure 1.4 presents a global fit on the triangle (1.43) with all available flavor constraints included here @ 95% C.L. The red hashed blob indicates the best fit values of $\overline{\rho}$ and $\overline{\eta}$ at 68% C.L. The best fit values of the Wolfenstein parameters are thus:

$$\begin{aligned} A = 0.810^{+0.018}_{-0.024} \quad \lambda = 0.22548^{+0.00068}_{-0.00034} \\ \overline{\rho} = 0.1453^{+0.0133}_{-0.0073} \quad \overline{\eta} = 0.343^{+0.011}_{-0.012} \end{aligned} \tag{1.45}$$

We see on fig. 1.4 that all flavor observables are compatible with the SM CKM mechanism i.e. no significant departure from unitarity is observed until now.

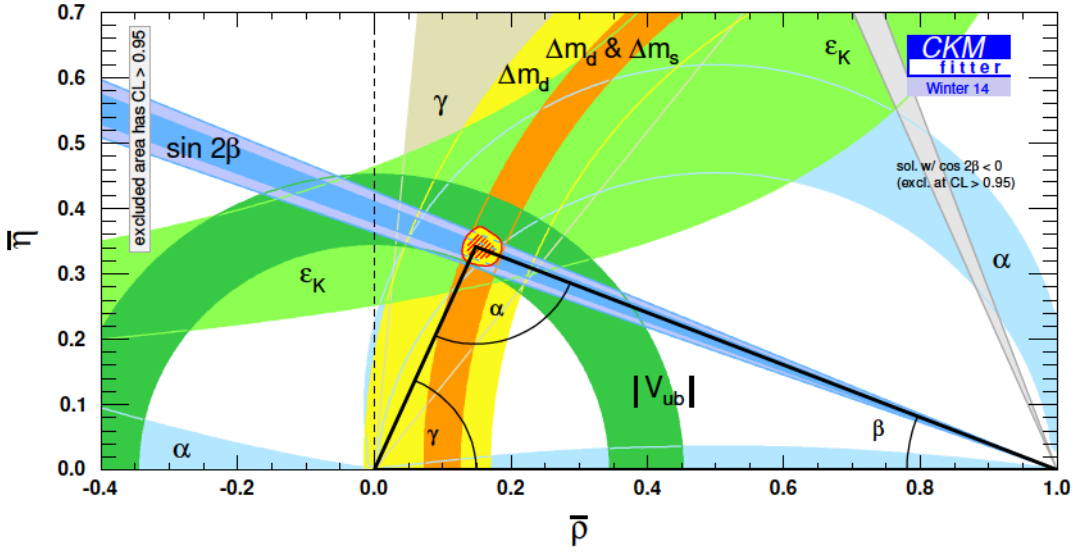

Figure 1.4 – Unitarity triangle test. All flavor observables are given at 95% C.L. The red hashed region represents the 68% C.L fitted value of the Wolfenstein parameters $\overline{\rho}$ and $\overline{\eta}$. Plot taken from the CKM fitter group [27], http://CKMfitter.in2p3.fr

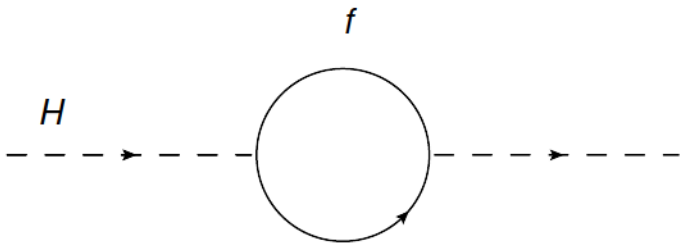

Figure 1.5 – Quantum corrections to the Higgs mass due to a Dirac fermion.

1.6 Limitations and open questions

There is much more to say about the SM, however for the sake of concision, we stop here and move on by giving some details on a few of the reasons that push the high energy physics community to think that despite all its virtues, the SM cannot be an ultimate theory of nature, if any such ultimate theory does exist at all.

1.6.1 The hierarchy problem

We start with the famous "gauge hierarchy problem". Beyond its formal presentation on which we will shed light below, it is of crucial importance to understand what the gauge hierarchy problem really is about. As stated in the introduction, the SM does not address the question of the quantification of gravity. The quantum effects of gravity should become relevant at most at a scale of the order of the Planck mass $M_P = \sqrt{\frac{\hbar c}{G_N}} \sim O(10^{19})$GeV. One can say that the Planck mass is the "natural" scale associated to gravity. If one wants to pick a natural scale for the SM, a good choice might be the vacuum expectation value $\nu \sim 246$ GeV which drives the spontaneous breaking of the electroweak symmetry. In its very essence, the gauge hierarchy problem consists in understanding why the electroweak scale is 17 orders of magnitudes below the Planck scale. Stated differently, since $M_P \propto \frac{1}{\sqrt{G_N}}$, it is equivalent to ask the question of the -apparent- weakness of the gravity interaction compared to the other interactions of the Standard Model.

More formally, the gauge hierarchy problem arises because the mass of the Higgs boson h receives radiative corrections which are driven naturally to huge values from all particles it coupled. Indeed, in the current state-of-the-art, the mass of the Higgs boson, as all masses in Quantum Field Theory, is computed perturbatively. That means the physical Higgs mass m_h^2 is given by $m_h^2 = m_{h^0}^2 + \sum_i (\Delta m_h^2)_i$ where the successive corrections $(\Delta m_h^2)_i$ have to decrease rapidly for the series to converge. Now, if we consider a Dirac fermion f which couples to the Higgs boson through a Yukawa interaction $-\lambda_f h f \overline{f}$, we can show via the diagram 1.5 that the first terms of this perturbative series are given by:

$$m_h^2 = m_{h^0}^2 - \frac{|\lambda_f|^2}{8\pi^2}\left[\Lambda_{UV}^2 + A m_f^2 \ln\left(\frac{m_f^2}{\Lambda_{UV}^2}\right)\right] \tag{1.46}$$

where A is an irrelevant dimensionless constant, Λ_{UV} the cutoff used to regularized the theory and $m_{h^0}^2$ is the "bare" mass. Λ_{UV} has to be seen as the energy scale at which the SM, seen as an effective field theory, breaks down. We see that we have naturally $\Lambda_{UV} \sim M_P$ if the SM is believed to be valid all the way up to the Planck scale. Indeed, we know that at this scale, the quantum effects of gravity become non negligible and the SM has to break down. Having $\Lambda_{UV} \sim M_P$ asks however serious naturalness problems as we know now that the physical Higgs mass is $m_h \approx 125$ GeV. However, for the physical mass m_h^2 to be of that order, we need the bare mass $m_{h^0}^2$ to cancel out the quadratic divergences $\propto \Lambda_{UV}^2$ at an incredible level of accuracy (see eq. (1.46)). An important point to notice is that this problem arises because scalar masses are not "protected" by any kind of symmetries in the SM. A mass is said to be protected by a symmetry if, in the limit where it vanishes, a symmetry is restored in the theory. In this case, just with dimensional analysis, one can show that no quadratic terms are allowed in the perturbative series, all terms being roughly of the form $m_0^2 \ln\left(\frac{\Lambda_{UV}^2}{m_0^2}\right)$ ensuring smoother divergences and guaranteeing that no accurate cancellations happened between the successive parameters of the series. This is exactly what occurs when a fermion mass is computed as in the limit $m_f \to 0$, the chiral symmetry is restored and the femions masses are protected from dangerous quadratic divergences. On the other hand, no symmetry protecting the Higgs mass, the nature has to pick couplings in the perturbative series which are very fine-tuned, any deviations from those high tuned couplings resulting in the mass to blow up. This kind of extremely accurate cancellation seems highly unnatural, unless a more fundamental theory of nature is at work, to explain that those couplings look tuned in the low energy effective theory as it will become clear later in this work. Finally, we conclude this section by pointed out that the gauge hierarchy problem is not really a problem if, despite highly unlikely, the SM is an ultimate theory of nature. In this case, $\Lambda_{UV} \to \infty$ and the SM being a renormalizable theory, all divergences can be exactly absorbed in counter-terms in eq. (1.46). Hence, the gauge hierarchy

problem is not an intrinsic problem of the SM but is rather the problem of the tuning of the SM with respect to a would-be BSM theory.

1.6.2 The cosmological connexion

We know today that most of the matter in the Universe (about 86%) escapes direct detection and interact very weakly with the fields of the SM. Maybe, one of the main evidence of this fact can be found in galaxy rotation curves. According to General Relativity (GR), the angular velocity of stars should decrease with the distance to the Galaxy core. But, observations have confirmed that this curve is approximately flat, the stars close to the core having roughly the same angular velocity that the ones at the edge of the Galaxy. The second evidence comes from gravitational lensing effects where light beams seem to be deflected without the presence of any apparent mass in the way. The more economical solution to these problems, if GR is to be preserved, is to introduce a new kind of matter which however has to interact very weakly with the ordinary matter. In particular, the constituents of this "dark" matter must does not own any electric nor color charges. These also have to be quite heavy and relatively stable to fit observational data. The Standard Model fails to introduce such kind of Weakly Interactive Massive Particles (WIMPs) in its spectrum and thus naturally call for an extension able to address this problem.

1.6.3 Unification of gauge couplings

An other interesting puzzle is the unification of the three gauge interactions in the SM. In perturbative QFT, all couplings being computed at finite order, they depend on an arbitrary energy scale Q. It is convenient for increasing the convergence of the series to fix this arbitrary scale at the typical energy at which the theory is probed. For instance, Q is fixed at the center of mass energy in the case where a coupling is measured via collisions. The evolution of a coupling with this energy scale can be obtained by computing the Renoramlization Group Equations (RGEs) of the theory (see [5]). The RGEs of a quantum field theory mainly depend on its gauge structure and particle spectrum. When solving the RGEs of a gauge coupling g_i, it is conventional to square it as appearing in the vertices of Feynman diagrams, i.e. to define $\alpha_i \equiv \frac{g_i^2}{4\pi}$. The dash-lines on Figure 2.1 present the evolution of the three SM α_i's with the energy scale Q. They seem to become of the same order of magnitude at a scale $Q_{GUT} = 10^{14-16}$ GeV. This suggest that in a more fundamental theory, this unification might be exact and the SM gauge group G_{SM} can be embed in a larger group G_{GUT}, where all gauge interactions get unified into a unique coupling constant at Q_{GUT}. Furthermore, doing so would reduce drastically the number of free parameters in the SM, thus increasing its predictability. However, such Grand Unified Theory would lead to serious phenomenological issues. For example, it generically predicts the decay of the proton. One has then to construct mechanisms that push the proton lifetime high enough, at values of the order of the lifetime of the Universe, to match the still non observation of proton decays (see [28, 29]). However, embedding a GUT in a supersymmetric framework helps. Such Supersymmetric Grand Unified theories (SUSY/GUT) have been an extensive area of research in the last decades. Several candidates have been proposed for a Grand Unified Group among which $SU(5)$ (see for instance the article of S. Raby in the PDG report [25]), $SO(10)$ [30] or $E(6)$ [31]. Currently, there is no consensus, even though some candidates seem more appealing. For instance, $SO(10)$ is able to include in its minimal model right-handed neutrinos. $SO(10)$ GUTs are thus able to explain quite easily neutrinos oscillations whereas $SU(5)$ fails to do so in a minimal way.

1.6.4 The flavor puzzle

Table 1.6 summarizes the mass spectrum and mixing parameters in the Standard Model. We also gave the mixing parameters in the neutrino sector assuming normal ordering between the neutrinos mass eigenstates i.e. $\Delta m^2_{31} = m^2_{\nu_3} - m^2_{\nu_1} > 0$. Several observations can be made when looking at these values. First of all, the fermion spectrum is highly hierarchical. The fermion masses span 6 orders of magnitude from the electron mass $m_e \sim 5.11 \times 10^{-1}$ MeV up to the top quark mass $m_\tau \sim 1.73 \times 10^5$ MeV. This seems quite weird that nature has chosen masses that are so different, and most certainly

Quarks		
Mass Spectrum		
m_u	m_c	m_t
$2.3^{+0.7}_{-0.5}$	$(1.275 \pm 0.025) \times 10^3$	$(173.21 \pm 0.51 \pm 0.71) \times 10^3$
m_d	m_s	m_b
$4.8^{+0.5}_{-0.3}$	95 ± 5	$(4.18 \pm 0.03) \times 10^3$
Mixing parameters		
θ_{12}^{CKM}	θ_{13}^{CKM}	θ_{23}^{CKM}
$0.2257^{+0.0009}_{-0.0010}$	$0.00359^{+0.00020}_{-0.00019}$	$0.0415^{+0.0011}_{-0.0012}$
δ^{CKM}		
$1.2023^{+0.0786}_{-0.0431}$		
Leptons		
Mass Spectrum		
m_e	m_μ	m_τ
0.511	105.66	1776.82 ± 0.16
Mixing parameters		
θ_{12}^{PMNS}	θ_{13}^{PMNS}	θ_{23}^{PMNS}
$33.48^{+0.78}_{-0.75}$	$8.50^{+0.20}_{-0.21}$	$42.3^{+3.0}_{-1.6}$
δ^{PMNS}		
306^{+39}_{-70}		

Figure 1.6 – Mass spectrum and mixing parameters in the SM. All masses are given in MeV. The fermion masses and CKM parameters are extracted from [25]. The quarks masses are given in the $\overline{\text{MS}}$ scheme, except for the top mass given in an on-shell scheme. The leptons masses are given in an on-shell scheme. The PMNS parameters are extracted from [34] and assume normal ordering among the neutrinos mass eigenstates.

an underlying dynamic involving new degrees of freedom must be at work to generate dynamically this spectrum. The fact that the fermions are gathered in only three families (why not four?) is also intriguing, no accepted explanation being available for now. Lastly, mixing angles in the quark sector are clearly smaller than in the neutrinos sector and we don't know why either. All these questions are collectively known as the "flavor puzzle". Several paths have been explored during the last decades to address this puzzle. For example, it has been proposed that discrete family symmetries could be at work in the leptonic sector (see [32]). Continuous flavor symmetries could be also relevant, for instance $SU(3)$ ([33]). These $SU(3)$ flavor models allow to address the question of the number of families as it is treated on the same foot as the number of color in QCD. In any case, the flavor puzzle of the SM raises very interesting questions and has provided a lot of literature over the last years even though no accepted explanation has emerged until now, largely due to the lack of experimental evidence for new physics in the flavor sector. Still, it is our belief that such peculiar patterns could not be left without explanation and that any serious BSM theory will have to face this puzzle to prove its value.

Chapter 2

A possible way out: Supersymmetry and the MSSM

After having described the Standard Model in chapter 1, we want to give details on a proposal which is trying to bring answers to the questions raised in section 1.6, namely Supersymmetry (SUSY). Supersymmetry constitutes one of the main proposal to complete the SM. It postulates the existence of a new symmetry relating bosons and fermions, each fermion of the SM being related to a bosonic "superpartner" and vice-versa. One important remark is that if SUSY is realized in nature, it has to be a broken symmetry to match the so-far non-observation of superpartners. SUSY has been extensively studied since the mid-70s and a wide literature exists on the topic that we will not have the time to start to summarize. This chapter is organized as follows. In section 2.1, we start by presenting the motivations which make SUSY a promising BSM. In section 2.2, we present the supersymmetric algebra and in section 2.3, we give some elements on superspaces and superfields which are needed for the rest of this chapter. Section 2.4 contains a general presentation of mechanisms used to break SUSY. Finally, section 2.5 is devoted to a presentation of the minimal supersymmetric model compatible with the SM, the Minimal Supersymmetric Standard Model (MSSM).

2.1 Motivations.

The first and historical reason for introducing SUSY is that it provides an extension of the Poincaré group $R^{1,3} \rtimes SO(1,3)$ in a very specific way. In 1967, S. Coleman and J. Mandula have derived a no-go theorem [1] on the impossibility of extending the spacetime symmetries beyond the Poincaré group. In its original form [35], it states that:

If (1) *the S matrix is based on a local, relativistic quantum field theory in four dimensional space-time,* (2) *there are only a finite number of different particles states associated with one-particle state of a given mass,* (3) *and there is an energy gap between the vacuum and the one particle state, then the most general Lie algebra of symmetries of the S matrix contains the Poincaré algebra and a finite number of Lorentz scalar operators that must belong to the Lie algebra of a compact Lie subgroup.*

Saying differently, this theorem states that the most general symmetry group of a QFT in four dimensions is a direct product of the Poincaré group and a compact Lie group which describes the internal symmetries of the theory. It means that, if we try to extend the spacetime symmetries above the Poincaré group we over-constrain spacetime resulting in vanishing S-matrix elements. However this theorem was derived under the specific assumption that the generators form a Lie algebra i.e. they obey to commutation relations and have a bosonic nature. R. Haag, J. Lopuszanski and M. Sohnius have shown [36] that it is possible to circumvent this theorem if one extends the Poincaré group with fermionic generators obeying anti-commutation relations. The extended spacetime algebra is called the Super-Poincaré algebra and the transformations associated are referred to as supersymmetric.

[1] Generically, a no-go theorem proves the impossibility of a result in physics.

Furthermore, one can show that the Super-Poincaré algebra (see sec. 2.2) provides the unique non-trivial extension of the Poincaré algebra assuming a single spinorial generator Q. Then, for a 4D-QFT, if one wants to extend the spacetime symmetries above the Poincaré group these have to be of supersymmetric nature.

The second and main motivation for introducing SUSY is that it solved the hierarchy problem introduced in sec. 1.6. Let us remind that the Higgs boson receives quadratic corrections from all fermions with which it couples. If we note m_{h^0} the bare or unrenormalized Higgs mass, these are of the form:

$$m_h^2 = m_{h^0}^2 + \frac{|\lambda_f|^2}{8\pi^2}\left[-\Lambda_{UV}^2 + 6m_f^2 \ln\left(\frac{\Lambda_{UV}}{m_f}\right)\right] \tag{2.1}$$

SUSY introduces to each fermion of mass m_f one pair of superpartner Weyl scalar fields (one for each chirality of the femion) of degenerate mass m_s. Each scalar field contributes to the Higgs boson self-energy as:

$$m_h^2 = m_{h^0}^2 + \frac{\lambda_s}{16\pi^2}\left[+\Lambda_{UV}^2 - 2m_s^2 \ln\left(\frac{\Lambda_{UV}}{m_s}\right)\right] \tag{2.2}$$

When we sum up the contributions of the two superpartners, one sees that the quadratic divergences cancel out if we impose:

$$\lambda_f^2 = \lambda_s \tag{2.3}$$

that is, if we are in the limit of exact supersymmetry. In this case, the fermion and the bosons should have the exact same mass $m_f^2 = m_s^2$ contradicting badly experiments as no superpartner has been observed so far. Hence SUSY has to be broken. However, if broken SUSY is still believed to provide a solution to the hierarchy problem, the terms which break SUSY must respect eq. (2.3). Such terms are called "soft" and SUSY is said to be softly broken. Still, having a softly broken SUSY results in $m_f^2 \neq m_s^2$ and logarithmic corrections to the Higgs boson self-energy survive:

$$\delta m_{h^0}^2 \propto \lambda\left(m_s^2 - m_f^2\right)\ln\left(\frac{\Lambda_{UV}^2}{m_s m_f}\right) \tag{2.4}$$

and, if we do not want to fine-tune excessively the parameters of the perturbative series, one must has $\left(m_s^2 - m_f^2\right) \lesssim 1$ TeV^2. Thus, the superpartners of the SM fermions are expected to have a mass in the TeV range. This argument has played a crucial role to motivate the construction of the Large Hadron Collider (LHC).

The third argument is that the MSSM improves also the unification of the three SM gauge couplings compared to the situation depicted in subsection 1.6.3. Let us have a look at the RGEs of the three gauge coupling constants g_1, g_2, g_3 in the case of the SM and the MSSM:

$$\beta_{g_i} \equiv \frac{d}{dt}g_i = \frac{1}{16\pi^2}b_i g_i^3, \quad (b_1, b_2, b_3) = \begin{cases} \left(\frac{41}{10}, \frac{-19}{6}, -7\right) & \text{Standard Model} \\ \left(\frac{33}{5}, 1, -3\right) & \text{MSSM} \end{cases} \tag{2.5}$$

where $t = \ln\left(\frac{Q}{Q_O}\right)$ with Q the RG scale and Q_0 the subtraction scale. We see that the coefficients b_i are modified in the MSSM due to the extended particles spectrum. As it turns out, these modifications occur just in the right way to improve significantly the gauge couplings unification around $M_{GUT} \sim 10^{16}$ GeV. Note that at 1-loop, one can linearize the running if we take the inverse of the quantities $\alpha_i = \frac{g_i^2}{4\pi}$. The running of the α_i's are depicted in fig. 2.1 in the cases of the SM and of the MSSM. We see that, even in the case of the MSSM, this unification is not perfect. M_{GUT} is then generally defined as the scale at which α_1 and α_2 cross: $\alpha_1(M_{GUT}) \equiv \alpha_2(M_{GUT})$. As stated in subsection 1.6.3, this apparent unification is taken as a hint that a GUT theory should exist able to completely unify the gauge couplings above M_{GUT}. Also, merging SUSY and a gauge GUT group seem quite appealing as it allows to protect the proton lifetime as threshold corrections due to the SUSY spectrum have now to be taken into account (see [38]).

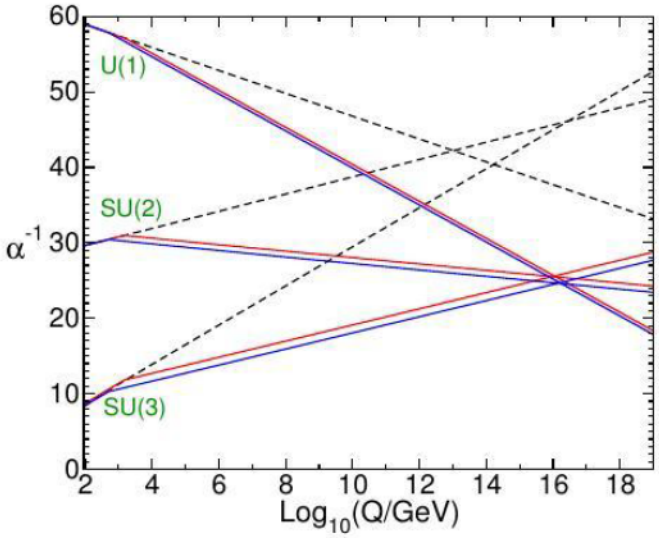

Figure 2.1 – Evolution of the inverse gauge couplings α_a^{-1} as defined in chapter 1 in the SM (dashed lines) and in the MSSM (solid lines). In the MSSM, the superpartner masses are collectivelly varied between 500 GeV and 1.5 TeV. Figure taken from [37].

The fourth motivation for SUSY is that it allows to incorporate gravity effects when we make SUSY transformations spacetime dependent i.e. when we gauge it [39]. Indeed, in this case, one has to introduce a spin $\frac{3}{2}$ particle called a gravitino whose superpartner is a spin 2 particle which can be identified as the graviton, the boson responsible for transmitting gravity effects, due to its coupling to the General Relativity (GR) energy momentum tensor. Unfortunately, supergravity does not constitute a coherent quantum description of gravity as the coupling between the graviton and the energy momentum tensor is dimensionfull and thus introduce non-renormalizable interactions in the theory. For an introduction to supergravity see [40].

The fifth argument in favor of SUSY is that it allows to dynamically trigger EWSB by radiative corrections. Indeed, in the SM, the condition $\mu^2 < 0$ (see eq. (1.16)) is enforced manually. In the MSSM, the running of μ^2 naturally drives it from a positive value at M_{GUT} to a negative value at M_{SUSY} mainly due to the strong coupling of the Higgs boson to the top quark [41].

Finally, in models with R-parity conservation – a global $\mathbb{Z}_2$ symmetry to be introduced in section 2.5– the SUSY spectrum incorporates good candidates for dark matter [42]. These can be of different natures depending on the exact mechanism responsible for the mediation of SUSY breaking. However in order to be stable, the dark matter candidate has to be the Lightest Supersymmetric Particle (LSP) of the SUSY spectrum to forbid subsequent decays. A common case arises when the supersymmetric partners of the four SM neutral gauge bosons and of the two Higgs bosons [2], the neutral gauginos and higgsinos, mix among each others after EWSB. This mixing results in four physical fields, called the neutralinos. The lightest of them is, in most cases, the LSP and can then be identified as a good dark matter candidate [43] as it is weakly coupled to the SM fields and does not possess electric nor color charges.

[2] As we will see later two Higgs doublets, instead of one, are needed in the MSSM.

2.2 Supersymmetric algebra.

Let us start this section by briefly recalling the Poincaré algebra. Basically, the usual Minkowski space is invariant under four translations, three rotations and Lorentz boosts. The translations are generated by the momentum 4-vector P_μ. The rotations are generated by the three kinetic moment operators J_k corresponding to the three space axis. Finally, the three Lorentz boosts can be generated by operators noted K_i. The J_k and K_i can be merged in a rank 2 tensor $M_{\mu\nu}$ according to $M_{ij} = \epsilon_{ijk}J_k$ and $M_{0i} = -K_i$ with ϵ_{ijk} the 3D totally antisymetric Levi-Civitta tensor. The Poincaré algebra can then be written as:

$$\begin{aligned}
[P_\mu, P_\nu] &= 0 \\
[M_{\mu\nu}, P_\lambda] &= i\left(g_{\nu\lambda}P_\mu - g_{\mu\lambda}P_\nu\right) \\
[M_{\mu\nu}, M_{\rho\sigma}] &= \left(ig_{\nu\rho}M_{\mu\sigma} + g_{\mu\sigma}M_{\nu\rho}\right. \\
&\quad \left. -g_{\mu\rho}M_{\nu\sigma} - g_{\nu\sigma}M_{\mu\rho}\right)
\end{aligned} \tag{2.6}$$

In its most simple form, the SuperPoincaré algebra consists of extending eq. 2.6 with 2 two-components Weyl spinors operators Q_α and $Q^\dagger_\alpha$ conjugate from each other where $\alpha = 1, 2$ is a spinorial indice. One can then show (see [37, 43]), that the extra fermionic generators must obey the following anti-commutation relations:

$$\begin{aligned}
\{Q_\alpha, Q_\beta\} &= \{Q^\dagger_{\dot\alpha}, Q^\dagger_{\dot\beta}\} = 0 \\
\{Q_\alpha, Q^\dagger_{\dot\beta}\} &= -2\sigma^\mu_{\alpha\dot\beta}P_\mu
\end{aligned} \tag{2.7}$$

Here a dotted indice (resp un-dotted) indicates that the spinor is right-handed (resp left-handed).

Furthermore, one also has commutation relations with the generators of the Poincaré algebra:

$$\begin{aligned}
[Q_\alpha, P_\mu] &= \left[Q^\dagger_{\dot\alpha}, P_\mu\right] = 0 \\
[M_{\mu\nu}, Q_\alpha] &= i\left(\sigma_{\mu\nu}\right)_\alpha{}^\beta Q_\beta \\
\left[M_{\mu\nu}, Q^{\dagger\dot\alpha}\right] &= i\left(\bar\sigma_{\mu\nu}\right)^{\dot\alpha}{}_{\dot\beta} Q^{\dot\beta}
\end{aligned} \tag{2.8}$$

The tensors $\sigma_{\mu\nu}, \bar\sigma_{\mu\nu}$ can be obtained by anti-symmetrizing the Pauli matrices σ_μ and their definitions are recalled in appendix A. The spinorial indices can be raised and lowered with the anti-symmetric metrics $\epsilon^{\alpha,\beta}$, $\epsilon^{\dot\alpha,\dot\beta}$ defined as:

$$\forall\alpha,\beta \in \{1,2\};\ \epsilon^{\alpha\beta} = \epsilon^{\dot\alpha\dot\beta} = -\epsilon^{\beta\alpha} = -\epsilon^{\dot\beta\dot\alpha} \text{ with } \epsilon^{12} = +1. \tag{2.9}$$

As we are using only one independent fermionic generator, we name this algebra the $\mathcal{N} = 1$ Super-Poincaré algebra. Higher dimensional generalization of equations (2.7),(2.8) exist with $\mathcal{N} = 2, 3...$ independent fermionic generators. However, until now, only the case $\mathcal{N} = 1$ is of phenomenological relevancy. In particular, the SUSY $\mathcal{N} = 2$ spectrum contains only vector-like fermions, meaning that both chiralities fall in the same representation of the gauge group, thus violating the SM $SU(2)_L$ gauge structure. So, we will logically restrict the rest of this work to the case $\mathcal{N} = 1$. Several remarks can now be made.

First, it can be deduced from angular momentum conservation that since Q carries a spin $1/2$, it turns a fermionic state into a bosonic one and vice-versa:

$$Q_\alpha|\text{fermion}\rangle = |\text{boson}\rangle,\ \ Q_\alpha|\text{boson}\rangle = |\text{fermion}\rangle \tag{2.10}$$

The boson and the fermion which are related by Q form an irreducible representation of the Super-Poincaré algebra called a supermultiplet. Second, in the context of SUSY, it is more natural to work with two-components Weyl fermions. Hence to each SM Dirac fermion made out of two Weyl fermions $\Psi_f = \begin{pmatrix}\xi_\alpha \\ \chi^{\dot\alpha}\end{pmatrix}$ (see appendix A.1) SUSY transformations will associate two scalars, one for each chirality

of the Dirac field, which was exactly what was needed to cancel the quadratic divergences in 2.1 and solve the hierarchy problem. Furthermore, the Hermitian conjugate of a left handed field transforms as a right-handed one: $\psi^\dagger_{\dot\alpha} \equiv (\psi_\alpha) = \left(\psi^\dagger\right)_{\dot\alpha}$. This gives us the freedom to work only with left-handed fields and that is what we are going to do from now on. Indeed, this convention is particularly useful when discussing GUTs. Third, one can show that the number of fermionic and bosonic d.o.f. in a supermultiplet must match. The most simple supermultiplet, called a chiral (or matter) supermultiplet is simply formed with a Weyl fermion and a complex scalar [3]. Fourth, from the first line of eq. (2.8), it follows that $P^2 = P_\mu P^\mu$ commutes with Q and that, if SUSY is unbroken, the members of a supermultiplet share the same mass.

Of course, as it was briefly discussed in section 2.1, this contradict badly experimental observations as no superpartners has been observed so far. Hence, if one wants to study its phenomenology, one has to break SUSY, but in a smart way, as it will be discussed in section 2.4.

2.3 Superspaces and superfields.

In this section, we would like to introduce the formalism of superspaces and superfields. This formalism is very elegant as it allows to reinterpret SUSY transformations introduced in 2.2 as translations on an extended Minkowski manifold called a superspace.

A systematic approach to write Lagrangians manifestly invariant under SUSY transformations can then be developed. We begin this section by introducing Grassmann variables which are anti-commuting coordinates needed to extend the Minkowski space to a superspace. We then continue by introducing superfields, in particular the important subclasses of chiral and vector superfields are properly defined. Finally, we end this section by developing a systematic method to build a SUSY Lagrangian in a superspace out of chiral and vector superfields. A very good review on Supersymmetry can be found in [37], also, a useful reference to get familiar with the formalism of superspaces is [44].

2.3.1 Grassmann coordinates

Superspaces can be obtained by adding to the usual spacetime coordinates $x_\mu = (t, x, y, z)$, anti-commuting coordinates described by a 2 two-component Weyl spinor θ^α (and its complex conjugate $\theta^\dagger_{\dot\alpha}$):

$$x_\mu \longrightarrow x_\mu,\ \theta^\alpha,\ \theta^\dagger_{\dot\alpha} \tag{2.11}$$

A field defined over those coordinates is called a superfield and incorporates as components the fields of the associated supermultiplet. To better understand the features of anticommuting coordinates, let us first consider the case of a single component Grassmann number η. First, it anticommutes so that $\{\eta, \eta\} = 0$ and $\eta^2 = 0$. It follows immediately that every function of η is exactly equal to its finite, order two, Taylor series:

$$f(\eta) = f_0 + f_1\eta \tag{2.12}$$

as higher order terms vanish. We can define the derivative operator through:

$$\frac{df}{d\eta} = f_1 \tag{2.13}$$

To define an integration over η, one has to impose linearity and the integration by parts formula:

$$\int d\eta\ f(\eta + \eta') = \int d\eta\ f(\eta); \qquad \int d\eta\ \frac{df}{d\eta} = 0 \tag{2.14}$$

From these definitions, it follows that the only possible definition of the integral operator is via:

$$\int d\eta\ f(\eta) = f_1 \tag{2.15}$$

[3] Actually, this is not generically true. if one wants to use SUSY off-shell i.e. in loop processes, one has to add a third "auxiliary" field which gets integrated out on-shell (see sec 2.3)

The Grassmann numbers have then the very peculiar feature that integrating them or differentiating them give the same result. This is a direct consequence of the anticommuting nature of these numbers.

We can now discuss a few properties of Grassmann numbers doublets $\theta_\alpha = (\theta_1, \theta_2)$; $\theta^\dagger_{\dot\alpha} = (\theta_1^*, \theta_2^*)^T$ needed for the superspace formalism. These objects anti-commute with each others such that:

$$\theta_1\theta_1 = \theta_2\theta_2 = 0; \qquad \theta_1\theta_2 = -\theta_1\theta_2 \tag{2.16}$$

Using the anti-symmetric metric (2.9), we can define Lorentz invariant combinations:

$$\begin{aligned} \theta\theta \equiv \theta^\alpha\theta_\alpha \quad &= \epsilon^{\alpha\beta}\theta_\beta\theta_\alpha = -2\theta_1\theta_2, \\ \theta^\dagger\theta^\dagger \equiv \theta^\dagger_{\dot\alpha}\theta^{\dagger\dot\alpha} \quad &= \epsilon^{\dot\alpha\dot\beta}\theta^\dagger_{\dot\alpha}\theta^\dagger_{\dot\beta} = +2\theta_1^*\theta_2^* \end{aligned} \tag{2.17}$$

We understand here why it is interesting to work with two component Weyl spinors and not four component Dirac spinors as it is usually the case in non-SUSY QFT. Indeed, it allows us to form Lorentz invariant more straightforwardly as we do not need to call the Dirac bar-conjugation trick . From these definitions, we can generalize equations (2.13), (2.15) to the case of Grassmann doublets:

$$\frac{\partial}{\partial\theta^\alpha}\theta^\beta = \delta^\beta_\alpha; \qquad \frac{\partial}{\partial\theta^\dagger_{\dot\alpha}}\theta^\dagger_{\dot\beta} = \delta^{\dot\alpha}_{\dot\beta}; \qquad \int d\theta_\alpha(f_0 + f_1\theta^\beta) = f_1\delta^\beta_\alpha \tag{2.18}$$

Furthermore, we can define integration measures over the quantities defined in equation (2.17):

$$d^2\theta \equiv -\frac{1}{4}d\theta^\alpha d\theta^\beta\epsilon_{\alpha\beta}, \qquad d^2\theta^\dagger \equiv -\frac{1}{4}d\theta^\dagger_{\dot\alpha}d\theta^\dagger_{\dot\beta}\epsilon^{\dot\alpha\dot\beta}, \qquad d^4\theta \equiv d^2\theta d^2\theta^\dagger \tag{2.19}$$

so that:

$$\int d^2\theta\ \theta\theta = 1, \qquad \int d^2\theta^\dagger\ \theta^\dagger\theta^\dagger = 1, \qquad \int d^4\theta\ \theta\theta\theta^\dagger\theta^\dagger = 1 \tag{2.20}$$

An important consequence of these definitions, which will be used abundantly in subsection 2.3.3, is that integrating a general superfield with the measures just defined will pick out the coefficients of $\theta\theta$ or $\theta^\dagger\theta^\dagger$ (see eq. (2.22)):

$$\begin{aligned} \int d^2\theta\ \mathbf{S}\left(x, \theta, \theta^\dagger\right) &= b(x) + \theta^\dagger\zeta^\dagger(x) + \theta^\dagger\theta^\dagger d(x) \\ \int d^2\theta^\dagger \mathbf{S}\left(x, \theta, \theta^\dagger\right) &= c(x) + \theta\eta(x) + \theta\theta d(x) \\ \int d^2\theta d^2\theta^\dagger \mathbf{S}\left(x, \theta, \theta^\dagger\right) &= d(x) \end{aligned} \tag{2.21}$$

With all these definitions, we are finally ready to talk about superspaces.

2.3.2 Superspaces and superfields

A superfield is a field defined over each point of the superspace coordinates $S = S\left(x_\mu, \theta, \theta^\dagger\right)$ (see (2.11)). As the Grassmann coordinates anticommute, a generic superfield can be expanded to a finite Taylor series and its generic expression is given by:

$$\mathbf{S}(x, \theta, \theta^\dagger) = a + \theta\xi + \theta^\dagger\chi^\dagger + \theta\theta b + \theta^\dagger\theta^\dagger c + \theta^\dagger\bar\sigma^\mu\theta v_\mu + \theta^\dagger\theta^\dagger\theta\eta + \theta\theta\theta^\dagger\zeta^\dagger + \theta\theta\theta^\dagger\theta^\dagger d \tag{2.22}$$

Here, a, b, c and d are complex scalar fields, v_μ is a complex vector field and ξ, χ, η, ζ are Weyl spinor fields. The bosonic and fermionic numbers of d.o.f. do indeed match. The bosonic fields bring $4 \times 2 + 4 \times 2 = 16$ real d.o.f. and the Weyl spinors $4 \times 2 \times 2 = 16$ d.o.f. also. Note that we haven't add any extra Lorentz nor spinor indices to S. Hence, for the sake of simplicity, we consider S to be a commuting scalar superfield in the rest of this section.

Now that we have the expression for a general superfield, it might be interesting to find a representation in terms of differential operators of the SUSY generators Q, $Q^\dagger$ satisfying eq. (2.7). To do this,

it is useful to rewrite the SUSY algebra in terms of commutation relations. These can be obtained using the Grassmann valued variables θ, $\theta^\dagger$ and the result is:

$$\begin{aligned}[\theta Q, \theta Q] &= \left[\theta^\dagger Q^\dagger, \theta^\dagger Q^\dagger\right] = 0, \\ \left[\theta Q, \theta^\dagger Q^\dagger\right] &= 2\theta\sigma^\mu\theta^\dagger P_\mu, \\ [\theta Q, P_\mu] &= \left[\theta^\dagger Q^\dagger, P_\mu\right] = 0\end{aligned} \tag{2.23}$$

From these expressions, one can construct a general element of a SUSY transformation X:

$$X\left(y_\mu, \epsilon^\alpha, \epsilon^\dagger_{\dot\alpha}\right) = \exp\left(-i\left(\epsilon^\alpha Q_\alpha + \epsilon^\dagger_{\dot\alpha} Q^{\dagger\dot\alpha} + y_\mu P^\mu\right)\right) \tag{2.24}$$

where ϵ, $\epsilon^\dagger$ are two Weyl spinors parameterizing the SUSY transformation.

It can be shown (see section 2.5 of [44]) that when X acts on $\mathbf{S}$, it translates the supercoordinates of $\mathbf{S}$ according to:

$$X\left(x_\mu, \epsilon, \epsilon^\dagger\right)\mathbf{S}\left(x, \theta, \theta^\dagger\right) = \mathbf{S}\left(x_\mu + y_\mu + i\epsilon\sigma^\mu\theta^\dagger + i\epsilon^\dagger\bar\sigma^\mu\theta, \theta + \epsilon, \theta^\dagger + \epsilon^\dagger\right) \tag{2.25}$$

We can expand eq. (2.25) to get the infinitesimal SUSY transformations $\delta_S\left(\xi, \xi^\dagger\right)$ acting on $\mathbf{S}$:

$$\begin{aligned}\delta_\epsilon\mathbf{S}\left(x, \theta, \theta^\dagger\right) &= -i\left[\epsilon Q + \epsilon^\dagger Q^\dagger\right]\mathbf{S}\left(x, \theta, \theta^\dagger\right) \\ &= \left[\epsilon^\alpha\frac{\partial}{\partial\theta^\alpha} + \epsilon^\dagger_{\dot\alpha}\frac{\partial}{\partial\theta^\dagger_{\dot\alpha}} + i\left(\epsilon\sigma_\mu\theta^\dagger + \epsilon^\dagger\bar\sigma^\mu\theta\right)\frac{\partial}{\partial x_\mu}\right]\mathbf{S}\end{aligned} \tag{2.26}$$

which gives expressions for the representation of Q and $Q^\dagger$ in terms of differential operators $\hat Q$, and $\hat Q^\dagger$:

$$\hat Q_\alpha = i\frac{\partial}{\partial\theta^\alpha} - \left(\sigma^\mu\theta^\dagger\right)_\alpha\partial_\mu, \qquad \hat Q^{\dagger\dot\alpha} = i\frac{\partial}{\partial\theta^\dagger_{\dot\alpha}} - \left(\bar\sigma^\mu\theta\right)^{\dot\alpha}\partial_\mu \tag{2.27}$$

where we have used the notation $\partial_\mu \equiv \frac{\partial}{\partial x_\mu}$.

The next step is to build SUSY covariant derivatives D_α, $D^{\dagger\dot\alpha}$ which commute with global SUSY transformations defined in eq. (2.26):

$$\delta_\epsilon\left(D_\alpha\mathbf{S}\right) = D_\alpha\left(\delta_\epsilon\mathbf{S}\right) \tag{2.28}$$

With all this machinery at our disposal, it is easy to check that the following operators:

$$D_\alpha = \frac{\partial}{\partial\theta^\alpha} - i\left(\sigma^\mu\theta^\dagger\right)_\alpha\partial_\mu, \qquad D^{\dagger\dot\alpha} = \frac{\partial}{\partial\theta^\dagger_{\dot\alpha}} - i\left(\bar\sigma^\mu\theta\right)^{\dot\alpha}\partial_\mu \tag{2.29}$$

satisfy the condition (2.28). We finally have all tools needed to properly define vector and chiral superfields. These will turn to be crucial ingredients when discussing the MSSM.

2.3.2.1 Chiral superfield

A chiral superfield is defined by imposing the following constraints on a generic superfield:

$$D^\dagger_{\dot\alpha}\Phi = 0. \tag{2.30}$$

A field satisfying this constraint is said to be a chiral (or left-chiral) superfield. Its complex conjugate is called an anti-chiral (or right-chiral) superfield and satisfy the constraint:

$$D_\alpha\Phi^* = 0 \tag{2.31}$$

The names of right and left-chiral superfields match with the handiness of the fermionic component of the supermultiplet as we are about to see below. An important remark is that the product of two chiral

superfields is still a chiral superfield whereas the product of a chiral and of an anti-chiral superfield is a vector superfield (see 2.3.2.2). To solve the constraint (2.30), we have to use a trick and perform a shift over the superspace coordinates x_μ, $x_\mu \to y^\mu \equiv x^\mu + i\theta^\dagger \bar{\sigma}^\mu \theta$. Re-expressing the covariant derivative $D^{\dagger\dot{\alpha}}$ in terms of $y^\mu, \theta, \theta^\dagger$, one would immediately see that the condition (2.30) is satisfied if the superfield does not depend on $\theta^\dagger$.

Hence, one can Taylor expand it:

$$\Phi_L = \phi^\dagger(y) + \sqrt{2}\theta\psi(y) + \theta\theta F(y), \tag{2.32}$$

where $\phi(y)$ is a complex scalar field, $\psi(y)$ a left two components Weyl field (hence the name) and $F(y)$ an auxiliary complex scalar field. The auxiliary field F is needed to make the number of bosonic and fermionic d.o.f. match off-shell. However, this is not a propagating field as its Lagrangian does not include a kinetic term. Hence, one can use its equation of motion to eliminate it. One says that F has been integrated out going on-shell.

If we reexpress (2.32) with $x_\mu, \theta, \theta^\dagger$, we end with the general expression of Φ_L in terms of component fields:

$$\Phi_L = \phi(x) + \sqrt{2}\theta\psi(x) + \theta\theta F(x) + i\theta^\dagger\bar{\sigma}^\mu\theta\partial_\mu\phi(x) + \frac{1}{4}\theta\theta\theta^\dagger\theta^\dagger\partial_\mu\partial^\mu\phi(x) - \frac{i}{\sqrt{2}}\theta\theta\theta^\dagger\bar{\sigma}^\mu\partial_\mu\psi(x) \tag{2.33}$$

Again, all those derivations rely on the fact that a Taylor expansion of Grassmann numbers always ends. By comparing the expression for a general superfield (2.22) to (2.33) and using that $\sqrt{2}\delta_\epsilon\Phi_L = -i\left(\epsilon\hat{Q} + \epsilon^\dagger\hat{Q}^\dagger\right)\Phi_L$, we can deduce the transformation laws of the component fields:

$$\begin{aligned}
\delta_\epsilon\phi &= \epsilon\psi, \\
\delta_\epsilon\psi_\alpha &= -i\left(\sigma^\mu\epsilon^\dagger\right)_\alpha\partial_\mu\phi + \epsilon_\alpha F, \\
\delta_\epsilon F &= -i\epsilon^\dagger\bar{\sigma}^\mu\partial_\mu\psi
\end{aligned} \tag{2.34}$$

We now have made explicit the fact that a SUSY transformation rotates a fermion into a boson and vice-versa. Furthermore, we see that the auxiliary field F transforms as a total derivative and does not play any role in the action. Beside, auxiliary fields are very useful when discussing spontaneous SUSY breaking as one can give them a SUSY breaking VEV without breaking Lorentz invariance. Finally, let us point out that the relations for a right-chiral superfield are obtained in an analogous way to what was done here simply by complex conjugation $\Phi_R = \Phi_L^\dagger$.

2.3.2.2 Vector superfields

The other important class of superfield are vector (or real) superfields. A vector superfield $\mathbf{V}$ is defined by the constraint:

$$\mathbf{V} = \mathbf{V}^* \tag{2.35}$$

Applying this constraint to the expression of a generic superfield (2.22), we end with:

$$\begin{aligned}
V\left(x, \theta, \theta^\dagger\right) = a + \theta\xi + \theta^\dagger\xi^\dagger + \theta\theta b + \theta^\dagger\theta^\dagger b^* + \theta^\dagger\bar{\sigma}^\mu\theta A_\mu + \theta^\dagger\theta^\dagger\theta\left(\lambda - \frac{i}{2}\sigma^\mu\partial_\mu\xi^\dagger\right) \\
\theta\theta\theta^\dagger\left(\lambda^\dagger - \frac{i}{2}\bar{\sigma}^\mu\partial_\mu\xi\right) + \theta\theta\theta^\dagger\theta^\dagger\left(\frac{1}{2}D + \frac{1}{4}\partial_\mu\partial^\mu a\right)
\end{aligned} \tag{2.36}$$

where a, b and D are real scalar fields, ξ, λ are Weyl fields and A_μ is a vector field.

As it turns out, the number of independent fields in (2.36) can be reduced using a suitable generalization of gauge transformations. In the abelian case, a supergauge transformation acts on chiral and vector superfields as:

$$\begin{cases}
\Phi \longrightarrow e^{(2igq\mathbf{\Omega})}\Phi \\
\mathbf{V} \longrightarrow \mathbf{V} + i\left(\mathbf{\Omega}^* - \mathbf{\Omega}\right)
\end{cases} \tag{2.37}$$

where $\mathbf{\Omega}$ is a chiral superfield gauge transformation parameter, g the coupling constant and q the charge of the superfield.

If the non-SUSY Lagrangian is invariant under an abelian $U(1)$ symmetry, supersymmetrizing it would result in a Lagrangian in superspace invariant under (2.37). For the vector superfield, we can use the freedom introduced by (2.37) to eliminate a, b and ξ_α from (2.36). In this *Wess-Zumino* (WZ) gauge, the vector superfield $\mathbf{V}$ takes the form:

$$\mathbf{V}_{WZ} = \theta^\dagger \bar{\sigma}^\mu \theta A_\mu + \theta^\dagger \theta^\dagger \theta \lambda + \theta \theta \theta^\dagger \lambda^\dagger + \frac{1}{2} \theta \theta \theta^\dagger \theta^\dagger D. \tag{2.38}$$

In fact going to the Wess Zumino gauge is equivalent to partially fixing the supergauge while still maintaining the invariance under the usual non-SUSY gauge transformation on the component fields λ and A_μ.

In this Wess Zumino gauge, the component fields of $\mathbf{V}$ transform under global SUSY translations as:

$$\begin{aligned} \sqrt{2}\delta_\epsilon A^\mu &= i\epsilon \partial^\mu \xi - i\epsilon^\dagger \partial^\mu \xi^\dagger + \epsilon \sigma^\mu \lambda^\dagger - \epsilon^\dagger \bar{\sigma}^\mu \lambda, \\ \sqrt{2}\delta_\epsilon \lambda_\alpha &= \epsilon_\alpha D + \frac{i}{2} \left(\sigma^\mu \bar{\sigma}^\nu \epsilon\right)_\alpha \left(\partial_\mu A_\nu - \partial_\nu A_\mu\right), \\ \sqrt{2}\delta_\epsilon D &= -i\epsilon \sigma^\mu \partial_\mu \lambda^\dagger - i\epsilon^\dagger \bar{\sigma}^\mu \partial_\mu \lambda \end{aligned} \tag{2.39}$$

As the notation suggests, a vector supermultiplet in the WZ gauge contains a spin 1 vector field A_μ as well as a spin 1/2 fermion λ_α. In the case of the MSSM, it will then be used to describe gauge bosons and their fermionic associated superpartners called "gauginos". The field D plays an analogous role to F in the chiral case. It is a real scalar auxiliary field, which does not propagate, needed to match the number of bosonic and fermionic d.o.f. in $\mathbf{V}$ off-shell. However, as it does not propagate, one can eliminate it from the Lagrangian using its equation of motion going on-shell.

2.3.3 SUSY lagrangians in a superspace

In this subsection, we are going to give some elements on how to construct Lagrangians invariant under SUSY transformations in the superspace formalism. Here we restrict ourselves to the case of a SUSY gauge theory with a unique semi-simple gauge group whose coupling constant is noted g, either abelian or non-abelian. The condition of invariance of the Lagrangian under SUSY transformations can be expressed as:

$$\delta_\epsilon \int_x \mathcal{L}(x) = 0 \tag{2.40}$$

We have shown that the auxiliary fields of chiral and vector superfields transform into total derivatives under SUSY translations leaving the action (2.40) invariant. We can then construct SUSY invariant Lagrangians from F and D terms using integrals over fermionic coordinates to pick up the relevant components (see (2.21)) :

$$\mathcal{L}(x) \equiv \mathcal{L}_F + \mathcal{L}_D = \int d^2\theta \mathcal{L}_f + \int d^2\theta d^2\theta^\dagger \mathcal{L}_d + h.c \tag{2.41}$$

where in $\mathcal{L}_F$ only the F term of $\mathcal{L}_f$ appears whereas in $\mathcal{L}_D$ only the D term of $\mathcal{L}_d$ appears. We have added the hermitian conjugate as usual to enforce the reality of $\mathcal{L}(x)$.

Let us start by describing $\mathcal{L}_f$. $\mathcal{L}_f$ can be obtained via a holomorphic function of the chiral superfields of the theory $\{\Phi_i\}$, called a *superpotential* [4] :

$$\mathcal{L}_f = W\left(\{\Phi_i\}\right) = a^i \Phi_i + \frac{1}{2} M^{ij} \Phi_i \Phi_j + \frac{1}{6} y^{ijk} \Phi_i \Phi_j \Phi_k \tag{2.42}$$

where all Φ_i are left-handed chiral superfields and the couplings M_{ij} and y_{ijk} are totally symmetric under the interchange of the indices i, j, k, an implicit sum over repeated indices being understood. $W\left(\{\Phi_i\}\right)$ being a sum of product of chiral superfields, it is a chiral superfield itself. We want to stress

[4] We want to recall here that "holomorphic" means that the superpotential is an analytical function of the superfields taken as complex numbers.

that, to have a Lagrangian which is gauge singlet, a *Fayet-Iliopoulos* term of the form $a_i\Phi_i$ can be included in the superpotential only if Φ_i is a gauge singlet itself. Furthermore, we have restricted the content of W with terms at most trilinear on the superfields. This enforces the fact that no terms with mass dimension higher than 4 are present in the Lagrangian which is hence renormalizable.

We can then pick the F-term of (2.42) by projecting out the $\theta\theta$ component of W using integration:

$$\begin{aligned}\int d^2\theta\, W\left(\{\Phi_i\}\right) &= a^i F_i + M^{ij}\left(\phi_i F_j - \frac{1}{2}\psi_i\psi_j\right) + \frac{1}{2}y^{ijk}\left(\phi_i\phi_j F_k - \phi_i\psi_j\psi_k\right) \\ &= \frac{\partial W(\phi)}{\partial\phi_j}F_j - \frac{1}{2}\frac{\partial^2 W(\phi)}{\partial\phi_j\phi_k}\psi_j\psi_k\end{aligned} \tag{2.43}$$

In the last line, the superpotential is understood to be a function only of the scalar components of the superfields. An implicit sum over the superfield content on all repeated indices is implicitly understood. $\mathcal{L}_F$ provides a mass matrix for the fermions $M_{ij} \equiv \frac{\partial^2 W(\phi)}{\partial\phi^i\phi^j}$ and Yukawa type interactions of the form $y^{ijk}\phi_i\psi_j\psi_k$. An important remark is that the superpotential is neither a potential in the classical sense, neither a SUSY invariant Lagrangian on its own. As can be seen on eq. (2.43), W generates the interactions of the theory when differentiating it with respect to the scalar components of the superfields. Hence, one can think about the superpotential as a generating functional of the interactions of a SUSY theory.

Now, let us turn to $\mathcal{L}_d$. One can show, in the non-abelian case, that the gauge invariance of $\mathcal{L}_d$ restricts its form to :

$$\mathcal{L}_d = \Phi^{\dagger i}\left(e^{2gT^aV^a}\right)_i^{\ j}\Phi_j \tag{2.44}$$

with T^a the generators of the gauge group and V_a the associated vector superfields. On can write $\mathcal{L}_d$ in component and the result is, in the WZ gauge:

$$\begin{aligned}\mathcal{L}_D &= \int d^2\theta d^2\theta^\dagger \Phi^{\dagger i}\left(e^{2g_aT^aV^a}\right)_i^{\ j}\Phi_j \\ &= i\psi^{i\dagger}\bar\sigma^\mu\nabla_\mu\psi_i - \nabla_\mu\phi^{*i}\nabla^\mu\phi_i - \sqrt{2}g_a\left(\phi^{*i}T^a\psi_i\lambda^a - \lambda^\dagger\psi^{i\dagger}T^a\phi_i\right) \\ &+ g_a\left(\phi^{*i}T^a\phi_i\right)D^a + F^{*i}F_i\end{aligned} \tag{2.45}$$

where ∇_μ is the usual covariant derivative $\nabla_\mu = \partial_\mu - igq_iA_\mu$.

This Lagrangian involves kinetic terms for the scalars and fermions, interaction terms between scalar, fermions and gauge bosons through the coupling to the covariant derivative. It also involves interactions between the superpartners of gauge bosons λ_a called "gauginos" and the scalars and fermions. We are still missing kinetic terms and self-interactions for the vector supermultiplets though. To generate them, one can define a field-strength superfield as:

$$\mathcal{W}_\alpha = -\frac{1}{4}D^\dagger D^\dagger\left(e^{-2gV}D_\alpha e^{2gV}\right) \tag{2.46}$$

One can show that this superfield is chiral [5] and transforms under supergauge transformations in the ajoint representation:

$$\mathcal{W}_\alpha \longrightarrow e^{i2gT^a\Omega^a}\mathcal{W}_\alpha e^{-i2gT^a\Omega^a} \tag{2.47}$$

where $\{\Omega^a\}$ are the chiral superfields gauge parameters and T^a the generators of the gauge group. We can decompose $\mathcal{W}_\alpha$ over the generators of the gauge group $\mathcal{W}_\alpha = 2g_aT^a\mathcal{W}_\alpha^a$ with:

$$\begin{aligned}\mathcal{W}_\alpha^a &= -\frac{1}{4}D^\dagger D^\dagger\left(D_\alpha V^\alpha - igf^{abc}V^bD_\alpha V^c\right) \\ &= \lambda_\alpha^a + \theta_\alpha D^\alpha - \frac{i}{2}\left(\sigma^\mu\bar\sigma^\nu\theta\right)_\alpha F_{\mu\nu}^a + i\theta\theta\left(\sigma^\mu\nabla_\mu\lambda^{\dagger a}\right)_\alpha\end{aligned} \tag{2.48}$$

where all computations have been done in the WZ gauge and $F_{\mu\nu}^a = \partial_\mu A_\nu - \partial_\nu A_\mu + g_af^{abc}A_\mu^bA_\nu^c$ is the usual field strength tensor.

[5] $\mathcal{W}_\alpha$ is chiral i.e. $D^{\dagger\dot\beta}\mathcal{W}_\alpha = 0$ because $D^\dagger D^\dagger D^\dagger = 0$ by construction (see [44]).

The abelian case can then simply be obtained by setting the structure constants to zero: $f^{abc} = 0$. It follows that:

$$\begin{aligned}\mathcal{L}_{kin} &= \int d^2\theta \frac{1}{4}\mathrm{Tr}\left[\mathcal{W}^\alpha \mathcal{W}_\alpha\right] \\ &= \int d^2\theta \mathcal{W}^{a\alpha}\mathcal{W}^a_\alpha \\ &= D^a D^a + 2i\lambda^a \sigma^\mu \nabla_\mu \lambda^{\dagger a} - \frac{1}{2}F^{a\mu\nu}F^a_{\mu\nu} + \frac{i}{4}\epsilon^{\mu\nu\rho\sigma}F^a_{\mu\nu}F^a_{\rho\sigma}\end{aligned} \tag{2.49}$$

is both gauge and supersymmetric invariant.

With all these contributions at hand, the most general renormalizable Lagrangian for a non-abelian gauge supersymmetric theory is:

$$\mathcal{L} = \frac{1}{4}\int d^2\theta \left(\mathcal{W}^{a\alpha}\mathcal{W}^a_\alpha + \text{h.c}\right) + \int d^2\theta \left(W\left(\Phi_i\right) + \text{h.c}\right) + \int d^2\theta d^2\theta^\dagger \left(\Phi^{\dagger i}\left(e^{2g_a T^a V^a}\right)_i^{\ j}\Phi_j\right) \tag{2.50}$$

We end this section with a brief description of the scalar potential of 2.50. As already stated, the auxiliary fields F (see (2.33)) and D (see (2.38)) do not come with kinetic terms. Their Euler-Lagrange equations of motions are hence purely algebraic:

$$\begin{aligned} F_i + \frac{\partial W^\dagger}{\partial \phi^i} &= 0 \\ D^a + g\left(\phi_i^* T^a \phi^i\right) &= 0 \end{aligned} \tag{2.51}$$

One can then use these equations to eliminate F_i and D^a in favor of the scalar component fields. Plugging (2.51) in (2.50), one can then obtain the scalar potential of the theory:

$$V(\phi, \phi^*) = \frac{\partial W^\dagger(\phi^*)}{\partial \phi_i^*}\frac{\partial W(\phi)}{\partial \phi^i} + \frac{1}{2}\sum_l g_l^2 \sum_a \left(\phi_i^* T_l^a \phi^i\right)^2 . \tag{2.52}$$

In eq. (2.52), l sums over the gauge group of the theory with the corresponding gauge coupling g_l and generators T_l^a.

Hence, the scalar potential of a SUSY gauge theory is a sum of squared terms and is always positive whatever the field configuration. Beside, the form of $V(\phi, \phi^*)$ is completely fixed by the other interactions of the theory.

2.4 Breaking Supersymmetry.

As it has been shown in section 2.2, the Casimir operator P^2 commutes with the spinorial generators $Q, Q^\dagger$. This implies that every field in a given supermultiplet own the same mass if SUSY is unbroken. As we haven't detected scalar superpartners of the SM fermions so far [6], this clearly implies that SUSY, if it is realized in nature, must be a broken symmetry. This being said, we are then left with two possibilities to break SUSY.

2.4.1 Breaking SUSY spontaneously.

The first and most natural possibility is to break SUSY spontaneously. This can be achieved by allowing a chiral auxiliary field F_i or a vector auxiliary field D_i to develop a SUSY breaking VEV. The first of these two mechanisms is known as a "F-type" or O'Raifeartaigh SUSY breaking [45] and the second is known as a "D-type" or "Fayet-Iliopoulos" SUSY breaking [46]. However, there is a subtlety which comes into the game if one wants to break SUSY spontaneously. Indeed, one can show that the auxiliary field which takes a SUSY breaking VEV cannot belong to any of the MSSM superfields (see sec. 2.5) nor to a superfield whose VEV lies anywhere near the TeV scale.

This comes mainly from the supertrace constraint on the tree level mass matrix of a spontaneously broken SUSY spectrum. In the SUSY broken phase, the mass degeneracy inside supermultiplets is lifted, hence particles with different spins have different masses. One can then define the supertrace on a SUSY spectrum as:

$$\mathrm{STr}\left(m^2\right) \equiv \sum_j (-1)^j \left(2j+1\right) \mathrm{Tr}\left(m_j^2\right) \tag{2.53}$$

where m_j^2 correspond to the mass matrix of particles with spin j and the sum runs over all the particles of the SUSY spectrum, the fermions contributing with opposite sign than the bosons.

One can then prove (see [47]) that this supertrace must vanish $\mathrm{STr}\left(m^2\right) = 0$ for a spontaneously broken SUSY theory [7] in the observable sector. This has strong consequences on how spontaneously broken SUSY can be achieved. For example, it can be shown that in the most optimistic case, due to the supertrace, if SUSY is to be broken in the observable sector, light color triplets scalars (squarks) lighter than m_u or m_d should be present in the spectrum which is clearly ruled out by experiment. Instead, physicists came up with the idea that the source of SUSY breaking should exist in a "hidden" sector. By "hidden", we mean either that the superfield is neutral under the SM gauge group or, within the context of extra-dimension models, is localized on a different brane of the one on which we are living. Still, we then have to construct models which allow the superfield in the visible sector to couple this hidden sector SUSY breaking VEV. Such mediation models can be construct. They have all the common feature that the messenger field has to be flavor blind, i.e. it respects the $U(3)^6$ flavor symmetry of chapter 1, in order to lead to an acceptable flavor phenomenology. In the first of these models, the gravity-mediated SUSY breaking (see for instance [48]), gravity, which is naturally flavor blind, plays the role of the messenger [8]. The second model, the gauge-mediated SUSY breaking model [50], couples the two sectors via loop effects involving new chiral supermultiplets through gauge interactions. Finally the third one, the anomaly mediated SUSY breaking mechanism involves extra-dimensions and mediates the SUSY breaking to the visible sector via the superconformal anomaly [51].

[6] Hopefully it will not be the case anymore soon!

[7] A condition is needed however: The gauge group of the SUSY theory must own a non-anomalous U(1) symmetry. This is the case of the MSSM as $U(1)_Y \in G_{SM}$.

[8] Note however that, in this last case, the flavor blindness of gravity does not guarantee by itself that the generated soft terms are flavor blind. The flavor blindness of soft terms can be achieved only if one makes further simplifications on the structure of the non-renormalizable terms used to communicate SUSY breaking to the visible sector (see [37]). These simplifications have lead to the well-known minimal-supergravity (mSUGRA) ansatz which have been the subject of several phenomenological studies (see for instance [49] and references therein) .

2.4.2 Soft SUSY breaking.

The second possibility would be to break SUSY explicitly. However, the operators used to do so would generically reintroduce quadratic divergences in the quantum corrections to the Higgs mass, thus spoiling SUSY as a solution to the hierarchy problem (see sec 2.1). However a trick can be used to circumvent this obstacle. Indeed, it has been proved that no quadratic divergences are reintroduced if only SUSY breaking operators with positive dimension are used [52], and thus to all orders in perturbation theory. Such operators are called "soft" and are used abundantly in phenomenological approaches as an effective parameterization at low scales of the mechanism which drives the spontaneous breaking of SUSY. Stated otherwise, if we see the MSSM as an effective theory, we can simply ignore the specific dynamic which drives SUSY breaking (see subsection 2.4.1) and simply parameterize it by adding extra soft terms to the SUSY Lagrangian. The "soft" nature of these terms guarantees that SUSY is still valid as a solution to the hierarchy problem. All possible soft terms have been classified and the most general Soft SUSY breaking Lagrangian is [9]:

$$\mathcal{L}_{soft} = -\left(\frac{1}{2}M_a\lambda^a\lambda^a + \frac{1}{6}a^{ijk}\phi_i\phi_j\phi_k + \frac{1}{2}b^{ij}\phi_i\phi_j + t^i\phi_j\right) + \text{h.c - } \left(m^2\right)^i_j\,\phi^{j\dagger}\phi_i \tag{2.54}$$

This lagrangian gives masses to the gauginos and scalars and also contains bilinear and trilinear scalar couplings. Clearly, all these terms break SUSY as they contain only gauginos or scalars but not both simultaneously. As stated above, the advantage of this approach is that we can break SUSY without relying on a specific model of mediation. The disadvantage is also clear. Indeed a lot of new parameters, considered as free here, are introduced by $\mathcal{L}_{soft}$. Beside, as the coupling matrices will have generically arbitrary complex and flavor structures, they will introduce many new sources of flavor and CP violation which will, without further restrictions, contradict experimental observations. This fact will give rise to what is called the "New physics flavor problem", discussed in section 2.5 in the case of the Minimal Supersymmetric extension of the SM that we will now describe.

[9] We neglect here the possibility of adding soft terms of the form $c_i^{jk}\phi^{*i}\phi_j\phi_k$. Indeed, constructing viable models of spontaneous SUSY breaking generally requires c_i^{jk} to be negligibly small.

Chiral supermultiplets			
	Spin 0	**Spin $\frac{1}{2}$**	**SU(3)$_C$, SU(2)$_L$, U(1)$_Y$**
Q	$\widetilde{Q}_L = \left(\widetilde{u}_L, \widetilde{d}_L\right)$	$Q_L = (u_L, d_L)$	$\left(\mathbf{3}, \mathbf{2}, \frac{1}{3}\right)$
$\overline{U}$	$\widetilde{u}_R^*$	$\overline{u}_R$	$\left(\overline{\mathbf{3}}, \mathbf{1}, -\frac{4}{3}\right)$
$\overline{D}$	$\widetilde{d}_R^*$	$\overline{d}_R$	$\left(\overline{\mathbf{3}}, \mathbf{1}, +\frac{2}{3}\right)$
L	$\widetilde{L}_L = (\widetilde{\nu}_L, \widetilde{e}_L)$	$L_L = (\nu_L, e_L)$	$(\mathbf{1}, \mathbf{2}, -1)$
$\overline{E}$	$\widetilde{e}_R^*$	$\overline{e}_R$	$\left(\overline{\mathbf{1}}, \mathbf{1}, 2\right)$
H_u	$H_u = \left(H_u^+, H_u^0\right)$	$\widetilde{H}_u = \left(\widetilde{H}_u^+ \widetilde{H}_u^0\right)$	$(\mathbf{1}, \mathbf{2}, 1)$
H_d	$H_d = \left(H_d^0, H_d^-\right)$	$\widetilde{H}_d = \left(\widetilde{H}_d^0, \widetilde{H}_d^-\right)$	$(\mathbf{1}, \mathbf{2}, -1)$
Gauge supermultiplets			
	Spin 0	**Spin $\frac{1}{2}$**	**SU(3)$_C$, SU(2)$_L$, U(1)$_Y$**
G^a	$\widetilde{G}^a$	G^a	$(\mathbf{8}, \mathbf{1}, 0)$
W	$\widetilde{W}^i$	W^i	$(\mathbf{1}, \mathbf{3}, 0)$
B	$\widetilde{B}^0$	B^0	$(\mathbf{1}, \mathbf{1}, 0)$

Figure 2.2 – MSSM supermultiplets and their gauge properties. The superfields are labeled with a capital letter. A tilde is used to label the superpartners of the SM fields. The L/R label on the superpartners refers to the chirality of the associated SM Weyl field. We have suppressed color and family indices on matter fields to alleviate the notation. $a = 1...8$ enumerates the vector superfields of $SU(3)_C$ and $i = 1..3$ the vector superfields of $SU(2)_L$. Note that here, we have not included right-handed neutrinos supermultiplets in the MSSM field content.

2.5 The MSSM.

The MSSM is the minimal renormalizable supersymmetric extension of the Standard Model [53]. The MSSM is "minimal" in the sense that it introduces the least possible number of new particles in its spectrum to get a proper renormalizable SUSY realization of the SM. It is based on the following assumptions:

$\Rightarrow$ The Standard model is extended by $\mathcal{N} = 1$ supersymmetry.

$\Rightarrow$ The MSSM is invariant under the SM gauge group.

$\Rightarrow$ The SUSY soft mass scale is near the EW scale.

$\Rightarrow$ $\mathcal{R}$-parity is conserved.

The third point is required if the MSSM is still believed to provide a solution to the hierarchy problem. Indeed, one can show that if the average mass scale of superpartners largely exceeds the EW scale, the MSSM gets once again fine-tuned due to the large hierarchy between the two scales. The $\mathcal{R}$-parity is required to stabilize the proton and will be discussed in subsection 2.5.1. The superpotential of the MSSM is:

$$W_{MSSM} = Y_u^{ij}\overline{U}_i Q_j \cdot H_u - Y_d^{ij}\overline{D}_i Q_j \cdot H_d - Y_e^{ij}\overline{E}_i L_j \cdot H_d + \mu H_u \cdot H_d \tag{2.55}$$

The objects $Q, \overline{U}, \overline{D}, L, \overline{E}$ are $SU(2)$ quark-doublet, quark-singlet, leptons-doublet and leptons singlet superfields whose corresponding supermultiplets are listed in table 2.2. The bar on the representation indicates that all singlet superfields $\overline{U}, \overline{D}$ and $\overline{E}$ transform under the complex conjugate representation of the respective doublet [10].

[10] For instance, an infinitesimal $SU(3)$ rotation acts on Q as $Q \to (\mathbb{1} + i\alpha^a T^a)$ with α^a the gauge parameters and $T^a = \lambda^a/2$ the $SU(3)$ generators. Q is said to transform under the $SU(3)$ fundamental representation $\mathbf{3}$. On the other hand, this same rotation will act on $\overline{U}$ as $\overline{U} \to (\mathbb{1} - i\alpha^a (T^a)^*)\,\overline{U}$. $\overline{U}$ or $\overline{D}$ will be said to transform under the complex conjugate fundamental representation of $SU(3)$ noted $\overline{\mathbf{3}}$. But, due to the hermiticity of the $SU(3)$ algebra, one has

The "$\cdot$" indicates a SU(2) invariant dot product of two doublets. For instance, $Q \cdot H_u = Q^\alpha \epsilon_{\alpha\beta} H_u^\beta$ where $\epsilon = i\sigma_2$ is used to contract $SU(2)$ indices.

$Y_u^{ij}, Y_d^{ij}, Y_e^{ij}$ are the exact same 3×3 Yukawa coupling matrices as in the SM. μ is a supersymmetric Higgs mass parameter needed due to the extended Higgs sector (see below). We see here, as foreseen previously, that chiral superfields are naturally used to handle both the SM fermions together with their superpartners. The usual naming convention wants that to designate scalar SM fermions superpartners, we add a "s" (for scalar) before the name of the SM field and a tilde on the scalar field itself. Hence, the scalar superpartners of the quarks (resp leptons) are called squarks (resp: sleptons). For example, the superpartner of the down quark (resp: muon) is named a sdown (resp: smuon) and is designated by the complex scalar field $\widetilde{d}$ (resp: $\widetilde{\mu}$). In the same way, the SM gauge bosons are promoted to vector superfields whose gauge supermultiplets contain both the gauge boson and its associate fermionic superpartner. The name of the gauge superpartner is formed by adding a suffix "ino" at the end of the SM gauge boson. Hence, winos, binos, gluinos and Higgsinos are the names of respectively the superpartners of the W, B, gluons and Higgs bosons. Here again, a tilde is used over the SM gauge boson when we refer to its superpartner, for example, winos, binos and gluinos are Weyl fermions noted as $\widetilde{W}, \widetilde{B}$ and $\widetilde{G}$. An important remark is that within the MSSM, to each SM Weyl fermion (of definite chirality) is associated an independent superpartner. So, to a SM Dirac fermion is associated two distinct scalar fields. The naming convention wants that we use a L/R index on the scalar field to designate the chirality of the associated SM Weyl fermion.

The MSSM Higgs sector is a little bit peculiar. Indeed, contrary to the SM case, in the MSSM not one but two weak Higgs doublets H_u and H_d are needed in (2.55) and there are deep reasons for that. The first one is that in section 2.3, we have build the superpotential as a holomorphic function of chiral superfields to get $\mathcal{L}_F$ (see eq. (2.41)) SUSY invariant. In other terms, $W(\Phi_i)$ depends only on chiral superfields, but not on their complex conjugates. Hence, we are forced to introduce two independent weak doublets with opposite hypercharge H_u and H_d to give mass to the up and down fermions separately. In the SM, we had just re-expressed H_u as $H_u = i\sigma_2 H_d^\dagger$ but in the MSSM, this trick cannot be used anymore without spoiling the holomorphicity of $W(\Phi_i)$. The second reason comes from anomaly cancellation. Indeed, due to the extended scalar spectrum we can show that both H_u and H_d are needed if we want to preserve the gauge symmetries at the quantum level.

Note that in the limit of exact SUSY, we got a proper extension of the SM just by introducing one extra free Higgs mass parameter μ. Of course, SUSY cannot be an exact symmetry of nature and the situation will be dramatically deteriorated once we will add soft terms in the MSSM Lagrangian as discussed in sec 2.5.2.

On the other hand, this SUSY μ term seems to pose something of a puzzle. Indeed, the μ term in eq. (2.55) leads to:

$$\left|\mu^2\right| \left(|H_u^+|^2 + |H_d^-|^2 + |H_u^0|^2 + |H_d^0|^2\right) \tag{2.56}$$

in the scalar potential of the theory. For the EWSB to be triggered one needs approximately $\mu \sim 100\ \text{GeV} - 1\ \text{TeV}$ if one wants to avoid too large cancellations between soft terms and terms in (2.56). The fact that μ should be, roughly, of the same magnitude as the SUSY mass scale is referred to as the μ problem (see [54] for the historical paper). One proposal to solve this puzzle, the so-called Guidice-Masiero mechanism proposes to generate this term dynamically via supergravity breaking effects [55]. Another proposal, the Next-to-MSSM proposes to extend the superfield content of the MSSM by one extra gauge singlet (see [56]). A good review of the μ problem and its solutions can be found in [57].

2.5.1 $\mathcal{R}$-parity

As stated at the beginning of this section, the MSSM is uniquely defined by the choice of the superpotential (2.55). However, there are other gauge invariant and renormalizable terms that one could

$(T^a)^* = (T^a)^T$ and a term of the form $\overline{U}Q$ is gauge invariant. A theory in which the gauge group acts on right-handed singlets and left-handed doublets through representations which are conjugate from each others is called a *chiral* theory. A counter-example of theory which is not chiral can be found in $\mathcal{N} = 2$ SUSY. Indeed, in this theory, it is not possible to make right and left-handed components of superfields transform differently under the gauge group.

include in the superpotential. These are:

$$\begin{aligned} W_{\Delta L=1} &= \frac{1}{2}\lambda_e^{ijk} L_i \cdot L_j \bar{E}_k + \lambda_L'^{ijk} L_i \cdot Q_j \bar{D}_k + \mu_L^i L_i \cdot H_u \\ W_{\Delta B=1} &= \frac{1}{2}\lambda_B^{ijk} \bar{U}_i \bar{D}_j \bar{D}_k \end{aligned} \tag{2.57}$$

where we have restored family indices $i = 1, 2, 3$. The problem with these terms is that they violate two symmetries accidentally preserved by the Yukawa interactions in the SM, namely the total baryon B and lepton L numbers. Indeed, $W_{\Delta L=1}$ and $W_{\Delta B=1}$ violate respectively L and B by one unit. One can be convinced of that if we remember that $B(Q_i) = +\frac{1}{3}$, $B(\bar{U}_i) = B(\bar{U}_i) = -\frac{1}{3}$ and $L(L_i) = +1$, $L(\bar{E}_i) = -1$ with all others B and L numbers vanishing. B and L violating processes have never been seen experimentally, in particular non-vanishing λ_L and λ_B couplings would result in proton decay through for instance, $p \to e^+\pi^0$. For this reason, the idea has came up to impose a $\mathbb{Z}_2$ symmetry, the so-called matter $\mathcal{R}$-parity, which is multiplicatively conserved and defined for each particle as:

$$P_R = (-1)^{3(B-L)+2s} \tag{2.58}$$

with s the spin of the particle.

From eq. (2.58), it follows that every SM field has $P_R = +1$ (because of the $(-1)^{2s}$ factor) while all s-particles have $P_R = -1$. Angular momentum conservation implies in turn that at each interaction vertex, the product of the $\mathcal{R}$-parity of all particles involved is equal to $+1$. It is then clear that terms in (2.57) do not conserve $\mathcal{R}$-parity and are thus forbidden. Furthermore, important phenomenological consequences of $\mathcal{R}$-parity conservation are that:

1. At each interaction vertex, the total number of s-particles involved is always even.
2. Each sparticle other than the LSP must eventually decay in a state that contains an odd number of LSP.
3. The LSP should thus be absolutely stable as it carries $P_R = -1$ and cannot decay any further in s-particles.

Beside, due to point 3, if the LSP is also chargeless and colorless, it is a good dark matter candidate.

To end this section we want to stress that, imposing an exact $\mathbb{Z}_2$ symmetry by hand, to make the MSSM phenomenologically viable, might seems quite frustrating theoretically. However, from a model building point of view, $\mathcal{R}$-parity might emerge as a conserved subgroup after a continuous $U(1)$ symmetry has been spontaneously broken [58].

2.5.2 MSSM soft parameters

The most general set of soft parameters (2.54) compatible with gauge invariance, $\mathcal{R}$-parity conservation and the particle content of the MSSM is given by:

$$\begin{aligned} \mathcal{L}_{soft} = &-\frac{1}{2}\left(M_3\tilde{G}\tilde{G} + M_2\tilde{W}\tilde{W} + M_1\tilde{B}\tilde{B} + \text{ h.c}\right) \\ &- \left(\tilde{u}_R^* A_U \tilde{Q}_L H_u - \tilde{d}_R^* A_D \tilde{Q}_L H_d - \tilde{e}_R^* A_E \tilde{L}_L H_d + \text{ h.c}\right) \\ &- \tilde{Q}_L^\dagger M_Q^2 Q_L - \tilde{L}_L^\dagger M_L^2 \tilde{L}_L - \tilde{u}_R^* M_U^2 \tilde{u}_R - \tilde{d}_R^* M_D^2 \tilde{d}_R - \tilde{e}_R^* M_E^2 \tilde{e}_R \\ &- M_{H_u}^2 H_u^* H_u - M_{H_d}^2 H_d^* H_d - (b H_u H_d + \text{ h.c}) \end{aligned} \tag{2.59}$$

Here, A_U, A_D and A_E are complex 3×3 in family space soft trilinear coupling matrices. The third line of (2.59) consists in soft mass terms for the squarks and sleptons. Each mass matrix $M_Q^2, M_L^2, M_U^2, M_D^2, M_E^2$ is again a 3×3 matrix in family space. They however have to be hermitian to guarantee the reality of the mass eigenvalues. Both type of matrices imply potential additional sources of flavor and CP violation in the MSSM. Therefore, their structures are highly constrained by phenomenology. Finally, we do have Higgs squared mass terms $M_{H_u}^2$ $M_{H_d}^2$ as well as a bilinear term b which contribute to the Higgs potential.

As already pointed out in subsection 2.4.2, adding soft terms to parameterize SUSY breaking introduce a lot of parameters, considered as free if the breaking mechanism is not specified. Indeed, (2.59) introduces no less than 105 new masses, phases or mixing angles that cannot be rotated away by a redefinition of the flavor basis in the quark or lepton supermultiplets. These new parameters will involve extra sources of flavor or CP violation. Indeed, extra phases in soft terms can overproduce electric dipole moment [59] beyond experimental limits. This is known as the CP problem.

New sources of flavor and CP violation can also disrupt the GIM mechanism which suppress the FCNCs to acceptable low levels in the SM. Developing a mechanism able to keep soft terms under control so that they do not introduce unacceptable large FCNCs is known as the SUSY flavor problem. Beside, within the MSSM, most of the entries in all those terms must be of the order of the SUSY soft mass scale M_{soft} or M^2_{soft} depending on the linear or squared dependence in (2.59). This is needed to avoid to reintroduce large logarithmic corrections to the Higgs mass which would spoil the MSSM as a solution to the hierarchy problem. This suggest that a more fundamental dynamic at higher scale should be at work in order to generate a *hierarchical* structure in (2.59) dynamically. For example, the spontaneous breaking of a flavor symmetry, discrete or continuous, might give rise to a hierarchy in the soft terms making them compatible with phenomenology (see [60] and references therein).

Again, a lot of flavor models exist which aim at solving (at least partially) the SUSY flavor and CP problems. However, if we consider SUSY through the eyes of a phenomenologist, three approaches can be described aiming at maintaining the contributions of the soft terms to flavor observables under control:

Soft supersymmetry breaking universality: The first approach, called the soft supersymmetry breaking universality, consists in three idealized assumptions on the soft terms structure. The first one is that the soft squared-mass matrices are flavor-blind, i.e. they are simply proportional to the unity matrix:

$$M_Q^2 = m_{Q_0}^2 \mathbb{1},\ M_U^2 = m_{U_0}^2 \mathbb{1},\ M_D^2 = m_{D_0}^2 \mathbb{1},\ M_L^2 = m_{L_0}^2 \mathbb{1},\ M_E^2 = m_{E_0}^2 \mathbb{1} \tag{2.60}$$

where $m_{Q_0}^2, m_{L_0}^2 ...$ are real scalars fixing the overall scale of the corresponding mass matrix. Then, SUSY contributions to FCNCs will only arise from small mixing induced by the trilinear couplings because all squarks and sleptons will be degenerate in mass. Beside, making the further assumption that the trilinear couplings are each proportional to the corresponding Yukawa coupling matrix:

$$A_U = A_{U_0} Y_u,\ A_D = A_{D_0} Y_d,\ A_E = A_{E_0} Y_e \tag{2.61}$$

will guarantee that only the squarks and sleptons of the third family will induce large trilinear couplings.

Finally one still has to deal with potential dangerous CP violation effects which could arise from complex phases in the soft terms. If (2.60) is assumed, all squarks and sleptons mass matrices as well as Higgs mass terms $m_{H_u}^2, m_{H_d}^2$ do not introduce CP violating effects as all universal couplings $m_{Q_0}^2, m_{L_0}^2 ...$ have to be real. Beside, by appropriate phase redefinitions of the scalar and fermion components of the Higgs supermultiplets H_u and H_d, one can make b (see (2.5.2)) and μ (see (2.55)) also real. So, the potential only new sources of CP violation could lie in the gauginos mass parameters and trilinear coupling matrices. The third assumption will hence consist in enforcing the reality of these complex parameters:

$$\mathrm{Im}(M_1) = \mathrm{Im}(M_2) = \mathrm{Im}(M_3) = \mathrm{Im}(A_{U_0}) = \mathrm{Im}(A_{D_0}) = \mathrm{Im}(A_{E_0}) = 0 \tag{2.62}$$

enforcing that the only source of CP violation is the usual CKM phase.

With the above assumptions we do have, in principle, a SUSY model which is phenomenologically viable. However, all these conditions (2.60), (2.61) and (2.62) should presumably arise due to a more fundamental mediation mechanism or due to the spontaneous breaking of a flavor symmetry. Hence these conditions should be taken as boundary conditions, rather than scale invariant constraints, which hold at the high scale at which the mechanism responsible for flavor dynamic decouples from the usual MSSM spectrum. This will in turn imply that all these quantities will have to be running down, using the appropriate RGEs, to a low scale, either M_Z or M_{SUSY} where experiments take place. Hence, flavor violation effects will be generated by the RGEs. These RGE induced flavor violating effects will

be small due to the idealized high scale boundary conditions. We also want to stress that (2.60), (2.61) and (2.62) depict idealized boundary conditions. These have to be thought of as representing a limit in which soft terms are perfectly harmless. One can then study small departures from this limit [61] keeping flavor observables under control.

Alignment The second approach one can take consists in assuming that the squarks squared-mass matrices are aligned in flavor space with the corresponding Yukawa matrix [62]. Concretely, it means that, starting from the SuperCKM basis in which the Yukawas couplings are diagonal, the matrix which rotates the squark mass matrix to its diagonal form has small mixing angles. This ensure that flavor-changing effects are suppressed enough and low scale SUSY processes are kept within experimental ranges. Beside, it has been argued that the alignment paradigm could potentially also adress the SUSY CP problem [63].

Decoupling Finally, in the "decoupling" or "irrelevancy" paradigm the sparticle masses are extremely heavy. Therefore, supersymmetric sources of CP violation and flavor changing neutral currents are suppressed as the SUSY spectrum is decoupled. However, if soft terms are completely arbitrary, the degree of suppression needed to be not in contradiction with data generically requires M_{Soft} to be well above the TeV scale, at least for some of the scalar masses. Such high soft breaking scale seems to play against the MSSM as a solution to the hierarchy problem. However, one can consider more "natural" spectra in which only the third scalar generation is light whereas the first two are kept heavy [64]. This allows to kept radiative corrections in the Higgs mass under control, as this is precisely the stops, which couple dominantly to the Higgs, which are kept light. Furthermore, this paradigm is also well motivated by the fact that the LHC has not discovered s-partners so far. This implies that, if SUSY is realized in nature, the scalar spectrum is probably quite heavy. Hence, a natural spectrum seems a quite pragmatic solution to explain that SUSY has not been yet discovered if, at low scale, the MSSM, or any -not too far from minimality- extension of it can stabilize, at least partially, the electroweak scale.

2.5.3 A glance at the MSSM mass spectrum

Disclaimer: In this section, we do not aim at giving an exhaustive description of all matter sectors within the MSSM but rather at illustrating the mixing mechanisms at work on the specific example of the neutralinos. The other sectors (squarks, sleptons, Higgs...) will be described in this work whenever necessary.

After EWSB, the different gauge eigenstates of the MSSM will mix among each other to propagating mass eigenstates if the quantum numbers which distinguish them refer to broken symmetries. For example, the s-partners of the neutral weak and Higgs bosons $\widetilde{H}_u^0, \widetilde{H}_d^0, \widetilde{B}^0, \widetilde{W}^0$ can only be distinguish by the third component of the weak isospin[11]. But, after EWSB, the $SU(2)_L$ symmetry is broken. Hence, these four gauge eigenstates mix each other and give rise to four mass eigenstates called *neutralinos* and noted $\widetilde{\chi}_i$, $i = 1, 2, 3, 4$. Specifically, if we define the gauge eigenstate basis as $\psi^0 = \left(\widetilde{B}, \widetilde{W}^0, \widetilde{H}_d^0, \widetilde{H}_u^0\right)$, the neutralino mass term in the MSSM Lagrangian is:

$$\mathcal{L}_{\widetilde{\chi}_i}^{mass} = -\frac{1}{2}\left(\psi^0\right)^T M_{\widetilde{\chi}} \psi^0 + \text{ h.c} \tag{2.63}$$

where the hermitian mass matrix $M_{\widetilde{\chi}}$ can be parameterized as:

$$M_{\widetilde{\chi}} = \begin{pmatrix} M_1 & 0 & -c_\beta s_W m_Z & s_\beta s_W m_Z \\ 0 & M_2 & c_\beta c_W m_Z & -s_\beta c_W m_Z \\ -c_\beta s_W m_Z & c_\beta c_W m_Z & 0 & -\mu \\ s_\beta s_W m_Z & -s_\beta c_W m_Z & -\mu & 0 \end{pmatrix} \tag{2.64}$$

with $c_\beta \equiv \cos(\beta)$, $s_\beta \equiv \sin(\beta)$, $c_W \equiv \cos(\theta_W)$, $s_W \equiv \sin(\theta_W)$. Here we have to define a very useful MSSM parameter, the β angle defined through $\tan(\beta) \equiv \frac{v_u}{v_d}$ with $v_u = \langle H_u^0 \rangle$ and $v_d = \langle H_d^0 \rangle$ the VEVs

[11] Explicitly the T^3 eigenvalues of these eigenstates are: $T^3(\widetilde{H}_u^0) = -\frac{1}{2}$, $T^3(\widetilde{H}_d^0) = +\frac{1}{2}$, $T^3(\widetilde{B}^0) = 1$, $T^3(\widetilde{W}^0) = +3$.

of the neutral components of the two MSSM Higgs doublets. M_1 and M_2 are just the soft gaugino mass terms and μ is the soft Higgs mass term of $\mathcal{L}_{soft}$ (see (2.59)). This mass matrix can be diagonalize by a 4×4 unitary matrix $Z_{\widetilde{\chi}^0}$ to obtain mass eigenstates defined as:

$$\begin{aligned} \widetilde{\chi}_i^0 &= (Z_{\widetilde{\chi}^0})_{ij} \psi_j^0 \\ Z_{\widetilde{\chi}^0}^* M_{\widetilde{\chi}} Z_{\widetilde{\chi}^0} &= \text{diag}\left(m_{\widetilde{\chi}_1^0}, m_{\widetilde{\chi}_2^0}, m_{\widetilde{\chi}_3^0}, m_{\widetilde{\chi}_4^0}\right) \end{aligned} \tag{2.65}$$

where by construction the mass eigenstates $\widetilde{\chi}_i$ are mass-ordered i.e. $m_{\widetilde{\chi}_1^0} < m_{\widetilde{\chi}_2^0} < ... < m_{\widetilde{\chi}_4^0}$. Thus, usually $\widetilde{\chi}_1^0$ is the LSP and the classic dark matter candidate in most spectra, unless there is a lighter gravitino or $\mathcal{R}$-parity is not conserved. It is interesting to point out that M_3, the gluino soft mass, has not appeared in $M_{\widetilde{\chi}}$. Indeed, as s-particles share the same quantum numbers as their SM counterparts, if M_3 would have appeared in $M_{\widetilde{\chi}}$, the $SU(3)_C$ would have been broken which is unacceptable. Note also, that one can always use phase redefinitions on $\widetilde{B}$ and $\widetilde{W}$ to set M_1 and M_2 real and positive. $\langle H_u^0 \rangle$ and $\langle H_d^0 \rangle$ can also be render real and positive by using the freedom we have in setting the vacuum alignment direction in the Higgs potential. The phase of μ cannot be rotated away in the same way. Nevertheless, it is usual to assume μ real to avoid too large CP violating effects such as electric dipole moments in the electron or in the neutron. However, the sign of μ will remain unconstrained and is thus a true physical parameter.

We want to end this section by giving a few definitions which will be useful in the next chapters. After $M_{\widetilde{\chi}}$ has been diagonalized, each mass eigenstate $\widetilde{\chi}_i^0$ is truly a superposition of the different Higgsinos and gauginos:

$$\widetilde{\chi}_i^0 = (Z_{\widetilde{\chi}^0})_{i1} \widetilde{B}^0 + (Z_{\widetilde{\chi}^0})_{i2} \widetilde{W}^0 + (Z_{\widetilde{\chi}^0})_{i3} \widetilde{H}_d^0 + (Z_{\widetilde{\chi}^0})_{i4} \widetilde{H}_u^0 \tag{2.66}$$

with $\forall i = 1, .., 4 \sum_{j=1}^4 |(Z_{\widetilde{\chi}^0})_{ij}|^2 = 1$ due to the unitarity of $Z_{\widetilde{\chi}^0}$. We say that $\widetilde{\chi}_i^0$ is more bino-like, wino-like or Higgsinos-like depending on which term dominates in the decomposition (2.66). For example, $\widetilde{\chi}_1^0$ is said bino-like if $|(Z_{\widetilde{\chi}^0})_{11}| \gg |(Z_{\widetilde{\chi}^0})_{21}|, |(Z_{\widetilde{\chi}^0})_{31}|, |(Z_{\widetilde{\chi}^0})_{41}|$.

Chapter 3

The SUSY-$SU(5)$ GUT model or the art to stick to minimality

In this chapter, we would like to give an introduction to one specific type of Supersymmetric Grand Unified theory, the one based on the simple Lie Group $SU(5)$. This Lie Group will play a crucial role in the subsequent chapters as all the phenomenological work which will be developed in the rest of this thesis will assume an underlying $SU(5)$ internal symmetry at the GUT scale. This chapter is organized as follows. The first section, sec. 3.1 is somehow complementary to sec. 1.6. Indeed, in this section, we will develop some additional limitations of the SM that SUSY/GUT are specifically able to address. Furthermore, the motivations to pick $SU(5)$ as a grand unified group will be also investigated. In section 3.2, the structure of $SU(5)$ and its associate field content will be presented. Finally, section 3.3 is going to be devoted to the presentation of a few important consequences that follow from SUSY/GUT models. In particular, and also the main focus of this thesis is not on this issue, the question of the instability of the proton will be briefly sketched. As we are not going to provide an exhaustive introduction to group theory, the interested reader is invited to refer to the references [65] for further details.

3.1 Introduction

Motivations for GUTs: As already stated, the purpose of a Grand Unified Theory is to embed the SM gauge group G_{SM} in a larger Grand Unified (GU) group. This embedding enforces the equality of the three SM gauge couplings at a very high scale $g_1 = g_2 = g_3 \equiv g_{GUT}$. But Grand Unified Theories have also others virtues. Indeed, we were not completely exhaustive when we have discussed the limitations of the SM in section 1.6 and there are at least two more questions that the SM is not able to address on which we would like to shed light here.

First, there is the question of charge quantization. Mathematically, any eigenvalue is possible for an abelian $U(1)$ group and thus, it is not clear why in the SM the electric and hyper charges are quantized in units of $\frac{1}{3}$. The second reason concerns *gauge anomalies*. Indeed, we have already mentioned that gauge anomalies appear when an internal symmetry group is broken at the quantum

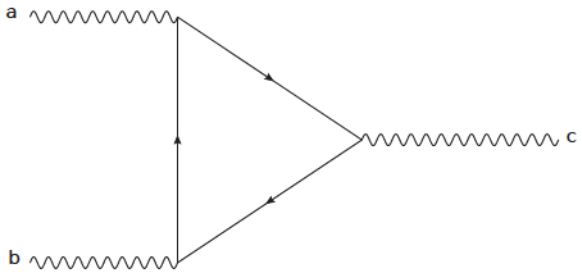

Figure 3.1 – Anomalous triangle diagram in the SM.

level, when computing radiative corrections, although the tree level Lagrangian respects the symmetry. In the SM, gauge anomalies appear and can be computed through the triangle diagram depicted on fig. 3.1. For a gauge group with generators T^a, this diagram is proportional to:

$$\mathcal{A}^{abc} = \mathrm{Tr}\left[T^a, \{T^b, T^c\}\right] \tag{3.1}$$

where every field configuration has to be computed. In the SM, eq. (3.1) is simply proportional to the sum of the fermion electric charges in one generation. As it turns out, the gauge anomalies seem to miraculously disappear in the SM due to a precise cancellation between the electric charges of the leptons and the quarks in each generation. Clearly, the two puzzles described above seem a-priori related. Indeed, one can hope that a theory able to explain why the electric charges are quantized the way they are could simultaneously address the question of anomaly cancellation within a SM family. In fact, this is not the case every time. For instance, the $SU(5)$ GUT adress the former even though anomaly cancellation still looks miraculous. Going to a higher rank (see below) GU group, for instance $SO(10)$, allows however to lift these cancellations to an intrinsic feature.

Why should we pick SU(5) as the GU group? Historically, the first attempt to build a GUT was due to J. Pati and A. Salam in 1974 [66]. Their theory was based on the internal group $SU(4)_C \times SU(2)_L \times SU(2)_R$. The original idea was to embed the quarks and leptons of a given family in a unique representation where the charged lepton was seen as the "fourth" color. However, one can immediately see that this GUT is not really one. Indeed, even with a discrete symmetry relating the two $SU(2)$, the Pati-Salam Group still implies at least two independent coupling constants. Thus, it does not reach the goal of unifying all SM gauge interactions. It is hence desirable to obtain a simple group capable of unifying all SM gauge couplings into one. But, which Lie Group should we use? First, if one wants to embed G_{SM} in a larger group, one needs a group with a rank at least equal to the one of G_{SM}, which is 4. We recall here, that the rank of a Lie Group is defined as the maximal number of generators which can be diagonalized simultaneously. These have to be diagonal due to Schur Lemna (see [65]) and, in the case of interest, these correspond to T^3, the third generator of $SU(2)$, T^3 and T^8 -the third and eight generator of $SU(3)$- and Y, the hypercharge generator. There are 9 simple or semi-simple Lie Groups of rank 4 that could potentially do the job. The first constraint that will help restrict further this set of candidates is that the GU group should obviously include $SU(3)$ as one of its subgroups. Second, as it has already been pointed out, particles and anti-particles transform differently in the SM. Hence, the GU group should own *complex representations* able to accomplish this distinction. One is then left with $SU(5)$ as the only simple group able to fulfill these requirements.

The first non-SUSY $SU(5)$ GUT was originally proposed by S. Glashow and H. Georgi in 1974 [67]. This model belongs to past now, as it has been excluded by precise LEP gauge coupling measurements [68]. From a theoretical point of view, this is not a big deal though. Indeed, we have seen in section 2.1 that the unification of gauge couplings works way better in the MSSM than in the SM anyway. It is thus natural to supersymmetrize the now ruled out non-SUSY Glashow-Georgi model. Beside, this embedding can be done in a quite straightforward manner. Just promote every SM field to a superfield and use two Higgs doublets instead of one to avoid gauge anomalies. This being established, the minimal supersymmetric $SU(5)$ model [69] has to be seen as the prototype of SUSY Grand Unified theory. In this sens, it constitutes a laboratory to study the consequences of embedding the SM gauge group in a higher rank group at very high scale. Of course, as all prototypes, it has flaws. Maybe, the best known of them is that SUSY/GUTs and, specifically the minimal SUSY $SU(5)$ predicts proton decay with a substantial rate [69] which highly restricts its parameter space. However, additional mechanisms exist and can be added to the core model to push the proton lifetime beyond lower bounds provided by current experiments. We will give some details about one of them in the rest of this chapter.

3.2 Introduction to $SU(5)$ and field content

After this general introduction, we would like to give more formal details about the SUSY $SU(5)$ theory. Although the model is ruled out by now, it will be helpful to discuss the $SU(5)$ structure and field content in the non-SUSY case. This will allow to easily supersymmetrize it in the second part of this section.

3.2.1 The Glashow-Georgi model:

Following [6], we recall that a general tensor $\Psi^{ij\cdots}_{kl\cdots}$ transforms under an $SU(N)$ rotation as:

$$\psi^{ij\cdots}_{kl\cdots} \to U^i_m U^j_n U^s_k U^t_l \cdots \psi^{mn\cdots}_{st\cdots} \tag{3.2}$$

where all indices run from 1 to N. The $N \times N$ unitary matrices U^i_m are given by:

$$[U]^i_m = [\exp(i\alpha^a T^a)]^i_m \,. \tag{3.3}$$

An $SU(N)$ group has N^2-1 generators represented by the hermitian and traceless matrices $T^a = \frac{\lambda^a}{2}$ ($a = 1 \cdots N^2-1$) where the λ_a are generalized Gell Mann matrices normalized to $\mathrm{Tr}\left(\lambda^a\lambda^b\right) = 2\delta^{ab}$. In the case of $SU(5)$, these $5^2-1 = 24$ generalized Gell-Mann matrices are, for example:

$$\lambda^3 = \begin{pmatrix} 0 & & & & \\ & 0 & & & \\ & & 0 & & \\ & & & 1 & \\ & & & & -1 \end{pmatrix}, \qquad \lambda^0 = \frac{1}{\sqrt{15}} \begin{pmatrix} 2 & & & & \\ & 2 & & & \\ & & 2 & & \\ & & & -3 & \\ & & & & -3 \end{pmatrix}. \tag{3.4}$$

The $SU(3)_C \times SU(2)_L \times U(1)_Y$ decomposition is obtained by identifying the first three indices of an $SU(5)$ multiplet Ψ_i with color indices. These are conventionally noted with greek letters $\alpha, \beta = 1,2,3$. The remaining two weak-isospin indices are noted with latin letters $r, s = 4,5$. The hypercharge value follows then from the normalization of the generators (see section 3.3).

One can show from the SM fermion content (1.11) that all fields of one family fit into two important representations of the $SU(5)$ group, namely the 5-dimensional (anti-)fundamental representation $\overline{\mathbf{5}}$ and the 10-dimensional antisymmetric representation $\mathbf{10} = [\mathbf{5} \times \mathbf{5}]_a$. $\overline{\mathbf{5}}$ contains the down-type anti-quark and the leptons:

$$\overline{\mathbf{5}} = \left(\overline{\mathbf{3}},\, \mathbf{1}, \frac{1}{3}\right) \oplus \left(\mathbf{1},\, \overline{\mathbf{2}}, -\frac{1}{2}\right) = (d^c_R,\, d^c_B,\, d^c_G,\, e,\, -\nu)^T_L = \begin{pmatrix} d^c \\ \epsilon_2 L \end{pmatrix} \tag{3.5}$$

whereas $\mathbf{10}$ contains the quark doublet, the up-type anti-quark singlet and the charged anti-lepton singlet:

$$\begin{aligned} \mathbf{10} = [\mathbf{5} \times \mathbf{5}]_a &= \left(\overline{\mathbf{3}}, \mathbf{1}, -\frac{2}{3}\right) \oplus \left(\mathbf{3}, \mathbf{2}, \frac{1}{6}\right)_a \oplus (\mathbf{1}, \mathbf{1}, 1) \\ &= \frac{1}{\sqrt{2}} \left(\begin{array}{ccc:cc} 0 & -u^c_G & u^c_B & -u_R & -d_R \\ u^c_G & 0 & -u^c_R & -u_B & -d_B \\ -u^c_B & u^c_R & 0 & -u_G & -d_G \\ \hdashline u_R & u_B & u_G & 0 & -e^c \\ d_R & d_B & d_G & e^c & 0 \end{array}\right)_L = \begin{pmatrix} \epsilon_3 u^c & Q \\ -Q^T & \epsilon_2 e^c \end{pmatrix} \end{aligned} \tag{3.6}$$

where the subscript a indicates that one has to pick the antisymmetric part of the representation. The lower indices R, B, G refer to the color of the quark (Red, Blue, Green). All fields have been taken left-handed thanks to the charge conjugation trick $(\Psi_R)^c = C\Psi_R = (\Psi^c)_L \equiv \Psi^c_L$ with $C = i\gamma_2\gamma_0$, the 4×4 Dirac charge conjugation matrix. Note that in the last step of eqs (3.5) and (3.6), we have used a shorthand notation where $\epsilon_2 \equiv i\sigma_2$ (resp: ϵ_3) is the 2D (resp: 3D) Levi-Civita antisymmetric tensor. Most generally in what follows, ϵ_n will be understood to be the n-dimensional antisymmetric tensor with the convention $\epsilon_{12\cdots n} \equiv +1$.

The gauge bosons live as usual in the adjoint representation of the group. For $SU(5)$, this is a **24** which decomposes under G_{SM} as:

$$\mathbf{24} = (\mathbf{8},\mathbf{1},0) \oplus (\mathbf{1},\mathbf{3},0) \oplus (\mathbf{1},\mathbf{1},0) \oplus (\mathbf{3},\mathbf{2},-\frac{5}{6}) \oplus (\overline{\mathbf{3}},\mathbf{2},\frac{5}{6}) \tag{3.7}$$

This representation contains the gluons, the W bosons and B boson in its decomposition. Moreover, the adjoint **24** introduces also 12 more bosons which are not present in the SM. These transform as :

$$A_\alpha^r = (\mathbf{3},\mathbf{2}) \text{ and } A_r^\alpha = (\overline{\mathbf{3}},2) \tag{3.8}$$

under $SU(3)_C \times SU(2)_L$. These extra gauge bosons are commonly named X and Y and noted:

$$A_\alpha^r = (X_\alpha, Y_\alpha)\,, A_r^\alpha = \begin{pmatrix} X^\alpha \\ Y^\alpha \end{pmatrix} \tag{3.9}$$

These gauge bosons, due to their internal quantum number assignment -X and Y are scalars which own both non-vanishing color and electric charges-, violate Lepton and Baryon number, thus opening proton decay channels (see sec 3.3). Specifically, their electric charges are equal to:

$$Q_X = -\frac{4}{3},\ Q_Y = -\frac{1}{3} \tag{3.10}$$

Finally, all these bosons can be merged into a single object if one decomposes an element of the adjoint representation over the basis of the generators:

$$A_\mu = \sum_{\alpha=1}^{24} A_\mu^\alpha T^\alpha = \frac{1}{\sqrt{2}} \left(\begin{array}{ccc:cc} & & & X_{R\mu}^* & Y_{R\mu}^* \\ & \frac{1}{\sqrt{2}}\sum_{a=1}^{8} G_\mu^a \lambda^a & & X_{B\mu}^* & Y_{B\mu}^* \\ & & & X_{G\mu}^* & Y_{G\mu}^* \\ \hdashline X_{R\mu} & X_{B\mu} & X_{G\mu} & \frac{1}{\sqrt{2}}W_\mu^3 & W_\mu^+ \\ Y_{R\mu} & Y_{B\mu} & Y_{G\mu} & W_\mu^- & -\frac{1}{\sqrt{2}}W_\mu^3 \end{array}\right) + \frac{B_\mu}{2\sqrt{15}} \begin{pmatrix} -2 & & & & \\ & -2 & & & \\ & & -2 & & \\ & & & 3 & \\ & & & & 3 \end{pmatrix} \tag{3.11}$$

where λ^a are the -$SU(3)$- Gell-Mann matrices and G_μ^a the eight gluon fields.

3.2.2 The Yukawa sector

To write Yukawa interactions in $SU(5)$ theories, two fundamental representations conjugated from each others are needed to form gauge invariant terms:

$$\mathbf{5}_H = \begin{pmatrix} T \\ H \end{pmatrix},\ \mathbf{5}_H^* = \begin{pmatrix} T^* \\ H^* \end{pmatrix} \tag{3.12}$$

where $H = \begin{pmatrix} H^+ \\ H^0 \end{pmatrix}$ is the usual SM Higgs doublet and T is a color triplet transforming as $(\mathbf{3},\mathbf{1})$ under $SU(3) \times SU(2)$. Note that T and T^* are extremely dangerous as they will open decay channels for the proton. To protect the proton from decaying too quickly, we will need to find a way to dynamically set the triplet masses at the GUT scale as it will be described in subsubsection 3.2.4.1. The most general $SU(5)$ Yukawa Lagrangian is then:

$$\mathcal{L}_Y = \mathbf{5}_F^c Y_5 \mathbf{10}_F \overline{\mathbf{5}}_H + \frac{1}{8}\epsilon_5 \mathbf{10}_F Y_{10} \mathbf{10}_F \mathbf{5}_H \tag{3.13}$$

where Y_5 and Y_{10} are matrices in generation space and the optional factor $\frac{1}{8}$ has been here taken for convenience.

We now have a look at each of the two terms in eq. (3.13), starting with the first one. We are interested in the coupling of the fermions with the light SM Higgs field, so this term can be rewritten as (see eqs (3.5) and (3.6)):

$$\begin{aligned} \mathbf{5}_F^c Y_5 \mathbf{10}_F \mathbf{5}_H^* &= \left(d^c - L\epsilon_2\right) Y_5 \begin{pmatrix} \epsilon_3 u^c & Q \\ -Q^T & \epsilon_2 e^c \end{pmatrix} \begin{pmatrix} T^* \\ H^* \end{pmatrix} \\ &\to d^c Y_5 Q H^* + L Y_5 e^c H^*. \end{aligned} \tag{3.14}$$

Rewritting the second term of eq. (3.14) as :

$$LY_5 e^c H^* = e^c Y_5^T L H^* \tag{3.15}$$

lead to the most well-known $SU(5)$ prediction:

$$Y_D = Y_E^T \tag{3.16}$$

i.e. that the Yukawa matrices in the charged lepton and down quark sectors are transposed from each other. Note that this relation is only valid at the GUT scale and one still has to evolve it down to the weak scale, where experiments are run, by RGEs. It turns out that this unification works relatively well for the third generation but it completely fails for the lighter first and second generations (see [70]). This problem can be overcome by adding either scalar multiplets [71] or Planck suppressed higher dimensional operators [69] [72]. We want to stress here that adding higher dimensional operators to the $SU(5)$ model should not be seen as a renouncement of minimality. Indeed, these operators would arise when integrating out degrees of freedom with masses lying between the GUT and Planck scales. But, a Grand Unified theory being itself an effective theory -it does not include gravity-, a GUT is not relevant to describe the dynamic between M_{GUT} and M_{Planck} where certainly, new physics must appear to properly handle the quantum effects of gravity.

Back to the second term in eq. (3.13), we see that it contains the 5D Levi-Civita tensor. Moreover, since this term is symmetric when we switch the two $\mathbf{10}_F$, only the symmetric part of Y_{10} survives. Hence, Y_{10} is symmetric as well. If we make the indices reappear, this term takes the form:

$$\epsilon_5 \mathbf{10}_F Y_{10} \mathbf{10}_F \mathbf{5}_H = \epsilon_{ijklm} \left(\mathbf{10}_F\right)^{ij} Y_{10} \left(\mathbf{10}_F\right)^{kl} \left(\mathbf{5}_H\right)^m \tag{3.17}$$

Using our convention to split the indices in color and electroweak indices, eq. (3.17) can be expanded to:

$$\begin{aligned} (3.17) \rightarrow & \, 2\epsilon_{\alpha\beta\gamma rs} \left(\mathbf{10}_F\right)^{\alpha\beta} Y_{10} \left(\mathbf{10}_F\right)^{\gamma r} \left(\mathbf{5}_H\right)^s \\ & + 2\epsilon_{\gamma r\alpha\beta s} \left(\mathbf{10}_F\right)^{\gamma r} Y_{10} \left(\mathbf{10}_F\right)^{\alpha\beta} \left(\mathbf{5}_H\right)^s \\ & = 2\epsilon_{\alpha\beta\gamma rs} \left(\mathbf{10}_F\right)^{\alpha\beta} \left(Y_{10} + Y_{10}^T\right) \left(\mathbf{10}_F\right)^{\gamma r} \left(\mathbf{5}_H\right)^s . \end{aligned} \tag{3.18}$$

The factor 2 comes from the two possibilities, $\left(\mathbf{10}_F\right)^{\gamma r}$ and $\left(\mathbf{10}_F\right)^{r\gamma}$. Clearly, we have $\epsilon_{\alpha\beta\gamma rs} = \epsilon_{\alpha\beta\gamma}\epsilon_{rs}$ so:

$$\begin{aligned} & 2\epsilon_{\alpha\beta\gamma}\epsilon^{\alpha\beta\delta} u_\delta^c \left(Y_{10} + Y_{10}^T\right) Q^{\gamma a} \epsilon_{rs} H^b \\ & = 4u_\delta^c \left(Y_{10} + Y_{10}^T\right) Q^{\delta r} \epsilon_{rs} H^s \end{aligned} \tag{3.19}$$

Finally, returning to an index free notation:

$$\frac{1}{8}\epsilon_5 \mathbf{10}_F Y_{10} \mathbf{10}_F \mathbf{5}_H = \frac{1}{2} u^c \left(Y_{10} + Y_{10}^T\right) Q H \tag{3.20}$$

leads to a symmetric up Yukawa matrix:

$$Y_U = Y_U^T . \tag{3.21}$$

This relation, and in particular its generalizations in the SUSY case to soft terms (see subsection 3.2.4), will play a central role in this thesis and its phenomenology will be extensively studied in the next chapters.

3.2.3 Spontaneous SU(5) symmetry breaking

Obviously, in order to be consistent with low energy data, the GU group needs to be broken down to the SM gauge group by a generalization of the Higgs mechanism described in subsection 1.4.1. To do this, a Higgs field $\mathbf{24}_H$ in the adjoint 24-dimensional representation can be used. If we impose a discrete symmetry $\mathbf{24}_H \rightarrow -\mathbf{24}_H$ which forbids cubic-terms -which would make the scalar potential unbounded from below- the most general $SU(5)$-symmetric Higgs potential takes the form:

$$V\left(\mathbf{24}_H\right) = -\frac{1}{2} m_1^2 \mathrm{Tr}\left(\mathbf{24}_H\right) + \frac{1}{4} a \left(\mathrm{Tr}\left(\mathbf{24}_H^2\right)\right)^2 + \frac{1}{2} b \mathrm{Tr}\left(\mathbf{24}_H^4\right) . \tag{3.22}$$

This potential has the following minimum if $b > 0$ and $a > -7/15b$:

$$\langle 0|\mathbf{24}_H|0\rangle = \text{diag}\,(2,2,2,-3,-3)\,v = v\lambda_0 \tag{3.23}$$

where v is related to m_1, a and b (see eq. (3.22)) by:

$$v^2 = 2m_1^2/\,(15a+7b)\,. \tag{3.24}$$

Note that the adjoint has taken a VEV in the λ_0 direction $\langle 0|\mathbf{24}_H|0\rangle \propto v\lambda_0$ (see eq. (3.4)). This guarantees that this VEV leaves the SM gauge group G_{SM} unbroken as it should be. In a second stage, the breaking of the electroweak symmetry has to be triggered. To do so, we need the two scalars 5-plets of subsection 3.2.2, the Higgs ϕ^4 potential can then be written :

$$V\,(H) = -\frac{\mu^2}{2}\mathbf{5}_H^*\mathbf{5}_H + \frac{\lambda}{4}\left(\mathbf{5}_H^*\mathbf{5}_H\right)^2 \tag{3.25}$$

where $\mathbf{5}_H$ takes a neutral VEV in the SM Higgs doublet direction:

$$\langle \mathbf{5}_H\rangle = \begin{pmatrix} 0 \\ 0 \\ 0 \\ 0 \\ \frac{v_0}{\sqrt{2}} \end{pmatrix},\ v_0^2 = \frac{2\mu^2}{\lambda}. \tag{3.26}$$

We will see later that, in order to stabilize the proton, we need a strong hierarchy between the two VEVs $v \gtrsim 10^{12}v_0$.

Eventually, a mixing term between the scalars $\mathbf{24}$ and $\mathbf{5}$ can also be added to the potential:

$$V\,(\mathbf{24}_H, \mathbf{5}_H) = \alpha \mathbf{5}_H^*\mathbf{5}_H \mathbf{Tr}\left(\mathbf{24}_H^2\right) + \beta \mathbf{5}_H^*\mathbf{\Phi}^2\mathbf{5}_H. \tag{3.27}$$

However as $\mathbf{24}_H$ and $\mathbf{5}_H$ are now coupled, $\langle \mathbf{24}_H\rangle$ also breaks the electroweak symmetry. But,in any cases $SU(3)_C$ has to be left intact in the low energy theory. One can then try to give a VEV to $\mathbf{24}_H$ in a direction slightly away from the SM neutral direction. One then look for solutions of the form:

$$\langle \mathbf{24}_H\rangle = \text{diag}\left(v, v, v, \left(-\frac{3}{2} - \frac{\epsilon}{2}\right)v, \left(-\frac{3}{2} - \frac{\epsilon}{2}\right)v\right) \tag{3.28}$$

where ϵ parameterized the deviation from the λ_0 SM neutral direction. Beside, we know that in the limit where no $\mathbf{24}_H - \mathbf{5}_H$ mixing is present i.e. if $\alpha = \beta = 0$, ϵ must vanish. The solution which satisfies these criteria looks like:

$$\epsilon = \frac{3}{20}\frac{\beta v_0^2}{bv^2} + \mathcal{O}\left(\frac{v_0^4}{v^4}\right) \tag{3.29}$$

Given that $v \sim \mathcal{O}\,(M_{GUT})$ and $v_0 \sim (M_W)$, the breaking of $SU(2)$ due to $\langle \mathbf{24}_H\rangle$ is much smaller than the one due to $\langle \mathbf{5}_H\rangle$. If we recompute the value of m_1^2 (the $\mathbf{24}_H$ mass parameter, see eq. (3.22)) and of μ^2, we end up with:

$$m_1^2 = \frac{15}{2}av^2 + 7\frac{15}{2}bv^2 + \alpha v_0^2 + \frac{9}{30}\beta v_0^2 \tag{3.30}$$

and

$$\mu^2 = \frac{1}{2}\lambda v_0^2 + 15\alpha v^2 + \frac{9}{2}\beta v^2 - 3\epsilon\beta v^2. \tag{3.31}$$

However, here we are confronted to a strong hierarchy problem similar to what was discussed in subsection 1.6.1. Indeed, we know that μ, the SM Higgs doublet mass parameter, has to be of the order of the weak scale $\mu \sim \mathcal{O}(M_W)$. But, looking at the right hand side of eq. (3.31), we see that, without imposing any constraint on α nor β, the natural thing to do to achieve such cancellation would be to set v at a value of the order of v_0 i.e. $v \sim v_0$.

But, this would completely destroy the model as one needs precisely a strong hierarchy between the two scales $v_0 \sim \mathcal{O}(M_W)$ and $v \sim \mathcal{O}(M_{GUT})$ to lead to an acceptable phenomenology. To avoid to spoil this hierarchy we need to tune α and β to one part in $\left(\frac{v^2}{v_0^2}\right) \sim 10^{24}$.

This extremely accurate tuning of the free parameters seems most likely to teach us that the theory at hand is incomplete. One then needs to introduce a more general framework in which these parameters would not have to be tuned so precisely. As we have argued in the last chapter, SUSY might constitute a solution to this problem. Beside, as already pointed out, the minimal $SU(5)$ non-SUSY GUT is ruled out anyway both by gauge couplings measurements -roughly, not enough d.o.fs are present in the spectrum when evolving the gauge couplings from M_{GUT} down to M_W to match the measured low energy values- and by a too high proton decay rate. SUSY helps for both problems as it doubles the number of d.o.fs in the spectrum and allows also to further suppress, at least partially, proton decay rate (see section 3.3). For these reasons, it is then natural to embed the $SU(5)$ GUT in a SUSY framework and that is what we are going to do now.

3.2.4 The SUSY SU(5) model

As stated in section 3.1, supersymmetrizing the Glashow-Georgi model is quite easy. Just promote every SM fermion (resp: boson) field to the corresponding chiral (resp: vector) superfield and introduce two independent Higgs superfields to enforce the holomorphy of the superpotential. Nonetheless, as this embedding will have strong consequences on the low energy phenomenology, we want to describe in this subsection the superpotential of the minimal SUSY-$SU(5)$ model in details.

We start with the Yukawa sector. Basically, its structure remains unchanged compared to the non-SUSY case. We need however two Higgs 5-plets $\mathbf{5}_H^u$ and $\mathbf{5}_H^d$ to cancel gauge anomalies. They contain the two MSSM Higgs doublets which give their masses to the up and down fermions, respectively. The Yukawa superpotential is then:

$$W_Y = \mathbf{5}_F^c Y_5 \mathbf{10}_F \mathbf{5}_H^d + \epsilon_5 \mathbf{10}_F Y_{10} \mathbf{10}_F \mathbf{5}_H^u \tag{3.32}$$

where all fields are chiral superfields and the subscript F indicates that the representation contains the associate matter (fermionic) multiplet of superfields. The symmetry relations on the Yukawa matrices derived in the non-SUSY case i.e. $Y_D = Y_E^T$ and $Y_U = Y_U^T$ are left unchanged in the SUSY version of the model. Even more, if we suppose that soft SUSY-breaking terms are generated above M_{GUT} and that the mediator of SUSY breaking is an $SU(5)$ singlet, two assumptions that are made in this thesis, one can show that these symmetry relations propagate to the soft terms of the MSSM eq. (2.59) (see [73]). Hence, with the notations of section 2.5, we have on the top of $Y_D = Y_E^T$ and $Y_U = Y_U^T$ also the following relations:

$$\begin{aligned} Y_D = Y_E^T \Rightarrow \begin{cases} M_D^2 = M_L^2 \\ A_D = A_E^T \end{cases} \\ Y_U = Y_U^T \Rightarrow \begin{cases} M_Q^2 = M_E^2 = M_U^2 \\ A_U = A_U^T \end{cases} \end{aligned} \tag{3.33}$$

Of all these relations, the last one will be interesting for us. Indeed, this thesis will be dedicated to the study of the low energy consequences of a GUT scale symmetric trilinear coupling in the up sector. We will give more details on this in the next chapters.

Back to the superpotential, although supersymmetrizing the Glashow-Georgi model helps with gauge couplings unification, it does not improve substantially the situation with regard to $Y_D = Y_E^T$. Then again, one has to add either higher dimensional operators or an extended Higgs sector to cure the bad mass relation and reconcile the minimal SUSY $SU(5)$ model with experiments ([74],[75]).

Now let us turn to the Higgs sector. The main change compared to the non-SUSY case is that the adjoint $\mathbf{24}_H$ has to be a complex multiplet in order to maintain an equal number of fermionic and bosonic d.o.fs within each supermultiplet. The superpotential for the adjoint $\mathbf{24}$ and the Higgs 5-plets takes then the form:

$$W(\mathbf{24}_H, \mathbf{5}_H) = M_{24}\mathrm{Tr}\left(\mathbf{24}_H^2\right) + \frac{\lambda}{3}\mathrm{Tr}\left(\mathbf{24}_H^3\right) + \alpha \mathbf{5}_H^d \mathbf{24}_H^2 \mathbf{5}_H^u \ + \mu \mathbf{5}_H^d \mathbf{5}_H^u. \tag{3.34}$$

$SU(5)$ will be broken to G_{SM} when $\mathbf{24}_H$ will take a VEV in the SM neutral direction:

$$\langle \mathbf{24}_H \rangle = \frac{2m'}{3\alpha} v \mathrm{diag}\left(1, 1, 1, -\frac{3}{2}, -\frac{3}{2}\right) \tag{3.35}$$

and the part of the now $SU(5)$ broken superpotential:

$$W = \mathbf{3}_H^d \mathbf{3}_H^u \left(\mu + \frac{2}{3}m'\right) + \mathbf{2}_H^d \mathbf{2}_H^u \left(\mu - m'\right) \tag{3.36}$$

will also suffer from a hierarchy problem similar to what was discussed in the non-SUSY case. Indeed, the breaking of $SU(5)$ to G_{SM} due to $\langle \mathbf{24}_H \rangle$ should both leave the MSSM Higgs doublets $\mathbf{2}_H^d$, $\mathbf{2}_H^u$ massless while sending the colored triplets $\mathbf{3}_H^d$, $\mathbf{3}_H^u$ at a mass of $\mathcal{O}(M_{GUT})$. This last condition is needed to stabilize the proton as it is the triplets which will mediate its decay. Formally, this doublet-triplet splitting can be achieved if we accept the tuning $\mu = m'$ (with μ, $\mu' \sim \mathcal{O}(M_{GUT})$). However, such conspiracy to keep the Higgs doublets exactly massless seems quite unsatisfactory and actually, models have been developed to achieve this more naturally. These models will unfortunately come at the price of dropping the minimality condition. Here, we want to describe the most known of them namely, the "missing partner mechanism" [76].

3.2.4.1 The missing partner mechanism

The idea behind the missing partner mechanism is to introduce in the superpotential a larger $\mathbf{50}$ representation that contains weak triplets but no doublets. Indeed, $\mathbf{50}$ decomposes under $SU(3) \times SU(2)$ as:

$$\mathbf{50} = (\mathbf{8},\mathbf{2}) \oplus (\mathbf{6},\mathbf{3}) \oplus \left(\overline{\mathbf{6}},\mathbf{1}\right) \oplus (\mathbf{3},\mathbf{2}) \oplus \left(\overline{\mathbf{3}},\mathbf{1}\right) \oplus (\mathbf{1},\mathbf{1})\,. \tag{3.37}$$

In fact, we need both $\mathbf{50}$ and $\overline{\mathbf{50}}$ to avoid gauge anomalies. We need also to extend the adjoint $\mathbf{24}$ to a $\mathbf{75}$ noted $\mathbf{\Sigma}$ in order to write $SU(5)$ invariant mixing terms between $\mathbf{5}_H^u$, $\mathbf{5}_H^d$ and $\mathbf{50}$, $\overline{\mathbf{50}}$.

The relevant part of the superpotential reads:

$$W = \frac{M}{2}\mathrm{Tr}\left(\mathbf{\Sigma}^2\right) + \frac{a}{3}\mathrm{Tr}\left(\mathbf{\Sigma}^3\right) + b\,\mathbf{50}\,\mathbf{\Sigma}\,\mathbf{5}_H^u + c\,\overline{\mathbf{50}}\,\mathbf{\Sigma}\,\mathbf{5}_H^d + \widetilde{M}\,\overline{\mathbf{50}}\,\mathbf{50} \tag{3.38}$$

where, and this is crucial, no mass term $\mathbf{5}_H^d \mathbf{5}_H^u$ is present. This is a direct consequence of the fact that the 50-dimensional representation does not contain any weak-doublet (see eq. (3.37)). $SU(5)$ will get broken to G_{SM} when Σ will get a VEV, $\langle \Sigma \rangle \sim \frac{M}{a}$. The resulting $SU(3) \times SU(2) \times U(1)$ invariant superpotential is:

$$W = \mathbf{3}_{\mathbf{50}}\frac{M\,b}{a}\,\mathbf{3}_H^u + \overline{\mathbf{3}}_{\mathbf{50}}\frac{M\,c}{a}\mathbf{3}_H^d + \widetilde{M}\overline{\mathbf{3}}_{\mathbf{50}}\mathbf{3}_{\mathbf{50}}, \tag{3.39}$$

where $\mathbf{3}_H^u$, $\mathbf{3}_H^d$ and $\mathbf{3}_{\mathbf{50}}$ are the $SU(3)$ triplets in the $\mathbf{5}_H^u$, $\mathbf{5}_H^d$ and $\mathbf{50}$ representations, respectively. We see here, that the Higgs colored triplets get a mass of order $M \sim \widetilde{M} \sim \mathcal{O}(M_{GUT})$ whereas the MSSM Higgs doublets remain massless. We have then achieved the goal of sending the triplets masses at the GUT scale while keeping the doublets massless without any fine-tuning of the parameters of the theory.

There is one caveat though. Indeed, one can show that having larger representations such as $\mathbf{50}$ or $\overline{\mathbf{50}}$ entering the RGEs of the theory breaks the perturbativity of the $SU(5)$ gauge coupling above the GUT scale. One has then to invoke a generalization of the mechanism described above, the "double missing partner mechanism" to guarantee both a solution to the doublet-triplet splitting problem and perturbativity of the GUT coupling up to the Planck scale (see [77] and [28]).

3.3 Physical consequences

In this section, we would like to review a few important consequences of GUTs which were already spotted in the previous sections. In particular, we are going to give some details on how fermion electric charges quantization follows naturally from a GU group and how this quantization is related to anomaly cancellations. We are also going to describe how proton decay channels open in GUTs and what are the conditions to push its lifetime high enough to enforce the stability of matter.

3.3.1 Charge quantization

We start with the question of fermion charge quantization. When the SM gauge group is embedded in a higher rank group, the electric and hyper charges are quantized because the eigenvalues of the generators of a non-abelian group are discrete. Beside, since the electric charge is an additive quantum number, it must be a linear combination of the diagonal generators of the GU group. We have mentioned previously that the number of diagonal generators of a group defines its rank. $SU(5)$ being of rank 4, it will have 4 diagonal generators. Clearly, Q has to commute with the generators of $SU(3)_C$, which is rank two. The only two diagonal generators which are left are $T^3 = \frac{\lambda_3}{2}$, the third component of the weak isospin, and $T^0 = \frac{\lambda_0}{2}$, the hypercharge generator.

We hence have:

$$Q = I^3 + \frac{Y}{2} = T^3 + cT^0 \tag{3.40}$$

where the normalization coefficient c can be obtained by comparing the eigenvalues of Y and T^0.

This leads to:

$$c = -\sqrt{\frac{5}{3}}. \tag{3.41}$$

which indeed yields to the correct electric charges for the fundamental representation:

$$Q\left(\mathbf{5}_F\right) = \begin{pmatrix} -\frac{1}{3} & & & & \\ & -\frac{1}{3} & & & \\ & & -\frac{1}{3} & & \\ & & & 1 & \\ & & & & 0 \end{pmatrix}. \tag{3.42}$$

The conjugate representation $\overline{\mathbf{5}}_F$ simply has opposite charges $Q\left(\overline{\mathbf{5}}_F^i\right) = -Q\left(\mathbf{5}_F^j\right)\delta_{ij}$. For a rank two tensor ψ , the electric charges can be calculated via:

$$\begin{aligned} Q\left(\psi_{ij}\right) &= Q_i + Q_j; \\ Q\left(\psi_i^j\right) &= Q_i - Q_j \end{aligned}. \tag{3.43}$$

One can show that for the fermionic ten-dimensional representation $\mathbf{10}_F$ or the adjoint $\mathbf{24}_H$, the electric charges are also correctly reproduced. Generalizations to higher order tensors of eq. 3.43 can be obtained in a similar manner.

Beside, in a GUT framework, also a relation between the color and electric charges emerges. Since the generators of $SU(N)$ are traceless, we get the relation:

$$N_c Q_d + Q_{e^c} = 0 \tag{3.44}$$

from eq. (3.42) where N_c is the number of colors. In $SU(3)_c$, $N_c = 3$, which enforces that the electric charges are quantized in unit of $\frac{1}{3}$. Hence, the pattern of gauge quantum numbers seems way less arbitrary when imposing a GU group than in the SM. We insist on the fact that the quantization of electric charges emerges only in the cases where the GU group is purely non-abelian. For instance, if $SU(5)$ is extended by a $U(1)$ factor as it is the case in flipped $SU(5)$ [78], electric charges do not have to be quantized anymore. However, a wide class of GUT models imply charge quantization as long as neutrinos are Majorana [79], which seems a reasonable assumption.

We now have a look at anomaly cancellations. In $SU(N)$ gauge theories, the SM anomaly eq. (3.1) simplifies to:

$$\mathcal{A}^{abc} = \mathrm{Tr}\left[t^a\{t^b, t^c\}\right] = \frac{1}{2}A\left(R\right)d^{abc} \tag{3.45}$$

where R is the representation at hand and f^{abc} are the constant structures of the group. $A(R)$ is independent of the choice of generators so that we are free to use $t^a = t^b = t^c = Q$ without loss of generality. This gives us the anomaly ratio of matter content:

$$\frac{A\left(\overline{\mathbf{5}}_F\right)}{A\left(\mathbf{10}_F\right)} = \frac{\mathrm{Tr}Q^3\left(\overline{\mathbf{5}}_F\right)}{\mathrm{Tr}Q^3\left(\mathbf{10}_F\right)} = \frac{3(\frac{1}{3})^2 + (-1)^3 + 0}{3\left(-\frac{2}{3}\right)^3 + 3\left(\frac{2}{3}\right)^3 + 3\left(-\frac{1}{3}\right)^3 + 1^3} = -1 \tag{3.46}$$

which shows that gauge anomalies cancel out between the $\mathbf{10}_F$ and $\overline{\mathbf{5}}_F$ representations. However, in the minimal SUSY $SU(5)$ model, this cancellation seems also to occur accidentally, although extending the GU group to the next well motivated candidate, $SO(10)$, allows to lift this cancellation to an intrinsic feature.

3.3.2 Proton decay

In, the SM, the total baryon and lepton numbers are accidentally conserved. This implies that operators inducing proton decay are forbidden, and thus, to any order in perturbation theory. Hence, in the SM, the proton is perfectly stable. On the other hand, in GUTs, the Higgs and others SM bosons got embedded in larger matter representations. These new vector and scalar representations imply that more degrees of freedom are present in the spectrum of the theory as we have seen in the last sections. These new d.o.fs are also colored and generally own a non vanishing electric charge. Thus, nothing prevents the proton from decaying through the exchange of these new particles. Since proton decay has not been seen, it is hence important to push the proton lifetime beyond currents experimental limits. In order to do so, particles mediating its decay have to get super-heavy decoupling masses, typically, at a magnitude of a few order below the GUT scale. The doublet-triplet splitting missing partner mechanism of subsubsection 3.2.4.1 was designed exactly to do this task. Beside, as the mediators of proton decay have to lie near the GUT scale, one can integrate them out. This will result in the appearance of higher dimension effective operators. From there, two cases should be distinguished. In non-SUSY GUTs, the main contribution arises from dimension 5 operators generated when integrating out the X ($Q_X = \pm\frac{4}{3}$) and Y ($Q_Y = \pm\frac{1}{3}$) d.o.fs of the adjoint representation 24_H (see eqs. (3.8) and (3.11)). These baryon number violating operators are of the form:

$$\mathcal{L}^{d=6}_{\Delta B=1} = \frac{g^2}{2M_X^2}\epsilon_{\alpha\beta\delta}\left(\overline{u}^c\right)^\alpha \gamma_\mu Q^{\delta b}\left(\overline{e}^c\gamma^\mu\epsilon_{b\alpha}Q^{\beta a} + \left(\overline{d}^c\right)^\beta \gamma^\mu\epsilon_{ab}L^a\right) + \text{ h.c} \tag{3.47}$$

where M_X is the common superheavy mass of the X and Y bosons. $\mathcal{L}^{eff}_{\Delta B=1}$ opens proton decay channels such as $p \to e^+\pi^0$ whose Feynman diagram is depicted on the left hand side of fig. 3.2. From this diagram, one can compute the proton decay rate which is equal to $\Gamma_p \sim 10^{-3}m_p^5/M_X^4$ with m_p, the mass of the proton. The 2012 PDG [25] gives $\tau_p > 10^{33}$ years, which leads to a lower bound on $M_X \geq 4\times 10^{15}$ GeV. The crucial point is that whereas in the SM case, the unification scale is relatively low $M_{GUT}^{SM} \sim 10^{14}$ GeV, in the SUSY case, this scale is pushed to $M_{GUT}^{SUSY} \sim 10^{16}$ GeV. We hence see that in the SM case, the lower bound on M_X allows to further exclude the minimal $SU(5)$ model whereas in the SUSY case, this bound can be accommodated thanks to the higher unification scale. In fact, in the SUSY case, new channels are open and dimension-6 operators will turn out to be sub-dominant, the main decay channels arising from lower dimensional effective operators. These dimension-5 operators are mediated by the exchange of superheavy colored Higgs triplets in the $\mathbf{5}^u_H$, $\mathbf{5}^d_H$ representations (see eq. (3.12)) needed to break the electroweak symmetry. When integrating out T^u and T^d, the dimension-5 effective superpotential is:

$$W_{d=5} = \frac{1}{2M_T}\epsilon_3\left(QY_{10}Q\right)\left(QY_5^TL\right) + \frac{1}{M_T}\left(d^cY_5u^c\right)\left(u^cY_{10}e^c\right) \tag{3.48}$$

with M_T the common superheavy mass of the Higgs triplets.

An example of decay, $p \to K^+\bar{\nu}_\tau$, arising from $W_{d=5}$ is given on the right hand side of fig. 3.2. These decays are extremely dangerous as the corresponding rate is only suppressed by $1/M_T^2$ instead of $1/M_X^4$ as it is the case for dimension 6 operators. Dimensions 5 operators can hence lower significantly the proton lifetime generally highly restricting the parameter space of the minimal SUSY $SU(5)$ model ([69, 80]). This has even lead the authors of [81] to claim the exclusion of the minimal SUSY $SU(5)$ model. However, later analysis showed that this claim was premature. Indeed, one has to remember that the minimal renormalizable version of the SUSY $SU(5)$ model is ruled out anyway. As already pointed out, Planck suppressed higher dimensional operators are needed to cure the bad leptons-quarks mass relations. These Planck non-renormalizable operators can in turn help to increase the lifetime of the proton of several orders of magnitude, pushing it above currents limits [69, 81].

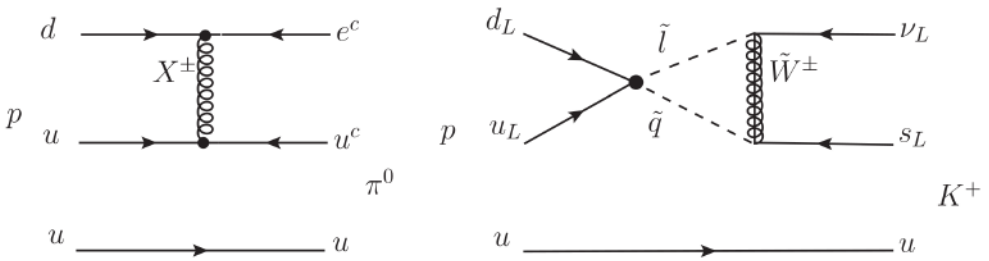

Figure 3.2 – Left: X and Y mediated dimension-6 proton decay $p \to e^+\pi^0$. Right: SUSY specific dimension-5 proton decay $p \to K^+\bar{\nu}_\tau$. On the right, the blob indicates the dimension-5 insertion that arises when integrating out the Higgs triplet fields.

We want to conclude this chapter by pointing out that until now, we had consciously omitted the question of neutrino masses. Indeed, the $\mathbf{10}_F$ and $\mathbf{5}_F$ representations cannot include right-handed neutrinos, making impossible to generate mass terms for them in a minimal way. It is thus clear that the $SU(5)$ model is crying for an extension. A first possibility is to assume that $\mathcal{R}$-parity is broken (see [82]). However, relaxing $\mathcal{R}$-parity conservation have dangerous phenomenological consequences. First, $\mathcal{R}$-parity violating terms can allow dark matter to decay, making it unstable. Second, these can mediate tree level proton decay through dimension-4 operators. These channels will decrease the proton lifetime dramatically. To avoid both problems, it seems that either additional discrete symmetries need to be invoked (see [83]) or a large hierarchy needs to be present in $\mathcal{R}$-parity violating couplings [84].

A second possibility is to extend the $SU(5)$ gauge group, to include the right handed neutrino as a gauge singlet, as it is for example the case in flipped $SU(5)$. In this context, it has even been suggested that dimension 6 operator contributions to proton decay can vanish if one imposes simple conditions on fermion mixing terms (see [85]). One can also extend the Higgs sector, for example by adding a second GUT breaking adjoint $\mathbf{24}'_H$ (see [28]). Lastly, one can also decide to extend the $SU(5)$ group to the next well motivated candidate for unification namely, $SO(10)$. Indeed, in $SO(10)$ all matter content of one family, including the right handed neutrino, gets unified into one 16-dimensional representation. One can then easily implement see-saw mechanisms (see subsubsection 1.4.2.2) allowing to generate naturally small neutrino masses in this framework.

Part II

New tests for SU(5)-like up-squarks

Chapter 4

Tasting the $SU(5)$ nature of supersymmetry at the LHC

In the last chapter, we have described the $SU(5)$ Grand Unified theory quite extensively. In particular, special care was given to the flavor sector where we have shown that the $SU(5)$ induced symmetry relations which hold in the Yukawa sector propagate to the soft terms in case of a supersymmetric theory.

In this chapter, we are going to show that this fact opens up intriguing possibilities to build relatively simple phenomenological tests on low scale SUSY spectra. The output of these tests will in turn indicate whether if the spectra point or not toward a high scale $SU(5)$-like dynamics.

Whereas most previous low energy studies where axed on the correlation of FCNC processes between the leptonic and hadronic sectors, our aim here is to stay confined within the up-squark sector where a new symmetry relation emerges, way more model independent.

Note that this chapter is inspired from the published references [86, 87].

4.1 Introduction

Unravelling whether or not Nature is $SU(5)$-symmetric at short distance constitutes a challenging open problem of particle physics. In particular, having clear evidence in favor of a GUT would allow to drastically reduce the number of free parameters in the SM. This will make the SM more predictive which is certainly something desirable from a theoretical point of view. But, as we have seen in the previous chapter, if a GUT is realized in nature the GU group definitely has to be broken at some very high scale, of the order of the unification scale $M_{GUT} \sim 10^{16}$ GeV, to be consistent with low energy data. We can be reasonably confident in the fact that future experiments will never be able, or at least not before a very long time, to directly probe such super high scale. If we want to have any chance to study the dynamics of a GUT, we hence have no choice but to evolve symmetric boundary conditions down to a low scale, where the symmetry is broken, either the weak or the SUSY scale accessible to experiments. We have already pointed out that the correct way to proceed to do so is by using the renormalization group equations which allow to evolve physical quantities with respect to the energy scale at which the theory is probed.

The problem is that, most probably if a $SU(5)$-like GUT is realized in nature, it has to be corrected by GUT scale threshold corrections and/or non-renormalizable operators arising from whatever extra degrees of freedom lie between M_{GUT} and M_{Planck}. These will in turn modify low energy predictions. But, in the present state of the art, we do not know exactly the scales at which these heavy degrees of freedom are supposed to manifest themselves. If the structure of a $SU(5)$ Grand Unified Theory predicts a certain symmetry relation between a set of observables to hold at M_{GUT}, for the above mentioned reasons, if we want to test this relation at M_{SUSY}, we have no choice but to make ad-hoc assumptions on the superheavy spectrum between M_{GUT} and M_{Planck} [88]. How sensitive the $SU(5)$-relation we want to test is to these assumptions will constitute a source of *model dependency*. Obviously, the less model dependent the relation is, the more robust the low scale predictions are.

Another source of theoretical uncertainty might also emerge from the differences in the inner structure of the RGEs governing the different observables one wants to evolve. For example, if a GUT implies an equality between two couplings λ and μ at M_{GUT} i.e. $\lambda(M_{GUT}) = \mu(M_{GUT})$ and that the RGEs of these two have widely different structure, for example if λ runs steeply whereas μ runs relatively smoothly, one can expect that the GUT scale equality will be spoiled quite severely at low scale. This might result in a higher model dependency with respect to the different threshold corrections which take a part in the running.

Let us take an example. We have already pointed out that $SU(5)$-like unification of matter fields predicts the relation $y_d = y_L^t$ between the Yukawa couplings of the down-type quarks and charged leptons to hold at M_{GUT}. If one wants to study the consequences of this unification at low energies, one has to evolve it down to M_{SUSY}. In fact, as the RGEs of the down quarks and charged leptons are fundamentally different - the two couplings belonging to two distinct flavor sectors- they will suffer from different renormalization effects and hence strong assumptions, for instance on the GUT scale spectrum, will have to be made in order to get testable predictions. This quark-lepton unification has been studied in different contexts quite extensively and a lot of literature exist on the subject (see [89] and references therein). However, according to our previous point, we see that this relation has a large model-dependency making the construction of generic $SU(5)$-tests quite an arduous task. It seems then, that a good testable GUT scale relation should both implies only couplings that stay confined within a given flavor sector, at least at tree level, and should also be left invariant under GUT threshold corrections.

In the rest of this chapter, we are going to point out that, in a SUSY context, beyond quark-lepton unification, generically $SU(5)$-like GUTs imply also a symmetry relation to hold within the up-type trilinear couplings, namely that these are symmetric at M_{GUT} i.e. that $A_U = A_U^T$. We will show that this relation is way less model dependent than quark-lepton unification relations. This being established, it will be possible to build relatively simple low energy tests to probe this $SU(5)$ symmetry relation for different squark spectra.

By "$SU(5)$-test", we will refer to a relation which encodes a correlation among different low scale observables, implied by a high scale $SU(5)$ symmetry. Obviously, a low scale $SU(5)$-test will never be "exact", the correlation among TeV scale observables being never rigorously preserved, a GUT scale symmetry is undeniably broken at scales accessible at colliders. Rather, we will develop a statistical method, based on a p-value test, to quantify with which significance one can asses a deviation in the $SU(5)$-test at hand, with respect to the limit case in which it would be exactly preserved at the TeV scale (see subsubsection 4.4.3.2). Thus, clearly, the methodology used in this chapter make that every $SU(5)$-test to be developed will be useful only to potentially reject the presence of a high scale $SU(5)$ symmetry, not to confirm it.

The rest of this chapter is organized as follows. Section 4.2 will be devoted to a general presentation of the up-squark sector in the context of SUSY-$SU(5)$ theories.

Section 4.3 will be dedicated to a phenomenological study of the $SU(5)$ GUT scale parameter space. We will show that in most of the parameter space, the discrepancies induced by the RGEs on our master relation $A_U = A_U^T$ remain small. As it will be needed in some cases, we will also show that, in the same manner, the discrepancies induced by the RGEs on the $SU(5)$ relation $M_Q^2 = M_U^2$ remain small as well. This will allow to treat the low-scale RGEs induced asymmetries as theoretical uncertainties.

Section 4.4 comprises the strategy and tools needed to setup $SU(5)$ tests at low energy. It includes in particular a new effective theory that we have developed to handle squark spectra presenting a sizable mass gap. Some elements of statistics will be given as well, useful for the tests that we are going to propose. We will then use these tools to build $SU(5)$ tests in various SUSY scenarios.

In section 4.5, we are going to propose $SU(5)$-tests in case where the SUSY scale is very high and all superpartners are decoupled. $SU(5)$ tests remain possible though indirectly, through SUSY-induced flavour-changing dipole operators on which we should give some details.

The second case to be developed in section 4.6 will be the one of natural SUSY spectra (see subsection 2.5.2) in which only the third scalar generation is accessible to the LHC. Depending on the

gauginos mass hierarchy, a test on stop flavour-violation involving charm tagging and a test involving top polarimetry are proposed.

Finally, in section 4.7, we will develop $SU(5)$ tests relying on Higgs detection in cascade decays considering spectra in which both stop-like squarks and scharm-like squarks are light. The conclusion will be given in section 4.8.

4.2 The up-type squark sector in $SU(5)$ theories

In this section, we are going to have a closer look at the up-type sector in SUSY theories as all $SU(5)$ tests to be developed in the next sections will involve, at least at tree level, observables confined to this sector. We start by a general presentation of the up-type squark mass spectrum. Then, we will discuss the relation to be exploited later, namely that the GUT scale up-type trilinear coupling is symmetric $A_U(M_{GUT}) = A_U^T(M_{GUT})$ in SU(5) theories. Finally, we will end with a qualitative discussion of the RGEs of the Yukawa and of the trilinear couplings. This will serve as a transition to the next section where the stability of $A_U = A_U^T$ will be tested against the RG flow.

4.2.1 The up-type squark mass spectrum

We start with a general presentation of the up-squark sector in the MSSM. For now, we want to focus on flavor mixing induced by soft terms, we hence neglect temporarily the diagonal and μ-electroweak corrections. We also define the following vectors: $\widetilde{u} = \left(\widetilde{u}_L\ \widetilde{c}_L\ \widetilde{t}_L\right)^T$ which contains the left up-squarks and $\widetilde{u}^c = \left(\widetilde{u}_L^c\ \widetilde{c}_L^c\ \widetilde{t}_L^c\right)^T$ which contains the left up anti-squarks. In all that follows, the interaction eigenstates will be noted with a superscript 0, for instance $\widetilde{u}^0$. With these assumptions, after electroweak symmetry breaking, the mass terms of the up-type squarks can be expressed as:

$$V_{squark} = \widetilde{u}^{0T} M_Q^2 \widetilde{u}^{0*} + \widetilde{u}^{0c\dagger} M_U^2 \widetilde{u}^{0c} + \widetilde{u}^{0c\dagger} A_u^\dagger \widetilde{u}^{0*} v_u + \widetilde{u}^{0T} A_u \widetilde{u}^{0c} v_u + \cdots \tag{4.1}$$

where v_u is the vev of the up-type Higgs doublet $\langle H_u \rangle = \begin{pmatrix} 0 & v_u/\sqrt{2} \end{pmatrix}^T$.

In matrix notation, eq. (4.1) gives:

$$V_{squarks} = \begin{pmatrix} \widetilde{u}^{0T} & \widetilde{u}^{0c\dagger} \end{pmatrix} \begin{pmatrix} M_Q^2 & \frac{v_u}{\sqrt{2}} A_u \\ \frac{v_u}{\sqrt{2}} A_u^\dagger & M_U^2 \end{pmatrix} \begin{pmatrix} \widetilde{u}^{0*} \\ \widetilde{u}^{0c} \end{pmatrix} \tag{4.2}$$

written in an interaction basis where the Yukawa matrix of the up-type quarks is not diagonal, such that:

$$\mathcal{L}_{Yuk} = v_u u^T Y_u u^c + \text{ h.c} + \cdots \tag{4.3}$$

In eq. (4.2), each element in the mass matrix is itself a 3×3 matrix. Note that left-handed antisquarks can be trade for right-handed squarks with a CP conjugation on the superfields. Beside, as the Lagrangian is real, it is possible to write $V_{squarks} = V_{squarks}^*$ and hence eq. (4.2) becomes:

$$V_{squarks} = \begin{pmatrix} \widetilde{u}_L^{0\dagger} & \widetilde{u}_R^{0\dagger} \end{pmatrix} \begin{pmatrix} M_Q^{2*} & v_u A_u^* \\ v_u A_u^T & M_U^{2*} \end{pmatrix} \begin{pmatrix} \widetilde{u}_L^0 \\ \widetilde{u}_R^0 \end{pmatrix} \tag{4.4}$$

where we have reintroduced explicitly chirality indices L/R. This gives the Yukawa Lagrangian:

$$\mathcal{L}_{Yuk} = \overline{u}_L v_u Y_u^* u_R + \text{ h.c. } + \cdots \tag{4.5}$$

The goal now is to express both the quarks and the squarks in terms of their mass eigenstates. This takes place in several steps. First, we start by rotating the quarks $u = (u\ c\ t)$ to their mass basis in which the Yukawa matrix Y_u is diagonal. We recall that Y_u can be diagonalized by a bi-unitary transformation:

$$\text{diag}\left(m_u, m_c, m_t\right) = V_{u_L} v_u Y_u^* V_{u_R}^\dagger \tag{4.6}$$

where V_{u_L} and V_{u_R} are the 3×3 unitary rotation matrices of the left and right-handed quarks. These define the quark mass eigenstate basis:

$$\begin{pmatrix} u_R \\ c_R \\ t_R \end{pmatrix} = V_{u_R} \begin{pmatrix} u_R^0 \\ c_R^0 \\ t_R^0 \end{pmatrix}, \quad \begin{pmatrix} u_L \\ c_L \\ t_L \end{pmatrix} = V_{u_L} \begin{pmatrix} u_L^0 \\ c_L^0 \\ t_L^0 \end{pmatrix}. \tag{4.7}$$

Another useful basis to work with when dealing with s-particles can be obtained by rotating the scalar gauge eigenstates $\left(\widetilde{u}^0\ \widetilde{c}^0\ \widetilde{t}^0\right)$ by exactly the same amount as their SM-counterparts:

$$\widetilde{u}_R^{SCKM} = \begin{pmatrix} \widetilde{u}_R \\ \widetilde{c}_R \\ \widetilde{t}_R \end{pmatrix} = V_{u_R} \begin{pmatrix} \widetilde{u}_R^0 \\ \widetilde{c}_R^0 \\ \widetilde{t}_R^0 \end{pmatrix}, \quad \widetilde{u}_L^{SCKM} = \begin{pmatrix} \widetilde{u}_L \\ \widetilde{c}_L \\ \widetilde{t}_L \end{pmatrix} = V_{u_L} \begin{pmatrix} \widetilde{u}_L^0 \\ \widetilde{c}_L^0 \\ \widetilde{t}_L^0 \end{pmatrix}. \tag{4.8}$$

This basis is known as the *Super-CKM* (or SCKM) basis. Here $\left(\widetilde{u}_L, \widetilde{c}_L, \widetilde{t}_L\right)$ are the superpartners of the physical mass eigenstates (u_L, c_L, t_L). Even though $\left(\widetilde{u}, \widetilde{c}, \widetilde{t}\right)_{L/R}$ are not mass eigenstates, it is very useful to work with squarks expressed in the SCKM basis when dealing with flavor violation, as all non-physical parameters of the CKM matrix have been rotated away. Beside, the supermultiplet structure is preserved as the scalar and fermionic component undergo the same rotation. In what follows, all matrices expressed in the SCKM basis will be noted with a hat on it as in for instance, $\widehat{\mathcal{M}}_{\widetilde{u}}^2$. In the SCKM basis $\left(\widetilde{u}_L, \widetilde{c}_L, \widetilde{t}_L, \widetilde{u}_R, \widetilde{c}_R, \widetilde{t}_R\right)$, reintroducing the electroweak contributions, the 6×6 up-squark mass matrix takes the form:

$$\widehat{\mathcal{M}}_{\widetilde{u}}^2 = \begin{pmatrix} \widehat{M}_Q^2 + m_u^2 - \frac{\cos(2\beta)}{6}\left(m_Z^2 - 4m_W^2\right)\mathbb{1}_3 & \frac{v_u}{\sqrt{2}}\widehat{A}_U - \cot(\beta)\,\mu m_u \\ \frac{v_u}{\sqrt{2}}\widehat{A}_U^\dagger - \cot(\beta)\,\mu^* m_u & \widehat{M}_U^2 + m_u^2 + \frac{2\cos(2\beta)}{3}m_Z^2 s_W^2 \mathbb{1}_3 \end{pmatrix} \tag{4.9}$$

where $s_W = \sin(\theta_W)$ and $m_u^2 = \mathrm{diag}\left(m_u^2, m_c^2, m_t^2\right)$. We recall that the β angle is defined through $\tan(\beta) = \frac{v_u}{v_d}$ with $\langle H_u\rangle = \begin{pmatrix} 0 & v_u/\sqrt{2}\end{pmatrix}^T$ and $\langle H_d\rangle = \begin{pmatrix} v_d/\sqrt{2} & 0\end{pmatrix}^T$ the vevs of the up and down MSSM Higgs doublets (see section 2.5). The flavor violating 3×3 blocks of $\widehat{\mathcal{M}}_{\widetilde{u}}^2$ are given by:

$$\widehat{M}_Q^2 = V_{u_L} M_Q^{2*} V_{u_L}^\dagger, \quad \widehat{M}_U^2 = V_{u_R} M_U^{2*} V_{u_R}^\dagger, \quad \widehat{A}_U = v_u^* V_{u_L} A_U^* V_{u_R}^\dagger. \tag{4.10}$$

In the electroweak broken phase, a useful expansion of $\widehat{\mathcal{M}}_{\widetilde{u}}^2$ can be obtained if the vev of the up-type MSSM Higgs doublet $\langle H_u\rangle$ is parameterized as $\langle H_u\rangle = \begin{pmatrix} 0 & \frac{v_u}{\sqrt{2}} + c_\alpha h\end{pmatrix}^T$ where h is the physical SM Higgs boson. $\widehat{\mathcal{M}}_{\widetilde{u}}^2$ takes then the approximate form:

$$\widehat{\mathcal{M}}_{\widetilde{u}}^2 = \begin{pmatrix} \widehat{M}_Q^2 + \mathcal{O}(v_u^2)\mathbb{1}_3 & \frac{v_u}{\sqrt{2}}\widehat{A}_U\left(1 + c_\alpha\frac{h}{v_u} + \cdots\right) + \mathcal{O}\left(v_u M_{SUSY}\right) \\ \frac{v_u}{\sqrt{2}}\widehat{A}_U^\dagger\left(1 + c_\alpha\frac{h}{v_u} + \cdots\right) + \mathcal{O}\left(v_u M_{SUSY}\right) & \widehat{M}_U^2 + \mathcal{O}(v_u^2)\mathbb{1}_3 \end{pmatrix} \tag{4.11}$$

if the SUSY scale M_{SUSY} is not too far above the electroweak scale, which is what is needed for the MSSM to solve the hierarchy problem. Note that until now, the squarks are still not mass eigenstates. The diagonalization of $\mathcal{M}_{\widetilde{u}}^2$ can be achieved with a 6×6 unitary rotation matrix $\mathcal{R}_{\widetilde{u}}$:

$$\mathrm{diag}\left(m_{\widetilde{u}_1}^2, \cdots, m_{\widetilde{u}_6}^2\right) = \mathcal{R}_{\widetilde{u}} \mathcal{M}_{\widetilde{u}}^2 \mathcal{R}_{\widetilde{u}}^\dagger, \tag{4.12}$$

which defines the squark mass eigenstate basis:

$$\begin{pmatrix} \widetilde{u}_L \\ \widetilde{c}_L \\ \widetilde{t}_L \\ \widetilde{u}_R \\ \widetilde{c}_R \\ \widetilde{t}_R \end{pmatrix} = \mathcal{R}_{\widetilde{u}} \begin{pmatrix} \widetilde{u}_1 \\ \widetilde{u}_2 \\ \widetilde{u}_3 \\ \widetilde{u}_4 \\ \widetilde{u}_5 \\ \widetilde{u}_6 \end{pmatrix} \tag{4.13}$$

with $m_{\widetilde{u}_i}$ the physical mass of the eigenstate $\widetilde{u}_i$. By convention, $\mathcal{R}_{\widetilde{u}}$ is defined such that the 6 $m_{\widetilde{u}_i}$ are mass ordered i.e. $m_{\widetilde{u}_1} < \cdots < m_{\widetilde{u}_6}$. Furthermore, by unitarity we have 6 relations $\forall i = 1, 2...6$: $\sum_{j=1}^{6} \left(\mathcal{R}^2_{\widetilde{u}}\right)_{ij} = 1$. We conclude by pointing out that, although for the sake of concision we have restricted this discussion to the up-type sector, all relations derived here can be easily extended to the down and lepton sectors.

4.2.2 The soft SUSY breaking sector of $SU(5)$ theories: the up sector case

We continue this section by giving some details on a symmetry relation already spotted in subsection 3.2.2. We recall that, the superpotential of a SUSY-$SU(5)$ Lagrangian contains the term:

$$W_{SU(5)} \supset \epsilon_5 Y_{10}^{ij} \mathbf{10}_i \mathbf{10}_j \mathbf{5}_H^u \tag{4.14}$$

where $i, j...$ are generation indices. We have shown in subsection 3.2.2 that if the superpotential contains a term of this form, symmetric in $\mathbf{10}_i \Longleftrightarrow \mathbf{10}_j$, the up-type Yukawa matrix is symmetric as well, i.e.:

$$Y_U = Y_U^T. \tag{4.15}$$

Beside, if SUSY breaking is mediated via a $SU(5)$ singlet, meaning that the soft terms are generated at a scale between M_{GUT} and M_{Planck} where the $SU(5)$ symmetry is exact, the relation (4.15) propagates to the soft breaking sector and we also have:

$$A_U = A_U^T. \tag{4.16}$$

A crucial point is that this relation is way less model dependent than the symmetry relations based on the quark-lepton complementarity. In particular, this relation is left invariant by whatever GUT scale non-renormalizable operator is added to $W_{SU(5)}$. To be precise, we see that for whatever $SU(5)$ invariant operator of the form $\mathcal{O}_{ij}\mathbf{10}_i\mathbf{10}_j$, the symmetric part of $\mathcal{O}_{ij}$ always vanishes during the contraction with the tensor $\mathbf{10}_i\mathbf{10}_j$. Thus, the property $A_U = A_U^T$ is independent of any assumption that can be made on the dynamics between M_{GUT} and M_{Planck}. Also, this relation remains exact in the SCKM basis. Indeed, if we note all matrices in the SCKM basis with a hat, the bi-unitary Yukawa diagonalization is $Y_U = V_{u_R}^\dagger \widehat{Y_U} V_{u_L}$ and the rotated SCKM trilinear term is $\widehat{A}_U = V_{u_L}^\dagger A_U V_{u_R}$. But, the fact that the Yukawa coupling is symmetric implies $V_{u_L} = V_{u_R}^*$, such that we can write $Y_U = V_{u_L}^T \widehat{Y_U} V_{u_L}$. We thus obtain $\widehat{A_U} = V_{u_L}^\dagger A_U V_{u_L}^*$ which is symmetric if A_U is. What we have found until now can be summarized by the implication:

$$\{SU(5) - \text{type SUSY GUT}\} \longrightarrow \{Y_U = Y_U^T, A_U = A_U^T \text{ at the GUT scale.}\} \tag{4.17}$$

If we have a look at eq. (4.9), we see that the only flavor violating contributions lie in the soft terms, the electroweak terms being diagonal in flavor space. Hence, a symmetric up-type trilinear coupling implies that the off-diagonal chirality flipping block $(\mathcal{M}^2_{\widetilde{u}})_{LR}$ of $\widehat{\mathcal{M}}^2_{\widetilde{u}}$ is symmetric as well. This property will be at the center of our attention in this chapter. Finding evidences in favor of a symmetric off-diagonal block in a weak scale mass matrix $\mathcal{M}^2_{\widetilde{u}}$ would constitute a rather striking hint in favor of the $SU(5)$ GUT scale hypothesis. Perhaps more importantly, finding evidences which disfavor this structure would tend to exclude $SU(5)$ as a candidate for the GU group.

4.2.3 Qualitative discussion of the RGEs in the up-squark sector

Obviously, the properties $Y_U = Y_U^T$ and $A_U = A_U^T$ are only true at or above the GUT scale, before $SU(5)$ gets spontaneously broken. One needs then to evolve these relations with the appropriate RGEs to scrutinize their structure at the TeV scale. Implication (4.17) then becomes:

$$\{SU(5) - \text{type SUSY GUT}\} \longrightarrow \{A_U \approx A_U^T \text{ at the TeV scale.}\} \tag{4.18}$$

where an asymmetry appears in A_U which has to be seen as a theoretical, model dependent, irreducible uncertainty induced by the running between M_{GUT} and M_{SUSY} . This asymmetry will be quantized in section 4.3. In what follows, we will be mostly interested in symmetry relations in the soft sector

to set up $SU(5)$ tests. However, as we have argued above, we also need the Yukawa coupling to stay symmetric if one wants to preserve $A_U = A_U^T$ in the SCKM basis. Thus, we need to scrutinize both beta functions. Starting the running from the GUT scale, the beta functions of the trilinear and Yukawa couplings β_{Y_U} and β_{A_U} will preserve the symmetry of Y_U and A_U as long as they are perfectly symmetric themselves i.e. $\beta_{Y_U/A_U} = \beta_{Y_U/A_U}^T$. Stated otherwise, above the GUT scale, when the $SU(5)$ symmetry is exact and, in the limit where the beta functions only contain terms which are symmetric in flavor space, Y_U and A_U will stay symmetric in the $SU(5)$ broken phase all the way down to the TeV scale. We are thus interested in non-symmetric terms in β_{Y_U} and β_{A_U} which spoil $Y_U = Y_U^T$ and $A_U = A_U^T$ below M_{GUT}. Here, we would like to discuss qualitatively these potential sources of asymmetry before providing a more quantitative phenomenological study in section 4.3. To do this, we will discuss the running of Y_U and A_U at one loop. The one-loop MSSM beta function of the Yukawa coupling is given by [90]:

$$16\pi^2\beta_{Y_U} = Y_U\left[3\mathrm{Tr}\{Y_U^\dagger Y_U\} + 3Y_U^\dagger Y_U + Y_D^\dagger Y_D - \frac{16}{3}g_3^2 - 3g_2^2 - \frac{13}{15}g_1^2\right]. \tag{4.19}$$

In this expression, at the GUT scale, the gauge terms $\beta_{Y_U} \supset Y_U g_i^2$, trace terms $\beta_{Y_U} \supset Y_U\mathrm{Tr}(Y_U^\dagger Y_U)$ and $\beta_{Y_U} \supset Y_U Y_U^\dagger Y_U$ are all symmetric by construction. The only GUT scale non symmetric contribution resides in the term $\beta_{Y_U} \supset Y_U Y_D^\dagger Y_D$. First, this term is suppressed by the elements of the CKM matrix once the quarks have been rotated to their physical mass eigenstates. Secondly, in a SUSY context, the relative magnitude of the up and down Yukawa sectors is set by $\tan(\beta) = \frac{v_u}{v_d}$ such that this term grows with $\tan(\beta)$. Given the low-energy quark masses, one can expect $Y_D^\dagger Y_D$ to be of the same order of magnitude as $Y_U^\dagger Y_U$ only at very high $\tan(\beta)$. Hence, we can expect Y_U to stay symmetric at low scale to a good approximation.

We turn now to the trilinear coupling beta function. This is given, at one-loop in the MSSM by [90]:

$$\begin{aligned}16\pi^2\beta_{A_U} = {} & A_U\left[3\mathrm{Tr}\{Y_U Y_U^\dagger\} + 5Y_U^\dagger Y_U + Y_D^\dagger Y_D - \frac{16}{3}g_3^2 - 3g_2^2 - \frac{13}{15}g_1^2\right] \\ & + Y_U\left[6\mathrm{Tr}\{A_U Y_U^\dagger\} + 4Y_U^\dagger A_U + 2Y_D^\dagger A_D + \frac{32}{3}g_3^2 M_3 + 6g_2^2 M_2 + \frac{26}{15}g_1^2 M_1\right].\end{aligned} \tag{4.20}$$

Again, at the GUT scale, the terms proportional to a trace or to a coupling constant are all symmetric by construction. However, the other terms are generically not symmetric, because A_U generically does not commute with $Y_U^\dagger Y_U$ nor does A_D with $Y_U Y_D^\dagger$. Thus, A_U stays symmetric to a good precision at the TeV scale only if the running is dominated by gauge contributions. In practice however, the running is dominated by the large gluino mass contribution M_3 due to the high value of α_3 compared to the other gauge couplings. Moreover, as the M_3 contribution is positive, it decreases A_U with the energy, such that non symmetric terms become smaller and smaller in β_{A_U}. Therefore, one can expect that although β_{A_U/Y_U} are not symmetric, the RGEs induced asymmetry on A_U at the TeV scale stays small in many concrete cases (see section 4.3).

Also, beyond the MSSM, one can check that Y_U and A_U stay symmetric at low energy to a good precision in many cases. The condition is that non-symmetric terms in eqs (4.15) and (4.16) do not dominate, and that the possible hidden sector do not contribute either. For example, a hidden SUSY breaking sector would need to be flavor singlet to not spoil the symmetry which is, as we have briefly argued in section 2.4, a rather common feature of mediation mechanisms.

$(M^2_{\mathbf{10}})_{ij}$		
$(1000)^2$	0	0
0	$(3270)^2$	$(557)^2$
0	$(557)^2$	$(1550)^2$

$(M^2_{\bar{\mathbf{5}}})_{ij}$		
$(860)^2$	0	0
0	$(374)^2$	0
0	0	$(412)^2$

$(A_U)_{ij}$		
0	0	0
0	0	$(A_U)_{23}$
0	$(A_U)_{32}$	-1500

$(A_D)_{ij}$		
0	0	0
0	0	$(A_D)_{23}$
0	$(A_D)_{32}$	400

$M_{1/2} = 1000$
$M^2_{H_{u,d}} = (1000)^2$
$\text{sign}(\mu) = +1$

Table 4.1 – Supersymmetry-breaking parameters at $Q = M_{\text{GUT}}$ of the MSSM reference scenario used in the numerical analysis. Masses and trilinear couplings are given in GeV.

4.3 Stability of the soft sector under the RG flow: quantitative discussion

In the previous section, we gave qualitative arguments that tend to show that $SU(5)$-like SUSY theories generically predict an up-type trilinear coupling approximately symmetric at low scales. In this section, we would like to quantify more precisely the size of the discrepancy induced by the RG flow on $A_U = A_U^T$. It is mandatory to know the magnitude of this asymmetry. Indeed, it constitutes an irreducible bound on the precision at which one can potentially test $A_U = A_U^T$. A too large asymmetry would imply that this relation is spoiled by large model-dependent quantum corrections making the task of constructing model-independent $SU(5)$ tests quite tedious. Note that also the stability of the $SU(5)$ symmetry relation $M_Q^2 = M_U^2$ (see eq. (4.21)) will be discussed at the end of this section, since certain tests to be proposed in the rest of this chapter will also rely partially on symmetry relations in the soft mass sector (see section 4.6).

4.3.1 Setup

We start by presenting the setup of the analysis. We remind that in a $SU(5)$ SUSY-GUT, the soft breaking SUSY parameters satisfy the following GUT scale boundary conditions:

$$\begin{aligned} M^2_{\mathbf{10}} \equiv M_Q^2 = M_U^2 = M_E^2 \\ M^2_{\bar{\mathbf{5}}} \equiv M_D^2 = M_L^2 \\ A_E = A_D^T \\ A_U = A_U^T \end{aligned} \tag{4.21}$$

Because the property we want to check is not sensitive to CP violation, we have also chosen to use only real soft breaking parameters, the only source of CP violation being the usual CKM matrix phase δ_{CKM}. To quantify the discrepancy between A_U and A_U^T, it is convenient to use a quantity normalized with respect to a SUSY scale. As all the phenomenological tests we are going to build involve observables confined to the up-squark sector, a reasonable choice of scale might be the average of the up-type squark mass eigenvalues. Therefore, we define the following quantity:

$$\mathcal{A}_{ij} = \frac{|\,(A_U)_{ij} - (A_U)_{ji}\,|}{\sqrt{\frac{1}{6}\text{Tr}\{\mathcal{M}^2_{\tilde{u}}\}}}, \qquad i \neq j. \tag{4.22}$$

normalized with respect to the trace of the up-squark mass matrix. Low scale SUSY spectra were computed using the spectrum calculator `SPhenoMSSM` obtained from the package `SPheno` [91] and from the Mathematica package `SARAH` [92]. This code solves the RGEs of the MSSM at two loops and computes low scale SUSY spectra from GUT scale boundary conditions on soft terms as well as weak scale SM parameters. We have also chosen to use the Supersymmetric Parameter Analysis (SPA)

ΔM_{Bs}	(17.76 ± 2.81) ps^{-1}
ϵ_K	(2.23 ± 0.26)
BR$(B_s^0 \to \mu\mu)$	$(3.12 \pm 2.08) \times 10^{-9}$
BR$(b \to s\gamma)$	$(355 \pm 68) \times 10^{-6}$
BR$(\tau \to \mu\gamma)$	$< 4.5 \times 10^{-8}$

Table 4.2 – Confidence interval on the Low-energy flavor constraints taken into account in the numerical analysis. The uncertainties quoted here already include both the experimental and theoretical errors, quadratically summed.

convention [93] in which SUSY spectra are outputted at $Q = 1$ TeV in the modified minimal dimensional reduction ($\overline{\text{DR}}$) scheme (see [94]). In this renormalization scheme, divergent integrals are regularized using a (regularization) scheme called Dimensional Reduction (DRED). In DRED, the dimension of the measure's integral is formally promoted to a complex parameter D but the Dirac tensors inside the integrand are still maintained to 4-dimensions. This scheme is very useful in SUSY because, contrary to the dimensional regularization scheme (DREG) in which the dimension of the full integral (measure + integrand) is promoted to a complex value, DRED allows to maintain full invariance of the Green functions under the Super Poincaré algebra.

A-priori, there are three asymmetries to be investigated: $\mathcal{A}_{12}$, $\mathcal{A}_{13}$ and $\mathcal{A}_{23}$ (see eq. (4.22)). However, only mixing in the $2-3$ sector seems relevant for phenomenology. Indeed, mixing terms in the $1-2$ and $1-3$ sectors of the trilinear couplings are way more constrained by phenomenology, in particular by low scale FCNC processes such as $D - \bar{D}$ mixing [95].

Also, mixing in these sectors can lead the superpartners to contribute too strongly in the SM fermion self-energies which would drive the TeV scale CKM matrix elements outside of their experimental measured values. Mostly, due to the hierarchical structure of the Yukawa couplings and, in particular, due to the large value of the top Yukawa coupling, the running is expected to be more severe in the $2-3$ sector and thus, we expect $\mathcal{A}_{12}, \mathcal{A}_{13} < \mathcal{A}_{23}$. Hence, we can safely restrict the analysis to $\mathcal{A}_{23}$.

We also needed to choose a $SU(5)$-symmetric reference scenario for the analysis. This reference scenario is given in tab. 4.1. In tab. 4.1, $M_{1/2}$ is the common gaugino mass and $M^2_{H_{u,d}}$ the common Higgs doublet mass i.e. we assume at $Q = M_{GUT}$, $M_{1/2} \equiv M_1 = M_2 = M_3$ and $M^2_{H_{u,d}} \equiv M^2_{H_u} = M^2_{H_d}$ in the notations of eq. (2.59).

In tab. 4.1, we have decided to take a diagonal $M_{\bar{5}}$ in order to maintain SUSY contributions to FCNC processes under control in the leptonic and down sectors.

$(A_U)_{23/32}$ and $(A_U)_{32/23}$ are the free parameters of the scan that we have varied assuming GUT scale $SU(5)$ boundary conditions on soft terms (see eq. (4.21)), in particular we have $(A_U)_{23} = (A_U)_{32}$ and $(A_D)_{23} = (A_E)_{23}$ at $Q = M_{GUT}$. We have also assumed a symmetric trilinear coupling in the down sector $(A_D)_{23} = (A_D)_{32}$ for simplicity. Finally, as well known in the MSSM, we have chosen a relatively large, negative, top trilinear coupling to increase the SM Higgs mass to a value compatible with its experimentally measured value.

4.3.2 Flavor constraints

In this section, we would like to describe the different constraints that we have taken into account in this analysis. These are all summarized in table 4.2. Expressions for all these constraints can be obtained with the full flavor structure of the MSSM using an effective Hamiltonian formalism (see sec 4.4.1 and [96] for expressions of B physics observables.)

This section has two purposes. First, we would like to discuss qualitatively these observables using a few relevant Feynman diagrams. Secondly, we will tabulate the up-to date experimental values as well as their uncertainties both experimental and theoretical. These two type of uncertainties will in turn be used to compute confidence intervals that will restrict the parameter space in the analysis of subsec. 4.3.3.

The constraints are the following:

- ϵ_K: We start by the description of the mixing parameter in the neutral Kaon system. We recall that the neutral Kaon $K^0\,(d\bar{s})$ and its associated anti-meson $\overline{K}^0\,(\bar{d}s)$ are related by a CP transformation as:

$$CP|K^0\rangle = -|\overline{K}^0\rangle \tag{4.23}$$

Hence the two linear combinations:

$$|K_1\rangle = \frac{1}{\sqrt{2}}\left(|K^0\rangle - |\overline{K}^0\rangle\right), \quad |K_2\rangle = \frac{1}{\sqrt{2}}\left(|K^0\rangle + |\overline{K}^0\rangle\right), \tag{4.24}$$

form CP eigenstates i.e. we have $CP|K_1\rangle = +|K_1\rangle$ and $CP|K_2\rangle = -|K_2\rangle$. Thus, if CP was an exact symmetry of the SM, $|K_1\rangle/|K_2\rangle$ should decay only to final states which have the same CP parity. For example, if one considers a set of neutral mesons π, the decay $K_1 \to \pi\pi$ would be possible but $K_1 \to \pi\pi\pi$ should be closed as $CP(\pi\pi) = +1$ and $CP(\pi\pi\pi) = -1$. Reciprocally for K_2, we expect the decay $K_2 \to \pi\pi\pi$ to be open but $K_2 \to \pi\pi$ to be closed due to CP conservation. But, we know that the CKM phase δ_{CKM} provides a small source of CP breaking in the weak interaction hamiltonian. Thus one expects that, although the two channels discussed above dominate, K_1 could decay to three pions and K_2 to two pions even if they do with a smaller branching ratio than in the CP conserving channels. That means that $|K_1\rangle$ and $|K_2\rangle$ are no longer eingenstates of the CP parity. The breaking of the CP parity in the weak interaction mixes $|K_1\rangle$ and $|K_2\rangle$, and the physical propagating eigenstates become:

$$|K_{S(L)}\rangle = \frac{1}{\sqrt{1+|\overline{\epsilon_K}|^2}}\left(|K_{1(2)}\rangle + \overline{\epsilon_K}|K_{2(1)}\rangle\right) \tag{4.25}$$

where the subscripts L, S stands for "Long" and "Short" which is no accident. Indeed, the dominant decay mode $K_L \to \pi\pi\pi$ has a much smaller width than $K_S \to \pi\pi$ which results in the lifetimes of K_L and K_S being widely different. As an illustration, the PDG gives $\tau(K_L) \sim 5 \times 10^{-8}$s and $\tau(K_S) \sim 0.89 \times 10^{-10}$s, this hierarchy makes possible the clear separation of these two states in a decay experiment. We will not go further in the description of CP violation in the kaon system. The important point to keep in mind is that the parameter $\bar{\epsilon}_K$ in eq. (4.25) allows two different kinds of CP violating phenomena. Direct CP violation manifests itself when a difference between a decay rate $\Gamma(P \to f)$ and the CP conjugate $\Gamma(\overline{P} \to \overline{f})$ is observed. Direct CP violation is parameterized via a parameter dubbed ϵ'_K. On the other hand, indirect CP violation manifests itself in mixing effects. This will result in a difference between the two widths $\Gamma(\overline{K}^0 \to K^0)$ and $\Gamma(K^0 \to \overline{K}^0)$ as well as in a mass difference $\Delta m_K = m_{K_L} - m_{K_S}$, these indirect effects are parameterized via a parameter dubbed ϵ_K. For a more extensive description of CP violation in the Kaon system, including expressions for the parameters ϵ_K and ϵ'_K, see refs. [97]. The important point for us is that, when the SM is supersymmetrized, extra-sources of indirect CP violation appear due to the extended scalar spectrum, thus participating in mixing effects. For example, the SM $\Delta S = 2$ box diagram can be supersymmetrized and is represented in fig. 4.1. Hence, indirect CP violation can set strong constraints in the parameter space of the soft sector. If we take the latest experimental PDG value (see [25]) combined with a theoretical uncertainty taken from [98], we have $\epsilon_K = (2.23 \pm 0.01(\text{exp}) \pm 0.26(\text{th})) \times 10^{-3}$ given at 1σ (68% CL). Also because theoretically, this value is subject to large QCD uncertainties, we have decided to normalize it to its SM prediction. A SM model prediction can be found in [99] and is equal to $\epsilon_K^{SM} = (1.85 \pm 15\%) \times 10^{-3}$. Combining these two results we find $\epsilon_K/\epsilon_K^{SM} = 1.20 \pm 0.37$. We hence see a discrepancy between the SM and experimental values which could possibly point toward NP effects. This has been the subject of several studies, see for instance [99]. From the values quoted above, we can get a 2σ confidence interval on that ratio equal to:

$$\epsilon_K/\epsilon_K^{SM} \in [0.83, 1.57] \text{ given at } 2\sigma \text{ (95\% CL)} \tag{4.26}$$

- ΔM_{B_s}: The second constraint we are going to consider is the mass difference in the strange B_s meson system. Similarly to the K system, the mesons $B_s\,(s\bar{b})$ and $\overline{B}_s\,(\bar{s}b)$ can oscillate among each other due to CP violation effects. Thus, an initially present B_s^0 state can evolved into a time dependant combination of B_s^0 and $\overline{B}_s^0$ flavor states. Actually, the frequency of this oscillation is fixed by the mass difference between the "light" and the "Heavy" states $\Delta M_{B_s} \equiv m_{B_H} - m_{B_L}$ where B_H and B_L are

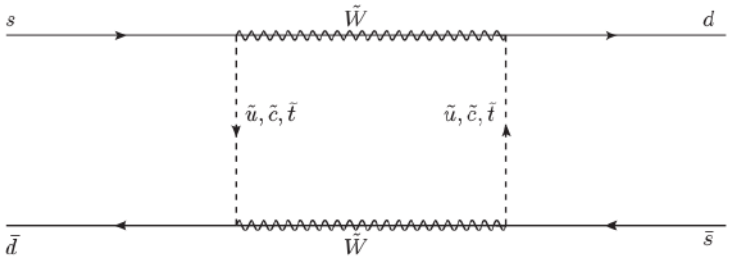

Figure 4.1 – SUSY box diagram contribution to $K^0 - \overline{K}^0$ mixing.

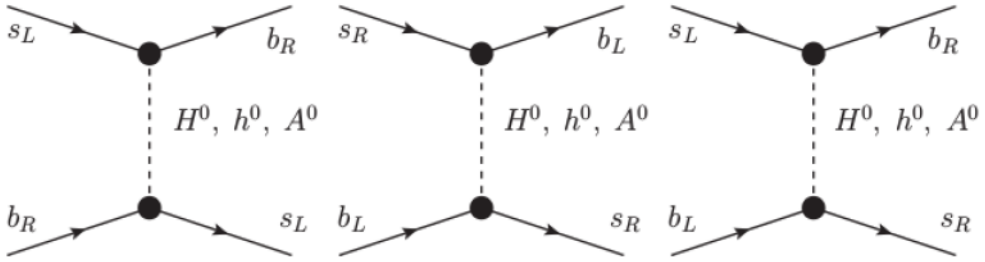

Figure 4.2 – MSSM contribution to B_s^0-$\overline{B}_s^0$ arising from Higgs penguins.

propagating eigenstates, superpositions of the flavor states B_s^0, $\overline{B}_s^0$ defined in a similar manner as in eq. (4.25). ΔM_{B_s} is known to set very strong constraints on the MSSM parameter space (see for instance [100] and [101] for a review in the large $\tan\beta$ case). ΔM_{B_s} is hence a very good probe to search for new physics effects. Especially, in the MSSM, sizable contributions to this observable arise in the large $\tan\beta$ region due to the extended Higgs sector, through penguin diagrams such as the one represented in fig. 4.2. The world average value quoted by the "Heavy Flavors Average Group" (HFAG [102]) gives :

$$\Delta M_{B_s} = 17.761 \pm 0.022 \text{ ps}^{-1} \tag{4.27}$$

obtained from measurements at LHCb and CDF. On the other hand, a SM value can be obtained from [100], taking into account NLO QCD effects, and is equal to $\Delta M_{B_s} = 16.1 \pm 2.8$ ps^{-1}. We hence see that this does not leave so much room for new physics effects. Although, for the analysis that follows, one also has to take into account a theoretical uncertainty on (4.27). We have decided to use the same theoretical uncertainty of ± 2.8 ps^{-1} used in the SM value quoted above. This error, when quadratically summed with the experimental error of 0.022 ps^{-1} allows us to deduce a confidence interval for ΔM_{B_s} equal to:

$$\Delta M_{B_s} \in [12.7,\ 22.7] \text{ ps}^{-1} \text{ given at } 2\sigma \text{ (95\%CL)} \tag{4.28}$$

Then again, one sees that the error is completely dominated by the theoretical uncertainty.

- $BR\left(B_s^0 \to \mu\mu\right)$: The third constraint considered is the rare muonic decay of the B_s^0 meson, $B_s^0 \to \mu^+\mu^-$. This process is very interesting to search for NP effects as it is clean theoretically. In particular, hadronic uncertainties are kept under control [96]. Beside in the SM, as the final state is purely leptonic and the initial state is a pseudoscalar, the decay in question is strongly helicity suppressed in view of the smallness of m_μ and equally importantly, do not receive photon-mediated one loop contributions [103]. As for the $B_s^0 - \overline{B}_s^0$ mixing, tree level exchanges of neutral scalar bosons can contribute to this process in extension of the SM and, in particular in the MSSM with general flavor mixing. Especially, penguin diagrams mediated by scalars and pseudoscalars can contribute significantly in the large $\tan\beta$ region. This process has been measured for the first time by the LHCb collaboration in 2013 [104] with a 3.5σ significance. The latest value reported by the HFAG group reads:

$$\text{BR}\left(B_s^0 \to \mu^+\mu^-\right) = (3.1 \pm 0.7) \times 10^{-9} \tag{4.29}$$

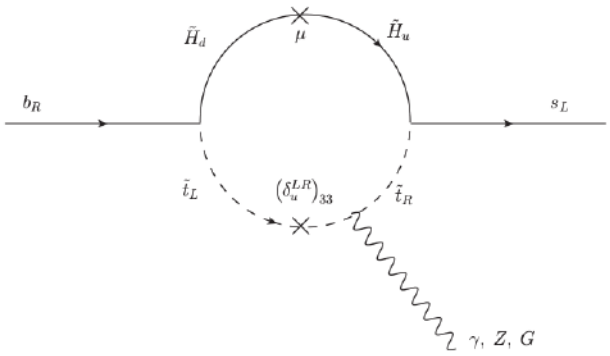

Figure 4.3 – One amplitude contribution to the transition $b \to s\gamma$ generated via chargino exchange. The crosses denote mass insertions.

to be compared with the SM value [105]:

$$\mathrm{BR}\left(B_s^0 \to \mu^+\mu^-\right)_{SM} = (3.56 \pm 0.17) \times 10^{-9} \tag{4.30}$$

which is in excellent agreement with the measured value, thus leaving once again little room for new physics effects. We have decided to include a theoretical uncertainty of $\pm 0.29 \times 10^{-9}$, taken from [100]. These two sources of uncertainties, when quadratically summed, allows us to deduce a 2σ confidence interval on that observable, equal to:

$$\mathrm{BR}\left(B_s^0 \to \mu^+\mu^-\right) \in [1.02, 5.18] \times 10^{-9} \text{ given at } 2\sigma, \ (95\%\mathrm{CL}). \tag{4.31}$$

- $\mathrm{BR}(B \to X_s\gamma)$: The fourth observable to be considered is the inclusive branching ratio of the B meson decay $B \to X_s\gamma$ where X_s represents any hadronic system containing a strange particle. Beside, the inclusive branching ratio of the hadronic process is known to be equal to a good precision to the branching of the partonic transition $b \to s\gamma$ due to the heavy-quark hadron duality [106]. The crucial point is that this transition $b \to s\gamma$ is loop-generated in the SM and most of its extensions. This loop suppression makes this observable sensitive to NP contribution and, in contrast to tree-level FCNCs mediated by neutral bosons and scalars (see fig. 4.2), this observable depends on the masses and couplings of the new heavy fermions. For instance, in the MSSM, magnetic and chromagnetic operators can be generated in the low scale theory. These effective operators can contribute to the $b \to s\gamma$ transition through loop diagrams mediated by gauginos and hence, can enhance significantly the branching ratio above its SM value, even in the case of small to moderate $\tan\beta$ (see [107]). As an illustration we have represented in fig. 4.3, the one loop amplitude generated by chargino exchanges, contributing to $b \to s\gamma$. The latest HFAG value gives:

$$\mathrm{BR}\left(b \to s\gamma\right) = (343 \pm 22) \times 10^{-6} \tag{4.32}$$

If one includes a theoretical uncertainty of $\pm 23 \times 10^{-6}$ obtained from [108], which takes into account NNLO QCD effects, one gets to the following 2σ confidence interval:

$$\mathrm{BR}\left(b \to s\gamma\right) \in [279, 407] \times 10^{-6} \text{ given at } (95\%) \text{ CL} \tag{4.33}$$

- $\mathrm{BR}\left(\tau \to \mu\gamma\right)$: The last flavor constraint to be considered is the charged lepton flavor violating (cLFV) transition $\tau \to \mu\gamma$. This observable has to be seen as the leptonic counterpart of the $b \to s\gamma$ transition discussed above. Also our analysis is focusing on the hadronic sector, we have decided to include this constraint as our model is $SU(5)$ symmetric at high scale, thus correlating flavor violation in the hadronic and leptonic sectors. This process violates explicitly the electronic as well as the muonic numbers. Thus in the SM, this process is sufficiently small so that it can never be observed. Furthermore, this process is very efficient in constraining the new sources of leptonic flavor violation predicted by the extensions of the SM, especially in a Grand Unified framework [109]. For now, cLFV has never

been observed and only upper-bounds have been set, most recently, by the BELLE [110] and BABAR [111] experiments. The result reads:

$$\mathrm{BR}\,(\tau \to \mu\gamma) < 4.5 \times 10^{-8} \text{ given at } 90\% \text{ CL} \tag{4.34}$$

As stated above, this branching ratio is strongly suppressed in the SM. Especially, being loop-generated, $\tau \to \mu\gamma$ is both GIM suppressed and suppressed by the tiny neutrino masses. Typically, using known oscillation parameters from the PMNS matrix, one can estimate that in the SM, $\mathrm{BR}\,(\tau \to \mu\gamma) \lesssim 10^{-54}$ (see [112]), well below the reach of any foreseeable experiments. Thus any observation of cLFV process would clearly indicate the presence of NP effects.

Table 4.2 summarized the different constraints taken into account in the numerical analysis with their associated 2σ confidence interval. To conclude this subsection, we would like to stress that, as we have seen, in many flavor observables, the error is completely dominated by the theoretical uncertainty thus limiting the predictability of these observables on NP models. This is due to several factors. Mainly, the accuracy of theoretical computations is limited by the unknown higher order corrections that one neglects when a perturbative computation is done, as well as by the numerical uncertainties originating from lattice computations. Increasing the accuracy of loop computations and of lattice numerical results is hence a crucial task to be able to discriminate the different models of NP in view of experimental data.

4.3.3 Results

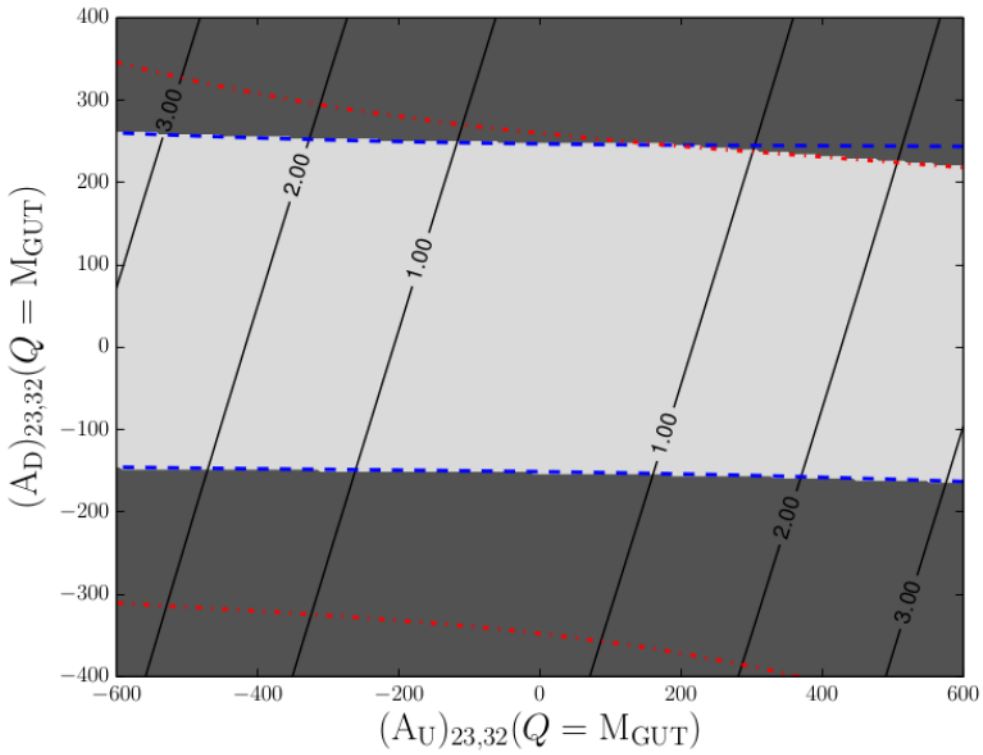

Figure 4.4 – The asymmetry $\mathcal{A}_{23}$ (black solid line) together with the 2σ exclusion bands from ΔM_{Bs} (blue dashed lines) and $\mathrm{BR}(B_s^0 \to \mu\mu)$ (red dashed-dotted lines) evaluated in the reference scenario of tab. 4.1 for the case of low $\tan\beta = 10$. The grey area represents the allowed zone once all constraints are taken into account.

In this section, we would like to present the results of the scan on the $2-3$ mixing elements of the trilinear couplings. We have considered two cases, depending on the value of $\tan\beta$. The figures 4.4 and 4.5 are the results respectively in the low $\tan\beta = 10$ and high $\tan\beta = 40$ regimes. The

black thick isolines represent $\mathcal{A}_{23}$ given at $Q = 1$ TeV and expressed in percent of the SUSY scale $M_{SUSY} = \sqrt{\frac{1}{6}\mathrm{Tr}\{\mathcal{M}^2_{\tilde{u}}\}}$. The colored lines represent the 2σ exclusion bands on the parameter space of the different flavor constraints (see table 4.2 and subsection 4.3.2). The grey area represents the region which survives once all constraints have been taken into account. A few remarks have to be formulated here.

First, it might be surprising that we have restricted the analysis to a single high scale reference scenario (see table 4.1). However, we have checked that the results presented in figures 4.4 and 4.5 depend only mildly of the high scale reference scenario, provided that one stays inside the GUT scale parameter space which leads to physical TeV scale spectra, i.e. one asks for tachyon-free spectra and correct EWSB.

Secondly, as can be seen from figures 4.4 and 4.5, we have restricted the range of $(A_U)_{23}$ and $(A_D)_{23}$ to $|(A_U)_{23}| < 600$ GeV and $|(A_D)_{23}| < 400$ GeV. This might seems quite stringent, however we have checked that outside this region the mass spectrum falls into a tachyonic regime.

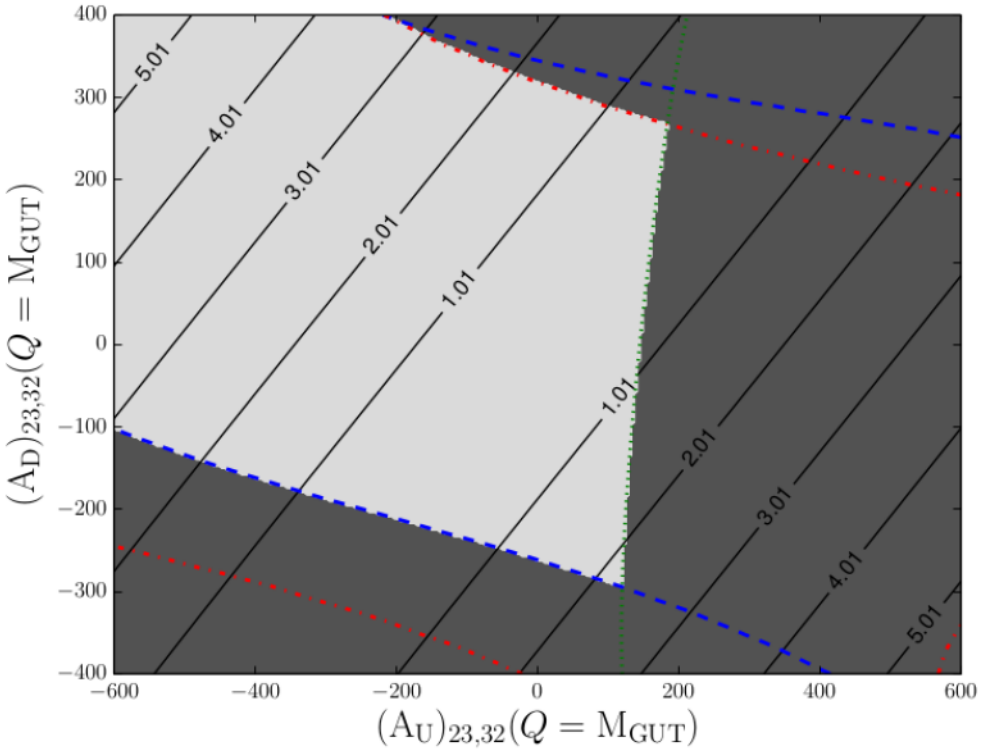

Figure 4.5 – Same as figure 4.4 for the case of high $\tan\beta = 40$. The green dotted line represents the 2σ lower bound on $\mathrm{BR}(b \to s\gamma)$.

We want now to discuss the effects of the constraints on the scan starting with the low $\tan\beta$ regime. We see on figure 4.4, that the leading constraint is ΔM_{B_s}. Also, we see that ΔM_{B_s} is roughly independent of $(A_U)_{23}$ in the low $\tan\beta$ regime. This can be explained by the weakness of up-squark loop effects in the low $\tan\beta$ regime. As we have chosen real soft breaking parameters, the K meson mixing parameter ϵ_K does not constitute a stringent constraint and we find in most of the parameter space $\epsilon_K/\epsilon_K^{SM} \sim 1$. Note also that in this regime, the 2σ exclusion band of $\mathrm{BR}(b \to s\gamma)$ is outside the region scanned. More interesting is the high $\tan\beta$ regime. Indeed, in this regime, up-squarks contributions to loop effects become important. For example, one sees that, the lower bound of $\mathrm{BR}(b \to s\gamma)$ increases significantly and closes the region $(A_U)_{23} \gtrsim 130$ GeV. Beside, both the $\mathrm{BR}\left(B_s^0 \to \mu\mu\right)$ lower bound and the ΔM_{B_s} upper bound closed a significant region of the parameter space.

In both regimes, $\mathrm{BR}(\tau \to \mu\gamma)$ never exceeds the experimental upper limit in the region scanned as we took a diagonal $M^2_{\bar{5}}$ at the GUT scale. Also, due to the large negative value of the stop trilinear coupling $(A_U)_{33} = -1.5$ TeV, the SM Higgs mass does not depend strongly on the value of $(A_U)_{23}$ or

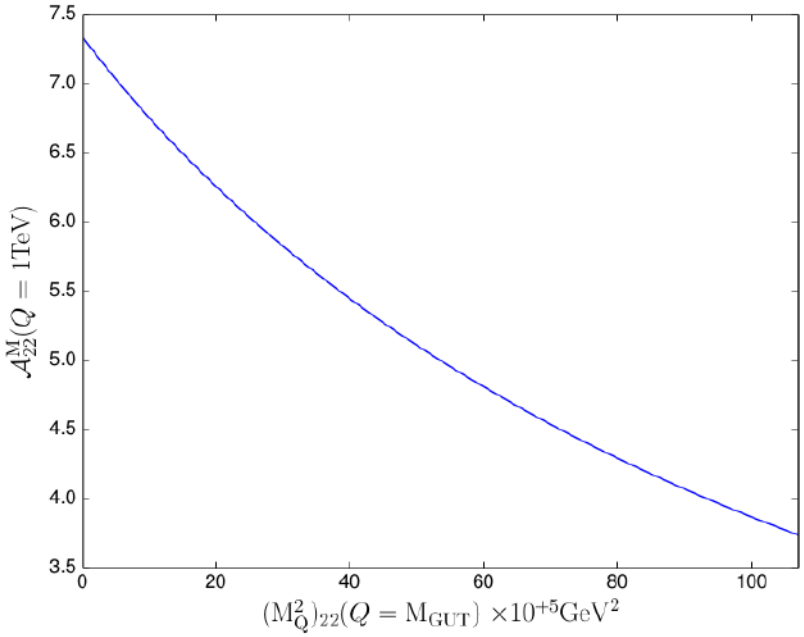

Figure 4.6 – Evolution of the TeV scale asymmetry $\mathcal{A}^{\rm M}_{22}$ as a function of $({\rm M}^2_Q)_{22}$. The same reference scenario than in subsection 4.3.1 has been used, except that now, the relevant GUT scale soft mass term is authorized to vary and the off-diagonal elements of the trilinear couplings have been fixed to vanishing values.

$(A_D)_{23}$ and is found to be about $m_{h^0} \sim 124$ GeV in the region scanned. This result is consistent with the latest ATLAS measure, $m_{h_0} = 125 \pm 0.41$ (sys+stat) GeV [113] if we remember that a theoretical uncertainty of ~ 3 GeV has to be quadratically summed with the experimental error (see [114] and subsection 4.3.2).

Coming back to the value of the asymmetry, we see that $\mathcal{A}_{23}$ never exceeds $\mathcal{A}_{23} \sim 5\%$ of M_{SUSY} in both the low and high $\tan\beta$ regimes, while staying at the level of a few percents in a large part of the parameter space. During the LHC era, testing A_u at such level of accuracy will be most probably difficult. Hence, the theoretical uncertainty $\mathcal{A}_{23}$ induced from the running between M_{GUT} and M_{SUSY} is kept under control and does not seem to constitute a limited factor which would spoil the $SU(5)$ tests to be proposed in the rest of this work.

4.3.4 Stability of the soft sector: the $M^2_Q = M^2_U$ case

As certain tests that will be proposed in this chapter will also rely on observables implying elements of the chirality conserving diagonal blocks of the up-squarks mass matrix, we would like to also comment on the stability of the $SU(5)$ symmetry relation $M^2_Q = M^2_U$ during the running toward the TeV scale. In the same way that we have defined the asymmetry $\mathcal{A}_{ij}$ in the trilinear sector (see eq. (4.22)), one can define a TeV scale asymmetry in the soft mass sector as:

$$\mathcal{A}^M_{ij} = \frac{\left|\left(M^2_Q\right)_{ij} - \left(M^2_U\right)_{ij}\right|}{\frac{1}{6}{\rm Tr}\{\mathcal{M}^2_{\tilde{u}}\}}, \quad . \tag{4.35}$$

We have used exactly the same reference scenario as in subsection 4.3.1, except that the off-diagonal elements of the trilinear couplings A_u and A_d have been set to vanishing values. We have investigated the value of this asymmetry by performing different scans on the elements of M^2_Q at the GUT scale, again assuming $SU(5)$ boundary conditions at the GUT scale, i.e. $M^2_Q = M^2_U$. Here we would like to present the results in the $(2,2)$ and in the $(2,3)$ sectors.

Figure 4.6 presents the TeV scale asymmetry $\mathcal{A}^{\rm M}_{22}$ given as a function of the GUT scale parameter $({\rm M}^2_Q)_{22}$, and expressed in percents of ${\rm Tr}\{\mathcal{M}^2_{\tilde{u}}\}$ (see eq. (4.35)). We see on that figure that the

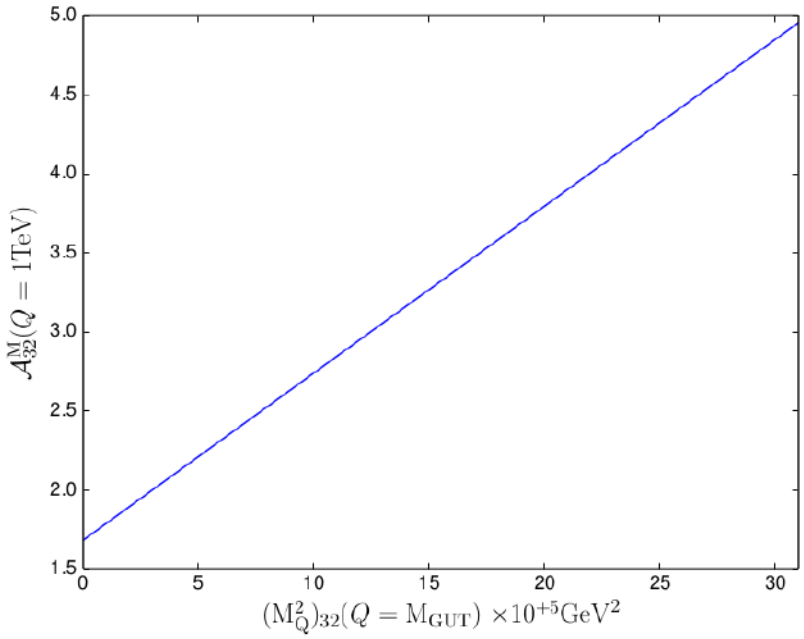

Figure 4.7 – Evolution of the TeV scale asymmetry $\mathcal{A}^{\mathrm{M}}_{32}$ as a function of $(\mathrm{M}^2_Q)_{32}$.

asymmetry reaches a maximum of $\sim 7.0\%$ for a vanishing $(\mathrm{M}^2_Q)_{22}$ and decreases when the soft mass term increases. We have scanned on the range $(\mathrm{M}^2_Q)_{22} \in \left[10^4, 10^7\right] \mathrm{GeV}^2$ since outside this interval the spectrum falls into a non-physical regime, due to the presence of tachyons in the low scale spectrum.

Figure 4.7 presents the TeV scale asymmetry $\mathcal{A}^{\mathrm{M}}_{32}$ given as a function of the GUT scale parameter $(\mathrm{M}^2_Q)_{32}$, and expressed in percents of $\mathrm{Tr}\{\mathcal{M}^2_{\tilde{u}}\}$ (see eq (4.35)). Here the asymmetry increases with the GUT scale mixing term until a maximum of $\sim 5\%$ is reach. Note also that the scan have been done on a range $(\mathrm{M}^2_Q)_{32} \in \left[3 \times 10^3, 3 \times 10^6\right] \mathrm{GeV}^2$ much narrower than in the $(2,3)$ sector. This seems quite intuitive, as it is well known that large mixing terms can quickly lead to a problematic phenomenology. In particular, we have checked that if $(\mathrm{M}^2_Q)_{32} > 3 \times 10^6 \mathrm{GeV}^2$, the squark contributions to SM loop processes become too important, driving the elements of the CKM matrix outside of their experimental measured values.

A very important remark to be made is that this asymmetry is completely spoiled in the $(3,3)$ sector. Indeed, we have checked that $\mathcal{A}^{\mathrm{M}}_{33}$ can reach $\sim 50\%$ of the SUSY scale $M_{SUSY} = \mathrm{Tr}\{\mathcal{M}^2_{\tilde{u}}\}$, this fact being due to the large value of the top Yukawa coupling which makes these soft terms running steeply.

All the plots which are presented here have been obtained imposing a low $\tan\beta = 10$ regime. However, we have checked that increasing $\tan\beta$ to a large value does not change significantly the results, the asymmetry in the different sectors staying at the same orders of magnitude.

Finally, all the flavor constraints of table 4.2 have also been imposed in these scans and turned out to be satisfied at 2σ on the entire ranges scanned in figures 4.6 and 4.7.

In conclusion, the $SU(5)$ symmetry relation $M^2_Q = M^2_U$ stays well preserved at the TeV scale only for the first two generations, the low scale asymmetry introduced by the running in the $(3,3)$ sector being important in front of the SUSY scale due to the large value of the top Yukawa coupling. So from now on, each time that we will invoke the $SU(5)$ hypothesis $M^2_Q \approx M^2_U$ on low scale spectra, it will be understood that this is assumed to hold only for the first two generations.

4.4 Strategies and tools for testing the $SU(5)$ hypothesis at the TeV scale

Any strategy that can be set up to test the $SU(5)$ relation $A_U = A^T_U$ necessarily relies on a comparison involving at least two up-squarks. Apart from this relation, the squark mass matrix is in general

arbitrary, so that each of the six up-type squarks can take any mass. Some of the squarks may be light enough to be produced *on shell* at the LHC while others may be too heavy so that they can only be produced *off shell* in intermediate processes. As a result, a panel of possibilities for setting $SU(5)$ tests will appear, depending on the exact feature of the up-squark spectrum. It can be convenient to split the possibilities of $SU(5)$ tests into three categories, depending on whether the test involves only virtual, both real and virtual, or only real up-type squarks.

It is the aim of this section to outline the tools that we are going to need to build $SU(5)$ tests in the next three sections. Note that $SU(5)$ tests on virtual up-type squarks will necessarily involve one-loop processes since, in this work, we are assuming that $\mathcal{R}$-parity (see subsection 2.5.1) is conserved at all vertices. In contrast, $SU(5)$ tests on real squarks can in principle rely on tree level processes only. Dealing with the eigenvalues and rotation matrices of the full 6×6 mass matrix is in general rather technical, and may constitute an obstacle on the quest for simple $SU(5)$ relations among observables. However, depending on the pattern of $\mathcal{M}^2_{\widetilde{u}}$, two expansions can be used to simplify this problem.

First, if the splitting between the eigenvalues of $\mathcal{M}^2_{\widetilde{u}}$ is small, the so-called Mass Insertion Approximation (MIA) can be used (see [115]). Basically, it consists in a Taylor expansion of the propagators into Feynmann integrals. This expansion is done with respect to small eigenvalues-splitting parameters $\Delta\widetilde{m}^2_{ij} \equiv \widetilde{m}^2_i - \widetilde{m}^2_j$ normalized to an appropriately chosen average mass scale $m^2_{\widetilde{q}}$. This expansion will be developed in subsection 4.4.2.

The second approach that we are going to use to simplify the handling of $\mathcal{M}^2_{\widetilde{u}}$ consists in an Effective Field Theory (EFT) applicable if the up-squark spectrum presents a sizable gap mass. Indeed, in this framework, an arbitrary number of heavy up-squarks can be integrated out of the MSSM Lagrangian. This results in an effective low energy Lagrangian for light squarks, way more practical to use. This framework will be developed in subsubsection 4.4.1.3 and will turn out to be very useful, especially when building $SU(5)$ tests dealing with natural SUSY spectra (see sec 4.6).

It is clear that the feasibility of the $SU(5)$ tests we will setup depends crucially on the amount of data available - whatever they involve real or virtual up-squarks. This feasibility needs to be quantified using appropriate statistical tools. All relevant statistical tools will be introduced in subsection 4.4.3. Whenever a $SU(5)$ test can be obtained through a definite relation among observables, we will use a frequentist p-value [116] approach in order to evaluate to which precision this relation can be tested for a given significance and amount of data.

4.4.1 Effective fields theories

In this section we would like to give a brief overview of the notion of Effective Field Theory (EFT) as it will be useful in the rest of this chapter. We start by presenting the idea behind the construction of an EFT in the simplest case of a scalar field theory. We continue by having a closer look to dimension-6 operators in a SUSY EFT. These will play a prominent role in the construction of the $SU(5)$ tests of section 4.5. We end this subsection by presenting a tree-level effective theory applicable if the up-type squarks spectrum presents a sizable mass gap. This EFT, that we have developed, will be very useful in sections 4.6 and 4.7. Many good pedagogical introductions to EFTs can be found in the literature. In particular, we refer to the references [117].

4.4.1.1 Generic idea

The core idea behind the notion of EFT is the following. All collider experiments are limited by an intrinsic upper-bound on the energy they are able to reach, at least directly, via on-shell processes. For example, the LHC is designed to reach a maximum energy of 14 TeV in the proton-proton center of mass frame. If one took into account the effects of parton PDFs in the proton, that means that the energy in the hard scattering process will be limited to a few TeV only. Hence, we see that particles with masses of say, 100 TeV, will play absolutely no direct role in the physics to be probed at the LHC. Even if one is able to construct a complete theory describing both d.o.fs with masses of $\mathcal{O}(1)$ TeV and masses of $\mathcal{O}(100)$ TeV, it will be desirable to shrink this theory to a less-ambitious one, which only deals with d.o.fs in the energy range we are interested in. Indeed, although all physical quantities relevant for LHC physics are in principle computable in the complete theory, generically, computations will be

easier to carry out in an EFT. Beside, if the gap between the heavy and light states is sufficiently large, the error made by using the EFT instead of the complete theory will be negligible.

Let us take the example of weak interaction. We know from chapter 1 that the complete, renormalizable theory of weak interaction is a gauge theory based on the group $SU(2)_L \times U(1)_Y$. However, as long as we are interested in processes which take place at an energy below the weak bosons mass scale, quantities such as the muon lifetime $\tau(\mu)$ or the electron-electron scattering cross-section $\sigma(ee \to AB)$ will be easier to compute in an EFT in which the weak bosons are decoupled. Such a theory has been constructed by Fermi in 1934 [118] long before the discovery of the weak bosons, and continues to be of great help, even though the SM has been developed since.

Reciprocally, if one has at hand a renormalizable theory $\mathcal{L}_R$ which is assumed to be incomplete, for instance, due to naturalness reasons, one can parameterize in a model-independent way the effects of the unknown, high scale physics, by adding non-renormalizable operators $\mathcal{L}_{NR}$ to the core Lagrangian $\mathcal{L}_R$. The resulting Lagrangian $\mathcal{L}_{eff} = \mathcal{L}_R + \mathcal{L}_{NR}$ will be again an EFT. This EFT will be perfectly fine as long as we use it at energies below the cutoff energy, at which the effects of the new physics are supposed to manifest themselves. For example, if SUSY is asked to provide a solution to the hierarchy problem, one knows that the SM, seen as an EFT, has to break down at the TeV scale where s-partners must appear. Another example of EFT whose Ultra Violet (UV) physics is unknown can be found in SUSY GUTs. Indeed, SUSY GUTs are assumed to be EFT, valid only up to the GUT scale, above which new physics effects are supposed to appear, perhaps linked to string theory, to properly incorporate the quantum effects of gravity. In the present work, we will be mainly interested in the first case, where the EFT is deduced from a larger, renormalizable SUSY theory supposed to be known.

We want now to adopt a more formal approach and give the generic recipe to construct an EFT from a renormalizable theory, restricting for simplicity to the case of a scalar field theory $\mathcal{L}(\phi, \partial_\mu \phi)$. This recipe goes through three steps:

1. First, we remind that a scalar field $\phi(x)$ can be Fourier expanded in term of ladder operators $a_p, a_p^\dagger$ as:

$$\phi(x) = \int \frac{d^3p}{(2\pi)^3} \frac{1}{\sqrt{2\omega_p}} \left(a_p e^{ipx} + a_p^\dagger e^{-ipx} \right) \tag{4.36}$$

where ω_p is the frequency/energy of the mode p. Then, the first step consists in picking a mass scale Λ. This mass scale allows to divide the fields of the theory ϕ into two types:

$$\phi = \phi_L + \phi_H \tag{4.37}$$

where ϕ_L contains the low-energy Fourier modes ($\omega_L < \Lambda$) and ϕ_H contains the high-energy modes ($\omega_L > \Lambda$) in the expansion (4.36). In fact, Λ represents the upper-bound of the energy range in which the EFT makes sense. Above Λ, the EFT will be of no use, and will give inconsistent results. This is perfectly fine as an EFT being "effective" is only physically relevant in a given, finite, energy range. Low energy physics, in which we are interested, can be then entirely described in terms of the ϕ_L fields. Everything we wish to know on the low energy physics (scattering amplitudes, decay rates etc...) can be computed from Green's functions of these light fields. These functions take the form:

$$\langle 0|T\left(\{\phi_L(x_1), \cdots, \phi_L(x_n))\}|0\right\rangle = \frac{1}{Z[0]} \left(-i\frac{\delta}{\delta J_L(x_1)}\right) \cdots \left(-i\frac{\delta}{\delta J_L(x_n)}\right) Z[J_L]\Big|_{J_L=0}. \tag{4.38}$$

where the generating functional $Z[J_L]$ is given by:

$$Z[J_L] = \int \mathcal{D}\phi_L \mathcal{D}\phi_H e^{iS(\phi_L,\phi_H) + i\int d^D x J_L(x)\phi_L(x)} \tag{4.39}$$

and where $S(\phi_L, \phi_H) = \int d^D x \mathcal{L}(x)$ is the action of the theory, D the dimension of space-time and J_L are source terms for the light fields.

2. The second step consists in computing the path integral over the high-frequency fields ϕ_H in eq. (4.39). If we define the Wilsonian effective action as:

$$e^{iS_\Lambda(\phi_L)} \equiv \int \mathcal{D}\phi_H e^{iS(\phi_L,\phi_H)} \tag{4.40}$$

one gets to:

$$Z[J_L] = \int \mathcal{D}\phi_L e^{iS_\Lambda \phi_L + i\int d^D x J_L(x)\phi_L(x)} \tag{4.41}$$

which does not depend on the heavy fields anymore. $S_\Lambda(\phi_L)$ depends by construction on the choice of cutoff Λ used to split the low-energy modes from the high-energy modes. Note that, this path integration comes at the price that, on scales $\Delta x^\mu = 1/\Lambda$, S_Λ is non-local anymore. This operation of removing the heavy fields of the theory is often referred to as "integrating out" the high-frequency modes of the functional integral.

3. Finally, during the third step, we have to take care of the non-locality of $S_\Lambda(\phi_L)$. To do so, we will expand $S_\Lambda(\phi_L)$ in terms of local operators composed of light fields. This expansion is called the (Wilsonian) Operator-Product Expansion (OPE) [119]. The OPE is only possible because $E << \Lambda$ by assumption. The result can be cast in the form:

$$S_\Lambda(\phi_L) = \int d^D x \mathcal{L}^{eff}_\Lambda(x), \tag{4.42}$$

where

$$\mathcal{L}^{eff}_\Lambda(x) = \sum_i C_i Q_i(\phi_L(x)) \tag{4.43}$$

is the "effective Lagrangian" and is composed of an infinite sum over local operators Q_i multiplied by coupling constants C_i called "Wilson coefficients". The Wilson coefficients contain all information about short-distance physics beyond the energy scale Λ. In general, all operators allowed by the symmetries of the low-energy theory are generated in the construction of the effective Lagrangian and appear in the sum. Thus, an effective Lagrangian constitutes a useful tool to describe low energy processes in a model-independent way.

4.4.1.2 One-loop effective operators

After having outlined the general construction of an EFT, we would like to focus on a specific type of EFT, namely SUSY EFT. Indeed, starting from a MSSM Lagrangian, if the up-squarks spectrum is heavy enough, the heavy squarks can be integrated out, resulting in a low-energy Lagrangian that contains the SM plus other light SUSY particles. But, we have checked that using other light s-partners to test $A_U \approx A_U^T$ does not provide attractive possibilities. In particular, gauginos are flavor-blind and bottom squarks depend on their own flavor structure.

Instead, we focus on the case where the entire SUSY spectrum is heavy and can be integrated out. If the SUSY scale M_{SUSY} is high enough, the procedure outlined in subsubsection 4.4.1.1, when applied to the MSSM Lagrangian, results in the following effective Lagrangian:

$$\mathcal{L}_{eff} = \mathcal{L}_{SM} + \mathcal{L}^{(5)} + \mathcal{L}^{(6)} + O(1/M^3_{SUSY}). \tag{4.44}$$

In equation (4.44), $\mathcal{L}_{SM}$ is the SM Lagrangian and $\mathcal{L}^{(n>4)}$ represents non-renormalizable operators of dimension n. We can truncate $\mathcal{L}_{eff}$ at order $O(1/M^3_{SUSY})$, because effective operators with dimension larger than 6 are not relevant for our present study. The dimension-6 Lagrangian takes the form:

$$\mathcal{L}^{(6)} = \sum_i \frac{\alpha_i}{M^2_{SUSY}} \mathcal{O}_i, \tag{4.45}$$

where the α_i are the dimensionless constants associated to the operators $\mathcal{O}_i$. This Lagrangian contains 59 independent operators, which have been first fully classified in ref. [120].

Now, we would like to go further, and restrict this set of 59 operators to only a few ones, which will be potentially useful to build $SU(5)$ tests. Mainly, we are looking for operators satisfying two conditions:

- At least one up-type trilinear vertex $(A_U)_{ij} h_u \tilde{Q}_i \tilde{U}_j$ should be present in the operator, as it encloses the $SU(5)$ relation we want to test.
- Fermions on the outgoing legs should be present, in order to access information on the flavor structure of the $(A_U)_{ij}$ coupling.

These two requirements naturally lead to the sector of up-type flavor-changing dipole operators of the form:

$$\mathcal{O}^V_{u,ij} = \bar{q}_i \sigma^{\mu\nu} u_j H_u V_{\mu\nu}|_{i \neq j} \tag{4.46}$$

where $V = (G, W, B)$ are the three Gauginos and $\sigma^{\mu\nu} \equiv \frac{i}{2}[\gamma^\mu, \gamma^\nu]$. The key point to obtain a test of the $SU(5)$ hypothesis is to be able to distinguish between $\mathcal{O}^V_{u,ij}$ and $\mathcal{O}^V_{u,ji}$. The generation of these operators and the possibilities they offer to build a $SU(5)$ test will be discussed in section 4.5.

4.4.1.3 Tree-level up-squark effective theory

Although the pattern of squark masses is arbitrary in full generality, a likely situation is that the masses exhibit some hierarchy. This is favored from naturalness considerations, from LHC bounds, as well as from certain classes of models. In such a situation, the physics of light squarks can be conveniently captured into a low energy effective theory, where heavy squarks have been integrated out. To do so, one has to look at the up-squark mass term in the MSSM Lagrangian:

$$\mathcal{L} \supset \tilde{u}^\dagger \mathcal{M}^2_{\tilde{u}} \tilde{u} \tag{4.47}$$

given in the SCKM basis, $\tilde{u} = \left(\tilde{u}_L, \tilde{c}_L, \tilde{t}_L, \tilde{u}_R, \tilde{c}_R, \tilde{t}_R\right)$. Let us reorganize this term as:

$$\mathcal{L} \supset \tilde{u}^\dagger \mathcal{M}^2_{\tilde{u}} \tilde{u} \equiv \Phi^\dagger \mathcal{M}^2_{\tilde{u}} \Phi = \left(\hat{\phi}^\dagger, \phi^\dagger\right) \begin{pmatrix} \hat{M}^2 & \tilde{M}^2 \\ \tilde{M}^{2\dagger} & M^2 \end{pmatrix} \begin{pmatrix} \hat{\phi} \\ \phi \end{pmatrix}. \tag{4.48}$$

Here, ϕ (resp: $\hat{\phi}$) is a column vector which contains the light (resp: heavy) up-squarks of the spectrum.

The relevant piece of the corresponding Lagrangian has the general form:

$$\mathcal{L} \supset |D\Phi|^2 - \Phi^\dagger \mathcal{M}^2_{\tilde{u}} \Phi + \left(\mathcal{O}\phi + \hat{\mathcal{O}}\hat{\phi} + \text{h.c}\right) \tag{4.49}$$

where $\mathcal{O}$ (resp: $\hat{\mathcal{O}}$) is a row vector containing all the interactions of the light (resp: heavy) up-squarks fields with the other fields of the MSSM Lagrangian, that are potentially exploited to probe the up-squark sector.

Let us compute the Euler-Lagrange equations of motion (EOMs) of ϕ and $\hat{\phi}$.

These EOMs take the form:

$$\partial^2 \hat{\phi}^\dagger + \hat{\phi}^\dagger \hat{M}^2 + \phi^\dagger \tilde{M}^{2\dagger} = \hat{\mathcal{O}} \tag{4.50}$$

$$\partial^2 \hat{\phi} + \hat{M}^2 \hat{\phi} + \tilde{M}^2 \phi = \hat{\mathcal{O}}^\dagger \tag{4.51}$$

where $\partial^2 \equiv \partial_\mu \partial^\mu$ is the d'Alembert operator. One can then go to momentum space with the replacement $\partial^2 \to -p^2$ in equations (4.50) and (4.51). As the mass matrix $\hat{M}$ is invertible, one can set these equations to the form:

$$\hat{\phi} = \frac{\tilde{M}^2 \phi - \hat{\mathcal{O}}^\dagger}{p^2 - \hat{M}^2} \tag{4.52}$$

$$\hat{\phi}^\dagger = \frac{\phi^\dagger \tilde{M}^{2\dagger} - \hat{\mathcal{O}}}{p^2 - \hat{M}^2} \tag{4.53}$$

Assuming that the norm of the heavy squark mass matrix $\hat{M}^2$ is large with respect to the typical momentum scale p^2 at which the theory is probed:

$$||\hat{M}^2|| = \sqrt{\sum_{i,j} \left|\hat{M}^2_{i,j}\right|^2} >> p^2, \tag{4.54}$$

the propagators in equations (4.52) and (4.53) can be Taylor expanded. Then, plug in these equations into the up-squarks Lagrangian (4.49), after a little bit of algebra, one is left with the following effective Lagrangian of light squarks:

$$\begin{aligned}\mathcal{L}_{\text{eff}} = |D\phi|^2 - \phi^\dagger \left[M^2 - \tilde{M}^{2\dagger}\hat{M}^{-2}\tilde{M}^2 - \frac{1}{2}\{\tilde{M}^{2\dagger}\hat{M}^{-4}\tilde{M}^2, M^2\} \right] \phi \\ + \left[\mathcal{O} - \hat{\mathcal{O}}\left(\hat{M}^{-2} - \hat{M}^{-4}D^2\right)\tilde{M}^2 - \frac{\mathcal{O}}{2}\tilde{M}^{2\dagger}\hat{M}^{-4}\tilde{M}^2 \right] \phi + \text{h.c}\end{aligned} \tag{4.55}$$

where the heavy squarks have been integrated out of the theory. Note that, in the derivation of eq. (4.55) a field redefinition:

$$\Phi \to \left(\mathbb{1} - \frac{1}{2}\tilde{M}^{2\dagger}\hat{M}^{-4}\tilde{M}^2 \right) \Phi \tag{4.56}$$

is needed in order to canonically normalize the kinetic terms of the squarks. The $\{,\}$ denoting here the anti-commutator. In this effective Lagrangian, we have kept only the leading and subleading terms of the $p^2\hat{M}^{-2}$ expansion relevant to build $SU(5)$ tests. The effective Lagrangian (4.55) contains in principle higher dimensional couplings and derivative terms, which are either subleading or irrelevant for the observables we are going to consider, and are thus neglected.

From eq. (4.55), we see that flavor violating couplings of the light squarks enter at first order and are controlled by $\hat{M}^{-2}\tilde{M}^2$. The flavor-conserving couplings will instead be modified at the second order. The mass matrix M^2, associated to the light squarks, receives a correction independent of M^2 at first order, and corrections proportional to M^2 at second order. The imprint of the heavy up-squarks in the Lagrangian of eq. (4.55) appears as corrections to the masses and couplings of the light up-squark states. Physically, these corrections have to be understood both as tree-level exchange of heavy up-squarks, and as the first term of the expansion with respect to the small parameter that describe mixing of heavy and light squarks. We emphasize the fact that the EFT developed here is applicable whatever the number of heavy up-squarks is contained in $\hat{\phi}$, while the others are assumed to be light enough to be accessible at the LHC.

4.4.2 Mass-insertion approximation

Supersymmetric models generically predict new sources of flavor and CP violation not present in the Standard Model. In particular, FCNC processes are present, for example through loop diagrams involving squarks and gauginos or Higgsinos. These occur via vertices of the type $q_i\,\widetilde{q}_j\,\widetilde{V}$ where $\widetilde{V} = \{\widetilde{G}, \widetilde{W}, \widetilde{B}, \widetilde{H}_{u/d}\}$ and q_i, $\widetilde{q}_j$ share the same electric charge. These processes are severely constrained by physical observables such as ϵ_K or $\text{BR}(b \to s\gamma)$. Note that obtaining perturbative expressions for these obervables, in terms of the fundamental parameters of the Lagrangian, is not straightforward. In particular, one has to deal with the diagonalization of the full 6×6 squark matrix. From a phenomenological point of view, it is thus desirable to find a procedure which allows to easily translate the bounds given by experiments on constraints upon the fundamental SUSY parameters, such as the elements of the mass matrices or the squark mixing angles.

The so-called Mass Insertion Approximation (MIA) (see [121], [122]), allows one to do exactly this task. Basically, it consists in a Taylor expansion of the superpartners propagators inside Feynman integrals. In the MIA, the up-squark mass matrix can be written in terms of the mass insertion parameters $\left(\delta_u^{MN}\right)_{ij}$, where $M, N = L, R$ denote chirality indices, as follows:

$$\mathcal{M}^2_{\tilde{u}} \approx m^2_{\tilde{q}} \left[\mathbb{1} + \begin{pmatrix} \delta_u^{LL} & \delta_u^{LR} \\ \delta_u^{RL} & \delta_u^{RR} \end{pmatrix} \right], \tag{4.57}$$

where $m^2_{\tilde{q}} = \frac{1}{6}\text{Tr}\left(\mathcal{M}^2_{\tilde{u}}\right)$ is an average squark mass and δ_u^{MN} are 3×3 matrices in flavor space, for example:

$$\left(\delta_u^{LL}\right) = \begin{pmatrix} \left(\delta_u^{LL}\right)_{14} & \left(\delta_u^{LL}\right)_{15} & \left(\delta_u^{LL}\right)_{16} \\ \left(\delta_u^{LL}\right)_{24} & \left(\delta_u^{LL}\right)_{25} & \left(\delta_u^{LL}\right)_{26} \\ \left(\delta_u^{LL}\right)_{34} & \left(\delta_u^{LL}\right)_{35} & \left(\delta_u^{LL}\right)_{33} \end{pmatrix}. \tag{4.58}$$

Beside, we have $\delta_u^{RL} = (\delta_u^{LR})^\dagger$ due to the hermiticity of $\mathcal{M}^2_{\tilde{u}}$.

Going back to the $SU(5)$ relation $A_U \approx A_U^T$ we are interested in, it translates on the chirality flipping, flavor violating, mass insertion matrices as:

$$\delta_u^{LR} = (\delta_u^{LR})^T, \tag{4.59}$$

or equivalently, in terms of the generation-mixing entries:

$$(\delta_u^{LR})_{12} = (\delta_u^{LR})_{21}, \;\; (\delta_u^{LR})_{31} = (\delta_u^{LR})_{13}, \;\; (\delta_u^{LR})_{32} = (\delta_u^{LR})_{23}. \tag{4.60}$$

Following [122], in what follow, we would like to work-out the explicit expression of the mass insertion parameters. However, for the sake of simplicity, we will restrict the discussion to chirality-conserving parameters. In the mass basis, the chirality-conserving insertion mass parameters take the following form:

$$\left(\delta^u_{ij}\right)_{MM} = \frac{1}{m^2_{\tilde{q}}} \left(\mathcal{R}^{\tilde{u}}_M\right)_{i\alpha} \left(\mathcal{R}^{\tilde{u}}_M\right)^*_{j\alpha} \Delta m^2_{\tilde{q}_\alpha}, \tag{4.61}$$

where $\mathcal{R}^{\tilde{u}}$ is the mixing matrix which rotates the up-squarks to their mass eigenstate basis, $m^2_{\tilde{q}} = \frac{1}{3}\sum_{\alpha=1}^3 m^2_{\tilde{q}_{M\alpha}}$ and $\Delta m^2_{\tilde{q}_\alpha} = m^2_{\tilde{q}_\alpha} - m^2_{\tilde{q}}$.

Assume that the following two constraints are satisfied:

$$\left|\left(\mathcal{R}^{\tilde{u}}\right)_{ik}\left(\mathcal{R}^{\tilde{u}}\right)^*_{jk}\right| \ll \left|\left(\mathcal{R}^{\tilde{u}}\right)_{ij}\left(\mathcal{R}^{\tilde{u}}\right)^*_{jj}\right|, \;\; \left|\left(\mathcal{R}^{\tilde{u}}\right)_{ik}\left(\mathcal{R}^{\tilde{u}}\right)^*_{jk}\Delta m^2_{\tilde{q}_j\tilde{q}_i}\right| \ll \left|\left(\mathcal{R}^{\tilde{u}}\right)_{ij}\left(\mathcal{R}^{\tilde{u}}\right)^*_{jj}\Delta m^2_{\tilde{q}_j\tilde{q}_i}\right| \tag{4.62}$$

where there is no summation over i, j, k and $\Delta m^2_{\tilde{q}_i\tilde{q}_j} \equiv m^2_{\tilde{q}_i} - m^2_{\tilde{q}_j}$. Then, an effective two generations framework can be used, in which the expression of the δ^u_{ij}'s simplifies to:

$$\left(\delta^u_{ij}\right)_{MM} = \frac{\Delta m^2_{\tilde{q}_j\tilde{q}_i}}{m^2_{\tilde{q}}} \left(\mathcal{R}^{\tilde{u}}_M\right)_{ij} \left(\mathcal{R}^{\tilde{u}}_M\right)^*_{jj}. \tag{4.63}$$

In a two generation framework, a wise choice consist in using the mass scale $m_{\tilde{q}} = \frac{1}{2}\left(m_{\tilde{q}_i} + m_{\tilde{q}_j}\right)$ as it has been shown to improve the accuracy of the MIA [121].

We would like to stress a point here. The MIA is often viewed in the literature as an expansion in terms of small off-diagonal, flavor violating, mass terms i.e., the expansion parameter is taken to be $\delta_{ij} = \Delta_{ij}/m^2_{\tilde{q}}$ where Δ_{ij} is an off-diagonal element of $\mathcal{M}^2_{\tilde{u}}$. This is a more restrictive expansion, and it has to be seen as a special case of the MIA as defined here. Indeed, we see from eq. (4.61), that one can obtain $\delta^u << 1$ via two different ways. Either the mixing angles $\mathcal{R}_{ij}$ are small, which is referred to as *alignment*, or the mass matrix is nearly degenerate $\Delta m^2_{\tilde{q}_\alpha}/m^2_{\tilde{q}} \ll 1$. Indeed, in the alignment paradigm, the quark and squarks mass matrices are nearly simultaneously diagonal in the SCKM basis. This in turn suppress SUSY contributions to FCNCs processes without requesting degenerate mass eigenstates. Alignment can be for example achieved when one constructs SUSY models with non-abelian flavor symmetries [123]. This being said, it is possible to define a MIA even though the mass matrix is not degenerate as long as the mixing angles are sufficiently small to compensate the hierarchical structure of $\mathcal{M}^2_{\tilde{u}}$ [121]. However, we will not consider this case here and we will consider that the MIA applies only when the squark spectrum is nearly degenerate i.e. we ask $\Delta m^2_{\tilde{q}_\alpha}/m^2_{\tilde{q}} \ll 1$ as the condition of validity of the MIA.

The MIA is commonly used in the broken electroweak phase with $\langle H \rangle \equiv v/\sqrt{2} \neq 0$. However, the effect of electroweak symmetry breaking in the mass matrix is small by assumption, as it participates in splitting the eigenvalues. In particular, this is verified whenever $M_{SUSY} >> v/\sqrt{2}$. Therefore electroweak breaking does not correct substantially the mean squark mass $\widetilde{m}_q$ by construction. As a result, the MIA can also be used in the unbroken electroweak phase. In this case, the VEVs have to be replaced by the original Higgs fields. Electroweak symmetry breaking appears in the squark mass matrices exclusively through the chirality-flipping mass insertion parameters δ^{LR} and δ^{RL}. More precisely, the latter are proportional to the VEV according to $\delta^{LR,RL} \propto v/M_{SUSY}$, while the chirality conserving ones are not. Thus, the use of the parameters δ^{LL} and δ^{RR} remain unchanged in the

unbroken phase. In contrast, for the chirality flipping, flavor violating, mass insertions we are interested in, we have to replace:

$$\left(\delta_u^{LR}\right)_{ij} \to \frac{\sqrt{2}H_u}{v_u}\left(\delta_u^{LR}\right)_{ij}, \tag{4.64}$$

for $i \neq j$. This is also a way to recover the physical Higgs boson in the complete mass matrix eq. (4.11).

4.4.3 Statistical tools

In this subsection we would like to introduce the statistical tools needed for the rest of this work. All discussions presented here will be developed in the context of the *frequentist* interpretation of probability theory.

In frequentist inference, the probability of an outcome of an experiment is defined as the relative frequency of that event to occur in the limit where the experiment is repeated an infinite number of times. For example, consider a discrete random variable X which can take values $X = \{x_1, ..., x_k\}$. If N is the number of times that X has been sampled, and $N(X = x_1)$ is the number of times where the random variable X has indeed picked the value x_1 during the N trials, then $P(X = x_1)$ is defined as:

$$P(X = x_1) = \lim_{N\to\infty} \frac{N(X = x_1)}{N}. \tag{4.65}$$

Clearly, the frequentist interpretation assumes that an experiment can be repeated a sufficiently number of times with uncorrelated outcomes, so that the limit (4.65) can converge.

An alternative interpretation of probability, which allows to define a probability when this last condition is not fulfilled, the *Bayesian* interpretation, will be discussed in the next chapter.

The rest of the section is organized as follows. In subsubsection 4.4.3.1, we introduce the notion of p-value, which is central in (frequentist) hypothesis testing, through one simple but intuitive example. In subsubsection 4.4.3.2, we proceed by introducing the notion of *expected precision*. This last quantity will play a central role as it will allow to quantify the feasibility of the $SU(5)$ tests to be proposed in the rest of this chapter. A very good review of all notions covered here can be found in ref. [116].

4.4.3.1 p-value

Assume that the data of an experiment are described by a continuous variable X. Let us recall that a statistical hypothesis consists in specifying a Probability Density Function (PDF) supposed to describe correctly the outcomes of X. If one has at disposal two hypothesis noted H_0 and H_1, the p-value asks the question of the exclusion of one of these two hypothesis, for example H_0, called the "null hypothesis", with regards to the data. Thus, the $p - value$ is defined as the probability, under the assumption of the null hypothesis, to obtain a result equals to, or more extreme to what was actually observed. For example, if the outcome of an experiment results in X taking a value x, then the p-value is defined either as $P(X \geq x|H_0)$ (right-tail event), $P(X \leq x|H_0)$ (left-tail event) or $2\min\left(P(X \geq x|H_0), P(X \leq x|H_0)\right)$ (for double-tail event). If that p-value is smaller than a certain threshold value, called the level of significance, one can exclude the null-hypothesis. The level of significance is purely arbitrary. In high energy physics, the consensus wants that the null-hypothesis can be rejected if the p-value is found to be less then $\alpha = 0.05$ (5%).

Let us take an example [1]. Consider an experiment set up to determine if a coin is fair or not. Assume that the coin has been flipped 20 times and that over these 20 times, the coin has turned up heads 14 times. Here, the null hypothesis would be that the coin is fair, i.e. $P(\text{Heads}) = P(\text{Tail}) = 0.5$ and the statistical test is the number of heads. If we consider a right-tailed test, the p-value of this result is the chance of a fair coin landing on heads *at least* 14 times out of 20 flips. This probability can be computed from binomial coefficients as:

$$P(N_{Heads} \geq 14) = \frac{1}{2^{20}}\left[\binom{20}{14} + \binom{20}{15} + \cdots + \binom{20}{20}\right] \approx 0.058 \tag{4.66}$$

[1] This example has been taken from en.wikipedia.org/wiki/P-value.

This probability is the p-value, considering only extreme results which favor heads, resulting in an one-tailed test. On the other hand, it would also have been possible to define a two-tailed test, which take into account the significance of the deviation in both directions, favoring either heads or tails.

Here the p-value test exceeds 0.05, so the observation is consistent with the null hypothesis, as it falls within the range of what would happen 95% of the time were the coin in fact fair. Hence, we fail to reject the null hypothesis at the 5% level. Although the coin did not fall evenly, the deviation from the expected outcome is small enough to be consistent with statistical fluctuations.

4.4.3.2 Expected precision

If the $SU(5)$ hypothesis implies that a certain set of observables, for example some LHC event rates, are constrained by a simple relation at the TeV scale, then one can use a p-value test to evaluate the potential of this test. In this context, the null hypothesis is that the GUT scale is symmetric under the $SU(5)$ group. Assume that, if the null hypothesis is true, there is a relation $R(\mathcal{O}_i)$ among observable quantities $\mathcal{O}_i$, that satisfies:

$$\mathrm{E}\left[R\left(\mathcal{O}_i\right)\right] = 0 \tag{4.67}$$

with E the expectation operator. Here, $R(x)$ is a continuous random variable, which depends on a (continuous) parameter x. We use a p-value test to quantify whether or not the *observed* value of R, denoted $\hat{R}$, is compatible with zero. This test is not trivial to perform in general but simplifies whenever the PDF of $\hat{R}$ can be approximated by a half-normal distribution [124]:

$$f_{\hat{R}}(x) = 2\mathcal{N}\left(x; \mu = 0, \sigma\right)\theta\left(x\right). \tag{4.68}$$

where θ is the unit step function defined as $\theta\left(x \geq 0\right) = 1$ and $\theta\left(x\right) = 0$ otherwise and where $\mathcal{N}\left(x; \mu, \sigma\right)$ is the normalized Gaussian PDF of standard deviation σ and mean μ.

In this case, the compatibility of $\hat{R}$ with the $\hat{R} = 0$ (e.g. $SU(5)$) hypothesis can be expressed in terms of a statistical significance Z. Suppose that one has computed the p-value associated to the test $\hat{R} = 0$. Then, one can define a statistical significance from p via the following formula:

$$Z = \Phi^{-1}\left(1 - p\right) \tag{4.69}$$

which translates the p-value into a significance given in terms of standard Gaussian deviations. Φ^{-1} is the inverse of the Gaussian cumulative distribution function [2]. Whenever $\hat{R}$ follows a half-normal distribution of the type eq. (4.68), the significance (4.69) simplifies to (see [116]):

$$Z = \frac{|\hat{R}|}{\sigma}. \tag{4.70}$$

For a given relation satisfying (4.67) and a hypothesized amount of data, one can evaluate the expected value of σ. If one fixes a certain threshold significance value Z, the quantity:

$$P_Z = Z\sigma \tag{4.71}$$

represents the *expected precision* at which the relation (4.67) can be tested, at the level of significance Z. In sections 4.5, 4.6 and 4.7, we will systematically report the value of P_Z, for different significance levels, when a relation like (4.67) will be available.

Let us take an example to be more concrete. Consider the relation:

$$aX_1 = bX_2. \tag{4.72}$$

The X_i are assumed to be normal variables, of mean μ_i and variance σ_i^2. Defining $R \equiv |aX_1 - bX_2|$, the PDF of R takes the form $f_R\left(x\right) = 2\mathcal{N}\left(x; \mu, \sigma\right)\theta\left(x\right)$, where the mean is $\mu = a\mu_1 - b\mu_2$ and the variance is given by $\sigma^2 = a^2\sigma_1^2 + b^2\sigma_2^2$. In order to compute the expected significance defined in eq.

[2] We recall that the Gaussian cumulative distribution function $\Phi\left(x\right)$ is defined as $\Phi\left(x\right) \equiv \int_{y=-\infty}^{x} \mathcal{N}\left(y, \mu, \sigma\right) \mathrm{d}y$ with $\mathcal{N}\left(y, \mu, \sigma\right)$ the Gaussian PDF of mean μ and standard deviation σ.

(4.71), we use this value of σ, under the assumption that the $SU(5)$ hypothesis is satisfied i.e. that $\mu = 0$.

In practice, it is useful to normalize R such that $E[R] \in [0,1]$. The expected precision can then be expressed in percents. Concretely, having $P_Z = 20\%$ means that a violation of the relation $E[R] = 0$ by 20% or more (i.e. $E[R] > 20\%$) can be assessed with a significance of $Z\sigma$. Beside, using a normalized quantity makes easier the task to interface $SU(5)$ tests with others studies.

Normalizing R implies that one frequently encounters the random variable $|A-B|/|A+B|$, where A and B are potentially correlated. We will use the following notations: $\mu_A \equiv E[A]$, $\mu_B \equiv E[B]$, $\sigma_A^2 \equiv V[A]$, $\sigma_B^2 \equiv V[B]$ and the correlation coefficient $\rho \equiv \frac{\text{Cov}[A,B]}{\sigma_A \sigma_B}$ where $\text{Cov}[A,B]$ is the covariance of A and B [3].

These notations allow to tabulate a set of approximations that we have used to derive the expected precision P_Z in the different cases to be considered in the rest of this chapter. In the Gaussian limit, when a ratio of random variable is described by the Fieller-Hinkley distribution [125], one has the following approximations:

$$\begin{aligned} E[A/B] &\approx E[A]/E[B] \\ V[A/B] &\approx \frac{1}{\mu_B^4}\left(\mu_A^2\sigma_B^2 + \mu_B^2\sigma_A^2 - 2\rho\sigma_A\sigma_B\mu_A\mu_B\right) \\ V[(A-C)/(A+C)] &\approx 4\frac{\mu_A^2\sigma_C^2 + \mu_C^2\sigma_A^2}{(\mu_A+\mu_C)^4} \approx 4V[A/(A+C)] \quad \text{with} \quad \text{Cov}[A,C] = 0. \end{aligned} \tag{4.73}$$

Also, for two large number of events N_A, N_C one has $N_{A/C} \approx \mu_{A/C} \approx \sigma^2_{A/C}$ and the following approximation holds:

$$V[|N_A - N_C|/(N_A+N_C)] = \frac{4N_AN_C}{(N_A+N_C)^3} \tag{4.74}$$

4.5 Case I: Heavy SUSY

We can now apply the strategy and tools developed in section 4.4 to build $SU(5)$ tests in various SUSY scenarios. In this section, we will assume that the SUSY scale is large with respect to the TeV scale probed by the LHC. This scenario introduces large logarithms into the perturbative series of the Higgs boson mass, thus increasing the fine-tuning of the model. Hence, heavy SUSY plays, a-priori, against the MSSM as a solution to the hierarchy problem.

On the other hand, it has recently been shown that the MSSM can accommodate, with a moderate fine-tuning, a 125 GeV Higgs in such scenarios, when the SUSY scale exceeds 10^{10} GeV [126] with even better unification than in standard low energy scenarios [127].

In such a situation, it is appropriate to integrate the whole SUSY spectrum. As discussed in section 4.4, the dimension-six operators that one should scrutinize to test the $SU(5)$ hypothesis are the up-sector dipoles:

$$\mathcal{L}^{(6)}_{1-\text{loop}} \supset \frac{\alpha^G_{ij}}{M^2_{SUSY}}\bar{q}_i\sigma^{\mu\nu}T^a u_j H_u G^a_{\mu\nu} + \frac{\alpha^W_{ij}}{M^2_{SUSY}}\bar{q}_i\sigma^{\mu\nu}T^I u_j H_u W^I_{\mu\nu} + \frac{\alpha^B_{ij}}{M^2_{SUSY}}\bar{q}_i\sigma^{\mu\nu}u_j H_u B_{\mu\nu}, \quad i \neq j. \tag{4.75}$$

Our ability to build a $SU(5)$-test relies crucially on distinguishing the chirality of the external SM fields at some level. The only quark for which this can be done is the top quark, as the lighter quarks hadronize too fast. Our test has therefore to rely on *top polarimetry* which itself relies on the chiral structure of the leading top decay $t \to bW$ (see [128]).

[3] We recall that the covariance of two random variables A and B is defined as: $\text{Cov}[A,B] \equiv E[(A-\mu_A)(B-\mu_B)]$.

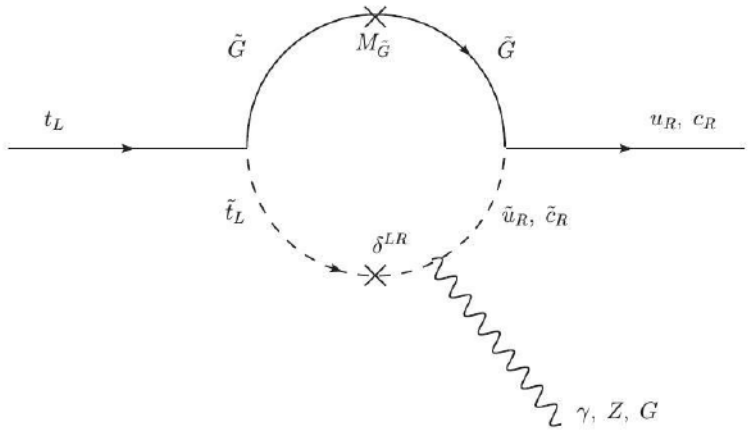

Figure 4.8 – One loop contribution to dipole-induced top decay via gluino exchange. The photon and gluon lines are attached to the loop in all possible ways.

We therefore focus only on the dipole operators involving a top quark:

$$\begin{aligned}\mathcal{L}^{(6)}_{1-\text{loop}} \supset & \frac{\alpha^G_{3i}}{M^2_{SUSY}}\bar{t}_L\sigma^{\mu\nu}T^a u_{Ri}H_u G^a_{\mu\nu} + \frac{\alpha^W_{i3}}{M^2_{SUSY}}\bar{u}_{Li}\sigma^{\mu\nu}T^a t_R H_u G^a_{\mu\nu} \\ & + \frac{\alpha^W_{3i}}{2M^2_{SUSY}}\bar{t}_L\sigma^{\mu\nu}u_{Ri}H_u W^3_{\mu\nu} + \frac{\alpha^W_{i3}}{2M^2_{SUSY}}\bar{u}_{Li}\sigma^{\mu\nu}T^I t_R H_u W^3_{\mu\nu} \\ & + \frac{\alpha^B_{3i}}{M^2_{SUSY}}\bar{t}_L\sigma^{\mu\nu}u_{Ri}H_u B_{\mu\nu} + \frac{\alpha^B_{i3}}{M^2_{SUSY}}\bar{u}_{Li}\sigma^{\mu\nu}t_R H_u B_{\mu\nu},\end{aligned} \tag{4.76}$$

where $i = 1, 2$ as we are only interested in flavor violating processes.

The operators given in eq. (4.75) are generated at one loop by penguin diagrams. They receive their main contributions from the chargino-down-squark, charged Higgs-down-quark and gluino-up-squark amplitudes. The latter is expected to dominate as it is enhanced by the QCD gauge coupling.

Moreover, contrary to the case of the down quarks, higher loop corrections in the up-sector from flavor changing self-energies are $\tan\beta$ suppressed [129], so that they cannot become large. We therefore end up with dipole operators mainly generated by the gluino loop represented on fig. 4.8.

From now on, we assume that the up-squark mass matrix is degenerate enough so that the MIA applies. The expression of the electroweak and chromo-dipoles operators are then given, in the electroweak unbroken phase and in the interaction basis, by:

$$\frac{\alpha^G_{3i}}{M^2_{SUSY}} = \frac{g_3^3}{16\pi^2 m^2_{\tilde{q}}}\left(7\sqrt{2}\frac{m_{\tilde{g}}\delta^{LR}_{3i}F^{(1)}_s(x_g)}{240v_u} - 5\frac{y_t\delta^{LL}_{3i}F^{(2)}_s(x_g)}{36}\right), \tag{4.77}$$

$$\frac{\alpha^W_{3i}}{M^2_{SUSY}} = \frac{g_1 g_3^2}{16\pi^2 m^2_{\tilde{q}}}\left(-\sqrt{2}\frac{m_{\tilde{g}}\delta^{LR}_{3i}F^{(1)}_{EW}(x_g)}{30v_u} + \frac{y_t\delta^{LL}_{3i}F^{(2)}_{EW}(x_g)}{9}\right), \tag{4.78}$$

$$\frac{\alpha^B_{3i}}{M^2_{SUSY}} = \frac{g_2 g_3^2}{16\pi^2 m^2_{\tilde{q}}}\left(-\sqrt{2}\frac{m_{\tilde{g}}\delta^{LR}_{3i}F^{(1)}_{EW}(x_g)}{180v_u} + \frac{y_t\delta^{LL}_{3i}F^{(2)}_{EW}(x_g)}{54}\right), \tag{4.79}$$

and the α_{i3} coefficients are obtained by replacements $\delta^{LR}_{3i} \to \delta^{LR}_{i3}$ and $\delta^{LL}_{3i} \to \delta^{RR}_{i3}$. Here, we have defined $x_{\tilde{g}} = \frac{m_{\tilde{g}}}{m_{\tilde{q}}}$. The form factors F_s, F_{EW} can be found in [115], [107] and are given in the appendix B. They all satisfy $F(1) = 1$ and $F(x) \to 0$ for $x \to \infty$.

The above expressions have been deduced from refs [115], [107] and by making use of section 4.4, in particular using eq. (4.64) to express these coefficients in the electroweak unbroken phase.

The coefficients of the Dipole EW operators after EWSSB,

$$\mathcal{L}^{(6)}_{1-\text{loop}} \supset \frac{\alpha^{\gamma}_{3i}}{M^2_{SUSY}} \bar{t}_L \sigma^{\mu\nu} u_{Ri} H_u F_{\mu\nu} + \frac{\alpha^{Z}_{3i}}{M^2_{SUSY}} \bar{t}_L \sigma^{\mu\nu} u_{Ri} H_u Z_{\mu\nu}, \tag{4.80}$$

are obtained by making the following rotation:

$$\begin{pmatrix} \alpha^{Z}_{ij} \\ \alpha^{\gamma}_{ij} \end{pmatrix} = \begin{pmatrix} c_w & -s_w \\ s_w & c_w \end{pmatrix} \begin{pmatrix} \alpha^{W}_{ij}/2 \\ \alpha^{B}_{ij} \end{pmatrix} \tag{4.81}$$

where $c_w = \cos\theta_W$, $s_w = \sin\theta_W$ are the cosine and sine of the Weinberg angle.

As already pointed out above, for the purpose of obtaining a $SU(5)$ test, the contributions we are interested in are the chirality flipped ones δ^{LR}.

The chirality-conserving contributions from δ^{LL} and δ^{RR} are suppressed by a factor $y_t v_u / m_{\tilde{g}} = m_t s_\beta / m_{\tilde{g}}$ with respect to the contributions from δ^{LR}. This factor is compensated if one considers that $\delta^{LR} \propto v_u A_u / m^2_{\tilde{q}}$ as it is usually the case in SUSY models with soft breaking (see eq. 4.11). However, the magnitude of the A_u-term can be larger that $m^2_{\tilde{q}}$ (for example from naive dimensional analysis [130]). One should therefore let $\delta^{LR} \sim \mathcal{O}(1)$.

Considering usual $SU(5)$ models, one should also notice that the symmetry relation $M^2_Q = M^2_U$ implies, at the TeV scale:

$$\delta^{LL}_{3i} \approx \delta^{RR}_{3i} \tag{4.82}$$

to a good approximation (see section 4.3).

We can now identify the consequences of the $SU(5)$ relation $A_u \approx A_u^T$ at the LHC. This relation implies the following equalities between the coefficients of the dipoles in eq. (4.76):

$$\alpha^{G}_{3i} = \alpha^{G}_{i3}, \qquad \alpha^{W}_{3i} = \alpha^{W}_{i3}, \qquad \alpha^{B}_{3i} = \alpha^{B}_{i3}. \tag{4.83}$$

Concretely, the dipole operators induce both new top decays and top production modes at the LHC. These processes will be discussed in subsection 4.5.2.

4.5.1 SU(5) test through single top polarimetry.

We have seen above that measuring the top spin is a necessary ingredient to build a $SU(5)$ test that distinguishes between the $\mathcal{O}^V_{3i}$ and $\mathcal{O}^V_{i3}$ dipole operators. The expected precision associated with such polarization-based test can be evaluated in a generic way. The top spin has to be measured with some polarization-sensitive observable z with distribution f_Z. For example, for the $t \to bW$ decay, z can be the leptonic angle between the top and the lepton from the W^-decay, or the b-quark energy in the case of a boosted top [128]. The usual way to proceed to get information on the top spin is to split the phase space into two subsets $\mathcal{D} = \mathcal{D}_+ + \mathcal{D}_-$. The total sample of N events is then split into two subsamples $N_\pm = N|_{z \in \mathcal{D}_\pm}$ satisfying:

$$N = N_+ + N_-, \qquad \mathrm{E}[N_\pm] = \mathrm{E}[N] \int_{\mathcal{D}_\pm} f_Z(z) \mathrm{d}z. \tag{4.84}$$

The choice of $\mathcal{D}_\pm$ is in general a freedom of the analysis, although it is preferable to have $N_+ \sim N_-$ to minimize the statistical error. In what follows, we will systematically choose the subsets of phase space $\mathcal{D}_\pm$ such that $\mathrm{E}[N_+] = \mathrm{E}[N_-]$ if the $SU(5)$ hypothesis is satisfied.

As a concrete example, assume that the distribution f_Z takes the following form:

$$f_Z(z) \propto (1 + \kappa P_t z), \tag{4.85}$$

with $z \in [-1, 1]$, $\kappa \in [0, 1]$ and where $P_t = \pm 1$ is the top helicity. The power of the $SU(5)$ test will then depend on the power of the spin-analyzing variable κ. The lepton angle in $t \to bW$ has a maximal spin-analyzer power, i.e. $\kappa = 1$ due to the chiral structure of the electroweak interaction. In that case, z is the top-lepton angle in the top rest frame. For the subdomains of z we choose $\mathcal{D}_+ = [0, 1]$ and $\mathcal{D}_- = [-1, 0[$ which match the usual definition of a forward-backward asymmetry.

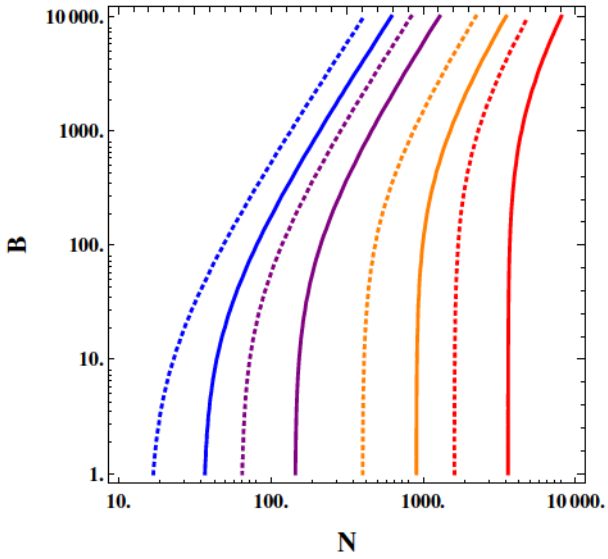

Figure 4.9 – Expected precision P_Z for top-polarization based $SU(5)$-tests as a function of the total number of signal and background events N and B. The spin-analyzing power is fixed to $\kappa = 1$. Dotted (plain) lines denote, respectively 2σ (3σ) significance levels. Blue, purple, orange, and red lines show then $P_{2,3} = 100\%,\ 50\%,\ 20\%$ and 10% isolines of expected precision.

With all these definitions, we can construct our first polarimetry-based test. Following subsubsection 4.4.3.2, one can define a normalized asymmetry out of N_+ and N_-:

$$R = \frac{2}{\kappa}\frac{|N_+ - N_-|}{N_+ + N_-}, \tag{4.86}$$

which satisfies:

$$\mathrm{E}[R] = \frac{\left||\alpha_{3i}|^2 - |\alpha_{i3}|^2\right|}{|\alpha_{3i}|^2 + |\alpha_{i3}|^2}. \tag{4.87}$$

Then, assuming B background events for the total signal, the expected precision defined in subsubsection 4.4.3.2 is equal to:

$$P_Z = Z\frac{2}{\kappa}\frac{(N+B)^{1/2}}{N}. \tag{4.88}$$

and is independent of the event numbers N_+, N_-.

Note that $P_Z \to \infty$ for $\kappa \to 0$ as, in this limit, no spin information is available. The expected precision is shown in fig. 4.9 as a function of the background and total number of events B and N. Obviously, the $SU(5)$ hypothesis starts to be testable when P_Z is lower than 100%.

In the no background event limit, i.e. if $B = 0$, we see that the hypothesis starts to be testable for $N \gtrsim 16$ at 2σ and for $N \gtrsim 36$ at 3σ significance. About 144, 900, and 3600 events are needed to test the relation at respectively 50%, 20% and 10% precision with 3σ significance. Clearly, and contrary to a mere signal discovery, a substantial amount of signal events is necessary in order to start to test the $SU(5)$ hypothesis.

4.5.2 Existing LHC searches.

Let us now discuss the various LHC processes that we expect to be relevant to perform the $SU(5)$ test eq. (4.86) described previously. The dipole-induced anomalous top couplings induce the two-body decays (see fig. 4.8):

$$t \to q\gamma, \quad t \to qZ, \quad t \to qG. \tag{4.89}$$

Among these decays, $t \to qZ$ and $t \to q\gamma$ carry information about the dipoles, that can be accessed through the polarization of the outgoing gauge bosons. The $t \to q\gamma$ process has been searched for at the Tevatron and LHC [131][135–137], the leading CMS bound is provided in table 4.3.

Dipole coefficients combinations	95% CL limits	SUSY
$\left(\lvert\alpha^{\gamma}_{31}\rvert^2+\lvert\alpha^{\gamma}_{13}\rvert^2\right)^{1/2} M^{-2}_{\rm SUSY}$	< 0.19 TeV^{-2} [131] (CMS)	$7\cdot 10^{-5}$ TeV^{-2}
$\left(\lvert\alpha^{\gamma}_{32}\rvert^2+\lvert\alpha^{\gamma}_{23}\rvert^2\right)^{1/2} M^{-2}_{\rm SUSY}$	< 0.65 TeV^{-2} [131] (CMS)	$7\cdot 10^{-5}$ TeV^{-2}
$\left(\lvert\alpha^{Z}_{31}\rvert^2+\lvert\alpha^{Z}_{13}\rvert^2\right)^{1/2} M^{-2}_{\rm SUSY}$	< 0.68 TeV^{-2} [132] (CMS)	$1\cdot 10^{-4}$ TeV^{-2}
$\left(\lvert\alpha^{Z}_{32}\rvert^2+\lvert\alpha^{Z}_{23}\rvert^2\right)^{1/2} M^{-2}_{\rm SUSY}$	< 3.44 TeV^{-2} [132] (CMS)	$1\cdot 10^{-4}$ TeV^{-2}
$\left(\lvert\alpha^{G}_{31}\rvert^2+\lvert\alpha^{G}_{13}\rvert^2\right)^{1/2} M^{-2}_{\rm SUSY}$	< 0.029 TeV^{-2} [133][134] (ATLAS)	$3\cdot 10^{-4}$ TeV^{-2}
$\left(\lvert\alpha^{G}_{32}\rvert^2+\lvert\alpha^{G}_{23}\rvert^2\right)^{1/2} M^{-2}_{\rm SUSY}$	< 0.063 TeV^{-2} [133][134] (ATLAS)	$3\cdot 10^{-4}$ TeV^{-2}

Table 4.3 – Leading experimental limits on dipole operators. All the limits are given at 95% confidence level. The SUSY contributions are given for $M_{\rm SUSY} = 1$ TeV, $\delta \sim 1$, and $\tan\beta = 5$.

We now turn to dipole-induced top production. All the LHC processes we can consider have the particularity of featuring a *single* top in their final state. For a proton-proton collider, the main partonic processes one can think about are $g\,q \to t$, $g\,q \to t\,Z$, $g\,q \to t\,\gamma$ and $g\,g \to t\,q$. Apart from the latter, various LHC searches have already been performed in these channels, see [131–134]. The sensitivities translated on dipole coefficients are given in table 4.3. The leading bounds on $\alpha^{\gamma}_{3i,i3}$, $\alpha^{Z}_{3i,i3}$, $\alpha^{G}_{3i,i3}$ come from CMS and ATLAS searches for rare top decays, top-γ production and single top production.

The typical order of magnitude for the SUSY dipole operators is indicated in the last column of table 4.3. We observe that all these bounds are far from the sensitivity required to probe SUSY contributions to dipoles, which are loop-suppressed.

For illustration, let us consider the ATLAS $gq \to t$ search discussed in refs. [133, 134]. Knowing the expected background $B \approx 10^5$ and the 95% confident level on $|\alpha^{G}_{3i}|^2 + |\alpha^{G}_{i2}|^2$ for $L = 14.2$ fb^{-1}, one can readily estimate the event rate by interpreting the significance as [4]:

$$Z = S/\sqrt{B+S}. \tag{4.90}$$

We obtain:

$$\sigma(qg \to t) \approx 52(|\alpha^{G}_{3i}|^2 + |\alpha^{G}_{i3}|^2)/M^4_{SUSY}\ \text{pb}^{-1}. \tag{4.91}$$

Using the typical SUSY-induced values of α^{G}_{3i} shown in table 4.3, and extrapolating to a luminosity of $L = 3000$ fb^{-1}, we find that only $S \sim 28$ signal events would be collected in this analysis. The background would need to be drastically reduced in order to achieve $Z \sim \mathcal{O}(1)$ significance. A mere discovery of the SUSY dipoles using these analyses being apparently difficult, applying top-polarimetry is even more compromised, as a substantial amount of events is necessary, as shown in fig. 4.9.

Beyond these possibilities, alternative kind of processes occurring via proton-proton collisions at large impact parameter, the ultra-peripheral collisions (see [138] for a review) own a good background rejection power, and thus might be used to probe SUSY dipole operators with high sensitivity. However, the possibilities they offer to build $SU(5)$ tests will not be investigated in this work, and we refer to [87] for further details.

4.6 Case II: Natural SUSY

The heavy SUSY scenario investigated in the previous section, although providing an explanation for the so-far un-discovery of s-partners at the LHC, has the clear disadvantage to spoil naturalness in the TeV region in most cases. In this section, we would like to investigate SUSY scenarios, more appealing, which maintain the stabilization of the electroweak scale while providing a coherent phenomenology.

These so-called *natural* SUSY scenarios have been first investigated in [64]. In the minimal case, these scenarios feature a third generation of light scalar squarks, while the other -first and second generation- scalar partners are kept heavy, thus being integrating-out of the TeV scale theory [139].

[4] The ATLAS statistical analysis is much more evolved, but we expect this estimation to be enough for qualitative discussions.

Natural scenarios have several virtues. First, as already pointed out, they allow to maintain naturalness in the model up to relatively high scale. Secondly, SUSY natural scenarios alleviate the SUSY flavor problem while suppressing SUSY contributions to FCNC processes at a reasonable level [64] as the first two generations of scalars are decoupled. From a theoretical point of view, these models are also well motivated by ultraviolet constructions like partially-supersymmetric composite models [140] or supergravity contributions generically present in five-dimensional models [141].

It is the aim of this section to scrutinize the potential of the natural SUSY framework to develop tests for the $SU(5)$ relation $A_U \approx A_U^T$. The up-squark EFT developed in 4.4.1.3 directly applies to natural SUSY spectra. Indeed, in these spectra, light degrees of freedom that will be active in the EFT consist in the two lightest squarks mass eigenstates $\tilde{u}_1$, $\tilde{u}_2$ which, in a natural framework, are mostly composed of stop squarks $\tilde{u}_{1/2} \sim \tilde{t}_{L/R}$. Thus, in the rest of this section, we will simply denote these mass eigenstates $\tilde{t}_1$ and $\tilde{t}_2$.

We will also assume that the lightest neutralino $\tilde{\chi}_1$ (see sec 2.5.3) is mostly bino like, i.e. $\tilde{\chi}_1 \sim \tilde{B}$ and that the next to lightest neutralino $\tilde{\chi}_2$ is mostly wino-like i.e. $\tilde{\chi}_2 \sim \tilde{W}$. This flavor content is well motivated by theories with gaugino mass unification at the GUT scale.

Two mass ordering will be considered in this section. In subsection 4.6.1, we consider spectra where the two stops are heavier than the gauginos. In subsection 4.6.1, the alternative case, with a wino heavier than the stops will be considered. These two mass hierarchies open different decay chains for the stops, thus allowing to build different $SU(5)$ tests. Both types of tests will be built using the up-squarks EFT of subsubsection 4.4.1.3. But, whereas in the first case, the test will be developed using LO operators of the EFT with flavor violating processes, the second test will imply NLO operators and flavor conserving processes, thus being complementary to the former one.

4.6.1 The $m_{\tilde{t}_{1,2}} > m_{\tilde{W}} > m_{\tilde{B}}$ case

We start with the case $m_{\tilde{t}_{1,2}} > m_{\tilde{W}} > m_{\tilde{B}}$. In order to build $SU(5)$ tests, we are interested in stops flavor-changing decays:

$$\tilde{t}_{1/2} \to \tilde{W}\, u/c \to \tilde{B}\, h\, u/c, \quad \text{and} \quad \tilde{t}_{1/2} \to \tilde{B}\, u/c. \tag{4.92}$$

Throughout this section, we will assume that one is able to count the number of event in these two channels by tagging the nature -$\tilde{W}$ or $\tilde{B}$- of the gaugino. However, we will not assume that one is able to disentangle the nature of the original stops, which are considered here as degenerate in mass. Then, N_L (resp: N_Y) denotes the event rate of the process with a wino $\tilde{W}$ (resp: a bino $\tilde{B}$) in the decay products. Also, one important remark is that, in the context of this chapter, the event rates N_L and N_Y will always be assumed to be measured with an efficiency of 100%.

Let us have a look at the up-squark effective Lagrangian eq. 4.55. As already stated, in natural SUSY spectra, the light states vector ϕ contains the stops and $\hat{\phi}$ contains the heavy squarks of the first two generations. Hence, we have in the SCKM basis :

$$\phi = \left(\tilde{t}_L, \tilde{t}_R\right), \quad \text{and} \quad \hat{\phi} = \left(\tilde{u}_L, \tilde{c}_L, \tilde{u}_R, \tilde{c}_R\right) \tag{4.93}$$

In order to build $SU(5)$ tests from the decay chains 4.92, we should scrutinize the operator that couples the stops to the bino $\tilde{B}$ and to the wino $\tilde{W}$. We are only interested in flavor violating couplings so that, we need to scrutinize only $\hat{\mathcal{O}}$ (see subsubsection 4.4.1.3). Beside, one can split $\hat{\mathcal{O}}$ as $\hat{\mathcal{O}} = \hat{\mathcal{O}}_{\tilde{W}} + \hat{\mathcal{O}}_{\tilde{B}}$ depending on whether the operator couples the stops to the bino or to the wino.

With the matter content of the MSSM, $\hat{\mathcal{O}}_{\tilde{W}}$ and $\hat{\mathcal{O}}_{\tilde{B}}$ are given by [142],[143]:

$$\hat{\mathcal{O}}_{\tilde{B}} \propto \left(u_L, c_L, -4u_R, -4c_R\right) \tilde{B} \quad \text{and} \quad \hat{\mathcal{O}}_{\tilde{W}} \propto \left(u_L, c_L\right) \tilde{W} \tag{4.94}$$

where the factor 4 comes from the different hypercharges of the left and right-handed top components. Beside, in eq. 4.94, the overall factors do not matter for the tests to be developed in this section and thus, are not explicitly written.

If we develop the Lagrangian 4.55, and keep only terms involving the stops $\tilde{t}_L$, $\tilde{t}_R$, their couplings to $\tilde{B}$ and $\tilde{W}$ do take the following matrix form:

$$\tilde{B}\begin{pmatrix} \frac{m_{13}^2}{\Lambda_1^2}u_L + \frac{m_{23}^2}{\Lambda_2^2}c_L - 4\frac{m_{34}^2}{\Lambda_1^2}u_R - \frac{m_{35}^2}{\Lambda_2^2}c_R \\ \frac{m_{16}^2}{\Lambda_1^2}u_L + \frac{m_{26}^2}{\Lambda_2^2}c_L - 4\frac{m_{46}^2}{\Lambda_1^2}u_R - \frac{m_{56}^2}{\Lambda_2^2}c_R \end{pmatrix}^T R(\tilde{\theta})\begin{pmatrix}\tilde{t}_1\\ \tilde{t}_2\end{pmatrix}, \tag{4.95}$$

$$\tilde{W}\begin{pmatrix} \frac{m_{13}^2}{\Lambda_1^2}u_L + \frac{m_{23}^2}{\Lambda_2^2}c_L \\ \frac{m_{16}^2}{\Lambda_1^2}u_L + \frac{m_{26}^2}{\Lambda_2^2}c_L \end{pmatrix} R(\tilde{\theta})\begin{pmatrix}\tilde{t}_1\\ \tilde{t}_2\end{pmatrix}. \tag{4.96}$$

In equations (4.95-4.96), and in the rest of this chapter, m_{ij}^2 will generically denote an element of the up-squark mass matrix, i.e. we have $m_{ij}^2 \equiv \left(\mathcal{M}_{\tilde{u}}^2\right)_{ij}$.

In eq. (4.95-4.96), Λ_1 and Λ_2 are then the two cut-offs in the stops effective theory, corresponding to the masses of the heavy squarks of the first and second generation i.e. we have $\Lambda_1 \equiv m_{11,44}^2$ and $\Lambda_2 \equiv m_{22,55}^2$ (see below).

$R(\tilde{\theta})$ is a 2×2 matrix which rotates the stops from their mass eigenstates to the SCKM basis. The mixing $\tilde{\theta}$ is left here as a free parameter, however one asks often for a large $\tilde{\theta}$, in particular to obtain a 125 GeV Higgs boson mass.

Note that, the GUT scale $SU(5)$ symmetry relations $M_Q^2 = M_U^2$ (see eq. 4.21) and $A_U = A_U^T$ imply the following identities between the coefficients of the mass matrix m_{ij}^2:

$$m_{15}^2 \approx m_{24}^2, \quad m_{16}^2 \approx m_{34}^2, \quad m_{26}^2 \approx m_{35}^2, \tag{4.97}$$

$$m_{12}^2 \approx m_{45}^2, \quad m_{13}^2 \approx m_{46}^2, \quad m_{23}^2 \approx m_{56}^2\,, \tag{4.98}$$

$$m_{11}^2 \approx m_{44}^2, \quad m_{22}^2 \approx m_{55}^2 \tag{4.99}$$

at the TeV scale, neglecting the effects of EWSSB.

Using eqs (4.97), (4.98) and (4.99), one can then show that both event rates N_Y and N_L are proportional to a common factor:

$$\begin{aligned} N_{Y,L} \propto & \left(\sigma_{\tilde{t}_1}c_{\tilde{\theta}}^2 + \sigma_{\tilde{t}_2}s_{\tilde{\theta}}^2\right)\left(m_{13}^4\Lambda_1^{-4} + m_{23}^4\Lambda_2^{-4}\right) \\ & + \left(\sigma_{\tilde{t}_1}s_{\tilde{\theta}}^2 + \sigma_{\tilde{t}_2}c_{\tilde{\theta}}^2\right)\left(m_{16}^4\Lambda_1^{-4} + m_{26}^4\Lambda_2^{-4}\right) \\ & + 2c_{\tilde{\theta}}s_{\tilde{\theta}}\left(\sigma_{\tilde{t}_1} - \sigma_{\tilde{t}_2}\right)\left(m_{13}^2m_{16}^2\Lambda_1^{-4} + m_{23}^2m_{26}^2\Lambda_2^{-4}\right) \end{aligned} \tag{4.100}$$

where $\sigma_{\tilde{t}_i}$ denotes the inclusive cross section of the flavor conserving production process $pp \to \tilde{t}_i\,\tilde{t}_i^*$ at the LHC.

To get a feeling on how eq. (4.100) is derived, consider the following example. Let us note $N_Y^{i,q}$, $N_L^{i,q}$ $(i = 1, 2)$ the event rates corresponding to the processes $\tilde{t}_i \to q\,\tilde{B}$ and $\tilde{t}_i \to q\,\tilde{W}$. For example, $N_Y^{1,u}$ denotes the event rate of the process $\tilde{t}_1 \to u\,\tilde{B}$. We have thus $N_Y^{1,u} \propto \sigma_{\tilde{t}_1}\mathrm{BR}\left(\tilde{t}_1 \to u\,\tilde{B}\right)$.

The branching ratio can be further split between left and right handed components, i.e. :

$$\mathrm{BR}\left(\tilde{t}_1 \to u\,\tilde{B}\right) = \mathrm{BR}\left(\tilde{t}_1 \to u_L\,\tilde{B}\right) + \mathrm{BR}\left(\tilde{t}_1 \to u_R\,\tilde{B}\right) \tag{4.101}$$

and we know that $\mathrm{BR}\left(\tilde{t}_1 \to u_L\,\tilde{B}\right)$ is proportional to the square of the coupling at the vertex $\tilde{t}_1\,u_L\,\tilde{B}$ in the effective stops Lagrangian. From eq. (4.95), one can deduce that:

$$\mathrm{BR}\left(\tilde{t}_1 \to u_L\,\tilde{B}\right) \propto \frac{\sigma_{\tilde{t}_1}}{\Lambda_1^4}\left(m_{13}^2c_{\tilde{\theta}} + m_{16}^2s_{\tilde{\theta}}\right)^2 \tag{4.102}$$

and similarly for the right handed branching ratio:

$$\mathrm{BR}\left(\tilde{t}_1 \to u_R\,\tilde{B}\right) \propto \frac{\sigma_{\tilde{t}_1}}{\Lambda_1^4}\left(m_{34}^2c_{\tilde{\theta}} + m_{46}^2s_{\tilde{\theta}}\right)^2 \tag{4.103}$$

Continuing this exercise for $N_Y^{2,u}$, $N_Y^{2,c}$, one has that the total event rate $N_Y = N_Y^{1,u} + N_Y^{2,u} + N_Y^{1,c} + N_Y^{2,c}$ is indeed proportional to the factor in eq. (4.100).

It is thus, in principle, possible to test the $SU(5)$ hypothesis using these simple decay rates. However, estimating precisely the overall factors relating N_L and N_Y to the quantity (4.100) is very challenging as this requires to know the realistic cross-section including all the kinematic selections.

Instead, we choose to follow an alternative strategy, in which the form of this factor will not really matter for the tests to be proposed. What will be crucial instead is that both event rates are proportional to the *same* factor.

Let us assume that one is able to experimentally tag charm jets in the processes (4.92) with a certain efficiency ϵ_c [5]. Let us note N_Y^c, N_L^c the event rates fractions corresponding to the events with a c-jet correctly tagged. $N_Y^{\not c} \equiv N_Y - N_Y^c$ and $N_L^{\not c} \equiv N_L - N_L^c$ then contain both up-quark events and miss-tagged charm jets.

Then, according to (4.100), the $SU(5)$ hypothesis implies :

$$\mathrm{E}\left[N_Y^c\right] = \epsilon_c \gamma_Y \mathrm{E}\left[N_Y\right], \qquad \mathrm{E}\left[N_L^c\right] = \epsilon_c \gamma_L \mathrm{E}\left[N_L\right] \tag{4.104}$$

where we have noted γ_Y, γ_L the actual fractions of charm events in N_Y and in N_L. Due to (4.100), one also has $\gamma \equiv \gamma_Y = \gamma_L$ and the four events rates N_Y^c, N_L^c, $N_Y^{\not c}$, $N_L^{\not c}$ are related by a simple relation. Indeed, when the $SU(5)$ hypothesis is verified, one has:

$$\frac{N_Y^c}{N_L^c} = \frac{N_Y^{\not c}}{N_L^{\not c}}. \tag{4.105}$$

Let us remark that the large QCD error on the underlying cross-section roughly cancels out in the above ratios of event rates. Moreover, no information on the stop mixing angle $\tilde{\theta}$ nor on the stops masses are needed to perform this test. Following subsection 4.4.3, we then define the normalized test quantity as:

$$R = \left| \frac{N_Y^c}{N_L^c} - \frac{N_Y^{\not c}}{N_L^{\not c}} \right| \Bigg/ \left| \frac{N_Y^c}{N_L^c} + \frac{N_Y^{\not c}}{N_L^{\not c}} \right| \tag{4.106}$$

such that:

$$\mathrm{E}\left[R\right] = \frac{|\gamma_Y - \gamma_L|}{\gamma_Y + \gamma_L}. \tag{4.107}$$

The expected precision (see subsection 4.4.3) associated with this test is found to be:

$$P_Z = \frac{Z}{2\epsilon_c^{1/2}} \left(\frac{1}{N_Y} + \frac{1}{N_L} \right)^{1/2} \left(\frac{1}{\gamma} + \frac{1}{\gamma - 1} - \frac{(1-\epsilon_c)\,\gamma}{(\gamma-1)^2} \right)^{1/2} \tag{4.108}$$

Let us remark that the power of this test vanish in different limit cases. One has $P_Z \to \infty$ if:

1. $\gamma \to 0$, meaning that no charm jets are expected.
2. $\gamma \to 1$, meaning that no up jets are expected.
3. $\epsilon_c \to 0$, meaning that no charm-jets can be tagged.

which is consistent as the test (4.106) relies on charm tagging.

4.6.1.1 Discussion

The expected precision (4.108) is plotted on fig. 4.11, where the charm fraction is set to $\gamma = 0.5$, and the charm tagging efficiency is set to $\epsilon_c = 0.5$. We see that $N_Y = N_L \gtrsim 27$ events are sufficient to start to probe the relation at 3σ significance, i.e. to have $P_3 < 100\%$. To evaluate the feasibility of this test, we have collected some typical values of cross sections expected at the LHC. The total

[5] We assume for what follows, that ϵ_c is independent from the channel considered. However the generalization of the results presented here, in case the efficiency is channel-dependent, is straightforward.

$m_{\tilde{t}}$ (GeV)	700	1000	1400	1800
$\sigma_{\tilde{t}\tilde{t}}$ (fb)	$89 \pm 10\%$	$8.6 \pm 15\%$	$0.71 \pm 20\%$	$0.08 \pm 25\%$

Figure 4.10 – Stops production cross sections at the LHC 14 TeV, computed at NLO+NLL and given as a function of the common stop mass $m_{\tilde{t}}$, with their associated uncertainty expressed in percent. Taken from [144] .

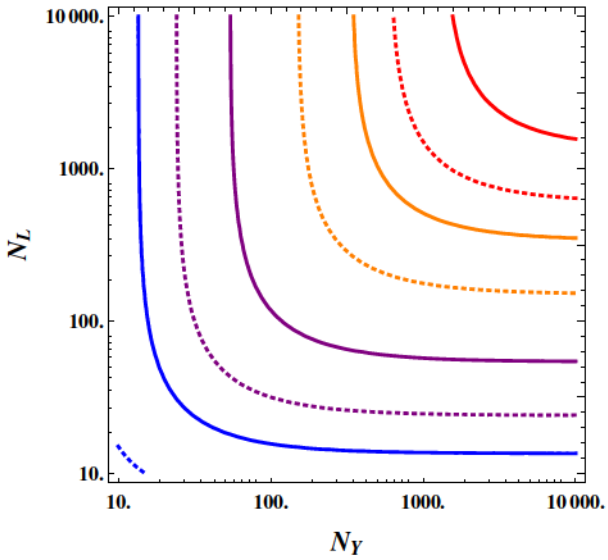

Figure 4.11 – Expected precision P_Z for the $SU(5)$ test on flavor-changing stop decays eq. (4.105). N_Y and N_L are respectively, the numbers of observed stop decays to bino and wino. The charm fraction is fixed to $\gamma = 0.5$ and the charm-tagging efficiency to $\epsilon_c = 0.5$. Dotted (plain) lines denote 2σ (3σ) significance. Blue, purple, orange and red lines show $P_{2,3} = 100\%, 50\%, 20\%$ and 10% isolines of expected precision.

production cross sections of stops pairs at next-to-leading order (NLO) and at next-to-leading log (NLL) $\sigma_{\tilde{t}\tilde{t}} \equiv \sigma(pp \to \tilde{t}\tilde{t}^*)$, taken from [144], are given in table 4.10 as a function of the common stop mass $m_{\tilde{t}}$, together with their associated uncertainties and for an energy in the proton-proton center of mass of 14 TeV.

From fig. 4.11, one sees that testing the relation with a level of significance of 3σ at a precision of 50%, 20% and 10% requires respectively $N_Y \sim N_L \sim 100$, 675 and 2700 events. For comparison, and using the values of table 4.10, assuming $\text{BR}\left(\tilde{t} \to q\, \tilde{B}\right) \sim \text{BR}\left(\tilde{t} \to q\, \tilde{W}\right) \sim 0.5$, with $L = 300\,\text{fb}^{-1}$ of integrated luminosity, one expects about 1340, 130, and 11 events for stop masses of $m_{\tilde{t}} = 700$, $m_{\tilde{t}} = 1000$, and $m_{\tilde{t}} = 1400$ GeV respectively.

4.6.2 The $m_{\tilde{W}} > m_{\tilde{t}_{1,2}} > m_{\tilde{B}}$ case

The second mass ordering we are going to consider is when one of the gauginos, the wino, is heavier than the stops. Then, kinematically, the stops are allowed to decay only into the bino $\tilde{B}$. Beside, contrary to the previous section, only flavor conserving decays will be considered. Then, the decays of interest are:

$$\tilde{t}_{1/2} \to t_{L/R}\, \tilde{B}. \tag{4.109}$$

Measuring the helicity of the top in eq. (4.109) potentially gives access to the stop mixing angle [145–147]. In this section, we point out that top-polarimetry potentially also provides a $SU(5)$ test.

From the up-squark effective Lagrangian (4.55) and from [142] and [143], one can deduce that the operator which couples the stops -$\tilde{t}_L, \tilde{t}_R$- to the bino $\tilde{B}$ is:

$$\mathcal{O} \propto \tilde{B}\,(t_L, -4t_R)\,. \tag{4.110}$$

As in eq. (4.94), the factor 4 comes from the mismatch in the values of the hypercharges between the left and right-handed top components. In the stop effective Lagrangian, the effective mass term mixes $\tilde{t}_L$ and $\tilde{t}_R$. The mass eigenstates $\tilde{t}_a$ and $\tilde{t}_b$ are then obtained, as usual, with a rotation:

$$\begin{pmatrix} \tilde{t}_a \\ \tilde{t}_b \end{pmatrix} = \begin{pmatrix} c_{\theta_t} & s_{\theta_t} \\ -s_{\theta_t} & c_{\theta_t} \end{pmatrix} \begin{pmatrix} \tilde{t}_L \\ \tilde{t}_R \end{pmatrix} \tag{4.111}$$

where c_{θ_t} and s_{θ_t} are the sine and cosine of the stop mixing angle θ_t.

However, there is something peculiar here. Indeed, we have labeled the mass eigenstates $\tilde{t}_a$, $\tilde{t}_b$ to emphasize that, for the purpose of the discussion that will follow (see the end of this section), and contrary to what was done in eq. (4.95), we do not want to make any assumption on the mass ordering here, i.e. we do not know a-priori whether $m_{\tilde{t}_a} < m_{\tilde{t}_b}$ or vice-versa. For this very same reason, we have denoted the stop mixing angle θ_t and not $\tilde{\theta}$ (see eq. 4.95), to underline that we do not consider a mass ordered eigenbasis.

Expanding the effective Lagrangian (4.55) with $\phi = \left(\tilde{t}_L, \tilde{t}_R\right)^T$ and making use of eq. (4.110), one can show that, at next-to-leading order in the EFT expansion, the coupling is distorted as:

$$\tilde{B}\left(t_L, -4t_R\right) \mathcal{K} R(\theta_t) \begin{pmatrix} \tilde{t}_a \\ \tilde{t}_b \end{pmatrix} \tag{4.112}$$

with the effective matrix $\mathcal{K}$ given by:

$$K = \begin{pmatrix} 1 & x \\ x & 1 \end{pmatrix}. \tag{4.113}$$

The parameter x depends on the elements of the up-squark mass matrix m^2_{ij}, and on the two cut-offs Λ_1 and Λ_2.

However, the exact form of x is not needed for what follows, and hence will not be given. Instead, in this mass ordering, the crucial signature lies in the fact that the matrix (4.113) is symmetric when the $SU(5)$ hypothesis is verified whereas it is not in full generality, when the $SU(5)$ constraints on low scale mass terms m^2_{ij} (see eqs. (4.97),(4.98),(4.99)) are not fulfilled. Beside, as the parameter x encloses the effects of the higher order operators in the stop effective Lagrangian, one has $x = 0$ at leading order and one expects $x << 1$ for the higher order corrections.

As in subsection 4.5.1, let us assume that the spin of the top is analyzed through distributions of the form $f_Z(z) \propto (1 + \kappa P_t z)$ with $z \in [-1, 1]$ and where $P_t = \pm 1$ is the helicity of the top.

The decay of the stops $\tilde{t}_a$ and $\tilde{t}_b$, leading to event rates noted N_a and N_b, are then splitted over the domains $D_- = [-1, 0[$ and $D_+ = [0, 1]$ such that:

$$N_a = N_{a+} + N_{a-} \text{ and } N_b = N_{b+} + N_{b-}. \tag{4.114}$$

These different event rates can then be deduced using eq. (4.84), and are given in the appendix C.

Then, from the event rates in eq. (4.114), one can define two forward-backward asymmetries:

$$A_a \equiv \frac{|N_{a+} - N_{a-}|}{N_{a+} + N_{a-}}, \quad \text{and} \quad A_b \equiv \frac{|N_{b+} - N_{b-}|}{N_{b+} + N_{b-}} \tag{4.115}$$

which potentially give access to the stop mixing angle θ_t.

Indeed, at leading order in the EFT expansion i.e. when $x = 0$, one can use the expressions of the decay rates $N_{a\pm}$ and $N_{b\pm}$ to deduce θ_t from measurements of forward-backward asymmetries.

For instance, one has:

$$\mathrm{E}\left[A_a\right] = \frac{\kappa}{2} \frac{15 - 17 c_{2\theta_t}}{17 - 15 c_{2\theta_t}} \quad \text{when } x = 0. \tag{4.116}$$

Thus, measuring one forward-backward asymmetry is enough to gain access to a leading order approximation of the stop mixing angle (see also [145]).

On the other hand, both A_a and A_b can be written in terms of the parameters x and θ_t using the full event rates expressions for $N_{a,b\pm}$ (see appendix C), at next-to-leading order in the EFT expansion. But in full generality, the coupling matrix $\mathcal{K}$ (see eq. (4.113)) is *a-priori* non-symmetric. Thus, one can

deduce two relations of the type $A_a = f(x_a, \theta_t)$ and $A_b = f(x_b, \theta_t)$, with *a-priori* $x_a \neq x_b$. Inversing these two relations to get $x_{a/b}$ as a function of $A_{a/b}$ and enforcing that the $SU(5)$ hypothesis is true i.e. that $x \equiv x_a = x_b$, one can get a $SU(5)$ test which can be set in the following normalized form:

$$R = \left| \frac{(A_a - A_b)\,(1606 + 450 c_{4\theta_t} + (1028\kappa - 2040\,(A_a + A_b)\,c_{2\theta_t}))}{(765 + 255 c_{4\theta})\,\kappa + 2040\,(A_a - A_b)\,c_{2\theta_t} - (1606 + 450 c_{4\theta_t})\,(A_a + A_b)} \right| \tag{4.117}$$

defined such that $\mathrm{E}[R] = 0$ if the $SU(5)$ hypothesis is verified.

The degree of dependency of the event rates $N_{a,b\pm}$ upon the higher order corrections in the EFT expansion, i.e. upon the x parameter, can be scrutinized by defining the following information quantity:

$$I[N_{a,b\pm}] \equiv \left| \frac{\partial \log N_{a,b\pm}}{\partial x} \right| \tag{4.118}$$

It turns out that this information depends crucially on the stop mixing angle θ_t. This can be seen on fig. 4.12, where $I[N_{a,b\pm}]$ is represented as a function of θ_t for $x = 0$ [6]. The information becomes small for $\theta_t \sim 0$ (no stop mixing) and vanishes exactly for $\theta_t = \pi/4$ (maximal stop mixing). In between these two limit cases, one has $I[N_{a\pm}] \sim O(1)$, $I[N_{b\pm}] \sim O(0.1)$, and the reverse for the interval $[\pi/4, \pi/2]$. From the $SU(5)$ test eq. (4.117), one can compute an expected precision (see subsubsection 4.4.3.2) which is found to be:

$$P_Z \approx Z \frac{(17 + 15 c_{2\theta_t})}{255\sqrt{2}\,(3 + c_{4\theta_t})\,\kappa} \left(\frac{3212 - 739\kappa^2 - 1020\,(\kappa^2 - 4)\,c_{2\theta_t} + (900 - 289\kappa^2)\,c_{4\theta_t}}{N_b} \right)^{1/2} \tag{4.119}$$

when $\theta_t \in [0, \pi/4]$. Indeed, in this case, the event rates N_{b+}, N_{b-} are less sensitive to x than the event rates N_{a+}, N_{a-}. The expected precision depends thus mainly on the amount of $\tilde{t}_b$ produced. For this reason, we have dropped the N_a dependence in P_Z in eq. 4.119. However, we have reported the full P_Z formula in appendix C. Note that, one would have a symmetric situation in the interval $\theta_t \in [\pi/4, \pi/2]$. Also, in the limit case where the top polarimetry-analyzing variable vanishes, i.e. when $\kappa \to 0$, the power of the test eq. (4.117) vanishes as well, i.e. we have $P_Z \to \infty$ which is consistent as the test relies on top-polarimetry.

As for $\theta_t \in [0, \pi/4]$, more $\tilde{t}_b$ than $\tilde{t}_a$ are needed to decrease the expected precision, scenarios where $\tilde{t}_b$ is the lightest are more interesting. For these values of the mixing angle, this lightest stop is mainly right-handed. The same reasoning can be applied in the complementary case, when $\theta_t \in [\pi/4, \pi/2]$. This time, a larger amount of $\tilde{t}_a$ is necessary. A spectrum where $\tilde{t}_a$ is the lightest stop is therefore more favorable for the $SU(5)$ test eq. (4.117). Again, this lightest stop would be mainly right-handed. We conclude that scenarios where the lightest stop is mainly right-handed are always more favorable to carry out the $SU(5)$ test discussed above, and thus, for any value of the stop mixing angle.

The expected precision is shown in fig. 4.13 for $\theta_t = 0.4$, as well as for $N_a = 20$ and 1000. We see that, with a spin-analyser efficiency of $\kappa = 0.5$ and $N_a = 20$ we have that $N_b \gtrsim 137$ events are needed to probe the relation at 3σ significance, i.e. to have $P_3 < 100\%$. Testing the relation with 50% or 20% precision at 3σ requires $N_b \sim 589$ and $N_b \sim 7560$. For comparison, assuming 300 fb^{-1} of integrated luminosity at the LHC 14 TeV, one expects about 26700, 2580, 213, and 24 events for stops with a mass of $m_{\tilde{t}} = 700, 1000, 1400$ and 1800 GeV (see table 4.10 for the production cross sections values).

4.7 Case III: Top-charm SUSY

In this section, we scrutinize spectra which feature a heavy first generation of up-type squarks and light second and third generations. That means that we assume that only stop-like and scharm-like squarks are accessible at the LHC. In the SCKM basis, at the GUT scale, the soft masses take then the form:

$$M_Q^2 = M_U^2 = \begin{pmatrix} \Lambda^2 & 0 & 0 \\ 0 & 0 & 0 \\ 0 & 0 & 0 \end{pmatrix} + \mathcal{O}(M_{SUSY}^2) \begin{pmatrix} 0 & 0 & 0 \\ 0 & \lambda_{22} & \lambda_{32} \\ 0 & \lambda_{32} & \lambda_{33} \end{pmatrix} \tag{4.120}$$

[6] Note that since x encodes the higher order corrections in the EFT expansion, setting $x \neq 0$ would result in only minor modifications to the results presented in fig. 4.12.

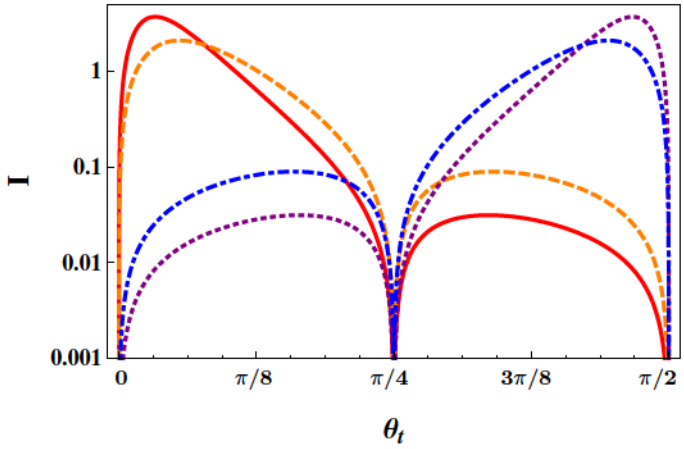

Figure 4.12 – Information content of the event rates $N_{a,b\pm}$ (see eq. (4.113)) plotted as a function of the mixing angle θ_t for $x = 0$. Plain, dashed, dotted and dot-dashed lines correspond to $I[N_{a+}]$, $I[N_{a-}]$, $I[N_{b+}]$, and $I[N_{b-}]$, respectively. The spin-analyzing power is set to $\kappa = 1$.

where the λ_{ij} form in general a hermitian matrix of $\mathcal{O}(1)$ parameters and $\Lambda >> M_{SUSY}$. Such a framework is immune against $D^0 - \bar{D}^0$ mixing induced by the up-squark sector ([107]) because the first up-squark generation is heavy. We also assume that the down-type squarks are either aligned or heavy in order to avoid FCNCs induced by the down sector. This assumption also avoid too large SUSY FCNC contributions in the leptonic sector due to the $SU(5)$ unification.

Phenomenologically, this top-charm SUSY framework constitutes an ideal playground to gain knowledge about how to test the $SU(5)$-like GUT hypothesis of our interest. Beside, it is also useful in order to carry out stop searches at the LHC taking into account flavor violation [148–152]. In particular, large top-charm mixing is found to both improve naturalness and to relax the constraints on stop masses [153].

4.7.1 Effective Lagrangian

The effective Lagrangian derived in subsubsection 4.4.1.3 directly applies to the top-charm SUSY spectrum, identifying the first up-squarks generation as the heavy fields $\hat{\phi} = (u_L,\, u_R)$, and the second and third generations as the light fields $\phi = (c_L,\, t_L,\, c_R,\, t_R)$. The blocks of the mass matrix $\mathcal{M}^2_{\tilde{u}}$ have then the form:

$$\hat{M}^2 = \begin{pmatrix} m^2_{11} & m^2_{14} \\ & m^2_{44} \end{pmatrix}, \quad \tilde{M}^2 = \begin{pmatrix} m^2_{12} & m^2_{13} & m^2_{15} & m^2_{16} \\ m^2_{42} & m^2_{43} & m^2_{45} & m^2_{46} \end{pmatrix}, \quad M^2 = \begin{pmatrix} m^2_{22} & m^2_{23} & m^2_{25} & m^2_{26} \\ & m^2_{33} & m^2_{35} & m^2_{36} \\ & & m^2_{55} & m^2_{56} \\ & & & m^2_{66} \end{pmatrix} \tag{4.121}$$

Using also the $SU(5)$ relation $M^2_Q \approx M^2_U$ (valid only for the first two generations), we have in addition:

$$m^2_{12} \approx m^2_{45} \quad \text{and} \quad m^2_{16} \approx m^2_{34}, \tag{4.122}$$

at the TeV scale. It is therefore natural to scrutinize the effects of the virtual first generation up-squarks on the light top-charm squarks. The $\hat{\mathcal{O}}\hat{M}^{-2}\tilde{M}^2\phi$ term in the effective Lagrangian eq. (4.55) induces flavor-changing decays of the light top-charm squarks into $u\,\tilde{B}$ and $u\,\tilde{W}$. But, in this case, distinguishing between the initial $\tilde{c}$ and $\tilde{t}$ seems difficult.

However, unlike for the Natural SUSY case, looking at the higher-dimensional operators is not the only possibility available, because a $SU(5)$ information from $A_u \approx A_u^T$ also remains at leading order in the low energy mass matrix M^2. This is the relation of the top-charm sector:

$$m^2_{26} \approx m^2_{35}. \tag{4.123}$$

We have therefore the possibility of testing the $SU(5)$ hypothesis using only the *real* up-squarks. From now on, we thus focus only on the top-charm sector.

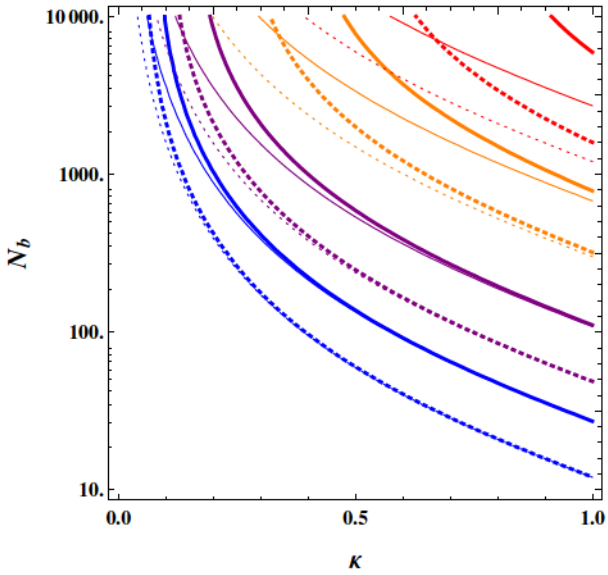

Figure 4.13 – Expected precision P_Z for the $SU(5)$ test on polarization of stop decays eq. (4.117) as a function of the spin-analyzer efficiency κ and of the amount of observed $\tilde{t}_b$ decays N_b. The number of $\tilde{t}_a$ decays is fixed to $N_a = 20$ (thick lines) and $N_a = 10000$ (thin lines). The stop mixing angle is fixed to $\theta_t = 0.4$. Dotted (plain) lines denote 2σ (3σ) levels of significance respectively. Blue, purple, orange and red lines show $P_{2,3} = 100\%, 50\%, 20\%$ and 10% isolines of expected precision.

4.7.2 $SU(5)$ test through Higgs production

Let us first consider a case where all stop and scharm masses are nearly degenerate. This possibility happens in particular in low-energy GUTs, where no large stop mixing is needed in order to have the correct Higgs mass, e.g [64]. Nearly-degenerate squarks imply that the MIA (see subsection 4.4.2) is valid for the stop and scharm sector, and :

$$m_{\tilde{t}_L} \sim m_{\tilde{t}_R} \sim m_{\tilde{c}_L} \sim m_{\tilde{c}_R} \equiv m_{\tilde{q}}. \tag{4.124}$$

These states should be produced in an equally abundant way at the LHC, as their production occurs mainly through flavor-blind gluon fusion.

The off-diagonal elements of the up-type trilinear matrix are identified with mass insertions:

$$\left(\delta_u^{LR}\right)_{ij} = v_u \left(A_u\right)_{ij} / \left(\sqrt{2} m_{\tilde{q}}^2\right). \tag{4.125}$$

The $SU(5)$ hypothesis $A_u \approx A_u^T$ then implies:

$$\left(\delta_u^{LR}\right)_{23} = \left(\delta_u^{LR}\right)_{32}. \tag{4.126}$$

To experimentally test this relation, one may scrutinize the flavor decomposition of the stop and scharm eigenstates. At first view, even in the MIA, such an analysis seems difficult because of the presence of additional mass-insertions δ_{23}^{LL}, δ_{23}^{RR} and $\delta_{22,33}^{LR}$. To overcome this issue, one should note the fundamental difference between $\delta_{23}^{LL,RR}$ and δ_{23}^{LR}. The chirality conserving insertions parameters relate to a truly bilinear term, i.e the scalar masses, while the chirality violating insertions parameters are induced by a trilinear term, the squark-Higgs scalar coupling. But, this fact is somehow hidden if one lets the Higgs be on its VEV. The physical Higgs exclusively couples to the LR components of the squarks eigenstates. Thus, in principle, detecting a Higgs gives an access to the coupling $\left(\delta_u^{LR}\right)_{23}$, i.e. to $(A_u)_{23}$.

The LHC SUSY processes of interest are therefore stop and scharm pair productions, followed by a flavor-violating decay into a squark and a Higgs boson in one of the decay chain. These processes are depicted in fig. 4.14. We further assume that the squarks decay into the bino-like lightest neutralino $\tilde{\chi}_1^0 \sim \tilde{B}$. These processes can be identified requiring a single top, a hard jet (from a charm quark),

a Higgs, and large missing transverse energy noted $\not{E}_T$. Higgs production through up-squark flavor-violating decays have been studied in refs [151, 154]. Note that, in the degenerate case, not all particles can be on-shell in the decay chain producing the Higgs. As in previous cases, this test has to rely on a distinction between the chiralities, which is possible only for the top quark. Reconstructing the events is necessary in order to select the ones where the Higgs comes from $\tilde{c}_{L,R} \to h\,\tilde{t}_{R,L}$ and reject the ones from $\tilde{t}_{L,R} \to h\,\tilde{c}_{R,L}$. The former of these processes is shown in the first row of fig. 4.14, the latter being shown in the second row. Other processes leading to the same final states are also possible but are suppressed by extra mass-insertions (see second row of fig. 4.14).

Provided that the cascade decay with $\tilde{c}_{L/R} \to h\,\tilde{t}_{R/L}$ can be isolated, top polarimetry then readily provides a $SU(5)$-test , as $\mathrm{BR}\left(\tilde{c}_L \to h\,\tilde{t}_R\right) \propto |\delta^{LR}_{23}|^2$ and $\mathrm{BR}\left(\tilde{c}_R \to h\,\tilde{t}_L\right) \propto |\delta^{LR}_{32}|^2$. Denoting the event rates from the relevant flavor-changing Higgs decay chain as N_{htc}, top-polarimetry provides a splitting of the events into $N_{htc} = N_{htc,+} + N_{htc,-}$, see subsection 4.5.1. The $SU(5)$ test then takes the form:

$$R = \frac{|N_{htc,+} - N_{htc,-}|}{N_{htc,+} + N_{htc,-}} \tag{4.127}$$

This situation is similar to the one of subsection 4.5.1 and will not be further discussed.

Instead, we focus on a somewhat different type of spectrum, where the stop mixing angle is large while the scharms are nearly degenerate. The MIA applies to the scharm sector, but not inside the stop sector. Instead, the stops are rotated to their exact mass eigenstates. After rotating the stops, the scharm-stop mass matrix takes the form:

$$M_{\tilde{t}} = \begin{pmatrix} m^2_{\tilde{c}} & 0 & 0 & 0 \\ & m^2_{\tilde{c}} & 0 & 0 \\ & & m^2_{\tilde{t}_1} & 0 \\ & & & m^2_{\tilde{t}_2} \end{pmatrix} + m^2_{\tilde{c}} \begin{pmatrix} 0 & \delta^{LR}_{22} & \delta^{LL}_{23} c_{\tilde{\theta}} - \delta^{LR}_{23} s_{\tilde{\theta}} & \delta^{LL}_{23} s_{\tilde{\theta}} - \delta^{LR}_{23} c_{\tilde{\theta}} \\ & 0 & \delta^{LR}_{32} c_{\tilde{\theta}} - \delta^{RR}_{23} s_{\tilde{\theta}} & \delta^{LR}_{32} s_{\tilde{\theta}} - \delta^{RR}_{23} c_{\tilde{\theta}} \\ & & 0 & 0 \\ & & & 0 \end{pmatrix} \tag{4.128}$$

Following the MIA approach, the first matrix above corresponds to the squarks mass eigenvalues, while the second matrix is treated as a mass insertion. Here, and contrary to subsection 4.5.1, the stops are rotated to a mass ordered basis, i.e. we have $m^2_{\tilde{t}_2} > m^2_{\tilde{t}_1}$. Note that the MIA is expected to be valid to a good precision for $m^2_{\tilde{t}_2} + m^2_{\tilde{t}_1} \sim 2m^2_{\tilde{c}}$ (see refs [121, 122]). For the rest of this section, we focus on the case $m^2_{\tilde{t}_2} > m^2_{\tilde{c}} > m^2_{\tilde{t}_1}$. Note that this ordering would happen naturally with degenerate stop-scharm soft masses and a hierarchical A_U with large $(3,3)$ element.

The physical Higgs couples only to the left-right mixing terms δ^{LR}. The vertices $h\tilde{c}_L\tilde{t}_1$, $h\tilde{c}_L\tilde{t}_2$, $h\tilde{c}_R\tilde{t}_1$, $h\tilde{c}_R\tilde{t}_2$ are respectively proportional to $\left|\delta^{LR}_{23} s_{\tilde{\theta}}\right|$, $\left|\delta^{LR}_{23} c_{\tilde{\theta}}\right|$, $\left|\delta^{LR}_{32} c_{\tilde{\theta}}\right|$, $\left|\delta^{LR}_{32} s_{\tilde{\theta}}\right|$. Within this given mass ordering, the SUSY cascade decays are rather different than from the degenerate case discussed above. Flavor changing scharm decays going through $\tilde{t}_2$ are now suppressed because of $m^2_{\tilde{t}_2} > m^2_{\tilde{c}}$. As a consequence, contrary to the degenerate spectrum, top polarimetry is not useful anymore. On the other hand, real decays $\tilde{t}_2 \to h\,\tilde{c}$ and $\tilde{c} \to h\,\tilde{t}_1$ are now open.

We require again a single top, a hard jet, a Higgs, and large missing E_T from both sides of the decay chains. Two event topologies lead to this final state: the Higgs can either come from $\tilde{t}_2 \to h\,\tilde{c}_{R,L}$ or from $\tilde{c}_{R,L} \to h\,\tilde{t}_1$. These processes are shown in the first row of fig. 4.15. The first of these diagrams is proportional to $\left|\delta^{LR}_{23}\right|^2 c^2_{\tilde{\theta}} + \left|\delta^{LR}_{32}\right|^2 s^2_{\tilde{\theta}}$, while the second is proportional to $\left|\delta^{LR}_{23}\right|^2 s^2_{\tilde{\theta}} + \left|\delta^{LR}_{32}\right|^2 c^2_{\tilde{\theta}}$. These two types of event can be disentangled using the topology of the decay chain. We denote the event rates associated with these two diagrams N_{hj} and N_{ht} respectively. For maximal stop mixing ($c_{\tilde{\theta}} = s_{\tilde{\theta}}$), the two quantities become equal so that the power of the test is expected to vanish.

Contrary to the degenerate case, the stops and scharms have different production rates. Moreover, the theoretical predictions suffer from a large QCD error. One way to get rid of that error is by normalizing N_{hj}, N_{ht} by appropriately chosen event rates. In order to normalize N_{ht}, we ask for the measurement of flavor conserving decay-chains of $\tilde{c}-$pairs into two jets plus large missing E_T. The corresponding event rate is noted N_{jj}. Because of stop mixing, the same process cannot be used to normalize N_{hj}. Instead we ask for one of the two $\tilde{t}_2$ to decay into $Z\,\tilde{t}_1$. This event rate is noted N_{Zt}. These processes are depicted in the second row of fig. 4.15.

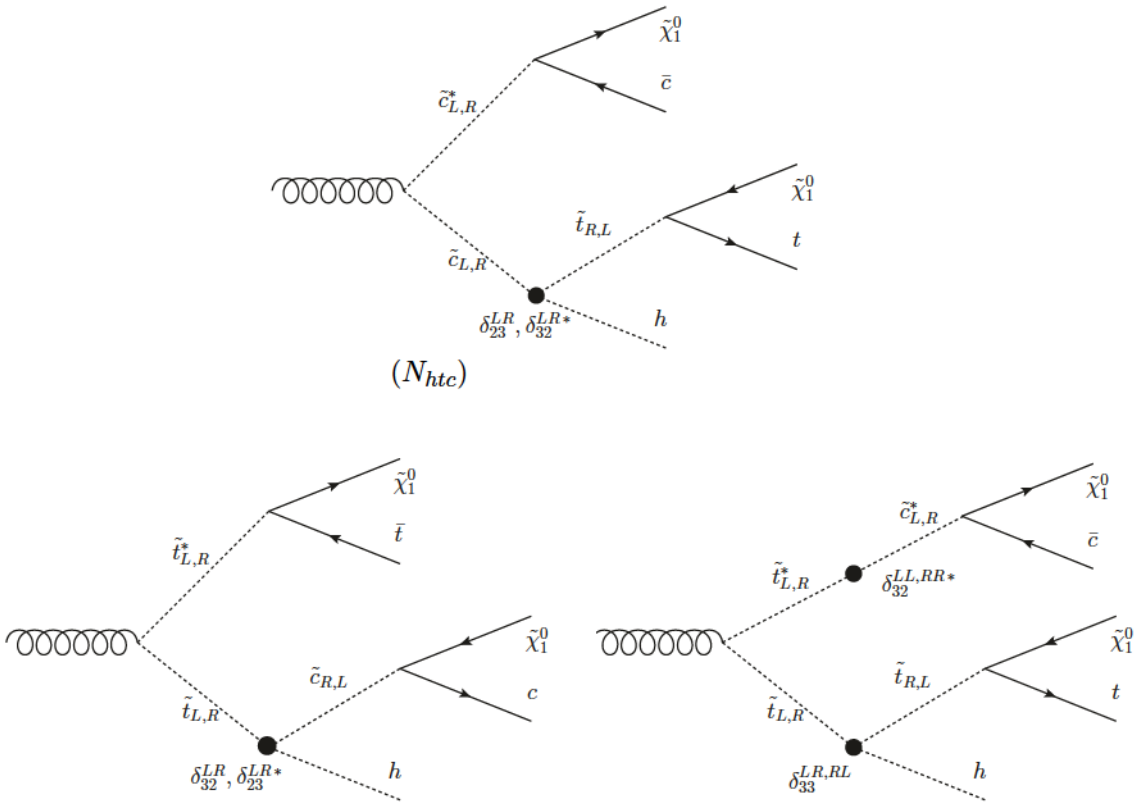

Figure 4.14 – Cascade decays in case of a nearly degenerate top-charm spectrum. The dots represent mass-insertions. First row: cascade decays used for the $SU(5)$ test defined in eq. (4.127). Second row: other processes leading to the same final state.

Note that, as in section 4.6, we are assuming that all these event rates can be measured with a detection efficiency of 100%. Normalizing N_{hj} by N_{Zt} and N_{ht} by N_{jj} cancels the cross-sections, leaving only the ratio of partial decay widths:

$$\mathrm{E}\left[\frac{N_{hj}}{N_{Zt}}\right] = \frac{\Gamma\left(\tilde{t}_2 \to h\,\tilde{c}_{L,R}\right)}{\Gamma\left(\tilde{t}_2 \to Z\,\tilde{t}_1\right)}, \qquad \mathrm{E}\left[\frac{N_{ht}}{N_{jj}}\right] = \frac{\Gamma\left(\tilde{c}_{L,R} \to h\,\tilde{t}_1\right)}{\Gamma\left(\tilde{c}_{L,R} \to c\,\tilde{B}\right)} \tag{4.129}$$

If we define now the quantity :

$$\begin{aligned}\eta \equiv \mathrm{E}\left[\frac{N_{ht}}{N_{jj}}\right] \Big/ \mathrm{E}\left[\frac{N_{hj}}{N_{Zt}}\right] &= \frac{\Gamma\left(\tilde{c}_{L,R} \to h\,\tilde{t}_1\right)}{\Gamma\left(\tilde{t}_2 \to h\,\tilde{c}_{L,R}\right)} \frac{\Gamma\left(\tilde{t}_2 \to Z\,\tilde{t}_1\right)}{\Gamma\left(\tilde{c}_{L,R} \to c\,\tilde{B}\right)} \\ &\approx \frac{m_{\tilde{c}}^2 - m_{\tilde{t}_1}^2}{m_{\tilde{t}_2}^2 - m_{\tilde{c}}^2} \frac{m_{\tilde{t}_2}^2 - m_{\tilde{t}_1}^2}{m_{\tilde{c}}^2 - m_{\tilde{B}}^2}\end{aligned} \tag{4.130}$$

where the approximation in the last line of eq. 4.130 is obtained by neglecting the SM masses, one sees that this factor can be evaluated using extra information from kinematic analysis, for example using the kinematic edges of the ht, hj and Zt invariant masses.

The normalized $SU(5)$ test then reads:

$$R \equiv \frac{1}{c_{2\tilde{\theta}}} \left|\frac{N_{hj}}{N_{jj}} - \eta\frac{N_{ht}}{N_{Zt}}\right| \Big/ \left(\frac{N_{hj}}{N_{jj}} + \eta\frac{N_{ht}}{N_{Zt}}\right) \tag{4.131}$$

which satisfies:

$$\mathrm{E}\left[R\right] = \frac{\left|\delta_{23}^{LR} - \delta_{32}^{LR}\right|}{\delta_{23}^{LR} + \delta_{32}^{LR}}. \tag{4.132}$$

Following the procedure of subsubsection 4.4.3.2, one can then compute the expected precision associated to the test eq. (4.15), which is found to be:

$$P_Z \approx \frac{Z}{2c_{2\tilde{\theta}}} \left(\frac{1}{N_{hj}} + \frac{1}{N_{ht}}\right)^{1/2}. \tag{4.133}$$

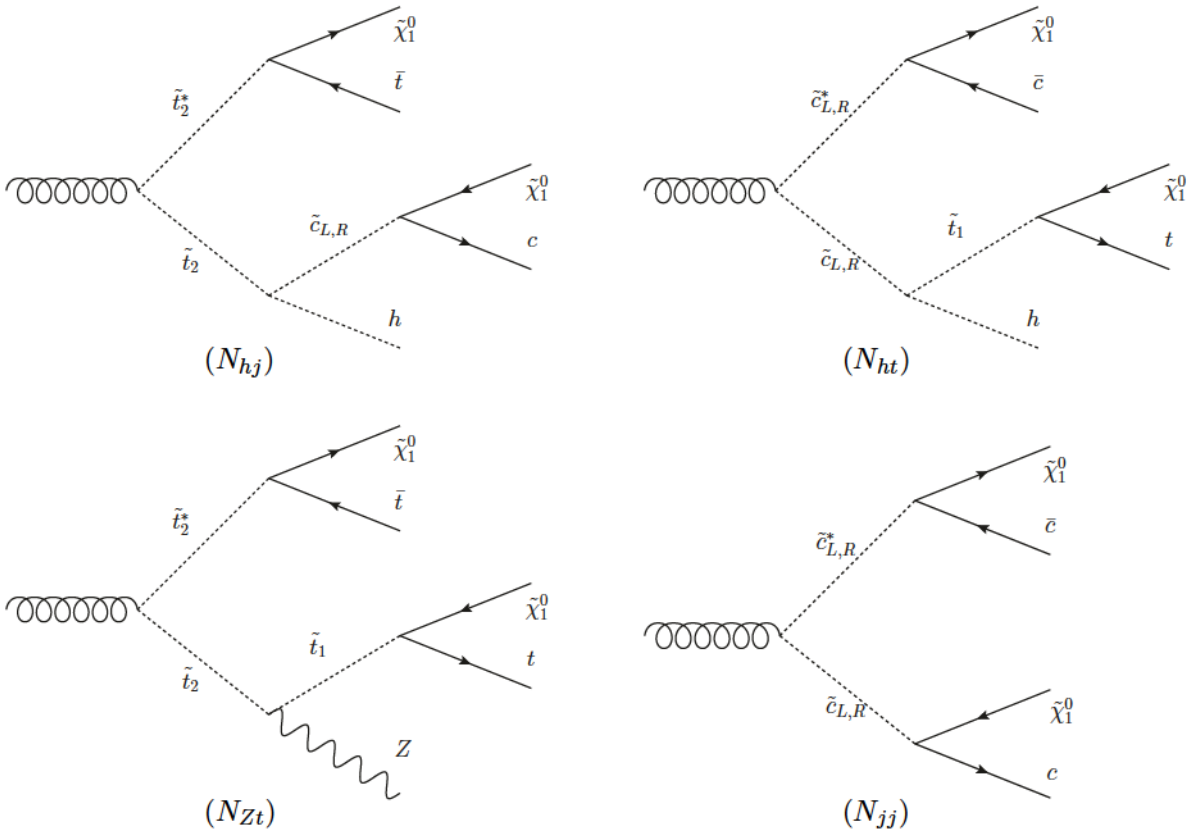

Figure 4.15 – Cascade decays used for the $SU(5)$ test based on Higgs detection defined in eq. (4.131).

Note that $P_Z \to \infty$ when $\tilde{\theta} \to \pi/4$, i.e. the power of the test vanish in the limit of maximal stop mixing as expected. Note also that in eq. (4.133), only the leading statistical uncertainty that comes from small flavor changing decay rates have been took into account.

4.7.2.1 Discussion

The expected precision is shown in fig. 4.16, for the intermediate value $\tilde{\theta} = 0.4$. Because of the mass ordering of this scenario, one expects $N_{hj} < N_{ht}$ as the $\tilde{t}_2$ is heavier than the scharms and thus produced less abundantly. Assuming $N_{hj} << N_{ht}$ and $\tilde{\theta} = 0.4$, testing the relation with 50%, 20% and 10% precision at 3σ significance requires respectively $N_{hj} \gtrsim 19$, 116 or 464 events. Roughly twice less events are needed if $\tilde{\theta} = 0$. For comparison, using the cross-section values of table 4.10, assuming flavor violating branching ratios of 0.05 and 300 fb^{-1} of integrated luminosity, one expects about 1340, 130 and 11 events for stop masses of $m_{\tilde{q}} = 700$, 1000 and 1400 GeV, respectively.

We want to conclude this section by pointing out that other possibilities of normalization of the N_{hj}, N_{ht} event rates are in principle possible - using either observed or theoretical event rates. In any case, the approach relies on evaluating the appropriate η parameter such that the expectation value of the test $\mathrm{E}[R]$ takes the form of eq. (4.132). The expected precision P_Z will then take the form of eq. (4.16) as long as the statistical uncertainties coming from the flavor changing event rates N_{hj} and N_{ht} dominate.

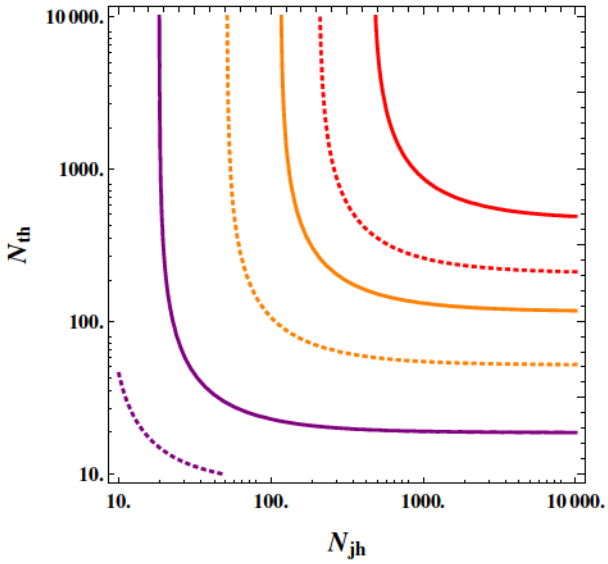

Figure 4.16 – Expected precision P_Z for the $SU(5)$ test based on Higgs detection in SUSY cascade decays eq. (4.131). N_{hj} and N_{ht} are the number of observed cascade decays from $\tilde{t}_2$ and $\tilde{c}_{L,R}$ pair production, respectively (see fig. 4.15). One fixes the stop angle to $\tilde{\theta} = 0.4$. Dotted (plain) lines denote 2σ (3σ) level of significance, respectively. Purple, orange and red lines respectively show $P_{2,3} = (50\%, 20\%, 10\%)$ isolines of expected precision.

4.8 Conclusion

In this chapter, we have explored the low energy consequences of supersymmetric theories, mainly the MSSM, equipped with a GUT scale $SU(5)$ symmetry. The $SU(5)$-MSSM constitutes the prototype of SUSY-GUTs theories and, as such, has been extensively studied in the past, especially the correlations of FCNCs between the hadronic and leptonic sectors have received a lot of attention. On the other hand, the originality of our approach was to stay confined within the up-squarks sector. In particular, we have shown that, a so far unstudied property of the up-type soft terms allowed to construct a variety of $SU(5)$ tests at low scale. Indeed, as we have argued, a SUSY model which is $SU(5)$ symmetric implies, in the up-squark sector, that the trilinear coupling is symmetric as well. As a happy coincidence, it turns out that the inner flavor structure of this relation makes it well stable under quantum corrections, the asymmetry induced by the RG flow staying, at the TeV scale of the order of $\mathcal{O}(10\%)$ at maximum. That makes clear the fact that, if a $SU(5)$-like grand unification is realized in nature, it should leave a footprint in the low scale up-squarks spectrum. This being said, this chapter have been devoted to the study of the consequences of this symmetry property among low scale observables, potentially accessible at the LHC. Three typical SUSY spectra have been investigated.

In section 4.5, "heavy" SUSY spectra were considered, in which the SUSY breaking scale is much higher than the TeV scale. Clearly in such a context, the relevant procedure was to scrutinize a low scale theory, with the s-partner spectrum integrated out. We showed that, a possibility to build a $SU(5)$ test remains if one looks at the SUSY induced effective dipole operators. Unfortunately, the current experimental sensitivity of experiments seems too low to hope disentangling the SUSY contributions to the dipole operators at colliders in the near future, thus making this test hardly applicable in practice.

In section 4.6, "natural" SUSY spectra -which feature a light third s-partner generation- have been showed to provide $SU(5)$ tests for two typical mass orderings. On one hand, if one assumes that the stops are heavier than the gauginos, one can constructs a particularly simple leading order test, from counting the number of decay events of the stops in each of the channels opened. On the other hand, if one assumes that one of the gauginos (the wino) is heavier than the stops, then one needs to push the EFT expansion of subsubsection 4.4.1.3 beyond the leading order to gain access to a $SU(5)$ footprint in the up-squark sector. Although this fact substantially complexifies the task of finding simple tests, we managed to extract a test relating stops forward-backward asymmetries.

Finally in section 4.7, we have explored the potentiality of the "Top-Charm" SUSY framework

to test the $SU(5)$ hypothesis. In these kind of spectra, the only decoupled generation is the first one, which is assumed to be very heavy, the stop-like and the scharm-like squarks lying near the TeV scale. In this framework, Higgs production through flavor violating squark decays have been shown to provide a test, assuming that one uses appropriate flavor conserving event rates to normalize the Higgs production event rates.

Table 4.4 gives a summary of the different $SU(5)$ tests that appear in the various SUSY scenarios outlined above. The typical amount of events to reach an expected precision of 50% at 3σ is also shown for each of these tests. The number of needed events ranges roughly from about 10 to about 100. For this required precision, the tests involving top-polarimetry require typically $\mathcal{O}(100)$ events as they rely on the shape of the kinematic distribution.

In any case, we see that the feasibility of all these tests have been quantified using a p-value frequentist approach, in which the null-hypothesis was the presence of a GUT scale $SU(5)$ symmetry. We hence insist on the fact that all tests developed in this chapter have been geared to only reject the $SU(5)$ hypothesis with a given significance, not to confirm it.

On the other hand, the next chapter will be devoted to a more global numerical analysis, which could be used to both reject and/or confirm the $SU(5)$ hypothesis. Beside, and complementary to what was done here, this analysis will rely on Bayesian statistics, thus transcending the intrinsic limitations of the frequentist approach.

	Heavy SUSY	Natural SUSY		Top-charm SUSY	
		$m_{\tilde{t}_{1,2}} > m_{\tilde{B},\tilde{W}}$	$m_{\tilde{W}} > m_{\tilde{t}_{1,2}} > m_{\tilde{B}}$	$m_{\tilde{t}_{L,R}} \sim m_{\tilde{c}_{L,R}}$	$m_{\tilde{t}_2} > m_{\tilde{c}_{L,R}} > m_{\tilde{t}_1}$
Squarks involved	virtual	virtual/real		real	
Top polarimetry	yes	no	yes	yes	no
Charm-tagging	no	yes	no	no	no
Higgs detection	no	no	no	yes	yes
$\tilde{\theta}$-dependence	no	no	yes	no	yes
$P_3 = 50\%$	144	72	108	144	10

Table 4.4 – Summary of the $SU(5)$-tests appearing in the various SUSY scenarios considered. The last line shows the typical number of events needed to reach a 50% precision at 3σ.

Chapter 5

A Bayesian analysis

This chapter will be devoted to the presentation of more global $SU(5)$ tests that those presented in chapter 4. The general framework to set up such tests will be the one of model comparison in Bayesian inference [155]. The central goal of this chapter will be the numerical computation of Bayes factors [156] using Markov Chain Monte Carlo (MCMC) algorithms [157] to test the $SU(5)$ hypothesis $A_U \approx A_U^T$ on low scale SUSY spectra. The rest of this chapter is organized as follows. As this has not become a widely familiar topic for high energy physicists yet, we will give in section 5.1 a brief introduction to Bayesian statistics. Section 5.2 will be devoted to the presentation of the analysis, in particular the numerical strategy used will be detailed. Finally, section 5.3 will be devoted to the presentation and to a discussion of the results of the analysis.

5.1 The Bayesian Context

This section is devoted to the presentation of the main ideas at the core of the Bayesian formulation of statistics. Very briefly, the frequentist school assumes that, when measuring a parameter from data, sufficiently high series of measurements converge to the true value of the parameter of interest, considered as constant. In contrast Bayesians argue that, when inferring a parameter, one has to take into account a subjective, a-priori distribution, reflecting our current knowledge on what that parameter should be, to formulate meaningful results. Bayes' theorem then provides a prescription to update the inferred value when more data become available. In short, one can say that for frequentists "truth" is fixed and observations are random whereas Bayesians argue that a probability is a statement about the possible states of the truth.

The difference is hence of a philosophical nature, and the debate between the two schools has been going on for years, triggering a lot of literature (see for instance [158] for a defense of the frequentist interpretation). Anyway, it is not our aim here to go deeper into this debate. Nonetheless, we would like to sketch a few of the reasons that have allowed the Bayesian interpretation to become very popular over the last years, thus making people think that it constitutes a more natural formulation of the concepts raised by the theory of probability. Indeed, currently Bayesian statistics find applications well beyond the scope of high energy physics, whether it is in psychology, biology or economy. Hence, in subsection 5.1.1, we will present a few of the limitations and, we believe inconsistencies, that arise in a frequentist formulation of probability, thus motivating the introduction of the Bayesian interpretation. Subsection 5.1.2 will be devoted to the presentation of the main concepts and results of the Bayesian theory. Especially, the notions of prior and posterior probability distributions, as well as the Bayes theorem, will be introduced. Finally, subsection 5.1.3 will focus on one application of the Bayesian theory, namely model comparison. In particular, the Bayes factor, which will be largely used in the rest of this chapter, will be presented. Note that this section has been prepared using the following references [159], [160] and [156].

5.1.1 Limitations of the frequentist approach

As we argued in subsection 4.4.3, in the frequentist approach, a definition of a probability of an event can be:

The number of times the event occurs over the total number of trials, in the limit of an infinite series of equiprobable repetitions.

This definition of probability is unsatisfactory in several aspects:

1. First, the fact that we define a probability in terms of relative equiprobable outcomes, render this definition clearly circular. Indeed, it was the very first notion of "probable" that we were trying to define. Other definitions try to escape this point by replacing the word "equiprobable" by "if all the cases are equally possible" ignoring that in this context, "possible" is a synonym of "probable". There is no way out. This statement does not provide a definition of "probability" but at most, gives a useful rule to evaluate it, in case we already know what a probability is.

2. Secondly, this definition cannot deal with unrepeatable experiments. For example, questions such as: "What is the probability that it was snowing in Dublin during the Paris 1998 final soccer world cup?" or in a cosmological context, questions related to the observational properties of the Universe as a whole cannot be answered in a frequentist context. Back to particle physics, for the same reasons, the frequentist interpretation has difficulties to deal properly with systematic uncertainties.

3. The definition only holds exactly for an infinite sequence of repetitions. But, in real life, we always have a finite number of measurements, sometimes with only a small number of them. Defining "how many repetitions" are sufficient for a probability to converge become then a tricky question, which has to be answered in every single case. In practice, one often forget about this issue of "infinite series" requirement and tend to use this definition, and the results that go with it, for whatever number of events we have at disposal.

The Bayesian interpretation of probability circumvent most of these caveats. Indeed, the definition 5.1.1 is replaced by the following, more intuitive definition:

A probability is a measure of the degree of belief *about a proposition.*

A-priori, this definition seems too vague to be of any utility. We then need some explanation of its meaning, a tool to evaluate what a "degree of belief" is, and we should look at such a tool, the Bayes theorem, in the next subsection. On the other hand, this definition seems however to be more powerful than the frequentist one on several points:

1. It is very general, and one can apply this definition to any event, independently of the repeatability of the event. Hence, one doesn't need to assume that a series of *equiprobable* measurements have to be made to compute a probability. Rather, a probability will be conditional, in a sense to be precised later on, on our *subjective* state of knowledge about the measurement. This last condition has been often considered as a weak point of the Bayesian interpretation, but it should not be. Let us consider, for example, a mass measurement. In frequentist methods based on maximum likelihood tests, in certain circumstances, for example if the signal to background ratio is low, unless special care is taken, one might end with negative best-fit estimates, which obviously make no sense for a mass value. On the opposite, in a Bayesian context one can guarantee that, by taking into account relevant prior information on the measurand, the final result will be enforced to be positive. Beside, the Bayes theorem ensures that, our a-priori state of knowledge on the measurand become less and less relevant as more and more data become available, the two approaches -frequentist and Bayesian- being asymptotically equivalents.

2. It can deal effortlessly with systematic errors. For example, if one wants to measure a BSM signal at colliders, let us say through a reconstructed invariant mass measurement, one has to take into account systematic errors which originate, for instance, from the finite energy resolution of the calorimeters, or from some electronic delay in the trigger system. In a frequentist context, one often deals with these systematics by the non-frequentist procedure of generating many pseudo-experiments, from Monte-Carlo simulations, whereas from one pseudo-experiment to the next, the values of all nuisance parameters are varied within their assumed distributions. In a Bayesian treatment, the nuisance parameters are removed from the start by marginalization, which mean that they are simply integrated out assuming some prior probability density function (PDF).

3. In a Bayesian treatment, one only has to deal with data which were actually observed, while frequentist methods focus on the distribution of possible data that have not been obtained. As a consequence, the opinion of an experimenter, for example through a specific distribution choice, on data that have not been observed yet, might influence the outcome of a frequentist result. This is clearly illogical as the results of inferences should not depend on what could have happened but, should only depend on what was actually observed. This problem is circumvented from the start in a Bayesian setup, as inferences are by construction conditional on what was observed.

5.1.2 The Bayes theorem, priors and posteriors, or the doom of the "false idol of objectivity"

After this qualitative discussion, we would like to go deeper into the formalism of Bayesian statistics. Clearly, in Bayesian statistics, the concept of conditional probability is absolutely central. We recall that if we note $P(A|B)$, the value of the probability of the event A assuming that B has been realized, or more commonly "the probability of A *knowing* B", the axioms of probability imply:

$$p(A, B|I) = p(A|B, I)p(B|I) \tag{5.1}$$

where in eq. (5.1), I represents any information that is assumed to be true, and $p(A, B|I)$ represents the *joint probability* of A and B knowing I. Eq. (5.1) simply says that the joint probability of A and B equals to the probability of A given that B occurs, times the probability of B occurring on its own, where all probabilities are assumed to be conditional on the true information I. If one is only interested on the probability of B alone, independently of A, the sum and products rules imply that:

$$p(B|I) = \sum_A p(A, B|I) \tag{5.2}$$

where the sum runs over all possible outcomes for proposition A. The quantity on the left-hand-side of eq. 5.2, where the proposition A has been summing out, is called the *marginal probability* of B. Since we have $p(A, B|I) = p(B, A|I)$, eq. (5.1) directly implies that:

$$p(B|A, I) = \frac{p(A|B, I)p(B|I)}{p(A|I)}. \tag{5.3}$$

This result is known as the Bayes theorem in honors of Thomas Bayes [1], an 18^{th} century English pastor and mathematician [2]. One can get a better insight at the Bayes theorem if we replace the proposition A by some observed data, which are generically noted d, and the proposition B by an hypothesis one wants to assess, noted H:

$$p(H|d, I) = \frac{p(d|H, I)p(H|I)}{p(d|I)}. \tag{5.4}$$

Let us have a look at the different ingredients of eq. (5.4). On the left-hand side, $p(H|d, I)$ represents the probability of the hypothesis H to be true, once the data d have been taken into account. For

[1] See for instance, en.wikipedia.org/wiki/Thomas_Bayes for a short biography of Thomas Bayes.

[2] As the author of this thesis is french, he would to point out that the Bayes theorem has been rediscovered and its interpretations extended, ten years later, by the French mathematician and physicist Pierre-Simon Laplace, see en.wikipedia.org/wiki/Pierre-Simon_Laplace.

this reason, $p(H|d,I)$ is called the *posterior* probability of the hypothesis given the data, or more shortly just the *posterior*. On the right-hand side, $p(H|I)$ represents the probability of the hypothesis irrespectively of any data. Stated otherwise, this probability represents the *degree of belief* of the hypothesis H before one has took into account the information brought by the data. For this reason, $p(H|I)$ is called the probability *prior* to the data, or simply the *prior*.

$p(d|H,I)$ represents the likelihood, which encodes how the degree of plausibility of the hypothesis changes when we acquire new data. The likelihood must then be considered as a function of the hypothesis, for fixed data (the one that have been actually observed). For this reason, as the data are fixed, we can shortcut the notation and simply write $\mathcal{L}(H) \equiv p(d|H,I)$. As the likelihood is a function of the hypothesis, not the outcome -in this case, the data-, it should not be viewed as a probability density function. The likelihood is thus, a-priori, not normalized. We hence also need a normalization constant, $p(d|I)$ called the marginal likelihood and which is equal to :

$$p(d|I) \equiv \sum_H p(d|H,I)p(H|I) \tag{5.5}$$

where the sum runs over all the possible outcomes for the hypothesis H. We hence see that the Bayes theorem teaches us how to update the prior -which represents our *degree of belief* before the data were considered- when new data are acquired, through the computation of the posterior. The Bayes theorem gives thus a prescription on how to learn from experiments.

From here, two applications of the Bayes theorem are possible. Model comparison allows to discriminate two competitive models in view of data, we will give some details on this in subsection 5.1.3. On the other hand, parameter inference allows to infer a model's parameter from a set of data, a prior pdf being given. Let us say for example one wants to infer a set of parameters of a given model noted $\mathcal{M}$. In eq. (5.4), the proposition I is then "the model $\mathcal{M}$ is true", simply noted $\mathcal{M}$, while the hypothesis H is "the set of parameters of the model takes the value θ", simply noted θ. The Bayes theorem gives then:

$$p(\theta|d,\mathcal{M}) = \mathcal{L}(\theta)\frac{p(\theta|\mathcal{M})}{p(d|\mathcal{M})}. \tag{5.6}$$

The marginal likelihood $p(d|\mathcal{M})$ is irrelevant for this application, but will play a crucial role when we will discuss model comparison in subsection 5.1.3. Often, all parameters of the model are not relevant for the problem at hand. Assume for instance, that the vector of parameters takes the form $\theta = (\phi, \psi)$, where ϕ is the parameter one wants to infer, and ψ represents the parameter we are not interested in, called a nuisance parameter. A nuisance parameter can represent for instance, a parameter in the distribution of some given background rate. In Bayesian inference, one get rid of nuisance parameters by marginalizing them, i.e. integrating them out of the posterior:

$$p(\phi|d,\mathcal{M}) \propto \int \mathcal{L}(\phi,\psi)p(\phi,\psi|\mathcal{M})\mathrm{d}\psi. \tag{5.7}$$

Then one can get an estimate of the parameter ϕ by extracting some characteristic of the distribution (5.7) such as the mean, the standard deviation or the correlation matrix among the components (in case ϕ is multidimensional), or by simply plotting the distribution (5.7). However, there are very little cases where this integration can be computed analytically and most of the time, one has to use numerical techniques such as Monte Carlo Markov Chains (see section 5.2) or Nested Sampling Algorithms [161] to sample the marginalized posterior.

5.1.3 Bayes factors and model comparison

We would like now to focus on model discrimination in Bayesian statistics. In model comparison, it is useful to think about a model as a given hypothesis but also as a set of parameters which characterize the hypothesis. Going back to eq. (5.4) and specifying a model noted $\mathcal{M}$, the hypothesis H is now "model $\mathcal{M}$ is true", and there is no additional true information I.

The prime tool for model selection is the marginal likelihood, also called in this context the *Bayesian evidence*. It corresponds to the normalization integral at the denominator of the right-hand side in the

$\lvert\log(B_{01})\rvert$	Odds	Probability	Strength of evidence
< 1.0	$\lesssim 3:1$	< 0.750	Inconclusive
1.0	$\sim 3:1$	~ 0.750	Weak evidence
2.5	$\sim 12:1$	~ 0.923	Moderate evidence
5.0	$\sim 150:1$	~ 0.993	Strong evidence

Figure 5.1 – The empirical calibrated Jeffrey scale. A value of Bayes factor B_{01} of 3 (resp: 1/3), 12 (resp: 1/12), and 150 (resp: 1/150) indicating a weak, moderate and strong evidence for (resp: against) the model $\mathcal{M}_0$.

Bayes theorem eq. (5.4). The Bayesian evidence can be re-written, on a continuous parameter space Ω_M as:

$$p(d|\mathcal{M}) \equiv \int_{\Omega_\mathcal{M}} p(d|\theta,\mathcal{M})p(\theta|\mathcal{M})\mathrm{d}\theta \tag{5.8}$$

where we have conditioned explicitly the probabilities to the model considered $\mathcal{M}$. We hence see that the Bayesian evidence is nothing more than the average of the likelihood $p(d|\theta,\mathcal{M})$ under the prior, given a chosen model $\mathcal{M}$. From the evidence, the model posterior probability given the data can be obtained using Bayes theorem to invert the conditioning:

$$p(\mathcal{M}|d) \propto p(\mathcal{M})p(d|\mathcal{M}) \tag{5.9}$$

where again, we have dropped an irrelevant constant that depends only on the data. In eq. (5.9), $p(\mathcal{M})$ is simply the prior associated to the model itself. Let us assume that one wants to compare two compelling models, noted $\mathcal{M}_0$ and $\mathcal{M}_1$. Then, the quantity of interest is the ratio of the posterior probabilities, or posterior odds, given by:

$$\frac{p(\mathcal{M}_0|d)}{p(\mathcal{M}_1|d)} = \frac{p(d|\mathcal{M}_0)}{p(d|\mathcal{M}_1)}\frac{p(\mathcal{M}_0)}{p(\mathcal{M}_1)}. \tag{5.10}$$

Due to possible differences on the prior choices, a choice between two models is often not based directly on the ratio of the posterior odds, but rather on the ratio of the models evidence:

$$B_{01} \equiv \frac{p(d|\mathcal{M}_0)}{p(d|\mathcal{M}_1)} \tag{5.11}$$

called the *Bayes factor*. This is the central quantity for model comparison. A value of $B_{01} > 1$ (resp: $B_{01} < 1$) represents an increase (resp: decrease) of the *degree of belief* of $\mathcal{M}_0$ with respect to $\mathcal{M}_1$. Thus, the Bayes factor gives a formal way of evaluating the relative probabilities of two models, in light of the data.

We know turn to the numerical interpretation of the Bayes factor. The Bayes factor is often interpreted against an empirical calibrated scale, named the Jeffrey scale [162]. This scale states that the odds of $\mathcal{M}_0$ against $\mathcal{M}_1$ go as $3:1$, $12:1$ and $150:1$, corresponding to weak, moderate and strong evidences, respectively. For example, a Bayes factor of 5 (resp: 1/5) indicates a weak evidence for (resp: against) $\mathcal{M}_0$. Furthermore, notice that the relevant quantity in tab. 5.1 is the logarithm of the Bayes factor. This indicates that the evidence in favor of one of the models accumulates only slowly. Indeed, to cross the different thresholds of evidence, one needs to increase the Bayes factor by one order of magnitude each time.

Beside, in case of nested models, a simplification of the Bayes factor -important for us in the rest of this chapter- can be worked out. Two models $\mathcal{M}_0$ and $\mathcal{M}_1$ are called *nested* if when the parameters of $\mathcal{M}_1$ take a certain value, one retrieves $\mathcal{M}_0$. For example, let us consider the case where the set of the $\mathcal{M}_1$ model parameters is $\theta = (\phi,\psi)$ and $\mathcal{M}_0$ is obtained whenever $\psi = 0$, i.e. we have $\mathcal{M}_0 = \mathcal{M}_1(\phi,\psi=0)$. If on the top of that, the priors are separable i.e. :

$$p(\phi,\psi|\mathcal{M}_1) = p(\psi|\mathcal{M}_1)p(\phi|\mathcal{M}_0) \tag{5.12}$$

then the Bayes factor simplifies to the following expression:

$$B_{01} = \left.\frac{p(\psi|d,\mathcal{M}_1)}{p(\psi|\mathcal{M}_1)}\right|_{\psi=0} \tag{5.13}$$

known as the Savage Dickey Density Ratio (SDDR, see [163], [164]). In eq. (5.13), the numerator is the marginal posterior under the more complex model evaluated at the simpler model's parameter value. The denominator is then simply the prior density of the more complex model evaluated at the same point. The SDDR is particularly suited for testing only one extra parameter at the time. Indeed, in such a case, the marginal posterior $p(\psi|d,\mathcal{M}_1)$ is a 1-dimensional function and normalizing it to unity only requires a 1-dimensional integral which is easily computable using standard numerical techniques. Hence, the SDDR will be of great help for us, and we will go back to it in section 5.2.

An important remark has to be made here. Let us assume that one wants to compare two models, one simple model parameterized by only one parameter, and a more complex model which requires two parameters. It is clear that by constructing models with more and more free parameters, one can always make them fit better the data than models containing a smaller number of them. It is thus important that the Bayes factor discriminates models, not only with respect to their goodness of fit to the data, but also as to know if the extra parameter is really needed by the data.

To gain an intuition on how it works, let us consider the following example. Consider two compelling nested models: $\mathcal{M}_0$ assigns to a quantity θ a vanishing value i.e. $\theta = 0$ and $\mathcal{M}_1$ assigns to θ a Gaussian prior distribution with mean 0 and variance Σ^2. Assume that we perform a measurement of θ described by a normal likelihood of standard deviation σ, and with the maximum likelihood value lying λ standard deviation away from 0 i.e. $|\theta_{\max}/\sigma| = \lambda$. In this case, the Bayes factor can be computed analytically from eq. (5.11) and is equal to:

$$B_{01} = \sqrt{1+(\sigma/\Sigma)^{-2}}\exp\left(-\frac{\lambda^2}{2(1+(\sigma/\Sigma)^2)}\right). \tag{5.14}$$

From eq. (5.11) a few limit cases can be discussed.

First, if $\lambda \gg 1$, the exponential term dominates and $B_{01} \ll 1$. This corresponds to a situation where the parameter θ is measured at many standard deviations from the mean value, it is thus intuitive that the complex model $\mathcal{M}_1$ is favored by the Bayes factor.

Secondly, assume that $\lambda \lesssim 1$ and $\sigma/\Sigma \ll 1$ meaning that, in the vicinity of zero, the likelihood is more sharply peaked than the prior. We have then $B_{01} \sim \Sigma/\sigma$ and evidence accumulates in favor of the simpler model proportional to Σ.

What does it mean? In fact, Σ represents the quantity of information which is bringing in the model by the extra parameter θ. If $\Sigma \gg 1$, the prior is only weakly informative, and will not really help constraining the data. On the other hand, if $\Sigma \ll 1$, than the constraining power of the parameter is high, its introduction in the model brings a real capital gain when trying to constrain the data. If the θ parameter typical range is in good agreement with the data, compared to the simpler model $\mathcal{M}_0$, than it is clear that the Bayes factor will favor $\mathcal{M}_1$.

In fact this example shows that the Bayes factor encodes the Occam's razor, an old philosophical principle which states that when comparing two models with the same predictions, the simplest should always be privileged. Also, as a concluding remark, let us note that contrary to frequentist goodness-of-fits tests, Bayesian model comparison always requests at least two models, maintaining that it is pointless to reject a model unless another, which fits better the data, is available

5.2 Numerical strategy

In this section we would like to present the numerical strategy used in our analysis. This section is structured as follows. We start by defining what we want to compute i.e. we define the models that we want to compare. Then, we continue by presenting the MCMC algorithm used to evaluate the posterior and prior probabilities. We conclude this section by giving some details on two tools used in this analysis: `SPheno`, a fast spectrum calculator already encountered in section 4.3 and `XSUSY`, a

package aimed at quickly computing squark decay branching ratios and production cross sections, both tools implementing the full flavor structure of the MSSM, as presented in subsection 4.2.1 (see also [96]).

5.2.1 Definition of the models

As already pointed out, the purpose of this analysis is to compute Bayes factors to disentangle the possible presence of remnants of a high scale $SU(5)$ symmetry in low scale squark spectra.

As in the previous chapter, our analysis will focus on mixing between the second and third generations. And, in the same way, we will consider that the crucial $SU(5)$ signature lies in the asymmetry of the trilinear coupling in the $(2,3)$ sector $\mathcal{A}_{23}$ being small, where compared to the definition 4.22, we have replaced the factor $1/6$ by a factor $1/4$, since only two flavors are active in this analysis (see below). Beside, we do not take the absolute value in $\mathcal{A}_{23}$ here, since we want to study the distribution of $\mathcal{A}_{23}$ on an interval symmetric around 0. To define the two models of interest, we will even consider that this SUSY scale asymmetry is exactly vanishing if the $SU(5)$ hypothesis is verified. We hence define the two following models at the TeV scale:

$$\mathcal{M}_0 = \{SU(5) \text{ hypothesis verified} \rightarrow \mathcal{A}_{23} = 0\} \tag{5.15}$$

$$\mathcal{M}_1 = \{SU(5) \text{ hypothesis not verified} \rightarrow \mathcal{A}_{23} \neq 0\}\,. \tag{5.16}$$

We have indeed nested models since $\mathcal{M}_0 = \mathcal{M}_1(\mathcal{A}_{23} = 0)$. The Bayes factor $B_{01} = \frac{p(d|\mathcal{M}_0)}{p(d|\mathcal{M}_1)}$ then reduces to the following SDDR:

$$\begin{aligned} S &= \frac{p'(\mathcal{A}_{23}|d,\mathcal{M}_1)}{\int \mathrm{d}\mathcal{A}_{23}\, p'(\mathcal{A}_{23}|d,\mathcal{M}_1)} \frac{1}{p(\mathcal{A}_{23}|\mathcal{M}_1)}\bigg|_{\mathcal{A}_{23}=0} \\ &= \frac{p(\mathcal{A}_{23}|d,\mathcal{M}_1)}{p(\mathcal{A}_{23}|\mathcal{M}_1)}\bigg|_{\mathcal{A}_{23}=0} \end{aligned} \tag{5.17}$$

where we have noted the unnormalized marginal posterior $p'(\mathcal{A}_{23}|d,\mathcal{M}_1)$ with a tilde. In the first line of eq. (5.17), the integral on the denominator of the right-hand side serves to normalize it to unity (see subsection 5.1.3).

We now turn to how to compute this SDDR in practice.

5.2.2 A MCMC algorithm

When we want to compute the SDDR eq. (5.17), two PDFs need to be evaluated: the normalized posterior $p(\mathcal{A}_{23}|d,\mathcal{M}_1)$, and the prior $p(\mathcal{A}_{23}|\mathcal{M}_1)$. The SDDR will then just be the ratio of the value of these two PDFs at $\mathcal{A}_{23} = 0$. We start by commenting the procedure used to compute the posterior $p(\mathcal{A}_{23}|d,\mathcal{M}_1)$.

We have decided to use a Markov Chain Monte Carlo method based on the standard Metropolis Hasting algorithm [157]. These methods are very useful to sample a target distribution, in this case the posterior, by exploring randomly a configuration space which can be potentially high dimensional.

5.2.2.1 Preliminary remarks

Before describing the algorithm, a few preliminary remarks have to be made:

1. In all that follows, we will assume an effective two generations framework i.e., the first generation of the up-type squarks is decoupled (cf case Top Charm SUSY, sec. 4.7). In this analysis we work with squarks given in their mass eigenbasis i.e. the up-squark spectrum is composed of the first four mass eigenstates $\tilde{u}_1, \cdots, \tilde{u}_4$ given in a mass ordered basis.

2. This analysis is aimed to test one spectrum at a time. In practice, this spectrum is provided through a "Standard Les Houches accord" (SLHA) file [165, 166] whose supersymmetric parameters are assumed to be taken at $Q = 1$ TeV. This file contains every parameter needed to

diagonalize the TeV scale spectrum i.e., it contains the different sfermion masses and trilinear couplings, the gaugino masses, the parameters describing the Higgs sector ($\tan\beta$, μ, the mass of the peudo-scalar Higgs m_A) and the SM parameters ($V_{\rm CKM}$, gauge couplings, m_Z etc..). In the following, we shall call this spectrum, the "reference spectrum".

3. We have decided to perform the random walk in the space of the TeV scale soft matrices. More precisely, a point in our parameter space is defined as :

$$x_i = \begin{cases} M^2_{Q_i} = \begin{pmatrix} (M^2_Q)_{11} & (M^2_Q)_{12} \\ (M^2_Q)_{21} & (M^2_Q)_{22} \end{pmatrix}_i \\ M^2_{U_i} = \begin{pmatrix} (M^2_U)_{11} & (M^2_U)_{12} \\ (M^2_U)_{21} & (M^2_U)_{22} \end{pmatrix}_i \\ A_{U_i} = \begin{pmatrix} (A_U)_{11} & (A_U)_{12} \\ (A_U)_{21} & (A_U)_{22} \end{pmatrix}_i \end{cases} \tag{5.18}$$

where all 2×2 soft matrices are assumed to be taken at $Q = 1$ TeV in the SCKM basis.

4. In the posterior PDF expression $p(\mathcal{A}_{23}|d,\mathcal{M}_1)$, the data d will be understood to be a set of observables build out of:
   (a) the squark mass eigenvalues: $m_{\tilde{u}_1},\cdots,m_{\tilde{u}_4}$.
   (b) the elements of the squark rotation matrix $(\mathcal{R}_{\tilde{u}})_{ij}$.
   (c) the decays branching ratios of the squarks into a charm or a top plus the lightest neutralino. That means we consider the following 8 flavor violating branching ratios: $\mathrm{BR}(\tilde{u}_i \to t/c\ \tilde{\chi}_1)$, $i = 1\cdots 4$.
   (d) the squark/anti-squark pair production cross sections at a proton-proton collider, i.e. we consider the 4 cross sections: $\sigma_{\tilde{u}_i\tilde{u}_i^*} \equiv \sigma(\mathrm{p\,p} \to \tilde{u}_i\,\tilde{u}_i^*)$, $i = 1\cdots 4$.

5. At each step of the MCMC, the soft matrices are diagonalized using the low scale version of `SPheno`. That means that the flag 1 of the block MODSEL is set to 0 (see: [91]) in our reference spectrum. The branching ratios and the cross sections are calculated using `XSUSY`, a package aimed at phenomenological studies in a general flavor violating MSSM. We will justify this choice and give a brief description of both tools in subsection 5.2.3.

6. We insist on the fact that, contrary to what is usually done, we do not use the MCMC presented here to converge toward a region of the parameter space favored by data. The purpose being to use the random walk to fill histograms approximating the conditional PDFs.

7. To evaluate the prior and posterior PDFs, we construct a histogram $\mathcal{B}$, which consists in a series of N_{bins} discretized values of $\mathcal{A}_{23}$: $\mathcal{B} = \{\mathcal{A}_1, \mathcal{A}_2, \cdots, \mathcal{A}_{N_{\rm bins}}\}$ where $\mathcal{A}_1 < \cdots < \mathcal{A}_{N_{\rm bins}}$ and the width of a bin is given by: $\mathrm{width(Bin)} = (\mathcal{A}_{N_{\rm bins}} - \mathcal{A}_1)/N_{\rm bins}$.

5.2.2.2 Algorithm: The posterior PDF case.

The general scheme is then as follows:

0. Initialisation: First of all, we use the reference spectrum to construct a set of observables dubbed $\mathcal{O}^j_{\rm Ref}$. We do not want to be more specific here, but $\mathcal{O}^j_{\rm Ref}$ might be for example an event rate, a mass eigenvalue or some combination of the elements in $\mathcal{R}_{\tilde{u}}$ representing the scharm/stop flavor content of a squark (see section 5.3). Note that this step is only done once, before the random walk starts.

1. Likelihood definition: We then need to define a goodness function measuring the "relevance" of a certain point in the configuration space. In this case, the goodness function is a standard Gaussian likelihood, defined at step i as:

$$\mathcal{L}(x_i) = \exp(-\frac{\chi^2_i}{2}) \tag{5.19}$$

where the χ_i^2 is defined as:

$$\chi_i^2 = \sum_j \frac{\left(\mathcal{O}^j_{\mathrm{MC}_i} - \mathcal{O}^j_{\mathrm{Ref}}\right)^2}{(\sigma^j)^2}. \tag{5.20}$$

Here $\mathcal{O}^j_{\mathrm{MC}_i}$ (resp: $\mathcal{O}^j_{\mathrm{Ref}}$) are a set of TeV scale observables computed from the Markov chain at step i (resp: from the reference scenario, see step 0). To each observable $\mathcal{O}^j$ is assigned an uncertainty noted σ^j.

2. Asymmetry computation, step i: From the diagonalized spectrum at step i, we can compute the asymmetry $\mathcal{A}^i_{23}$ (see eq. (4.22)), properly normalized to the sum of the squark mass eigenvalues.

3. Jump: A new point is evaluated at step $i+1$ as:

$$x_{i+1} = \begin{cases} (M^2_{Q_{i+1}})_{lk} = (M^2_{Q_i})_{lk} + M^2_{\mathrm{SUSY}}\, b\, \lambda_{lk} \\ (M^2_{U_{i+1}})_{lk} = (M^2_{U_i})_{lk} + M^2_{\mathrm{SUSY}}\, b\, \mu_{lk} \quad l,k = 1,2. \\ (A_{U_{i+1}})_{lk} = (A_{U_i})_{lk} + M_{\mathrm{SUSY}}\, b_A\, \epsilon_{lk} \end{cases} \tag{5.21}$$

where λ_{lk}, μ_{lk} and ϵ_{lk} are numbers generated randomly [3] with a Gaussian distribution of mean zero and unit standard deviation.

In eq. (5.21), M^2_{SUSY} is a mass scale which fixes the scale of the soft terms, and b (resp: b_A) is a parameter which controls the size of the jump in the scalar mass terms (resp: trilinear couplings) direction. All three parameters are free, the values used in this analysis will be given in section 5.3.

4. Likelihood computation, step $i+1$: From the soft matrices sampled at step 3, we diagonalize the spectrum with the low scale version of `SPheno` (see remark 5).

   If the soft matrices sampled lead to a non-physical spectrum (presence of tachyons, loop corrections too high), we discard the sampling and go back to step 3.

   With the spectrum properly diagonalized, we can compute the likelihood $\mathcal{L}(x_{i+1})$ at step $i+1$, calling eventually `XSUSY` if one of the observables $\mathcal{O}^j_{MC_{i+1}}$ implies a branching ratio or a cross section calculation.

5. Asymmetry computation, step $i+1$: With the spectrum at step $i+1$, we can compute the asymmetry on this point of the Markov Chain, noted $\mathcal{A}^{i+1}_{23}$.

6. Metropolis-Hasting algorithm: If $\mathcal{L}(x_{i+1}) > \mathcal{L}(x_i)$, the point is accepted. In this case, we jump to the next step on the chain and go back to step 1 with the replacement $x_i \to x_{i+1}$.

   Otherwise, the point is accepted with a certain probability u i.e. if $\mathcal{L}(x_{i+1}) > u\mathcal{L}(x_i)$ then go back to step 1 with $x_i \to x_{i+1}$ and if $\mathcal{L}(x_{i+1}) < u\mathcal{L}(x_i)$, the point is rejected and we stay on the same point of the chain i.e. go back to step 1 with $x_i \to x_i$.

   Here u is a number randomly generated with a uniform distribution over the interval $[0,1]$. This step is the Metropolis-Hasting algorithm itself. The last condition is requested to prevent the chain from staying stuck indefinitely in a region of the parameter space.

7. Histogram filling: If the point x_{i+1} is accepted by the Metropolis-Hasting algorithm, then we use the asymmetry computed at step $i+1$ to fill the histogram, i.e. $\mathrm{Bin}(\mathcal{A}^{i+1}_{23}) \to \mathrm{Bin}(\mathcal{A}^{i+1}_{23}) + 1$.

   Otherwise, we fill the histogram with the asymmetry computed at step i, i.e. $\mathrm{Bin}(\mathcal{A}^{i}_{23}) \to \mathrm{Bin}(\mathcal{A}^{i}_{23}) + 1$.

[3] we have used the random number generator of `Octave` v3.8.2 which is a free software, equivalent to `MATLAB`, available at [167].

Looking at the algorithm 5.2.2.2, it is clear that the outcome at step $i+1$ depends only on the outcome at step i, thus this algorithm is "memoryless" and we have a Markov Chain in the mathematical sense [168].

Also, we have implemented a burn-in phase, i.e. given a free integer N_{burn}, we skip the step 7 during the N_{burn} first iterations of the chain, such that the algorithm can reach a numerical stability before starting filling histograms.

We have summarized the algorithm on figure 5.2. Note that the arrows marked in red on fig. 5.2 correspond to the initialization step (see step 0).

5.2.2.3 Algorithm: The prior PDF case.

Using this setup to compute the prior probability $p(\mathcal{A}_{23}|\mathcal{M}_1)$ leads to a much more simple algorithm. Indeed, in this case, no observable need to be computed and the Metropolis-Hasting step is skipped, the Markov Chain being then allowed to explore freely the parameter space of soft matrices, in the limit where each sampling (see step 3) leads to a physical spectrum.

The main steps used to compute $p(\mathcal{A}_{23}|\mathcal{M}_1)$ then are:

1. Jump: This is exactly the same step as in step 3.
2. Diagonalization, step i: With the soft matrices sampled at step 1, and the reference spectrum, one can diagonalize the spectrum at step i using `SPheno`.

   If the spectrum is unphysical, then go back to step 1.
3. Asymmetry computation, step i: With the spectrum properly diagonalized, one can compute $\mathcal{A}_{23}^i$.
4. Histogram filling: The histogram representing $p(\mathcal{A}_{23}|\mathcal{M}_1)$ is filled with $\mathcal{A}_{23}^i$, i.e. $\text{Bin}(\mathcal{A}_{23}^i) \to \text{Bin}(\mathcal{A}_{23}^i) + 1$.

Note also that as the prior does not depend on the data (i.e. the obervables), the prior needs to be simulate only once in subsections 5.3.2-5.3.4 in which different sets of observables are used to constrain the Markov Chain.

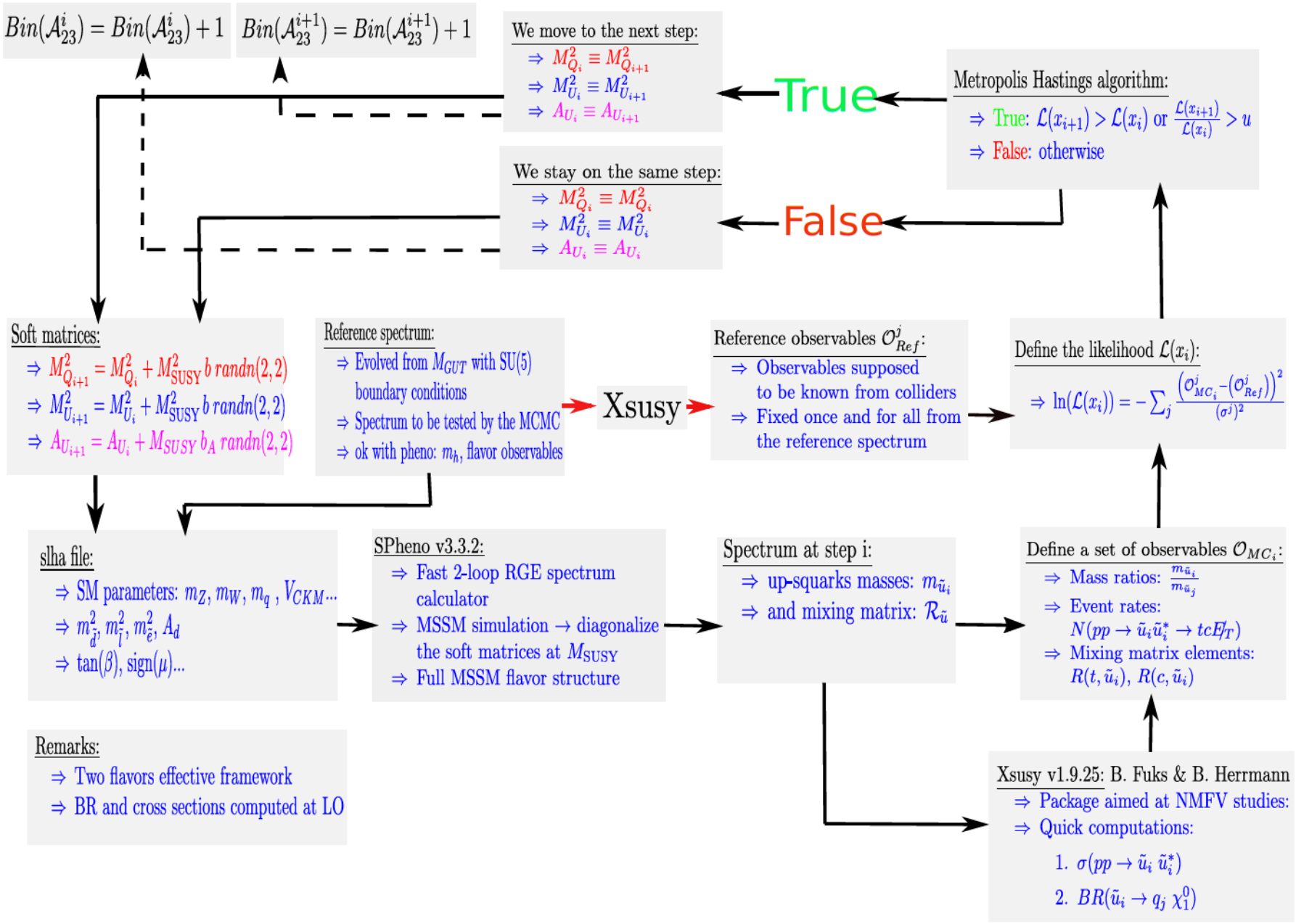

Figure 5.2 – MCMC algorithm used to compute the posterior PDF $p(\mathcal{A}_{23}|d, \mathcal{M}_1)$. $randn(n, m)$ generates a random matrix of size $n \times m$ with elements distributed according to a Gaussian distribution of mean 0 and unit standard deviation. The red arrows correspond to the initialization step (see step 0) which is only done once.

5.2.3 Tools

In this subsection, we would like to give a brief overview of the two main tools used in this analysis, `SPheno` and `XSUSY`.

5.2.3.1 SPheno

We start by describing `SPheno`. As already pointed out, `SPheno` is a fast spectrum calculator written in Fortran. `SPheno` computes low scale SUSY mass spectra from high scale boundary conditions on soft terms inspired by a variety of SUSY breaking mechanisms such as, gauge mediated SUSY breaking, anomaly mediated SUSY breaking, gravity mediated SUSY breaking and diverse models inspired from string theory.

To do so, it solves the MSSM RGEs at two loop orders to run the gauge and Yukawa couplings between $Q = m_Z$, the Z boson pole mass, and the high scale, which can either be fix or deduced from the requirement of the unification of the first two gauge couplings i.e. $g_1 = g_2$. At the high scale, the boundary conditions for the soft parameters are set, and the gauge and Yukawa couplings as well as the soft terms are then running down to the SUSY scale, which can be either user-defined or equal to $Q_{\text{SUSY}} = \sqrt{m_{\tilde{u}_1} m_{\tilde{u}_6}}$. Then, at Q_{SUSY}, the gauge and Yukawa couplings can be used as input, to compute the pole masses of SUSY particles at one loop. Note also that this procedure has to be repeated several times until the relative difference in the SUSY mass spectrum computed between two successive iterations decreases below a certain user-defined, precision threshold.

In our case, we were interested by directly computing the SUSY scale spectrum from boundary conditions on soft terms given at the same low-scale. It is possible to do so with `SPheno`, using a general MSSM simulation (see [91]). In this case, obviously, the running between the high and SUSY scales is skipped but, nonetheless the gauge and Yukawa couplings are running up between M_Z and M_{SUSY}, to compute $\tan\beta$ in a consistent manner.

Also, originally, `SPheno` was designed in its first versions to neglect flavor and CP violation in the soft sector, it is now able to properly take care of complex phases as well as mixing terms in the soft terms [91], allowing for phenomenological studies in a general flavor and CP violating MSSM.

`SPheno` can be freely downloaded in its most recent version on the following website [4].

5.2.3.2 XSUSY

`XSUSY` is a package, written in `C++`, aimed at phenomenological studies in the MSSM with general flavor violation. Given a low scale SUSY spectrum, it can compute fastly gaugino, squark, squark-antisquark pair production cross sections at a proton-proton collider such as the LHC. In addition, it can also compute squark, gluino, and gaugino decay branching ratios, all computations being done in a non-minimal flavor violating (NMFV) MSSM.

Very shortly, a new physics model is said to violate flavor in a non-minimal way when flavor-violating processes can occur through couplings not only related to the Yukawa couplings. Stated more formally, a NMFV model is a model in which the flavor group is not only broken by spurions [5] build out of Yukawa couplings.

In a NMFV-MSSM, obviously, the squark mass matrix $\mathcal{M}^2_{\tilde{u}}$ owns non-vanishing, non-diagonal flavor violating entries at the TeV scale. In the SCKM basis, if we note $(\mathcal{M}^2_{\tilde{u}})^{ab}_{ij}$ a generic element of the up-squark mass matrix where $a, b = L, R$ are chirality indices and $i, j = 1...6$ are generation indices, one can then parameterize these flavor violating entries, in a model independent way, with the following parameters:

$$\delta^{ab}_{ij} = \frac{(\mathcal{M}^2_{\tilde{u}})^{ab}_{ij}}{\sqrt{(\mathcal{M}^2_{\tilde{u}})^{aa}_{ii}(\mathcal{M}^2_{\tilde{u}})^{bb}_{jj}}} \tag{5.22}$$

[4] spheno.hepforge.org/

[5] We recall that the spurion method consists in promoting a coupling constant to a fictitious non-dynamical field whose charge is fixed such that the symmetry of interest, for example the flavor symmetry, is re-established in the Lagrangian [47]. The observed value of the coupling constant will then just be the VEV of the spurion. This method, even though looking quite abstract, is very useful to constrain the form of higher order operators in an effective theory context. For an example of the usefulness of the spurion method applied to flavor physics, see [169], [170].

$(M^2_{\mathbf{10}})_{ij}$		
$(10000)^2$	0	0
0	$(609)^2$	$(841)^2$
0	$(841)^2$	$(1564)^2$

$(M^2_{\bar{\mathbf{5}}})_{ij}$		
$(8600)^2$	0	0
0	$(1180)^2$	0
0	0	$(1317)^2$

$(A_u)_{ij}$		
0	0	0
0	0	-575
0	-575	-1055

$(A_d)_{ij}$		
0	0	0
0	0	0
0	0	-70

$M_{1/2} = 962$
$M^2_{H_{u,d}} = (1343)^2$
$\text{sign}(\mu) = +1$

Table 5.1 – Boundary conditions on soft parameters at $Q = M_{\text{GUT}}$ of our reference spectrum to be tested by the MCMCs. Masses and trilinear couplings are given in GeV.

normalized to the diagonal entries of the mass matrix. Note that despite the notation, the δ^{ab}_{ij}'s are not mass insertion parameters (see subsection 4.4.2), no approximation being made on the mass matrix, and in particular on its hierarchy.

Back to `XSUSY`, one important remark is that it is a leading order software, all cross sections and branching ratios computations being done at tree level.

All formulas of cross sections implemented in `XSUSY`, given as an expression of the parameters (5.22), can be found in [148].

Also, other packages to compute squark production cross sections in a NMFV-MSSM such as `WHIZARD` [171] exist, our experience though tends to show that `XSUSY` is the quickest, time optimization being important as a high number of points have to be sampled for the MCMCs to converge (see section 5.3).

Lastly to conclude we have to point out that, unfortunately to this day, XSUSY is not a public software. However, a copy can be easily obtained by sending an email to its main author, Benjamin Fuks [6].

5.3 Results

In this section we would like to describe the results we got, using the setup described in section 5.2. In subsection 5.3.1, we start by describing the reference spectrum used in this analysis. Then, in subsections 5.3.2-5.3.4, we describe three different cases we have considered, corresponding to three different sets of observables, as well as their associated results.

5.3.1 Reference scenarios

We start by the description of the reference spectrum. When we were looking for a TeV scale spectrum to test this setup, several criteria had to be fulfilled:

1. Obviously, our reference spectrum had to derive from $SU(5)$ symmetric boundary conditions at the GUT scale, as we want to use it to test the $SU(5)$ hypothesis at the TeV scale.

2. The reference spectrum needed to lead to relatively low masses for the first four up-type squarks $\tilde{u}_1, \cdots, \tilde{u}_4$ in order to get substantial squark/anti-squark production rates at the LHC 14 TeV.

3. Also, a relatively high mixing between the second and third generations needed to be present, in order for flavor violating branching ratios, such as $\text{BR}(\tilde{u}_2 \to t\, \tilde{\chi}_1)$, to be non-negligible, in order to not suppress too strongly the different even rates defined in subsections 5.3.2-5.3.4.

4. As already stated, we are working in the context of the Top-Charm SUSY framework of section 4.7. Hence, we wanted the first generation to be much heavier than the first two ones.

[6] fuks@lpthe.jussieu.fr

5. Finally, obviously, we wanted our reference spectrum to pass the different flavor constraints of table 4.2, and also we wanted it to give a Higgs sufficiently heavy to agree with the ATLAS and CMS measurements.

In fact, when we were looking for a reference spectrum, we had to face a balance between different effects. On one hand, we wanted at the same time an up-squark spectrum as light as possible -in particular to get a Higgs boson heavy enough- and mixing terms as high as possible in order to get substantial flavor changing branching ratios. On the other hand, the flavor constraints tend to prefer a relatively heavy squark spectrum with near diagonal soft terms, but then the Higgs can become quickly too light compared to its experimental value, and the squark production cross sections too low to get a substantial statistic.

Finally, the best compromise we found is summarized in table 5.1. This table lists the GUT scale boundary conditions leading to a TeV scale spectrum satisfying the different constraints of list 5.3.1. When these are evolved down to $Q = 1$ TeV using `SPheno`, it leads to:

1. a relatively light squark spectrum for the first two generations. Indeed, we have $m_{\tilde{u}_1} = 1.15$ TeV and $m_{\tilde{u}_4} = 1.79$ TeV.

2. a first generation which is decoupled since we have $m_{\tilde{u}_5}, m_{\tilde{u}_6} \sim 10$ TeV. Thus, we made sure that the contributions to the TeV scale observables of these states are very low.

3. production cross sections relatively low, for example we have $\sigma(\text{pp} \to \tilde{u}_1\tilde{u}_1^*) = 1.7$ fb, and $\sigma(\text{pp} \to \tilde{u}_4\tilde{u}_4^*) = 0.04$ fb.

4. on the other hand, due to the high mixing, these cross section values are compensated by the decay branching ratios, in the channels of interest (see subsections 5.3.2-5.3.4), for example one has $\text{BR}(\tilde{u}_1 \to t\,\tilde{\chi}_1) = 80\%$ and $\text{BR}(\tilde{u}_1 \to c\,\tilde{\chi}_1) = 6\%$.

5. A spectrum which is in good agreement with phenomenology. For instance, one has $\Delta M_{B_s} = 17.5\ \text{ps}^{-1}$, $\text{BR}(B_s \to \mu\,\mu) = 2.88 \cdot 10^{-9}$. Note that we have $m_h = 122$ GeV, thus the Higgs boson is quite light but nonetheless in agreement with the ATLAS and CMS values if we accept a theoretical uncertainty of ± 3 GeV.

We have also defined a counter-example to test the efficiency of this setup in case the spectrum does not originate from $SU(5)$ symmetric boundary conditions. To do so, we started from the spectrum obtained from tab. 5.1 upon which we have imposed:

$$(A_U)_{23} = -(A_U)_{32} \text{ at Q= 1 TeV}, \tag{5.23}$$

corresponding to a maximally asymmetric situation. We shall note the SDDR associated to this counter-example S_c.

5.3.2 Case I

We are now in a position to apply the setup discussed in section 5.2 to the first example we have considered. Let us define the following TeV scale event rates:

1. $\underline{N_{tt}}$: The event rate associated to a di-top production plus missing transverse energy, through on-shell squark resonances i.e. N_{tt} is defined as:

$$N_{tt} \equiv N(\text{p p} \to \tilde{u}_i\tilde{u}_i^* \to t\,\bar{t}\,\not{E}_T) \tag{5.24}$$

$$= \mathcal{L}\sum_{i=1}^{4} \sigma_{\tilde{u}_i\tilde{u}_i^*}\text{BR}(\tilde{u}_i \to t\tilde{\chi}_1^0)^2. \tag{5.25}$$

where $\mathcal{L}$ is the integrated luminosity and $\sigma_{\tilde{u}_i\tilde{u}_i^*} = \sigma(\text{pp} \to \tilde{u}_i\tilde{u}_i^*)$ is the squark/anti-squark production cross sections computed with `XSUSY` with $\tilde{u}_1 \cdots \tilde{u}_4$ the four active mass eigenstates.

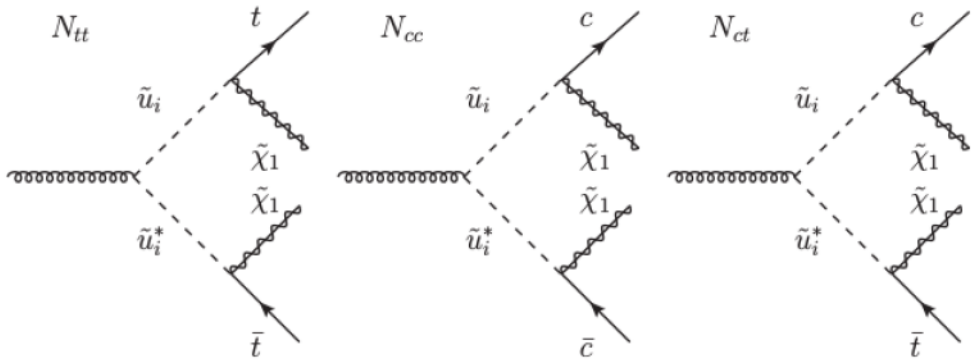

Figure 5.3 – Contributions to the different event rates defined in equations (5.24)-(5.28).

2. N_{cc}: The event rate associated to a di-charm production plus $\not{E}_T$, hence N_{cc} is defined as:

$$N_{cc} \equiv N(\mathrm{p\,p} \to \tilde{u}_i \tilde{u}_i^* \to c\,\bar{c}\,\not{E}_T) \tag{5.26}$$

$$= \mathcal{L} \sum_{i=1}^{4} \sigma_{\tilde{u}_i \tilde{u}_i^*} \mathrm{BR}(\tilde{u}_i \to c\tilde{\chi}_1^0)^2. \tag{5.27}$$

3. N_{ct}: The event rate associated to a charm and a top production, hence N_{ct} is defined as:

$$N_{ct} \equiv N(\mathrm{p\,p} \to \tilde{u}_i \tilde{u}_i^* \to c\,\bar{t}\,\not{E}_T) \tag{5.28}$$

$$= 2\mathcal{L} \sum_{i=1}^{4} \sigma_{\tilde{u}_i \tilde{u}_i^*} \mathrm{BR}(\tilde{u}_i \to c\tilde{\chi}_1^0) \mathrm{BR}(\tilde{u}_i \to t\tilde{\chi}_1^0). \tag{5.29}$$

Here, we are applying this analysis to the LHC and we have fixed $\sqrt{s}$, the proton-proton center of mass energy, to 14 TeV with an integrated luminosity of $\mathcal{L} = 300$ fb^{-1}. This typically gives for our reference spectrum, $N_{tt} = 328$, $N_{cc} = 51$ and $N_{ct} = 26$ events.

Feynman diagrams contributing to these different event rates are represented in figure 5.3.

We can now define the two ratios:

$$\frac{N_{cc}}{N_{tt}}, \quad \frac{N_{ct}}{N_{tt}} \tag{5.30}$$

which are the first two observables we consider here.

We still need to define the error on the event rate ratios (5.30). Generically, one can show from the Fieller-Hinkley distribution (see [125]) that the error on the ratio of two gaussian distributed even rates N_1/N_2 is, in the limit of large N_1, N_2, equal to:

$$\sigma_N^2 \equiv \frac{N_1^2}{N_2^3} - \frac{N_1}{N_2^2}. \tag{5.31}$$

This is the error we associate to the ratios (5.30) and typically, for our reference spectrum, using the numbers mentioned above, one has $\sigma_N(N_{ct}/N_{tt}) \sim 3\%$ and $\sigma_N(N_{cc}/N_{tt}) \sim 6\%$.

The third observable that we have taken into account is simply the mass ratio of the first two squarks:

$$\frac{m_{\tilde{u}_1}}{m_{\tilde{u}_2}} \tag{5.32}$$

where we have considered that this ratio was measured with an uncertainty of $\sigma = 10\%$ and which can be accessed, for example at the LHC, through kinematical edges in mass invariant distributions [172].

Finally, we have also defined a certain number of observables linked to the up-squark rotation matrix $\mathcal{R}_{\tilde{u}}$. If we note $\mathcal{R}_{\tilde{u}_i\tilde{q}_a}$ the flavor content of the interaction eigenstate $\tilde{q}_a$ in the mass eigenstate $\tilde{u}_i$ expressed in the SCKM basis, for instance $\mathcal{R}_{\tilde{u}_1\tilde{t}_L} \equiv (\mathcal{R}_{\tilde{u}})_{13}$, we can define the following ratios of mixing matrix elements:

$$\frac{\mathcal{R}_{\tilde{u}_1\tilde{t}_L}}{\mathcal{R}_{\tilde{u}_1\tilde{t}_R}}, \quad \frac{\mathcal{R}_{\tilde{u}_1\tilde{c}_L}}{\mathcal{R}_{\tilde{u}_1\tilde{c}_R}} \tag{5.33}$$

corresponding to the ratio of the left and right stop and scharm flavor content in the first mass eigenstate $\tilde{u}_1$.

The results from the MCMC simulation obtained after ~ 500000 iterations (see fig. 5.2) with the likelihood function (5.19) constrained by the observables (5.30), (5.32) and (5.33) are presented in figure 5.6. The left plot of fig. 5.6 is the simulated posterior $p(\mathcal{A}_{23}|d, \mathcal{M}_1)$ obtained using our reference scenario of tab. 5.1. The right plot is the posterior obtained imposing a maximally asymmetric trilinear coupling at $Q = 1$ TeV (see eq. (5.23)).

Computing the ratio of the posterior both for our reference spectrum and counter-example, normalized to the prior PDF (represented in figure 5.7) at $\mathcal{A}_{23} = 0$, one can deduce the SDDR (see eq. (5.17)) values S (reference spectrum) and S_c (counter-example) :

$$\underline{\text{Case I:}}\ S = 1.50,\ S_c = 1.00 \tag{5.34}$$

Comparing these values to the Jeffrey scale of tab. 5.1 clearly indicate that this set of observables does not allow to draw any conclusion for/against the $SU(5)$ hypothesis (i.e. the model $\mathcal{M}_0$ in eq. (5.15)), both tests being absolutely inconclusive.

In fact, the problem arises because we have taken only ratios of event rates, thus canceling most of the dependency of these observables with respect to the elements of the up-type trilinear coupling matrix $(A_U)_{23}$ and $(A_U)_{32}$.

Thus, these ratios do not constraint efficiently enough the posterior PDF for the SDDR to cross the different thresholds of evidence of the Jeffrey scale. In particular, to be decisive, observables need to constrain the posterior PDF so that it is highly peaked either on zero, resulting in an evidence for the $SU(5)$ hypothesis, or on a value sufficiently away from zero, to lead to an evidence against the $SU(5)$ hypothesis.

As an illustration, the figure 5.4 shows the dependency of both N_{ct} and N_{ct}/N_{tt} over the trilinear coupling matrix elements $(A_U)_{23}$ and $(A_U)_{32}$.

On the other hand, the event rates depend crucially of the up-type squark mass spectrum and, in particular of the soft mass matrices upon which the random walk is performed. Hence, we can expect a high variability of N_{tt}, N_{cc} and N_{ct} when we take a jump on the Markov chain (see eq. (5.21)).

This results that if these event rates are directly inputted in the likelihood function (5.19)-(5.20), the acceptance rate of the Metropolis-Hasting algorithm decreases dramatically.

One way to offset this drop is to considerably reduce the step size of the jump (fixed by the parameters b and b_A see tab. 5.2). But if we do so, we explore a much more narrow portion of the parameter space, which will make the MCMC converge much more slowly. Hence, a compromise has to be found between acceptance rate and exploration depth.

In any case, we are still trying to optimize the free parameters of the chain, in particular the values of the parameters b and b_A, to be able to both include directly the event rates N_{tt}, N_{cc} and N_{ct} in the analysis and to maintain an acceptable acceptance rate on the chain.

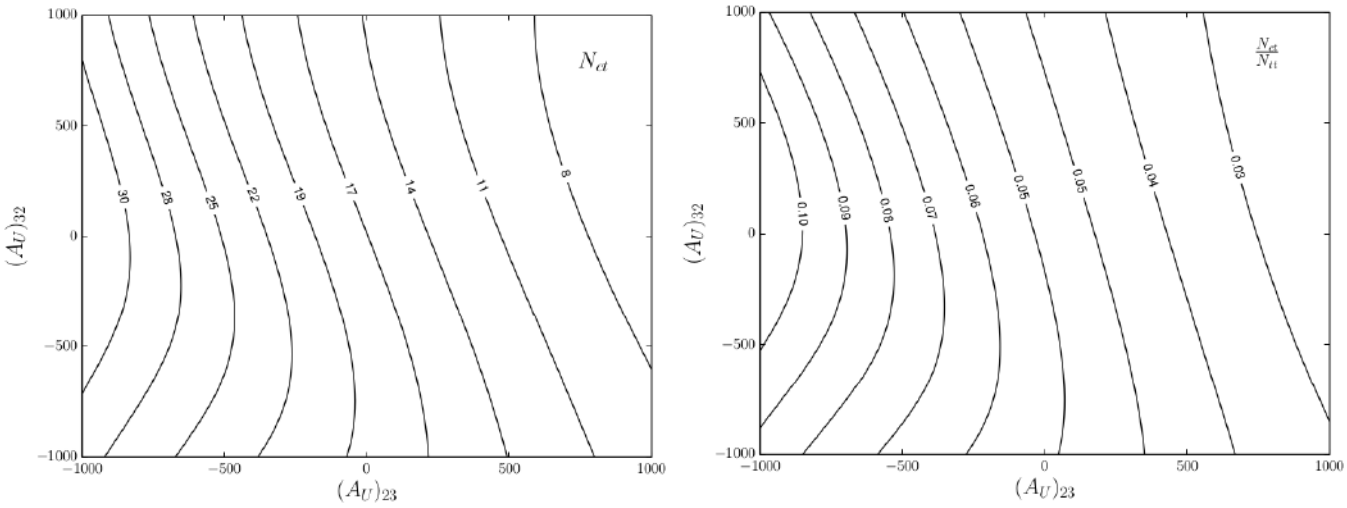

Figure 5.4 – Left: Dependance of the event rate N_{ct} as a function of the trilinear couplings $(A_U)_{23}$ and $(A_U)_{32}$ given at $Q = 1$ TeV. Right: Dependance of the ratio N_{ct}/N_{tt}. The integrated luminosity is fixed to $\mathcal{L} = 300$ fb^{-1}.

5.3.3 Case II

The second case that we have analyzed is the following. We are still considering that the event rate ratios of eq. (5.30) are known as well as the mass ratio (5.32) but, we are now considering that the full flavor decomposition of the first two mass eigenstates is known, i.e. we are assuming that the following mixing matrix elements have been measured at the LHC:

$$\begin{aligned} &\mathcal{R}_{\tilde{u}_1\tilde{t}_L}, \mathcal{R}_{\tilde{u}_1\tilde{t}_R}, \mathcal{R}_{\tilde{u}_1\tilde{c}_L}, \mathcal{R}_{\tilde{u}_1\tilde{c}_R} \\ &\mathcal{R}_{\tilde{u}_2\tilde{t}_L}, \mathcal{R}_{\tilde{u}_2\tilde{t}_R}, \mathcal{R}_{\tilde{u}_2\tilde{c}_L}, \mathcal{R}_{\tilde{u}_2\tilde{c}_R} \end{aligned} \tag{5.35}$$

with a relative error of $\sigma \sim 10\%$ each. These matrix elements can be measured by for example combining different branching ratio measurements in exclusive squark decay channels. Note that both top and charm polarimetry should be available to access to the flavor decomposition (5.35) of the mass eigenstates $\tilde{u}_1$ and $\tilde{u}_2$.

However, even though we gave arguments in the previous chapter, to be optimistic about the possibilities of accessing the chirality of the top at the LHC (see subsection 4.6.2 and references [128]), the prospects for measuring the chirality of a charm seem quite limited at a proton proton collider, in particular due to its relatively low mass compared to the top, the charm hadronizes fastly, which complicates the reconstruction of angular distributions.

So, in the context of LHC physics, the case developed in this subsection should be seen as relatively unrealistic and is done for illustration purposes, at least, as long as techniques to tag the chirality of a charm will not be developed.

In any case, taking the mixing matrix elements separately raises the time of convergence of the MCMC compared to subsection 5.3.2 and approximately 8.10^5 points needs to be sampled so that the posterior PDF converge to an acceptable level.

The results are presented in figure 5.8 where, as in figure 5.6, the left plot is the simulated posterior using our reference spectrum and the right plot is the simulated posterior imposing a maximally asymmetric trilinear coupling at the TeV scale (see eq. (5.23)).

From these PDFs, using the prior fig. 5.7, one can compute the values of the SDDR S and S_c:

$$\underline{\text{Case II:}}\ S = 1.85, \quad S_c = 0.25 \tag{5.36}$$

Looking at eq. (5.36), and at the Jeffrey scale tab. 5.1, one can deduce that a value of $S = 1.85$ is not high enough to support the $SU(5)$ hypothesis, even with weak evidence.

N_{bins}	$\mathcal{A}_1$	$\mathcal{A}_{N_{\text{bins}}}$
40	-2	2

M_{SUSY}	b	b_A
1600 GeV	0.06	0.20

N_{burn}
5000

Table 5.2 – Free parameters of the MCMCs. The left table represents the characteristics of the histogram used to evaluate the PDFs (see remark 7). The centered table represents the free parameters linked to step 3: M_{SUSY} is a scale fixing the overall scale of the soft matrices sampled, b and b_A are parameters setting the relative size of the jump in the soft mass terms and trilinear couplings directions, respectively. Finally, in the right table N_{burn} is the number of points which is discarded at the beginning of the MCMC, before the histogram starts to be filled.

On the other hand, the counter-example SDDR is equal to $S_c = 0.25 < 1/3$ and indicates, according to the Jeffrey scale, that the $SU(5)$ hypothesis is disfavored with a weak evidence.

Thus, in this Bayesian setup, should SUSY be realized in nature, counting the event rate ratios (5.30) and assuming that one has access to the mass ratio $m_{\tilde{u}_1}/m_{\tilde{u}_2}$ and to the different mixing matrix elements (5.35), could allow to exclude (weakly) the high scale $SU(5)$ hypothesis, if the up-type trilinear coupling matrix turned out to present a high asymmetry.

5.3.4 Case III

Finally, the last case that we have considered is the following. We are assuming that the same set of observables that in subsection 5.3.3 has been accessed experimentally, but our aim here, is to test this setup in a *limit case*, where all uncertainties have been shrunk to $\mathcal{O}(1\%)$. To do so, we are also assuming that an integrated luminosity of $\mathcal{L} = 3000$ fb^{-1} is available, corresponding to a high luminosity LHC.

As we are still considering ratios of event rates, the luminosity upgrade leaves them invariant. But, changing the luminosity does have an effect on the statistical uncertainty of these ratios (5.31), as they scale as $\propto 1/N$. Typically, for our reference spectrum, upgrading the luminosity to $\mathcal{L} = 3000$ fb^{-1} reduces the uncertainties by one order of magnitude, and one has $\sigma_N(N_{ct}/N_{tt}) \sim 0.3\%$ and $\sigma_N(N_{cc}/N_{tt}) \sim 0.6\%$.

Note also that taking such small uncertainties considerably raises the time of convergence of the MCMC, the likelihood function being highly peaked (see eq. (5.19)), since now approximately 1.6×10^6 points need to be sampled for the posterior PDF to converge to an acceptable level.

The results are presented in figure 5.9. From this figure, and the prior fig.5.7, one can deduce the values of the tests S and S_c:

$$\underline{\text{Case III:}}\ \ S = 3.05, \qquad S_c = 0.03 \tag{5.37}$$

From eq. (5.37), one sees that this time both tests are decisive. Indeed, using our reference spectrum, which derives from $SU(5)$ symmetric boundary conditions, leads to $S = 3.05 > 3$ which indicates a weak evidence for the $SU(5)$ hypothesis. On the other hand, imposing a maximally asymmetric trilinear coupling at the TeV scale (see eq. (5.23)), leads to a test $S_c = 0.03$, and as $S_c < 1/12$ (see tab. 5.1), it indicates a moderate evidence against the $SU(5)$ hypothesis.

We hence see that it is possible to cross a threshold of evidence in the Jeffrey scale, i.e. to go from inconclusive to weak evidence or from weak to moderate evidence, at the cost of drastically reducing the uncertainties attached to the observables inputted in the likelihood function.

It should be also clear now, that this MCMC allows more easily to exclude the $SU(5)$ hypothesis than to confirm it, a high asymmetry in the trilinear coupling A_U shifting the posterior PDF (fig. 5.9) sufficiently away from zero for the SDDR S_c to be small enough to point against the $SU(5)$ hypothesis.

Table 5.5 gives a summary of the results obtained using the simulation of fig. 5.2 with the three different cases discussed in this section.

Again, we insist on the fact that these results should still be seen as preliminary, different aspects of the MCMC being still tested. However, the fact that we managed to compute SDDRs which point against the $SU(5)$ hypothesis, even with a weak evidence, is promising and we expect that, once the analysis will be refined, in particular to include more observables in the likelihood function, for example heavier squark masses, or multiple squark decay branching ratios, this analysis will be able to exhibit

its full potential, in particular to exclude the $SU(5)$ hypothesis when the low scale asymmetry $\mathcal{A}_{23}$ is high.

Case I	Case II	Case III
$\mathcal{L} = 300$ fb^{-1}		$\mathcal{L} = 3000$ fb^{-1}
$\frac{m_{\tilde{u}_1}}{m_{\tilde{u}_2}}$ $(\sigma = 5\%)$	$\frac{m_{\tilde{u}_1}}{m_{\tilde{u}_2}}$ $(\sigma = 5\%)$	$\frac{m_{\tilde{u}_1}}{m_{\tilde{u}_2}}$ $(\sigma = 1\%)$
$\frac{N_{cc}}{N_{tt}}$ $(\sigma = \sigma_N)$	$\frac{N_{cc}}{N_{tt}}$ $(\sigma = \sigma_N)$	$\frac{N_{cc}}{N_{tt}}$ $(\sigma = \sigma_N)$
$\frac{N_{ct}}{N_{tt}}$ $(\sigma = \sigma_N)$	$\frac{N_{ct}}{N_{tt}}$ $(\sigma = \sigma_N)$	$\frac{N_{ct}}{N_{tt}}$ $(\sigma = \sigma_N)$
$\frac{\mathcal{R}_{\tilde{u}_1\tilde{t}_L}}{\mathcal{R}_{\tilde{u}_1\tilde{t}_R}}$ $(\sigma = 10\%)$	$\mathcal{R}_{\tilde{u}_1\tilde{t}_L}, \mathcal{R}_{\tilde{u}_1\tilde{t}_R}$ $(\sigma = 10\%)$	$\mathcal{R}_{\tilde{u}_1\tilde{t}_L}, \mathcal{R}_{\tilde{u}_1\tilde{t}_R}$ $(\sigma = 1\%)$
$\frac{\mathcal{R}_{\tilde{u}_1\tilde{c}_L}}{\mathcal{R}_{\tilde{u}_1\tilde{c}_R}}$ $(\sigma = 10\%)$	$\mathcal{R}_{\tilde{u}_1\tilde{c}_L}, \mathcal{R}_{\tilde{u}_1\tilde{c}_R}$ $(\sigma = 10\%)$	$\mathcal{R}_{\tilde{u}_1\tilde{c}_L}, \mathcal{R}_{\tilde{u}_1\tilde{c}_R}$ $(\sigma = 1\%)$
	$\mathcal{R}_{\tilde{u}_2\tilde{t}_L}$, $\mathcal{R}_{\tilde{u}_2\tilde{t}_R}$ $(\sigma = 10\%)$	$\mathcal{R}_{\tilde{u}_2\tilde{t}_L}, \mathcal{R}_{\tilde{u}_2\tilde{t}_R}$ $(\sigma = 1\%)$
	$\mathcal{R}_{\tilde{u}_2\tilde{c}_L}$, $\mathcal{R}_{\tilde{u}_2\tilde{c}_R}$ $(\sigma = 10\%)$	$\mathcal{R}_{\tilde{u}_2\tilde{c}_L}, \mathcal{R}_{\tilde{u}_2\tilde{c}_R}$ $(\sigma = 1\%)$
$S = 1.50$, $S_c = 1.00$	$S = 1.85$, $S_c = 0.25$	$S = 3.06$, $S_c = 0.03$

Figure 5.5 – Summary table of the different obervables taken into account in the three different cases discussed in this section. The associated errors, given in percents, are indicated in parenthesis. σ_N is the error on a ratio of event rates, and is defined in the text (see eq. (5.31)). The last line summarizes the SDDR obtained both for our reference spectrum noted S (see tab. 5.1) and our counter-example, noted S_c (see eq. (5.23)).

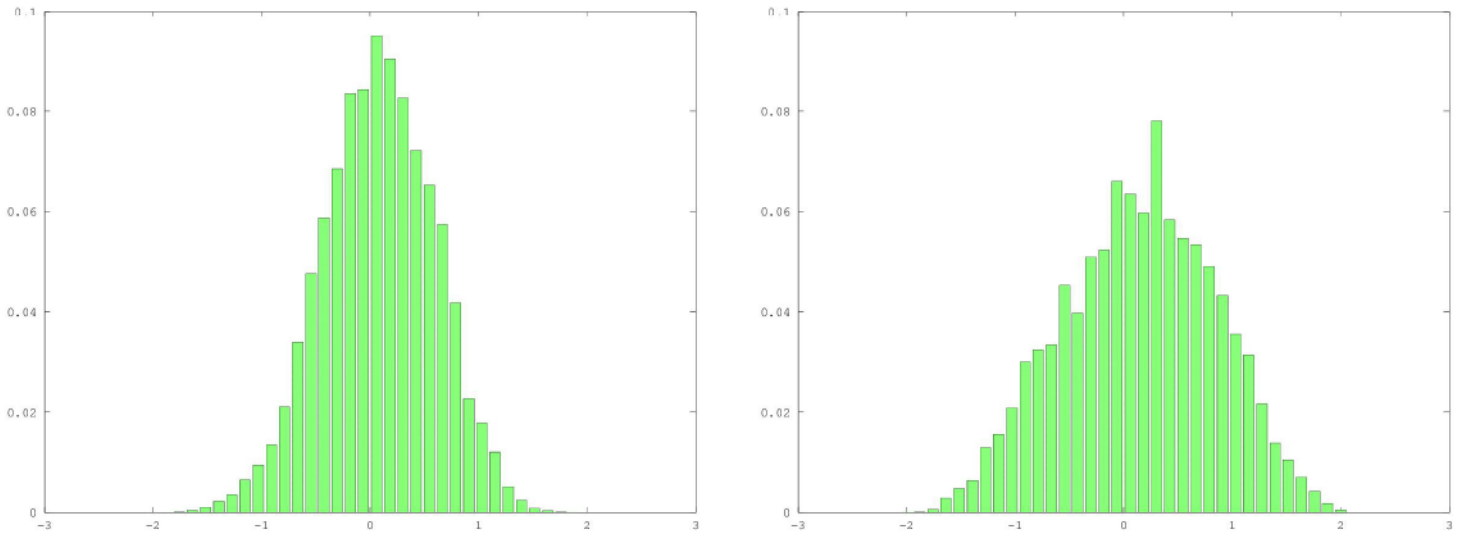

Figure 5.6 – Left: Posterior PDF $p(\mathcal{A}_{23}|d, \mathcal{M}_1)_{\text{Case I}}$ obtained from the MCMC simulation in the case I (see first column of tab. 5.5) for the reference spectrum. Right: Posterior PDF obtained in the case I with a maximally asymmetric trilinear coupling enforced at $Q = 1$ TeV (see counter-example eq. (5.23)). The SDDR obtained are $S = 1.50$ (reference spectrum) and $S_c = 1.00$ (counter-example).

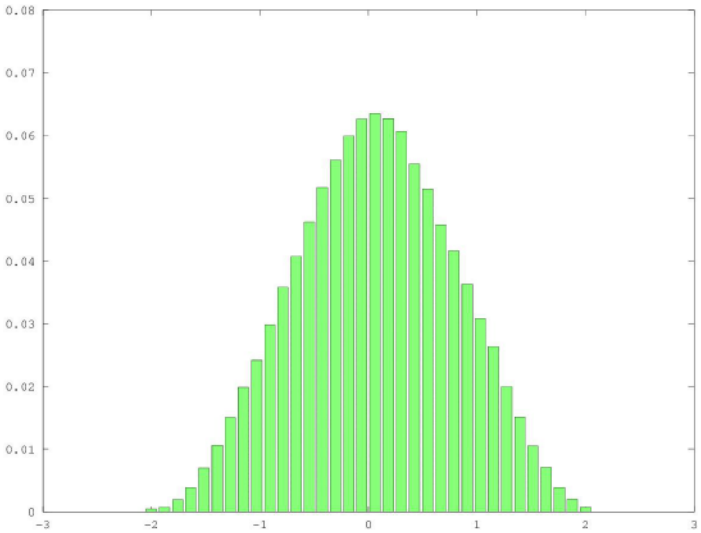

Figure 5.7 – Prior PDF $p(\mathcal{A}_{23}|\mathcal{M}_1)$ obtained from the MCMC simulation.

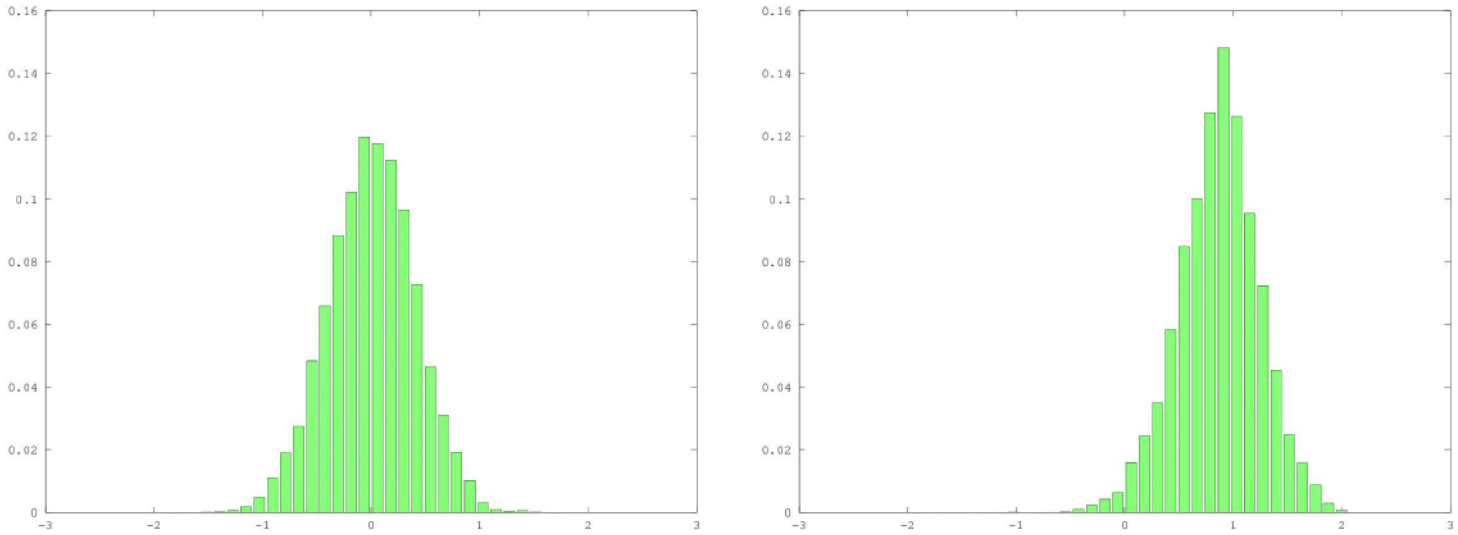

Figure 5.8 – Same as figure 5.6 for the case II (see second column of tab. 5.5) . The SDDR obtained are $S = 1.85$ and $S_c = 0.25$.

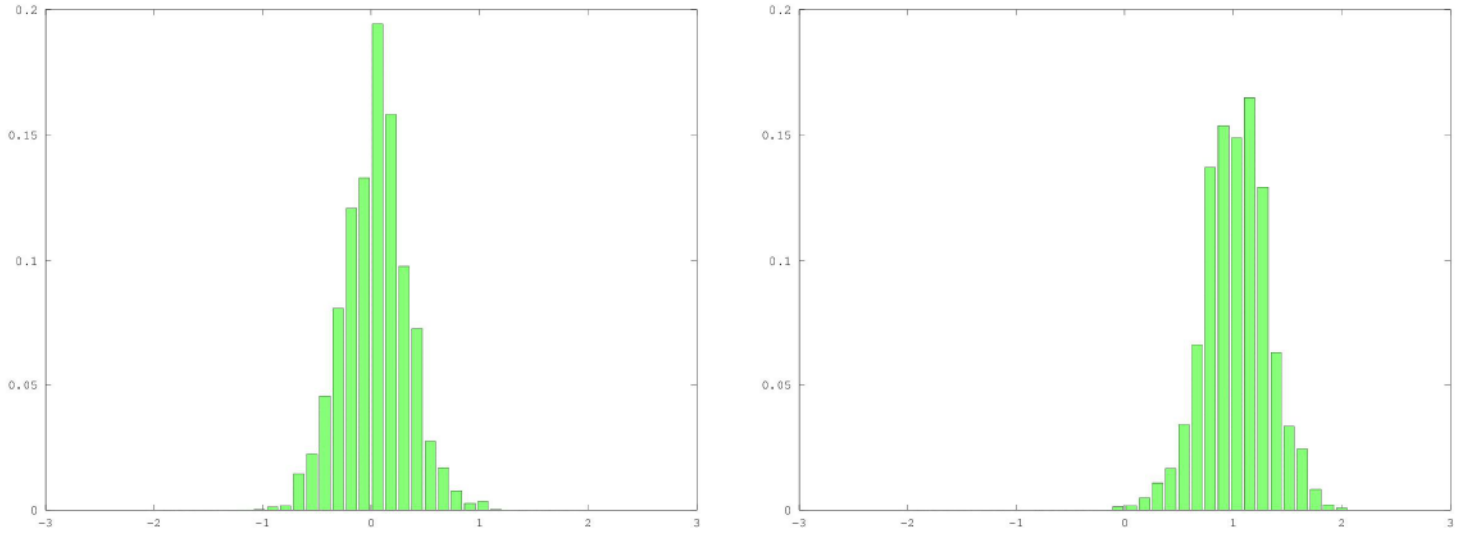

Figure 5.9 – Same as figure 5.6 for the case III (see third column of tab. 5.5) . The SDDR obtained are $S = 3.06$ and $S_c = 0.03$.

Conclusion

Supersymmetry stays among the best motivated frameworks to extend the Standard Model. In particular, its simple realizations (MSSM, NMSSM), allow to solve almost all questions unanswered by the Standard Model. Beside, when SUSY is embedded in a grand unified theory, the high number of free parameters introduced by the SUSY soft sector gets drastically reduced. The simplest SUSY/GUT models are based on the $SU(5)$ Lie group. As such, these models have received a lot of attention during the last decades. However, most studies seemed to focus mainly on the quark-lepton unification in the Yukawa sector.

In this thesis, we have taken advantage of the stability of the up-squark soft sector between the GUT and the TeV scales to build different low scale phenomenological tests on $SU(5)$ SUSY/GUT models. In chapter 5, we started by testing the stability of two GUT scale $SU(5)$ symmetry relations, $A_U = A_U^T$ and $M_Q^2 = M_U^2$ when these are running down to the TeV scale. These two relations seem well preserved by quantum corrections, the TeV scale asymmetries in both sectors staying at the maximum of the order of $\mathcal{O}(5)\%$. We have then explored the possibilities offered by these relations to build tests of the $SU(5)$ hypothesis within three different kind of SUSY spectra, well motivated by phenomenology.

In section 4.5, we started by investigating "Heavy SUSY" spectra, which feature a SUSY breaking scale well beyond the electroweak scale. A-priori, these spectra destabilize the electroweak scale and play against the MSSM as a solution to the hierarchy problem. However, we have mentioned studies that show that in certain circumstances SUSY spectra can accommodate a heavy breaking scale while still maintaining a Higgs boson at 125 GeV with moderate fine-tuning ([126] [127]).

In this framework, we managed to exhibit $SU(5)$ tests relying on the measurement of SUSY-dipole induced processes. Unfortunately, the current sensitivities of experiments to these effective operators seem too low for the tests to be determinant, even if, processes occurring via proton-proton collisions at large impact parameter -the ultra-peripheral collisions- might provide a way out.

In section 4.6, spectra featuring a light third scalar generation have been investigated. These spectra are called "natural" as they automatically stabilize the electroweak scale. In this context, we managed to exhibit two relations among low scale event rates, or among forward-backward asymmetries, depending on the exact mass ordering of the spectrum. When the stops are heavier than the wino and the bino, a leading order relation (relatively to the EFT developed in subsubsection 4.4.1.3), can be found, which assumes that a certain fraction of jets can be charm tagged at colliders. When one of the gaugino is heavier than the stops, the EFT expansion needs to be pushed at next-to-leading order where in the limit of the $SU(5)$ hypothesis, the coupling between the stops and the gauginos is symmetric. It is then possible to build $SU(5)$ tests relying on top polarimetry. For these tests, one needs typically 589 events in the channels of interest to assess a deviation of the test relation with a level of significance of 3σ where in comparison, if $m_{\tilde{t}} \sim 1$ TeV, about 2580 events are expected at the LHC with an integrated luminosity of 300 fb^{-1}.

Lastly, we have considered spectra which feature a large mixing between the second and third generation of scalar. In this "Top-Charm" SUSY framework, we managed to build tests with again, two typical mass ordering considered. In the case of a compressed spectrum, with the stops and scharms almost degenerate, it is possible to build $SU(5)$ tests relying on Higgs detection in squark cascade decays. Typically, about 144 events are needed then to assess a deviation of the test relation with a precision of 50% at a level of significance of 3σ. If only the scharms are nearly degenerate, a test can also be worked out, which depends on properly normalized event rates, and typically requires only 20 events to probe the test relation with a precision of 50%.

Finally, in chapter 5, we have used Bayesian model comparison methods to perform a numerical

analysis using a Markov Chain Monte Carlo algorithm. This analysis assume that some information have been collected on the up-squark spectrum at colliders, through the measurement of certain observables, such as event rates, squark masses, or elements of the squark mixing matrix. It is then possible to build Gaussian likelihood functions with these observables to set up a Markov Chain whose target distributions are the posterior probabilities. One can then deduce Bayes factors to test the possible presence of remnants of the $SU(5)$ unification in the low scale up-type trilinear coupling. We have applied this analysis to several sets of observables, both for an integrated luminosity of 300 fb^{-1} and of 3000 fb^{-1}, and have presented the associated preliminary results. Typically, the observables we have considered do not constrain the posterior probabilities enough for the Bayes factors to support the $SU(5)$ hypothesis, unless the uncertainties attached to these observables are shrunk to $\mathcal{O}(1\%)$. However, even with uncertainties of $\mathcal{O}(10\%)$, if enough information are available on the squark rotation matrix, it is possible to get a weak evidence against the $SU(5)$ hypothesis when a large asymmetry is enforced on the trilinear coupling matrix at the TeV scale. The preliminary conclusion is then, that this analysis seems to show its full potential when it is used to reject the $SU(5)$ hypothesis, using it to confirm the presence of a high scale unification appearing as more difficult.

Outlooks

I mainly see four outlooks, to continue the work developed in this thesis.

First, the MCMC analysis of chapter 5 still needs to be optimized, in particular the step size on the Markov Chain should be adjusted to lead to an optimal acceptance rate, while still exploring a sufficiently large portion of soft matrices parameter space. This optimization should allow in the medium-term, to include more observables in the analysis, in particular individual squark masses and decay branching ratios, thus allowing to constrain the posterior probabilities more efficiently.

Second, all the work developed in this thesis have been done under the assumption of a desert between the TeV and GUT scales. It should be interesting to extend this work to the case the $SU(5)$ symmetry is not realized at the GUT scale, but at an intermediate scale. For example, if the grand unified group consists of $SO(10)$, the breaking chain toward the SM gauge group might involve an intermediate $SU(5)$ symmetry. In such cases, extra-degrees of freedom, arising from the extended GUT representations might exist between the two scales, it should be then interesting to study their impact on the running of the two $SU(5)$ symmetry relations we were interested in.

Third of course, all the tests which have been developed in this thesis also hold when the GUT scale is symmetric under a GU group containing $SU(5)$ as a subgroup. Hence, the different tests worked out here can be straightforwardly extended in case of a $SO(10)$ SUSY/GUT theory which add only a right-handed neutrino in its matter content compared to $SU(5)$. Note however that extending the GU group beyond $SO(10)$, for instance to $E(6)$, would generally introduce new flavoured d.o.fs such as the so-called leptoquarks or un-higgs (see [31],[173, 174]) potentially feeding the RGEs of the soft terms. One can then ask to what extent the GUT scale symmetry relations we have considered in this work are spoiled by these new degrees of freedoms and if our low scale tests can still be carried out in such a context.

Finally, and perhaps more importantly, one should definitely perform an extended collider analysis, using Monte Carlo generators, to simulate the expected sensitivities to charm tagging and top polarimetry in the channels we used to build our tests, taking into account the different sources of background. Indeed, as all tests developed in chapter 4 rely on one of these two techniques, it is crucial to have a more quantitative idea of the expected sensitivities of the current detectors.

Conclusion en français

La supersymétrie reste un des meilleurs candidats de théorie de nouvelle physique au-delà du modèle standard. En particulier, ses réalisations simples (MSSM, NMSSM), résolvent presque toutes les questions laissées sans réponse par le modèle standard. De plus, lorsque la SUSY est plongée dans une théorie de grande unification, les nombreux paramètres libres du secteur doux se retrouvent réduit à quelques uns seulement. Parmi les modèles SUSY/GUT, ceux basés sur le groupe de Lie $SU(5)$ sont les plus simples. En tant que tels, ces modèles ont reçu beaucoup d'attention au cours des dernières décennies. Cependant, la plupart des études semblent s'être principalement concentrées sur l'unification quark-lepton dans le secteur de Yukawa.

Dans cette thèse, nous avons profité de la stabilité du secteur doux des squarks hauts entre l'échelle GUT et l'échelle du TeV pour construire différents tests phénoménologiques des modèles $SU(5)$ SUSY/GUT. Dans le chapitre 5, nous avons commencé par tester la stabilité de deux relations de symétrie réalisées à haute énergie dans les modèles $SU(5)$, à savoir $A_U = A_U^T$ et $M_Q^2 = M_U^2$, lorsque celles-ci sont évoluées vers l'échelle du TeV.

Ces deux relations semblent bien préservées par les corrections quantiques, les asymétries à l'échelle du TeV dans les deux secteurs restant au maximum de l'ordre de $\mathcal{O}(5)\%$. Nous avons ensuite utilisé la stabilité sous les RGEs de ces relations afin de construire des tests de l'hypothèse $SU(5)$ en considérant trois sortes de spectre SUSY différents, tous motivés par la phénoménologie.

Dans la section 4.5, nous commençâmes par investir les spectres "SUSY lourds", dont l'échelle de brisure de la supersymétrie se situe bien au-delà de l'échelle électrofaible. A-priori, ces spectres déstabilisent l'échelle électrofaible et semblent remettre en question la viabilité du MSSM comme solution du problème de la hiérarchie de jauge. Cependant, nous avons mentionné plusieurs études qui montrent que dans certaines circonstances ces spectres peuvent s'accommoder d'une échelle de brisure haute tout en maintenant un boson de Higgs à 125 GeV avec un ajustement fin modéré.

Dans ce contexte, nous avons réussi à exhiber des tests $SU(5)$ via des processus induits par des opérateurs dipolaires supersymétriques. Malheureusement à l'heure actuelle, les sensibilités des détecteurs semblent trop basses pour que ces tests puissent être déterminants même si, des collisions proton-proton à haut paramètre d'impact (les collisions ultra-périphériques) pourraient être utilisées pour sonder ces opérateurs de manière indirecte.

Dans la section 4.6, nous avons étudié des spectres contenant une troisième génération de squarks légers. Ces spectres sont appelés "naturels" étant donné qu'ils permettent de stabiliser automatiquement l'échelle électrofaible. Dans ce contexte, nous avons réussi à exhiber deux relations, impliquant soit des taux d'évènements, soit des asymétries avants-arrières, selon la hiérarchie de masse considérée. Lorsque les stops sont plus lourds que le wino et le bino, une relation à l'ordre dominant (relativement à la théorie effective développée dans la sous-section 4.4.1.3) peut être trouvée, à condition qu'une certaine fraction des jets issus d'un quark charm puisse être correctement identifiée aux collisionneurs. Lorsque l'un des jauginos est plus lourd que les stops, le développement de la théorie effective a besoin d'être poussé aux ordres supérieurs. Le couplage des stops aux jauginos étant symétrique dans la limite de l'hypothèse $SU(5)$, des tests reposant sur la mesure de l'hélicité du top deviennent alors possibles. Ces tests requièrent typiquement 598 évènements dans les canaux utilisés afin de sonder une déviation de notre relation test à une précision de 50% avec un niveau de significativité de 3σ. En comparaison, 2580 évènements sont attendus au LHC avec des stops de 1 TeV et pour une luminosité intégrée de 300 fb^{-1}.

Enfin, nous avons considéré des spectres présentant un large mélange entre la seconde et la troisième génération de scalaire. Dans ces spectres de SUSY "Top-Charm", nous avons réussi à construire des

tests en considérant à nouveau, deux hiérarchies dans le spectre de masse. Dans le cas d'un spectre compressé, où les stops et les scharms sont presque dégénérés, il est possible de construire des tests $SU(5)$ reposant sur la détection de bosons de Higgs dans les cascades de désintégration des squarks. Typiquement, environ 144 évènements sont nécessaires afin de sonder une déviation de notre relation test avec une précision de 50% à un niveau de significativité de 3σ. Si seulement les scharms sont dégénérés, un test reste possible en utilisant des taux d'évènements convenablement normalisés, faisant là-encore intervenir des processus contenant des bosons de Higgs dans leurs états finaux, produits via des désintégrations violant la saveur. Ce dernier test requiert typiquement seulement 20 évènements pour sonder la relation test avec une précision de 50%.

Finalement, dans le chapitre 5, nous avons utilisé des méthodes bayésiennes de comparaison de modèles afin de procéder à une analyse numérique en utilisant des algorithmes de Monte Carlo par chaine de Markov. Cette analyse suppose que certaines informations soient collectées aux collisionneurs sur le spectre des squarks hauts, via la mesure de certaines observables, telles que des taux d'évènements, des masses de squarks, ou des éléments de la matrice de mélange des squarks. Des fonctions de vraisemblance gaussiennes peuvent être construites pour mettre en place une chaine de Markov dont la distribution cible est la probabilité a postériori que l'on cherche à évaluer. Des facteurs de Bayes peuvent ensuite être déduits afin de tester la présence possible de rémanents d'une unification $SU(5)$ dans le couplage trilinéaire des squarks hauts à basse énergie. Nous avons appliqué cette analyse à plusieurs jeux d'observables, à la fois avec une luminosité intégrée de 300 fb^{-1} et de 3000 fb^{-1}, et avons présenté les résultats préliminaires associés. Typiquement, les observables que nous avons considéré ne contraignent pas suffisamment les probabilités a postériori pour que les facteurs de Bayes puissent supporter l'hypothèse $SU(5)$, à moins que les incertitudes associées aux observables ne soient réduites à $\mathcal{O}(1\%)$. Cependant, même avec des incertitudes de l'ordre de $\mathcal{O}(10\%)$, si suffisamment d'information est disponible sur la matrice de mélange des squarks, il est possible d'obtenir une évidence faible contre l'hypothèse $SU(5)$ lorsqu'une haute asymétrie est imposée dans le couplage trilinéaire à l'échelle du TeV. La conclusion préliminaire est donc que cette analyse semble montrer son plein potentiel lorsqu'elle est utilisée pour rejeter l'hypothèse $SU(5)$, l'utilisant pour confirmer la présence d'une unification à haute énergie semblant plus difficile.

Perspectives

Je vois principalement quatre perspectives pour continuer le travail développé dans cette thèse.

Premièrement, l'analyse MCMC du chapitre 5 a encore besoin d'être optimisée, en particulier afin d'ajuster la taille du pas sur la chaine de Markov pour arriver à un taux d'acceptation optimal, tout en explorant une partie significative de l'espace des paramètres des matrices douces. À moyen terme, cette optimisation devrait autoriser l'inclusion de plus d'observables dans l'analyse, en particulier des masses individuelles des squarks et des rapports de branchement ce qui devrait permettre de contraindre les probabilités a postériori plus efficacement.

Deuxièmement, tout le travail développé dans cette thèse l'a été sous l'hypothèse d'un désert entre les échelles GUT et du TeV. Il pourrait être intéressant d'étendre ce travail au cas où la symétrie $SU(5)$ n'est plus réalisée à l'échelle GUT mais à une échelle intermédiaire. Par example, si le groupe de grande unification est $SO(10)$, sa chaine de brisure vers le groupe de jauge du modèle standard peut impliquer une symétrie intermédiaire de type $SU(5)$. Dans de tels cas, des degrés de liberté supplémentaires peuvent être présents entre les deux échelles, à cause des représentations étendues du groupe de grande unification. Étudier leurs impacts sur l'évolution des deux relations de symétrie auxquelles nous nous sommes intéressés constitue donc une extension naturelle de ce travail.

Troisièmement, tous les tests qui ont été développés dans cette thèse peuvent être directement généralisés aux théories GUTs d'ordres supérieurs, lorsque le groupe de grande unification contient $SU(5)$ comme sous-groupe. En particulier, les différents tests développés devraient directement applicables au cas des théories SUSY/GUTs de type $SO(10)$ qui, comparativement à $SU(5)$, n'ajoutent que les neutrinos droits dans le spectre de matière. Cependant les théories SUSY/GUTs plus grandes que $SO(10)$, par exemple celles basées sur $E(6)$, introduisent généralement des degrés de libertés supplémentaires sensibles à la saveur, tels que les leptoquarks ou les higgs sombres, pouvant ainsi potentiellement modifier l'évolution des couplages trilinéaires. Il serait alors intéressant de se demander

dans quelle mesure l'évolution des relations de symétrie que nous avons considéré se trouve modifié, et si des tests de basse énergie peuvent toujours être construits dans un tel contexte.

Le quatrième point, peut-être le plus important, consisterait à mener une analyse détaillée aux collisionneurs, en utilisant des générateurs Monte-Carlo, afin de simuler les efficacités attendues pour l'identification des jets charmés et pour la mesure de l'hélicité du top, en tenant compte des différentes sources de bruit de fond. En effet, comme presque tous les tests développés dans le chapitre 4 reposent sur l'une de ces techniques, il est crucial d'avoir une idée quantitative plus précise des sensibilités attendues aux détecteurs actuels.

Appendix A

Conventions

A.1 Pauli and Dirac matrices.

We recall that a basis of $SU(2)$ is given by $(\mathbb{1}_2, i\sigma_1, i\sigma_2, i\sigma_3)$ where:

$$\sigma_1 = \begin{pmatrix} 0 & 1 \\ 1 & 0 \end{pmatrix}, \quad \sigma_2 = \begin{pmatrix} 0 & -i \\ i & 0 \end{pmatrix}, \quad \sigma_3 = \begin{pmatrix} 1 & 0 \\ 0 & -1 \end{pmatrix}, \tag{A.1}$$

are the three Pauli matrices and $\mathbb{1}$ is understood to be the 2×2 identity matrix. The Pauli matrices obey the $su(2)$ algebra commutation relations:

$$\left[\sigma^i, \sigma^j\right] = 2i\epsilon_{ijk}\sigma^k \tag{A.2}$$

The 4D-Clifford algebra $\{\gamma_\mu, \gamma_\nu\} = 2g_{\mu\nu}$ can be represented by the 4×4 Dirac matrices, given here in the chiral representation:

$$\gamma_0 = \begin{pmatrix} 0 & \mathbb{1} \\ \mathbb{1} & 0 \end{pmatrix}, \quad i = 1,2,3: \quad \gamma_i = \begin{pmatrix} 0 & \sigma^i \\ -\sigma^i & 0 \end{pmatrix}, \tag{A.3}$$

One can further define the "fifth" gamma matrix:

$$\gamma_5 = i\gamma_0\gamma_1\gamma_2\gamma_3\gamma_4 = \begin{pmatrix} -\mathbb{1} & 0 \\ 0 & \mathbb{1} \end{pmatrix}, \tag{A.4}$$

which satisfies $\{\gamma^5, \gamma^\mu\} = 0$.

A.2 Weyl spinors.

A Weyl spinor is a doublet of complex numbers $\psi = \begin{pmatrix} c_1 \\ c_2 \end{pmatrix}$ lying in the fundamental representation space of $SU(2)$. In the chiral representation, one can define left-handed ψ_α and right handed $\psi^{\dagger\dot{\alpha}}$ Weyl spinors. These have the virtue to have well defined transformation properties under the Lorentz group:

$$\psi_\alpha \to M_\alpha{}^\beta \psi_\beta, \quad \psi^{\dot{\alpha}} \to \left(\left(M^{-1}\right)^\dagger\right)^{\dot{\alpha}}{}_{\dot{\beta}} \psi^{\dot{\beta}} \tag{A.5}$$

where $M = M(\Lambda)$ is the two-dimensional representation of the Lorentz transformation Λ. The spinor indices $\alpha, \beta = 1,2$ and $\dot{\alpha}, \dot{\beta} = 1,2$ can be raised and lowered with the totally antisymmetric Levi-Civita tensor ϵ where $\epsilon_{\alpha\beta} = \epsilon_{\dot{\alpha}\dot{\beta}} = -\epsilon^{\alpha\beta} = -\epsilon^{\dot{\alpha}\dot{\beta}}$ with $\epsilon_{12} = +1$. Hermitian conjugation relates left and right handed Weyl spinors:

$$\psi^\dagger_{\dot{\alpha}} \equiv (\psi_\alpha)^\dagger = (\psi^\dagger)_{\dot{\alpha}}, \quad (\psi^{\dagger\dot{\alpha}})^\dagger = \psi^\alpha \tag{A.6}$$

Then, one can equally use either a left-handed Weyl spinor (with an undotted indice) or a right-handed Weyl spinor (with a dotted indice) to describe any particular fermionic degree of freedom. This gives us the freedom to make all right-handed spinors carry daggers while left-handed spinors do not.

Note that, as Weyl spinors are Grassmann valued, they anticommute:

$$\xi^\alpha \chi_\alpha = -\xi_\alpha \chi^\alpha \text{ and } \xi^\dagger_{\dot\alpha} \chi^{\dagger\dot\alpha} = -\xi^{\dagger\dot\alpha} \chi^\dagger_{\dot\alpha} \tag{A.7}$$

Then, one has to fix an ordering convention to suppress repeated indices. We fix that indices repeated as:

$$^{\alpha}{}_{\alpha} \text{ or } {}_{\dot\alpha}{}^{\dot\alpha} \tag{A.8}$$

can be suppressed. In particular, we have for the scalar product:

$$\begin{aligned} \xi\chi \equiv \xi^\alpha \chi_\alpha = \chi^\alpha \xi_\alpha \equiv \chi\xi, \\ \xi^\dagger \chi^\dagger \equiv \xi^\dagger_{\dot\alpha} \chi^{\dagger\dot\alpha} = \chi^\dagger_{\dot\alpha} \xi^{\dagger\dot\alpha} \equiv \chi^\dagger \xi^\dagger \end{aligned} \tag{A.9}$$

Finally, one can define two four-vectors of Pauli matrices via:

$$(\sigma^\mu)_{\alpha\dot\beta} \equiv \left(\mathbb{1}, \sigma^i\right)_{\alpha\dot\beta} \text{ and } (\overline{\sigma}^\mu)^{\dot\alpha\beta} \equiv \left(\mathbb{1}, -\sigma^i\right)^{\dot\alpha\beta}. \tag{A.10}$$

It is also useful to define antisymmetrized products of these two four-vectors:

$$(\sigma^{\mu\nu})_\alpha{}^\beta \equiv \frac{i}{2}(\sigma^\mu \overline{\sigma}^\nu - \sigma^\nu \overline{\sigma}^\mu)_\alpha{}^\beta \quad \text{and} \quad (\overline{\sigma}^{\mu\nu})^{\dot\alpha}{}_{\dot\beta} \equiv \frac{i}{2}(\overline{\sigma}^\mu \sigma^\nu - \overline{\sigma}^\nu \sigma^\mu)^{\dot\alpha}{}_{\dot\beta} \tag{A.11}$$

A.3 Dirac and Majorana spinors

One can define a four-component Dirac spinor out of two Weyl spinors (see sec A.2) of opposite chiralities:

$$\Psi_D \equiv \begin{pmatrix} \psi_L \\ \psi_R \end{pmatrix} = \begin{pmatrix} \xi_\alpha \\ \chi^{\dagger\dot\alpha} \end{pmatrix}. \tag{A.12}$$

and its Dirac conjugate form:

$$\overline{\Psi} = \Psi^\dagger \gamma^0 = \begin{pmatrix} \chi^\beta & \xi^\dagger_{\dot\alpha} \end{pmatrix} \tag{A.13}$$

which allows to form (Dirac) Lorentz invariant mass terms of the form $\overline{\Psi}\Psi$.

Note that γ_5 allows to define the two chirality projection operators:

$$P_L = \frac{1-\gamma_5}{2}, \quad P_R = \frac{1+\gamma_5}{2} \tag{A.14}$$

which makes the chirality assignment in Ψ_D consistent as:

$$P_L \Psi = \begin{pmatrix} \xi_\alpha \\ 0 \end{pmatrix} \text{ and } P_R \Psi = \begin{pmatrix} 0 \\ \chi^{\dagger\dot\alpha} \end{pmatrix}. \tag{A.15}$$

The charge conjugation of a Dirac spinor is defined as:

$$\Psi^c \equiv C\overline{\Psi}^T = \begin{pmatrix} \chi_\beta \\ \xi^{\dagger\dot\alpha} \end{pmatrix} \tag{A.16}$$

with $C = i\gamma_0\gamma_2$, the 4-D charge conjugation matrix. C satisfies the important identity $C^{-1}\gamma_\mu C = -(\gamma_\mu)^T$.

One can then define a 4 components Majorana spinor Ψ_M via the condition:

$$\Psi^c = \Psi. \tag{A.17}$$

A Majorana spinor is its own anti-particle and, when applying constraint A.17 to the general form of a Dirac spinor (A.12), one finds:

$$\Psi = \begin{pmatrix} \xi_\alpha \\ \xi^{\dagger\dot\beta} \end{pmatrix} \text{ and } \overline{\Psi} = \begin{pmatrix} \xi^\beta & \xi^\dagger_{\dot\alpha} \end{pmatrix} \tag{A.18}$$

Contrary to a Dirac spinor, a Majorana spinor has hence only two complex, anti-commuting degrees of freedom.

Appendix B

The dipole form factors

The form factors for the dipole penguin diagrams are given by:

$$F_s^{(1)} = \frac{10\left(19+172x+x^2\right)}{21\left(1-x\right)^4} + \frac{20x\left(18+15x-x^2\right)}{7\left(1-x\right)^5}\log x, \tag{B.1}$$

$$F_s^{(2)} = -\frac{12\left(11+x\right)}{5\left(1-x\right)^3} - \frac{6\left(9+16x-x^2\right)}{5\left(1-x\right)^4}\log x, \tag{B.2}$$

$$F_{EW}^{(1)} = \frac{10\left(1-8x-17x^2\right)}{3\left(1-x\right)^4} - \frac{20x^3\left(3+x\right)}{\left(1-x\right)^5}\log x, \tag{B.3}$$

$$F_{EW}^{(2)} = \frac{6\left(1+5x\right)}{\left(1-x\right)^3} - \frac{12x\left(2+x\right)}{\left(1-x\right)^4}\log x. \tag{B.4}$$

Appendix C

Event rates for $\tilde{t}_{a,b} \to t_{L/R}\tilde{B}$

Assuming a spin analyzer distribution $P_Z(z) \propto (1 + \kappa P_t z)$, the events rates of sec. 4.5.1 are given by:

$$N_{a+} = N_{aL}\frac{1-\kappa/2}{2} + N_{aR}\frac{1+\kappa/2}{2}, \tag{C.1}$$

$$N_{a-} = N_{aL}\frac{1+\kappa/2}{2} + N_{aR}\frac{1-\kappa/2}{2}, \tag{C.2}$$

$$N_{b+} = N_{bL}\frac{1-\kappa/2}{2} + N_{bR}\frac{1+\kappa/2}{2}, \tag{C.3}$$

$$N_{b-} = N_{bL}\frac{1+\kappa/2}{2} + N_{bR}\frac{1-\kappa/2}{2}, \tag{C.4}$$

with:

$$N_{aL} = N_a\frac{(c_{\theta_t} - x s_{\theta_t})^2}{(c_{\theta_t} - x s_{\theta_t})^2 + 16(s_{\theta_t} - x c_{\theta_t})^2}, \tag{C.5}$$

$$N_{aR} = N_a\frac{16(s_{\theta_t} - x c_{\theta_t})^2}{(c_{\theta_t} - x s_{\theta_t})^2 + 16(s_{\theta_t} - x c_{\theta_t})^2}, \tag{C.6}$$

$$N_{bL} = N_b\frac{(c_{\theta_t} - x s_{\theta_t})^2}{(c_{\theta_t} - x s_{\theta_t})^2 + 16(s_{\theta_t} - x c_{\theta_t})^2}, \tag{C.7}$$

$$N_{bR} = N_b\frac{16(s_{\theta_t} - x c_{\theta_t})^2}{(c_{\theta_t} - x s_{\theta_t})^2 + 16(s_{\theta_t} - x c_{\theta_t})^2}, \tag{C.8}$$

$$\tag{C.9}$$

Here N_a, N_b are the production rates of $\tilde{t}_a$, $\tilde{t}_b$.

The exact formula for the expected precision associated to the $SU(5)$ test eq. (4.117) is then simply:

$$P_Z \approx Z\frac{(17 + 15c_{2\theta_t})}{255\sqrt{2}\,(3 + c_{4\theta_t})\,\kappa}\left(\frac{3212 - 739\kappa^2 - 1020\left(\kappa^2 - 4\right)c_{2\theta_t} + \left(900 - 289\kappa^2\right)c_{4\theta_t}}{N_a} + \frac{3212 - 739\kappa^2 - 1020\left(\kappa^2 - 4\right)c_{2\theta_t} + \left(900 - 289\kappa^2\right)c_{4\theta_t}}{N_b}\right)^{1/2}. \tag{C.10}$$

Bibliography

[1] Abdus Salam and John C. Ward. On a gauge theory of elementary interactions. *Il Nuovo Cimento*, 19(1):165–170, 1961. ISSN 0029-6341. URL http://dx.doi.org/10.1007/BF02812723.

[2] Steven Weinberg. The Making of the standard model. *Eur.Phys.J.*, C34:5–13, 2004, arXiv:hep-ph/0401010.

[3] Lillian Hoddeson. *The rise of the standard model : particle physics in the 1960s and 1970s.* Cambridge University Press, New York, 1997. ISBN 978-0521578165.

[4] Cédric Weiland. Effects of fermionic singlet neutrinos on high- and low-energy observables, 2013, arXiv:1311.5860.

[5] Michael Peskin. *An introduction to quantum field theory.* Addison-Wesley, Reading, Mass, 1995. ISBN 978-0201503975.

[6] Tai-Pei Cheng and Ling-Fong Li. *Gauge theory of elementary particle physics.* Clarendon Press Oxford University Press, Oxford Oxfordshire New York, 1984. ISBN 978-0198519614.

[7] Ian Aitchison. *Gauge theories in particle physics : a practical introduction.* CRC Press, Boca Raton, FL, 2012. ISBN 978-1466513174.

[8] Chen N. Yang and Robert L. Mills. Conservation of isotopic spin and isotopic gauge invariance. *Phys. Rev.*, 96:191–195, Oct 1954. URL http://link.aps.org/doi/10.1103/PhysRev.96.191.

[9] François Englert and Robert Brout. Broken symmetry and the mass of gauge vector mesons. *Phys. Rev. Lett.*, 13:321–323, Aug 1964. URL http://link.aps.org/doi/10.1103/PhysRevLett.13.321.

[10] Gerald S. Guralnik, Carl R. Hagen, and Tom W. B. Kibble. Global conservation laws and massless particles. *Phys. Rev. Lett.*, 13:585–587, Nov 1964. URL http://link.aps.org/doi/10.1103/PhysRevLett.13.585.

[11] G. Arnison et al. Experimental Observation of Lepton Pairs of Invariant Mass Around 95-GeV/c**2 at the CERN SPS Collider. *Phys.Lett.*, B126:398–410, 1983.

[12] G. Arnison et al. Experimental Observation of Isolated Large Transverse Energy Electrons with Associated Missing Energy at s**(1/2) = 540-GeV. *Phys.Lett.*, B122:103–116, 1983.

[13] P. Bagnaia et al. Evidence for Z0 → e+ e- at the CERN anti-p p Collider. *Phys.Lett.*, B129: 130–140, 1983.

[14] M. Banner et al. Observation of Single Isolated Electrons of High Transverse Momentum in Events with Missing Transverse Energy at the CERN anti-p p Collider. *Phys.Lett.*, B122:476–485, 1983.

[15] Georges Aad et al. Observation of a new particle in the search for the Standard Model Higgs boson with the ATLAS detector at the LHC. *Phys.Lett.*, B716:1–29, 2012, arXiv:1207.7214.

[16] Serguei Chatrchyan et al. Observation of a new boson at a mass of 125 GeV with the CMS experiment at the LHC. *Phys.Lett.*, B716:30–61, 2012, arXiv:1207.7235.

[17] Young S. Kim. *Theory and Applications of the Poincaré Group*. Springer Netherlands, Dordrecht, 1986. ISBN 978-9401085267.

[18] Murray Gell-Mann. Symmetries of baryons and mesons. *Phys. Rev.*, 125:1067–1084, Feb 1962. URL http://link.aps.org/doi/10.1103/PhysRev.125.1067.

[19] Jean Iliopoulos. Introduction to the STANDARD MODEL of the Electro-Weak Interactions. pages 1–30, 2014, arXiv:1305.6779.

[20] Makoto Kobayashi and Toshihide Maskawa. CP Violation in the Renormalizable Theory of Weak Interaction. *Prog.Theor.Phys.*, 49:652–657, 1973.
Nicola Cabibbo. Unitary symmetry and leptonic decays. *Phys. Rev. Lett.*, 10:531–533, Jun 1963. URL http://link.aps.org/doi/10.1103/PhysRevLett.10.531.

[21] Ziro Maki, Masami Nakagawa, and Shoichi Sakata. Remarks on the unified model of elementary particles. *Progress of Theoretical Physics*, 28(5):870–880, 1962. URL http://ptp.oxfordjournals.org/content/28/5/870.abstract.

[22] Elena Giusarma, Roland de Putter, Shirley Ho, and Olga Mena. Constraints on neutrino masses from Planck and Galaxy Clustering data. *Phys.Rev.*, D88(6):063515, 2013, arXiv:1306.5544.

[23] Stanislav A. Barabash. Double beta decay experiments: beginning of a new era. 2012, arXiv:1209.4241.

[24] Renata Zukanovich Funchal, Benoit Schmauch, and Gaëlle Giesen. The Physics of Neutrinos. 2013, arXiv:1308.1029.
Emiliano Molinaro. Type I Seesaw Mechanism, Lepton Flavour Violation and Higgs Decays. *J.Phys.Conf.Ser.*, 447:012052, 2013, arXiv:1303.5856.
Stephen F. King. Neutrino mass models. *Rept.Prog.Phys.*, 67:107–158, 2004, arXiv:hep-ph/0310204.

[25] J. Beringer and *et al.* Review of particle physics. *Phys. Rev. D*, 86:010001, July 2012. URL http://link.aps.org/doi/10.1103/PhysRevD.86.010001.

[26] Lincoln Wolfenstein. Parametrization of the kobayashi-maskawa matrix. *Phys. Rev. Lett.*, 51: 1945–1947, Nov 1983. URL http://link.aps.org/doi/10.1103/PhysRevLett.51.1945.

[27] J. Charles, O. Deschamps, S. Descotes-Genon, H. Lacker, A. Menzel, et al. Current status of the Standard Model CKM fit and constraints on $\Delta F = 2$ New Physics. 2015, arXiv:1501.05013.

[28] Stefan Antusch, Ivo de Medeiros Varzielas, Vinzenz Maurer, Constantin Sluka, and Martin Spinrath. Towards predictive flavour models in SUSY SU(5) GUTs with doublet-triplet splitting. *JHEP*, 1409:141, 2014, arXiv:1405.6962.

[29] Toshifumi Yamashita. Doublet-Triplet Splitting in a SU(5) Grand Unification. *Phys.Rev.*, D84: 115016, 2011, arXiv:1106.3229.

[30] Takeshi Fukuyama. SO(10) GUT in Four and Five Dimensions: A Review. *Int.J.Mod.Phys.*, A28:1330008, 2013, arXiv:1212.3407.

[31] Felix Braam, Alexander Knochel, and Jürgen Reuter. An Exceptional SSM from E6 Orbifold GUTs with intermediate LR symmetry. *JHEP*, 1006:013, 2010, arXiv:1001.4074.

[32] Stephen F. King and Christoph Luhn. Neutrino Mass and Mixing with Discrete Symmetry. *Rept.Prog.Phys.*, 76:056201, 2013, arXiv:1301.1340.
Gui-Jun Ding, Stephen F. King, Christoph Luhn, and Alexander J. Stuart. Spontaneous CP violation from vacuum alignment in S_4 models of leptons. *JHEP*, 1305:084, 2013, arXiv:1303.6180.

[33] Stefan Antusch, Stephen F. King, and Michal Malinsky. Solving the SUSY Flavour and CP Problems with SU(3) Family Symmetry. *JHEP*, 0806:068, 2008, arXiv:0708.1282.

[34] M.C. Gonzalez-Garcia, Michele Maltoni, and Thomas Schwetz. Updated fit to three neutrino mixing: status of leptonic cp violation. *Journal of High Energy Physics*, 2014(11), 2014. URL http://dx.doi.org/10.1007/JHEP11%282014%29052.

[35] Sidney Coleman and Jeffrey Mandula. All possible symmetries of the s matrix. *Phys. Rev.*, 159: 1251–1256, Jul 1967. URL http://link.aps.org/doi/10.1103/PhysRev.159.1251.

[36] Rudolf Haag, Jan T. Łopuszański, and Martin Sohnius. All possible generators of supersymmetries of the s-matrix. *Nuclear Physics B*, 88(2):257 – 274, 1975. ISSN 0550-3213. URL http://www.sciencedirect.com/science/article/pii/0550321375902795.

[37] Stephen P. Martin. A Supersymmetry primer. *Adv.Ser.Direct.High Energy Phys.*, 21:1–153, 2010, arXiv:hep-ph/9709356.

[38] Waldemar Martens. *Threshold Corrections in Grand Unified Theories*. PhD thesis, Karlsruhe institute of technology, 2011. URL http://digbib.ubka.uni-karlsruhe.de/volltexte/1000023673.

[39] Stanley Deser and Bruno Zumino. Consistent supergravity. *Physics Letters B*, 62(3):335 – 337, 1976. ISSN 0370-2693. URL http://www.sciencedirect.com/science/article/pii/0370269376900897.

[40] Julius Wess. *Supersymmetry and supergravity*. Princeton University Press, Princeton, N.J, 1992. ISBN 0691025304.

[41] Roman Nevzorov. Theoretical aspects of electroweak symmetry breaking in SUSY models. *PoS*, QFTHEP2010:015, 2010, arXiv:1103.2141.

[42] Riccardo Catena and Laura Covi. SUSY dark matter(s). *Eur.Phys.J.*, C74:2703, 2014, arXiv:1310.4776.

[43] Bibhushan Shakya. The Status of Neutralino Dark Matter. *AIP Conf.Proc.*, 1604:98–104, 2014, arXiv:1312.7505.
Ian J.R Aitchison. Supersymmetry and the MSSM: An Elementary introduction. 2005, arXiv:hep-ph/0505105.

[44] Daniele Bertolini, Jesse Thaler, and Zachary Thomas. TASI 2012: Super-Tricks for Superspace. 2013, arXiv:1302.6229.

[45] Lochlainn O'Raifeartaigh. Spontaneous Symmetry Breaking for Chiral Scalar Superfields. *Nucl.Phys.*, B96:331, 1975.

[46] Pierre Fayet and John Iliopoulos. Spontaneously Broken Supergauge Symmetries and Goldstone Spinors. *Phys.Lett.*, B51:461–464, 1974.
Pierre Fayet. Supersymmetry and weak, electromagnetic and strong interactions. *Physics Letters B*, 64(2):159 – 162, 1976. ISSN 0370-2693. URL http://www.sciencedirect.com/science/article/pii/0370269376903191.

[47] Markus A. Luty. 2004 TASI lectures on supersymmetry breaking. pages 495–582, 2005, arXiv:hep-th/0509029.

[48] Ali H. Chamseddine, Richard Arnowitt, and Pran Nath. Locally supersymmetric grand unification. *Phys. Rev. Lett.*, 49:970–974, Oct 1982. URL http://link.aps.org/doi/10.1103/PhysRevLett.49.970.

[49] Irene Niessen. Supersymmetric Phenomenology in the mSUGRA Parameter Space. Master's thesis, Nijmegen U., IMAPP, 2008, arXiv:0809.1748. URL http://inspirehep.net/record/796204/files/arXiv:0809.1748.pdf.

[50] Michael Dine and Ann E. Nelson. Dynamical supersymmetry breaking at low-energies. *Phys.Rev.*, D48:1277–1287, 1993, arXiv:hep-ph/9303230.

[51] Lisa Randall and Raman Sundrum. Out of this world supersymmetry breaking. *Nucl.Phys.*, B557:79–118, 1999, arXiv:hep-th/9810155.
Gian F. Giudice, Markus A. Luty, Hitoshi Murayama, and Riccardo Rattazzi. Gaugino mass without singlets. *JHEP*, 9812:027, 1998, arXiv:hep-ph/9810442.

[52] Luciano Girardello and Marcus T. Grisaru. Soft breaking of supersymmetry. *Nuclear Physics B*, 194(1):65 – 76, 1982. ISSN 0550-3213. URL http://www.sciencedirect.com/science/article/pii/0550321382905120.

[53] Csaba Csaki. The Minimal supersymmetric standard model (MSSM). *Mod.Phys.Lett.*, A11:599, 1996, arXiv:hep-ph/9606414.

[54] Gian F. Giudice and Esteban Roulet. Conditions on supersymmetry soft breaking terms from GUTs. *Phys.Lett.*, B315:107–112, 1993, arXiv:hep-ph/9307226.

[55] Gian F. Giudice. A natural solution to the μ-problem in supergravity theories. *Physics Letters B*, 206(3):480 – 484, 1988. ISSN 0370-2693. URL http://www.sciencedirect.com/science/article/pii/0370269388916139.

[56] Markos Maniatis. The Next-to-Minimal Supersymmetric extension of the Standard Model reviewed. *Int.J.Mod.Phys.*, A25:3505–3602, 2010, arXiv:0906.0777.

[57] Nir Polonsky. The Mu parameter of supersymmetry. 1999, arXiv:hep-ph/9911329.

[58] Stephen P. Martin. Some simple criteria for gauged R-parity. *Phys.Rev.*, D46:2769–2772, 1992, arXiv:hep-ph/9207218.
Stephen P. Martin. Implications of supersymmetric models with natural R-parity conservation. *Phys.Rev.*, D54:2340–2348, 1996, arXiv:hep-ph/9602349.

[59] Richard L. Arnowitt, Bhaskar Dutta, and Y. Santoso. SUSY phases, the electron electric dipole moment and the muon magnetic moment. *Phys.Rev.*, D64:113010, 2001, arXiv:hep-ph/0106089.

[60] Stefan Antusch, Stephen F. King, Michal Malinsky, and Graham G. Ross. Solving the SUSY Flavour and CP Problems with Non-Abelian Family Symmetry and Supergravity. *Phys.Lett.*, B670:383–389, 2009, arXiv:0807.5047.

[61] Tatsuo Kobayashi, Masahiko Konmura, Daijiro Suematsu, Kiyonori Yamada, and Yoshio Yamagishi. Neutron electric dipole moment under nonuniversal soft SUSY breaking terms. *Prog.Theor.Phys.*, 94:417–434, 1995, arXiv:hep-ph/9410269.
Pran Nath and Richard L. Arnowitt. Nonuniversal soft SUSY breaking and dark matter. *Phys.Rev.*, D56:2820–2832, 1997, arXiv:hep-ph/9701301.
John R. Ellis, Keith A. Olive, and Pearl Sandick. Varying the Universality of Supersymmetry-Breaking Contributions to MSSM Higgs Boson Masses . *Phys.Rev.*, D78:075012, 2008, arXiv:0805.2343.

[62] Lawrence J. Hall and Lisa Randall. Weak-scale effective supersymmetry. *Phys. Rev. Lett.*, 65:2939–2942, Dec 1990. URL http://link.aps.org/doi/10.1103/PhysRevLett.65.2939.
Yosef Nir and Nathan Seiberg. Should squarks be degenerate? *Phys.Lett.*, B309:337–343, 1993, arXiv:hep-ph/9304307.

[63] Stephen M. Barr. Supersymmetric solutions to the strong CP problem. *Phys.Rev.*, D56:1475–1480, 1997, arXiv:hep-ph/9612396.
Stephen M. Barr. Flavor alignment solutions to the strong CP problem in supersymmetry. *Phys.Rev.*, D56:5761–5765, 1997, arXiv:hep-ph/9705265.

[64] Savas Dimopoulos and Gian F. Giudice. Naturalness constraints in supersymmetric theories with nonuniversal soft terms. *Phys.Lett.*, B357:573–578, 1995, arXiv:hep-ph/9507282.
Alex Pomarol and Daniele Tommasini. Horizontal symmetries for the supersymmetric flavor problem. *Nucl.Phys.*, B466:3–24, 1996, arXiv:hep-ph/9507462.
Andrew G. Cohen, David B. Kaplan, and A.E. Nelson. The More minimal supersymmetric standard model. *Phys.Lett.*, B388:588–598, 1996, arXiv:hep-ph/9607394.
Savas Dimopoulos, Kiel Howe, and John March-Russell. Maximally Natural Supersymmetry. *Phys.Rev.Lett.*, 113:111802, 2014, arXiv:1404.7554.

[65] Howard Georgi. *Lie algebras in particle physics*. Westview Press, A Member of the Perseus Books Group, Reading, Mass, 1999. ISBN 978-0738202334.
Pierre Ramond. *Group theory : a physicists survey*. Cambridge University Press, Cambridge, UK New York, 2010. ISBN 978-0521896030.
Jürgen Fuchs. *Symmetries, Lie algebras and representations : a graduate course for physicists*. Cambridge University Press, Cambridge, 2003. ISBN 978-0521541190.

[66] Jogesh C. Pati and Abdus Salam. Lepton number as the fourth "color". *Phys. Rev. D*, 10: 275–289, Jul 1974. URL http://link.aps.org/doi/10.1103/PhysRevD.10.275.

[67] Howard Georgi and Sheldon L. Glashow. Unity of all elementary-particle forces. *Phys. Rev. Lett.*, 32:438–441, Feb 1974. URL http://link.aps.org/doi/10.1103/PhysRevLett.32.438.

[68] Ugo Amaldi, Wim de Boer, and Hermann Fürstenau. Comparison of grand unified theories with electroweak and strong coupling constants measured at {LEP}. *Physics Letters B*, 260(3–4):447 – 455, 1991. ISSN 0370-2693. URL http://www.sciencedirect.com/science/article/pii/0370269391916418.

[69] Savas Dimopoulos and Howard Georgi. Softly broken supersymmetry and su(5). *Nuclear Physics B*, 193(1):150 – 162, 1981. ISSN 0550-3213. URL http://www.sciencedirect.com/science/article/pii/0550321381905228.
Radovan Dermíšek, Arash Mafi, and Stuart Raby. Supersymmetric grand unification under siege: Proton lifetime upper bound. *Phys. Rev. D*, 63:035001, Dec 2000. URL http://link.aps.org/doi/10.1103/PhysRevD.63.035001.
Borut Bajc, Pavel Fileviez Perez, and Goran Senjanovic. Minimal supersymmetric SU(5) theory and proton decay: Where do we stand? pages 131–139, 2002, arXiv:hep-ph/0210374.

[70] Paul Langacker. Grand unified theories and proton decay. *Physics Reports*, 72(4):185 – 385, 1981. ISSN 0370-1573. URL http://www.sciencedirect.com/science/article/pii/0370157381900594.

[71] Howard Georgi and Cecilia Jarlskog. A new lepton-quark mass relation in a unified theory. *Physics Letters B*, 86(3–4):297 – 300, 1979. ISSN 0370-2693. URL http://www.sciencedirect.com/science/article/pii/0370269379908426.

[72] Waldemar Martens, Luminita Mihaila, Jens Salomon, and Matthias Steinhauser. Minimal Supersymmetric SU(5) and Gauge Coupling Unification at Three Loops. *Phys.Rev.*, D82:095013, 2010, arXiv:1008.3070.

[73] Marco Ciuchini, Antonio Masiero, Luca Silvestrini, Sudhir K. Vempati, and Oscar Vives. Grand unification of quark and lepton FCNCs. *Phys.Rev.Lett.*, 92:071801, 2004, arXiv:hep-ph/0307191.

[74] Pran Nath. Hierarchies and textures in supergravity unification. *Phys.Rev.Lett.*, 76:2218–2221, 1996, arXiv:hep-ph/9512415.

[75] Tsedenbaljir Enkhbat. SU(5) unification for Yukawas through SUSY threshold effects. 2009, arXiv:0909.5597.

[76] Antonio Masiero, Dimitri V. Nanopoulos, Kyriakos Tamvakis, and Tsutomu Yanagida. Naturally massless higgs doublets in supersymmetric su(5). *Physics Letters B*, 115(5):380 – 384, 1982. ISSN 0370-2693. URL http://www.sciencedirect.com/science/article/pii/0370269382905226.
Benjamin Grinstein. A supersymmetric su(5) gauge theory with no gauge hierarchy problem. *Nuclear Physics B*, 206(3):387 – 396, 1982. ISSN 0550-3213. URL http://www.sciencedirect.com/science/article/pii/0550321382902759.

[77] Junji Hisano, T. Moroi, K. Tobe, and Tsutomu Yanagida. Suppression of proton decay in the missing partner model for supersymmetric SU(5) GUT. *Phys.Lett.*, B342:138–144, 1995, arXiv:hep-ph/9406417.

[78] John Ellis, Dimitri V. Nanopoulos, and J. Walker. Flipping su(5) out of trouble. *Physics Letters B*, 550(1–2):99 – 107, 2002. ISSN 0370-2693. URL http://www.sciencedirect.com/science/article/pii/S0370269302029568.
John Ellis, Azar Mustafayev, and Keith A. Olive. Constrained Supersymmetric Flipped SU(5) GUT Phenomenology. *Eur.Phys.J.*, C71:1689, 2011, arXiv:1103.5140.

[79] Kaladi S. Babu and Rabindra N. Mohapatra. Is there a connection between quantization of electric charge and a majorana neutrino? *Phys. Rev. Lett.*, 63:938–941, Aug 1989. URL http://link.aps.org/doi/10.1103/PhysRevLett.63.938.

[80] Junji Hisano, Hitoshi Murayama, and Tsutomu Yanagida. Nucleon decay in the minimal supersymmetric SU(5) grand unification. *Nucl.Phys.*, B402:46–84, 1993, arXiv:hep-ph/9207279.

[81] Hitoshi Murayama and Aaron Pierce. Not even decoupling can save minimal supersymmetric SU(5). *Phys.Rev.*, D65:055009, 2002, arXiv:hep-ph/0108104.
David Emmanuel-Costa and Soren Wiesenfeldt. Proton decay in a consistent supersymmetric SU(5) GUT model. *Nucl.Phys.*, B661:62–82, 2003, arXiv:hep-ph/0302272.
Goran Senjanovic. Proton decay and grand unification. *AIP Conf.Proc.*, 1200:131–141, 2010, arXiv:0912.5375.

[82] Borut Bajc and Luca Di Luzio. R-parity violation in SU(5). 2015, arXiv:1502.07968.
R. Barbier, C. Berat, M. Besancon, M. Chemtob, Aldo Deandrea, et al. R-parity violating supersymmetry. *Phys.Rept.*, 420:1–202, 2005, arXiv:hep-ph/0406039.

[83] Yoshio Koide and Joe Sato. An SU(5) SUSY model with R parity violation and radiatively induced neutrino masses. 2002, arXiv:hep-ph/0210188.
Yoshio Koide. Neutrino masses induced by R-parity violation in a SUSY SU(5) model with additional $\overline{\mathbf{5}}'_L + \mathbf{5}'_L$. *Physics Letters B*, 595(1–4):469 – 475, 2004. ISSN 0370-2693. URL http://www.sciencedirect.com/science/article/pii/S0370269304008895.

[84] Bobby S. Acharya, Gordon L. Kane, Piyush Kumar, Ran Lu, and Bob Zheng. R-Parity Conservation from a Top Down Perspective. *JHEP*, 1410:1, 2014, arXiv:1403.4948.

[85] Ilja Dorsner and Pavel Fileviez Perez. Could we rotate proton decay away? *Phys.Lett.*, B606:367–370, 2005, arXiv:hep-ph/0409190.

[86] Sylvain Fichet, Björn Herrmann, and Yannick Stoll. A new flavour imprint of SU(5)-like Grand Unification and its LHC signatures. *Physics Letters B*, 742:69 – 73, 2015. ISSN 0370-2693. URL http://www.sciencedirect.com/science/article/pii/S0370269315000155.

[87] Sylvain Fichet, Björn Herrmann, and Yannick Stoll. Tasting the SU(5) nature of supersymmetry at the LHC. *Journal of High Energy Physics*, 2015. URL http://dx.doi.org/10.1007/JHEP05%282015%29091.

[88] Paul Langacker and Nir Polonsky. Uncertainties in coupling constant unification. *Phys. Rev. D*, 47:4028–4045, May 1993. URL http://link.aps.org/doi/10.1103/PhysRevD.47.4028.
Lawrence J. Hall and Uri Sarid. Gravitational smearing of minimal supersymmetric unification predictions. *Phys. Rev. Lett.*, 70:2673–2676, May 1993. URL http://link.aps.org/doi/10.1103/PhysRevLett.70.2673.
Alakabha Datta, Sandip Pakvasa, and Utpal Sarkar. Gravitational uncertainties from dimension-six operators on supersymmetric GUT predictions. *Phys.Rev.*, D52:550–552, 1995, arXiv:hep-ph/9403360.
D. Ring, Shinichi Urano, and Richard L. Arnowitt. Planck scale physics and the testability of SU(5) supergravity GUT. *Phys.Rev.*, D52:6623–6626, 1995, arXiv:hep-ph/9501247.
Jon L. Chkareuli and Ilia G. Gogoladze. Unification picture in minimal supersymmetric SU(5) model with string remnants. *Phys.Rev.*, D58:055011, 1998, arXiv:hep-ph/9803335.

[89] Tomas Blazek and Stuart Raby. Supersymmetric grand unified theories and global fits to low-energy data. *Phys.Lett.*, B392:371–375, 1997, arXiv:hep-ph/9611319.
Daniel Auto, Howard Baer, Csaba Balazs, Alexander Belyaev, Javier Ferrandis, et al. Yukawa coupling unification in supersymmetric models. *JHEP*, 0306:023, 2003, arXiv:hep-ph/0302155.
Marco Ciuchini, Antonio Masiero, Paride Paradisi, Luca Silvestrini, Sudhir K. Vempati, et al. Soft SUSY breaking grand unification: Leptons versus quarks on the flavor playground. *Nucl.Phys.*, B783:112–142, 2007, arXiv:hep-ph/0702144.
Wolfgang Altmannshofer, Diego Guadagnoli, Stuart Raby, and David M. Straub. SUSY GUTs with Yukawa unification: A Go/no-go study using FCNC processes. *Phys.Lett.*, B668:385–391, 2008, arXiv:0801.4363.
Andrzej J. Buras, Minoru Nagai, and Paride Paradisi. Footprints of SUSY GUTs in Flavour Physics. *JHEP*, 1105:005, 2011, arXiv:1011.4853.

[90] Stephen P. Martin and Michael T. Vaughn. Two loop renormalization group equations for soft supersymmetry breaking couplings. *Phys.Rev.*, D50:2282, 1994, arXiv:hep-ph/9311340.

[91] Werner Porod. SPheno, a program for calculating supersymmetric spectra, SUSY particle decays and SUSY particle production at e+ e- colliders. *Comput.Phys.Commun.*, 153:275–315, 2003, arXiv:hep-ph/0301101.
Werner Porod and Florian Staub. SPheno 3.1: Extensions including flavour, CP-phases and models beyond the MSSM. *Comput.Phys.Commun.*, 183:2458–2469, 2012, arXiv:1104.1573.

[92] Florian Staub. Automatic Calculation of supersymmetric Renormalization Group Equations and Self Energies. *Comput.Phys.Commun.*, 182:808–833, 2011, arXiv:1002.0840.
Florian Staub. SARAH 4: A tool for (not only SUSY) model builders. *Comput.Phys.Commun.*, 185:1773–1790, 2014, arXiv:1309.7223.

[93] Juan Antonio Aguilar-Saavedra, A. Ali, Benjamin C. Allanach, Richard L. Arnowitt, Howard A. Baer, et al. Supersymmetry parameter analysis: SPA convention and project. *Eur.Phys.J.*, C46: 43–60, 2006, arXiv:hep-ph/0511344.

[94] Warren Siegel. Inconsistency of supersymmetric dimensional regularization. *Physics Letters B*, 94(1):37–40, 1980.
Karol Kovarik. *Precise predictions for sfermion pair production at a linear collider*. PhD thesis, Comenius University Bratislava, 2005. URL http://www.hephy.at/fileadmin/user_upload/Projekte/theorie_susy/diss_Kovarik_K.pdf.

[95] Wolfgang Altmannshofer, Andrzej J. Buras, Stefania Gori, Paride Paradisi, and David M. Straub. Anatomy and Phenomenology of FCNC and CPV Effects in SUSY Theories. *Nucl.Phys.*, B830: 17–94, 2010, arXiv:0909.1333.

[96] Piotr H. Chankowski and Lucja Slawianowska. B0(d,s) —> mu- mu+ decay in the MSSM. *Phys.Rev.*, D63:054012, 2001, arXiv:hep-ph/0008046.
Gino Isidori and Alessandra Retico. $B_{s,d} \to \ell^+\ell^-$ and $K_L \to \ell^+\ell^-$ in SUSY models with nonminimal sources of flavor mixing. *JHEP*, 0209:063, 2002, arXiv:hep-ph/0208159.
Miguel Arana-Catania, Sven Heinemeyer, Maria J. Herrero, and Siannah Penaranda. Higgs Boson masses and B-Physics Constraints in Non-Minimal Flavor Violating SUSY scenarios. *JHEP*, 1205: 015, 2012, arXiv:1109.6232.
Miguel Arana-Catania, Sven Heinemeyer, and Maria J. Herrero. Updated Constraints on General Squark Flavor Mixing. *Phys.Rev.*, D90(7):075003, 2014, arXiv:1405.6960.

[97] Eduardo de Rafael. Chiral Lagrangians and kaon CP violation. 1995, arXiv:hep-ph/9502254.
Maria Elvira Gamiz Sanchez. Kaon physics: CP violation and hadronic matrix elements. 2003, arXiv:hep-ph/0401236.

[98] Joachim Brod and Martin Gorbahn. Epsilon_K at Next-to-Next-to-Leading Order: The Charm-Top-Quark Contribution. *Phys.Rev.*, D82:094026, 2010, arXiv:1007.0684.

[99] Diego Guadagnoli. On the Consistency Between CP Violation in the K vs. Bd Systems within the Standard Model. 2011, arXiv:1102.2760.

[100] Patricia Ball and Robert Fleischer. Probing new physics through B mixing: Status, benchmarks and prospects. *Eur.Phys.J.*, C48:413–426, 2006, arXiv:hep-ph/0604249.

[101] Andrzej J. Buras, Piotr H. Chankowski, Janusz Rosiek, and Lucja Slawianowska. $\Delta M_{d,s}, B^0 d, s \to \mu^+\mu^-$ and $B \to X_s\gamma$ in supersymmetry at large $\tan\beta$
. *Nucl.Phys.*, B659:3, 2003, arXiv:hep-ph/0210145.

[102] Y. Amhis et al. Averages of b-hadron, c-hadron, and τ-lepton properties as of summer 2014. 2014, arXiv:1412.7515.

[103] Andrzej J. Buras and Jennifer Girrbach. Towards the Identification of New Physics through Quark Flavour Violating Processes. *Rept.Prog.Phys.*, 77:086201, 2014, arXiv:1306.3775.

[104] R Aaij et al. First Evidence for the Decay $B_s^0 \to \mu^+\mu^-$. *Phys.Rev.Lett.*, 110(2):021801, 2013, arXiv:1211.2674.

[105] Andrzej J. Buras, Robert Fleischer, Jennifer Girrbach, and Robert Knegjens. Probing New Physics with the $B_stomu + \mu-$ Time-Dependent Rate. *JHEP*, 1307:77, 2013, arXiv:1303.3820.

[106] Mikhail Shifman. Lectures on quark-hadron duality. *Czechoslovak Journal of Physics*, 52(2): B102–B135, 2002. ISSN 0011-4626. URL http://dx.doi.org/10.1007/s10582-002-0080-6.

[107] Wolfgang Altmannshofer. *Anatomy and phenomenology of flavor and CP violation in supersymmetric theories*. PhD thesis, Munich University, 2010.

[108] Mikolaj Misiak, H.M. Asatrian, Kay Bieri, Michal Czakon, Andrzej Czarnecki, et al. Estimate of B(anti-B —> X(s) gamma) at O(alpha(s)**2). *Phys.Rev.Lett.*, 98:022002, 2007, arXiv:hep-ph/0609232.

[109] Junji Hisano, Minoru Nagai, Paride Paradisi, and Yasuhiro Shimizu. Waiting for mu —> e gamma from the MEG experiment. *JHEP*, 0912:030, 2009, arXiv:0904.2080.

[110] K. Hayasaka et al. New search for tau —> mu gamma and tau —> e gamma decays at Belle. *Phys.Lett.*, B666:16–22, 2008, arXiv:0705.0650.

[111] B. Aubert and *et al.* Searches for lepton flavor violation in the decays $\tau^\pm \to e^\pm\gamma$ and $\tau^\pm \to \mu^\pm\gamma$. *Phys. Rev. Lett.*, 104:021802, Jan 2010. URL http://link.aps.org/doi/10.1103/PhysRevLett.104.021802.

[112] Andre de Gouvea and Petr Vogel. Lepton Flavor and Number Conservation, and Physics Beyond the Standard Model. *Prog.Part.Nucl.Phys.*, 71:75–92, 2013, arXiv:1303.4097.

[113] Georges Aad et al. Measurement of the Higgs boson mass from the $H \to \gamma\gamma$ and $H \to ZZ^* \to 4\ell$ channels with the ATLAS detector using 25 fb^{-1} of pp collision data. *Phys.Rev.*, D90(5):052004, 2014, arXiv:1406.3827.

[114] Benjamin C. Allanach, Abdelhak Djouadi, Jean L. Kneur, Werner Porod, and Pietro Slavich. Precise determination of the neutral Higgs boson masses in the MSSM. *JHEP*, 0409:044, 2004, arXiv:hep-ph/0406166.

[115] Fabrizio Gabbiani, Emidio Gabrielli, Antonio Masiero, and Luca Silvestrini. A Complete analysis of FCNC and CP constraints in general SUSY extensions of the standard model. *Nucl.Phys.*, B477:321–352, 1996, arXiv:hep-ph/9604387.

[116] Glen Cowan, Kyle Cranmer, Eilam Gross, and Ofer Vitells. Asymptotic formulae for likelihood-based tests of new physics. *European Physical Journal C*, 71:1554, February 2011, arXiv:1007.1727.

[117] David B. Kaplan. Effective field theories. 1995, arXiv:nucl-th/9506035.
Aneesh V. Manohar. Effective field theories . *Lect.Notes Phys.*, 479:311–362, 1997
, arXiv:hep-ph/9606222.
Ira Z. Rothstein. TASI lectures on effective field theories. 2003, arXiv:hep-ph/0308266.
Witold Skiba. TASI Lectures on Effective Field Theory and Precision Electroweak Measurements. 2010, arXiv:1006.2142.

[118] Fred L. Wilson. Fermi's Theory of Beta Decay. *American Journal of Physics*, 36:1150–1160, 1968.

[119] Stefan Hollands and Christoph Kopper. The operator product expansion converges in perturbative field theory. *Commun.Math.Phys.*, 313:257–290, 2012, arXiv:1105.3375.

[120] Bohdan Grzadkowski, Mateusz Iskrzynski, Mikolaj Misiak, and Janusz Rosiek. Dimension-Six Terms in the Standard Model Lagrangian. *JHEP*, 1010:085, 2010, arXiv:1008.4884.

[121] Guy Raz. The Mass insertion approximation without squark degeneracy. *Phys.Rev.*, D66:037701, 2002, arXiv:hep-ph/0205310.

[122] Gudrun Hiller, Yonit Hochberg, and Yosef Nir. Flavor Changing Processes in Supersymmetric Models with Hybrid Gauge- and Gravity-Mediation. *JHEP*, 0903:115, 2009, arXiv:0812.0511.
Gino Isidori, Yosef Nir, and Gilad Perez. Flavor Physics Constraints for Physics Beyond the Standard Model. *Ann.Rev.Nucl.Part.Sci.*, 60:355, 2010, arXiv:1002.0900.

[123] Ferruccio Feruglio, Claudia Hagedorn, and Luca Merlo. Vacuum Alignment in SUSY A4 Models. *JHEP*, 1003:084, 2010, arXiv:0910.4058.

[124] Mohammad Ahsanullah. *Normal and student's t distributions and their applications*. Atlantis Press, Paris, 2014. ISBN 978-94-6239-060-7.

[125] David V. Hinkley. On the ratio of two correlated normal random variables. *Biometrika*, 56(3): 635–639, 1969. URL http://biomet.oxfordjournals.org/content/56/3/635.abstract.

[126] Luis E. Ibanez and Irene Valenzuela. The Higgs Mass as a Signature of Heavy SUSY. *JHEP*, 1305:064, 2013, arXiv:1301.5167.

[127] Carlos Tamarit. Decoupling heavy sparticles in Effective SUSY scenarios: Unification, Higgs masses and tachyon bounds. *JHEP*, 1206:080, 2012, arXiv:1204.2645.

[128] Marek Jeżabek and J.H. Kühn. Lepton spectra from heavy quark decay. *Nuclear Physics B*, 320 (1):20 – 44, 1989. ISSN 0550-3213. URL http://www.sciencedirect.com/science/article/pii/0550321389902095.
Marek Jezabek. Top quark physics. *Nucl.Phys.Proc.Suppl.*, 37B:197, 1994, arXiv:hep-ph/9406411.
Jessie Shelton. Polarized tops from new physics: signals and observables. *Phys.Rev.*, D79:014032, 2009, arXiv:0811.0569.
Brock Tweedie. Better Hadronic Top Quark Polarimetry. *Phys.Rev.*, D90(9):094010, 2014, arXiv:1401.3021.

[129] Lars Hofer, Ulrich Nierste, and Dominik Scherer. Resummation of tan-beta-enhanced supersymmetric loop corrections beyond the decoupling limit. *JHEP*, 0910:081, 2009, arXiv:0907.5408.
Andreas Crivellin and Ulrich Nierste. Chirally enhanced corrections to FCNC processes in the generic MSSM. *Phys.Rev.*, D81:095007, 2010, arXiv:0908.4404.

[130] Felix Brummer, Sylvain Fichet, and Sabine Kraml. The Supersymmetric flavour problem in 5D GUTs and its consequences for LHC phenomenology. *JHEP*, 1112:061, 2011, arXiv:1109.1226.

[131] CMS Collaboration. Search for anomalous single top quark production in association with a photon. (CMS-PAS-TOP-14-003), 2014. URL http://cds.cern.ch/record/1700519.

[132] CMS Collaboration. Search for Flavour Changing Neutral Currents in single top events. (CMS-PAS-TOP-12-021), 2013. URL http://cds.cern.ch/record/1563579.

[133] The ATLAS collaboration. Search for single top-quark production via FCNC in strong interaction in $\sqrt{s} = 8$ TeV ATLAS data. (ATLAS-CONF-2013-063, ATLAS-COM-CONF-2013-064), 2013. URL http://cds.cern.ch/record/1562777.

[134] Georges Aad et al. Search for FCNC single top-quark production at $\sqrt{s} = 7$ TeV with the ATLAS detector. *Phys.Lett.*, B712(CERN-PH-EP-2012-032):351–369, 2012, arXiv:1203.0529.

[135] S. Chatrchyan *et al.* CMS collaboration. Search for Flavor-Changing Neutral Currents in Top-Quark Decays $t \to Zq$ in pp Collisions at $\sqrt{s} = 8$ TeV. *Phys. Rev. Lett.*, 112:171802, May 2014. URL http://link.aps.org/doi/10.1103/PhysRevLett.112.171802.

[136] CMS Collaboration. Search for flavor changing neutral currents in top quark decays in pp collisions at 8 TeV. Technical Report CMS-PAS-TOP-12-037, 2013.

[137] Efe Yazgan. Flavor changing neutral currents in top quark production and decay. (CMS-CR-2013-398):285–294, 2014, arXiv:1312.5435.

[138] Carlos A. Bertulani, Spencer R. Klein, and Joakim Nystrand. Physics of ultra-peripheral nuclear collisions. *Ann.Rev.Nucl.Part.Sci.*, 55:271–310, 2005, arXiv:nucl-ex/0502005.

[139] Christopher Brust, Andrey Katz, Scott Lawrence, and Raman Sundrum. SUSY, the Third Generation and the LHC. *JHEP*, 1203:103, 2012, arXiv:1110.6670.

[140] Michele Redi and Ben Gripaios. Partially Supersymmetric Composite Higgs Models. *JHEP*, 1008:116, 2010, arXiv:1004.5114.

[141] Emilian Dudas and Gero von Gersdorff. Universal contributions to scalar masses from five dimensional supergravity. *JHEP*, 1210:100, 2012, arXiv:1207.0815.

[142] Janusz Rosiek. Complete set of feynman rules for the minimal supersymmetric extension of the standard model. *Phys. Rev. D*, 41:3464–3501, 1990. URL http://link.aps.org/doi/10.1103/PhysRevD.41.3464.
Janusz Rosiek. Complete set of Feynman rules for the MSSM: Erratum. 1995, arXiv:hep-ph/9511250.

[143] Manuel Drees. *Theory and phenomenology of sparticles : an account of four-dimensional N=1 supersymmetry in high energy physics*. World Scientific, Singapore Hackensack, NJ, 2004. ISBN 978-9812565310.

[144] LHC SUSY Cross Section Working Group. URL https://twiki.cern.ch/twiki/bin/view/LHCPhysics/SUSYCrossSections.

[145] Maxim Perelstein and Andreas Weiler. Polarized Tops from Stop Decays at the LHC. *JHEP*, 0903:141, 2009, arXiv:0811.1024.

[146] Biplob Bhattacherjee, Sourav K. Mandal, and Mihoko Nojiri. Top Polarization and Stop Mixing from Boosted Jet Substructure. *JHEP*, 1303:105, 2013, arXiv:1211.7261.

[147] Geneviève Bélanger, Rohini M. Godbole, Lisa Hartgring, and Irene Niessen. Top Polarization in Stop Production at the LHC. *JHEP*, 1305:167, 2013, arXiv:1212.3526.

[148] Giuseppe Bozzi, Benjamin Fuks, Björn Herrmann, and Michael Klasen. Squark and gaugino hadroproduction and decays in non-minimal flavour violating supersymmetry. *Nucl.Phys.*, B787: 1–54, 2007, arXiv:0704.1826.

[149] Tobias Hurth and Werner Porod. Flavour violating squark and gluino decays. *JHEP*, 0908:087, 2009, arXiv:0904.4574.

[150] Benjamin Fuks, Björn Herrmann, and Michael Klasen. Phenomenology of anomaly-mediated supersymmetry breaking scenarios with non-minimal flavour violation. *Phys.Rev.*, D86:015002, 2012, arXiv:1112.4838.

[151] Alfred Bartl, Helmut Eberl, Elena Ginina, Björn Herrmann, Keisho Hidaka, et al. Flavor violating bosonic squark decays at LHC. *Int.J.Mod.Phys.*, A29(07):1450035, 2014, arXiv:1212.4688.

[152] Kamila Kowalska. Phenomenology of SUSY with General Flavour Violation. *JHEP*, 1409:139, 2014, arXiv:1406.0710.

[153] Monika Blanke, Gian F. Giudice, Paride Paradisi, Gilad Perez, and Jure Zupan. Flavoured Naturalness. *JHEP*, 1306:022, 2013, arXiv:1302.7232.

[154] Matthias Bruhnke, Björn Herrmann, and Werner Porod. Signatures of bosonic squark decays in non-minimally flavour-violating supersymmetry. *JHEP*, 1009:006, 2010, arXiv:1007.2100.

[155] George Box. *Bayesian inference in statistical analysis*. Wiley, New York, 1992. ISBN 978-0471574286.
Andrew Gelman. *Bayesian data analysis*. Chapman & Hall/CRC, Boca Raton, Fla, 2004. ISBN 978-1584883883.
Jayanta K. Ghosh. *An introduction to Bayesian analysis theory and methods*. Springer, New York, 2006. ISBN 978-0-387-35433-0.
William Bolstad. *Introduction to Bayesian statistics*. John Wiley, Hoboken, N.J, 2007. ISBN 978-0470141151.

[156] Roberto Trotta. Bayes in the sky: Bayesian inference and model selectio in cosmology. *Contemp.Phys.*, 49:71–104, 2008, arXiv:0803.4089.

[157] Christian Robert. *Monte Carlo statistical methods*. Springer, New York, 2010. ISBN 978-1441919397.

[158] Deborah Mayo. *Error and the growth of experimental knowledge*. University of Chicago Press, Chicago, 1996. ISBN 978-0226511986.

[159] Giulio D'Agostini. Probability and measurement uncertainty in physics: A Bayesian primer. 1995, arXiv:hep-ph/9512295.

[160] Aart F. de Vos. A primer in Bayesian Inference. URL http://personal.vu.nl/a.f.de.vos/primer/primer.pdf.

[161] Nicolas Chopin and Christian P. Robert. Properties of nested sampling. *Biometrika*, 97(3):741–755, 2010, arXiv:http://biomet.oxfordjournals.org/content/97/3/741.full.pdf+html. URL http://biomet.oxfordjournals.org/content/97/3/741.abstract.

[162] Harold Jeffreys. *Theory of probability*. Clarendon Press Oxford University Press, Oxford Oxfordshire New York, 1998. ISBN 978-0198503682.

[163] James M. Dickey. The weighted likelihood ratio, linear hypotheses on normal location parameters. *Ann. Math. Statist.*, 42(1):204–223, 1971. URL http://dx.doi.org/10.1214/aoms/1177693507.

[164] Jean-Michel Marin and Christian P. Robert. On resolving the savage–dickey paradox. *Electron. J. Statist.*, 4:643–654, 2010. URL http://dx.doi.org/10.1214/10-EJS564.

[165] Peter Z. Skands, Benjamin C. Allanach, Howard Baer, Csaba Balazs, Geneviève Bélanger, et al. SUSY Les Houches accord: Interfacing SUSY spectrum calculators, decay packages, and event generators. *JHEP*, 0407:036, 2004, arXiv:hep-ph/0311123.

[166] Benjamin C. Allanach, Csaba Balazs, Geneviève Bélanger, Markus Bernhardt, Fawzi Boudjema, et al. SUSY Les Houches Accord 2. *Comput.Phys.Commun.*, 180:8–25, 2009, arXiv:0801.0045.

[167] URL http://www.gnu.org/software/octave/.

[168] James R. Norris. *Markov chains*. Cambridge University Press, Cambridge, UK New York, 1998. ISBN 978-0521633963.

[169] Giancarlo D'Ambrosio, Gian F. Giudice, Gino Isidori, and Alessandro Strumia. Minimal flavor violation: An Effective field theory approach. *Nucl.Phys.*, B645:155–187, 2002, arXiv:hep-ph/0207036.

[170] Oram Gedalia and Gilad Perez. TASI 2009 Lectures - Flavor Physics. pages 309–382, 2011, arXiv:1005.3106.

[171] Wolfgang Kilian, Thorsten Ohl, and Jürgen Reuter. WHIZARD: Simulating Multi-Particle Processes at LHC and ILC. *Eur.Phys.J.*, C71:1742, 2011, arXiv:0708.4233.

[172] Christopher G. Lester, Michael A. Parker, and Martin J. White. Three body kinematic endpoints in SUSY models with non-universal Higgs masses. *JHEP*, 10:051, 2007, arXiv:hep-ph/0609298.

[173] Stephen F. King, Stephano Moretti, and Roman Nevzorov. Exceptional supersymmetric standard model. *Phys. Lett.*, B634:278–284, 2006, arXiv:hep-ph/0511256.

[174] Jurgen Reuter and Daniel Wiesler. Distorted mass edges at LHC from supersymmetric leptoquarks. *Phys. Rev.*, D84:015012, 2011, arXiv:1010.4215.